Institute of Organic Chemistry
Polish Academy of Sciences

Synthesis of N-doped polycyclic aromatic hydrocarbons built on 1,4-dihydropyrrolo[3,2-*b*]pyrroles via alkyne activation

Gana Sanil M.Sc.

A monothematic series of publications with a commentary presented to the Scientific Council of the Institute of Organic Chemistry of the Polish Academy of Sciences in order to obtain a doctorate in chemical sciences

Promotor: prof. dr hab. Daniel T. Gryko

Doctoral thesis completed as part of the project:

Project funded by the EU under the Marie Curie Action: H2020-MSCA-ITN-2019, GA nr 860762

"Develop C-H activation methods for the synthesis of new materials"

Acknowledgements:

I would like to extend my deepest gratitude to my supervisor, Prof. Daniel T. Gryko, whose support, guidance, and patience have been invaluable throughout my PhD journey. I am profoundly grateful for the opportunity to work under his mentorship, which has been a constant source of encouragement and inspiration. Without his continuous motivation and throughout help, this dissertation would not be possible.

I would also like to express my gratitude to all current and past members of the Daniel Gryko group for their support, welcoming work environment, valuable insights, and companionship. I would like to acknowledge Dr. Maciek Krzeszewski for his invaluable guidance and support during the first phase of my PhD studies. I sincerely thank Dr. Yevgen Poronik for always being there to troubleshoot problems in the lab and for insightful discussions. I would like to thank Dr. Olena Vakuliuk for her constant help and fruitful suggestions. Additionally, I wish to thank Dr. Mariusz Tasior, Dr. Beata Koszarna, Dr. Krzysztof Górski and Dr. Damian Kusy for their help and support. I would like to acknowledge the staff, and friends in the IOC, PAS for helpful discussions, support and assistance when I needed it most.

I would like to express my gratitude to my collaborators Prof. Denis Jacquemin and Dr. Wojciech Chaładaj for performing the theoretical studies. I wish to thank Prof. Michał Cyrański and Dr. Łukasz Dobrzycki for carrying out the X-ray analysis.

I would like to thank CHAIR- consortium - funded by the EU under the Marie Curie Action: H2020-MSCA-ITN-2019 for the financial support. I wish to thank all the members of the consortium including our project manager, Dr. Irène Arrata, for their companionship and delightful memories.

I wish to thank my friends Smrithi, Neeraj, Anil, Minu, Juby, Prachi, Vishali, Deepshikha, Jacqueline, Kitti, Güler, Nabeel and Vidhu for their kind support and encouragement. I would like to thank Prof. Gokulnath Sabapathi (IISER TVM) and Dr. Ajay Jayaprakash for their mentorship.

Finally, I would like to dedicate this thesis to my parents, my unwavering pillar of strength who have always believed in me and gave wings to my dreams. I am thankful to my partner, Vishnu, for always being there through thick and thin, holding me tight throughout this journey. I am forever grateful to my brother Rag for keeping my happiness at highest priority than his needs.

Abstract in English

In the quest for innovative materials, non-planar polycyclic aromatic hydrocarbons (PAHs) and their heterocyclic analogues with new molecular topologies are emerging as an important candidate. Particularly, introduction of non-hexagonal rings such as pentagons and heptagons into completely planar hexagonal backbone leads to the formation of uniquely curved architectures, acquiring distinct electronic, magnetic and mechanical properties that are significantly different from their planar counterparts. Moreover, doping of heteroatom to this framework is a direct approach to tune their inherent physical and chemical properties to enable novel applications. Considering the purely benzenoid structure, intramolecular alkyne benzannulation is one among the key reactions for C-C bond formation.

The main goal of my PhD dissertation is to design pathways to synthesize aza-doped non-planar polycyclic aromatic systems featuring unique curvature and to study their photophysical properties. I started my research with synthesizing tetraaryl-1,4-dihydropyrrolo[3,2-*b*]pyrroles (TAPPs) bearing alkynyl moieties as precursors by using optimized reaction conditions reported in our lab. In the first part of the thesis, several conditions to perform alkyne annulation reaction on the precursors were explored. It turned out that only cationic gold(I) complexes catalyze this reaction, albeit accompanied by 1,2-aryl shift leading to the formation of S-shaped polycyclic π-system (**Scheme 1**). The scope of this *6-endo-dig* type annulation was further explored on electronically different substituents for tunability with respect to the photophysical properties, as well as creating additional sites for functionalization. Additional optimization experiments to determine the factors affecting the reaction were also carried out. Steady state UV/Vis spectroscopy shows that the synthesized aza-doped PAHs primarily undergoes radiative relaxation upon photoexcitation resulting in high fluorescence quantum yields. The optical properties of both precursors and products were rationalized by density functional theory (Prof. Denis Jacquemin, France).

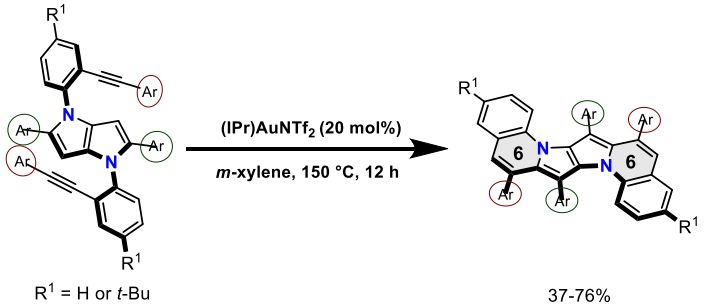

Scheme 1. Gold-catalyzed double *6-endo-dig* alkyne annulation accompanied by 1,2-aryl shift.

In the second part of my thesis, I worked on the same TAPP precursors to induce *7-endo-dig* type alkyne annulation to synthesize unique 7-5-5-7 type cyclized system. Exceptionally strong Brønsted acid $HNTf_2$ facilitated the 7-membered ring formation (**Scheme 2**). The scope studies revealed that this reaction is highly selective towards certain substrates where electron-donating and electron-withdrawing substituents are arranged in a specific manner. Additionally, I found that subsequent intramolecular direct arylation led to the formation of N-doped nanographene possessing four seven-membered rings with 7-7-5-5-7-7 type cyclic system. Newly synthesized dyes showed weak red emission. The presence of conjugated ring systems 7-5-5-7 and 7-7-5-5-7-7 causes the bathochromic shift of absorption and emission.

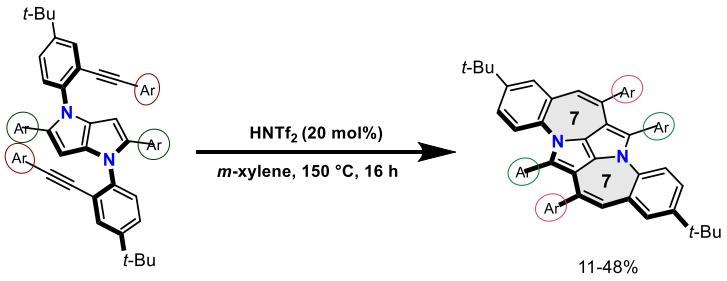

Scheme 2. $HNTf_2$-mediated double *7-endo-dig* alkyne annulation.

Abstract in Polish

Nieplanarne wielopierścieniowe węglowodory aromatyczne (WWA) i ich heterocykliczne analogi wyłaniają się jako ważni kandydaci w poszukiwaniach innowacyjnych materiałów. Zastąpienie niektórych sześcioczłonowych pierścieni w planarnych cząsteczkach WWA pierścieniami pięcio- lub siedmioczłonowymi, powoduje zakrzywienie ich struktury, co w istotny sposób wpływa na ich właściwości elektronowe, magnetyczne oraz mechaniczne. Dodatkowo, wprowadzenie heteroatomów do tych układów, pozwala dostrajać ich właściwości fizyczne oraz chemiczne do odpowiednich aplikacji. Jedną z najistotniejszych reakcji wykorzystywanych do tworzenia wiązania C–C w syntezie wielopierścieniowych węglowodorów aromatycznych jest wewnątrzcząsteczkowa benzannulacja alkinów.

Głównym celem mojej rozprawy doktorskiej jest zaprojektowanie ścieżek do syntezy aza-domieszkowanych, nieplanarnych wielopierścieniowych układów aromatycznych, charakteryzujących się unikalną krzywizną oraz zbadanie ich właściwości fotofizycznych. Swoje badania rozpoczęłam od syntezy alkinylowych pochodnych tetraarylo-1,4-dihydropirolo[3,2-*b*]piroli (TAPP), wykorzystując w tym celu optymalne warunki reakcji opracowane w Zespole X IChO PAN. W pierwszej części pracy przetestowałam szereg zestawów warunków benzannulacji alkinów na ww. prekursorach. Okazało się, że jedynie kationowe kompleksy złota(I) są zdolne do katalizowania tej reakcji, a dodatkowo towarzyszy jej przesunięcie 1,2-arylowe, prowadzące do powstania wielopierścieniowego układu π w kształcie litery S (**Schemat 1**). Następnie przeprowadziłam dodatkowe eksperymenty optymalizacyjne w celu określenia czynników wpływających na reakcję oraz zbadałam zakres stosowalności nowoopracowanej benzannulacji typu *6-endo-dig* dla prekursorów wyposażonych w różne podstawniki, co pozwoliło na dostrojenie właściwości fotofizycznych produktów, a także ich dalsze przekształcenie. Spektroskopia UV/Vis pokazuje, że zsyntetyzowane aza-WWA po wzbudzeniu ulegają przede wszystkim relaksacji radiacyjnej, co skutkuje wysoką wydajnością kwantową fluorescencji. Dodatkowo właściwości optyczne prekursorów i produktów zostały uzasadnione za pomocą obliczeń DFT. (prof. Denis Jacquemin, Francja).

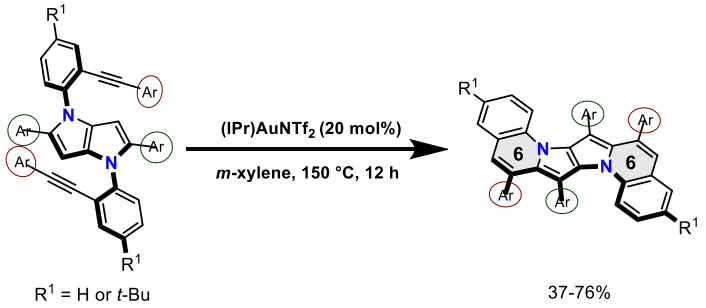

Schemat 1. Katalizowana kationowym kompleksem złota podwójna *6-endo-dig* annulacja z przesunięciem 1,2-arylowym.

W drugiej części mojej pracy pracowałam nad annulacją typu *7-endo-dig* ww. prekursorów w celu syntezy unikalnego układu sprzężonych pierścieni 7-5-5-7-członowych, co udało się osiągnąć wykorzystując wyjątkowo silny kwas Brønsteda – $HNTf_2$ (**Schemat 2**). Badania zakresu stosowalności metody wykazały, że jest ona wysoce selektywna w stosunku do substratów o określonym ułożeniu podstawników elektronodonorowych i elektronoakceptorowych. Ponadto odkryłam, że następcze wewnątrzcząsteczkowe bezpośrednie arylowanie prowadzi do powstania *N*-domieszkowanego nanografenu posiadającego cztery siedmioczłonowe pierścienie w układzie 7-7-5-5-7-7. Obecność sprzężonych pierścieni 7-5-5-7 i 7-7-5-5-7-7-członowych powoduje batochromowe przesunięcie absorpcji i emisji, a nowo zsyntetyzowane barwniki wykazują słabą, czerwoną emisję.

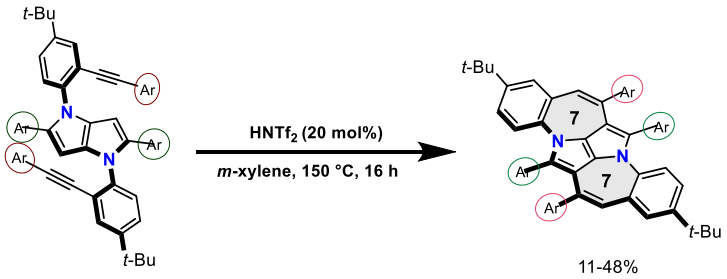

Schemat 2. Podwójna annulacja *7-endo-dig* alkinu z wykorzystaniem $HNTf_2$.

Table of Contents

Reprints of publications included as part of the doctoral dissertation.

List of publications for the doctoral dissertation

(1) **Sanil, G**.; Koszarna, B.; Poronik, Y. M.; Vakuliuk, O.; Szymański, B.; Kusy, D.; Gryko, D. T. The Chemistry of 1,4-Dihydropyrrolo[3,2-*b*]Pyrroles. *Adv. Heterocycl. Chem.* **2022**, *138*, 335–409. DOI:10.1016/bs.aihch.2022.04.002.

(2) **Sanil, G**.; Krzeszewski, M.; Chaładaj, W.; Danikiewicz, W.; Knysh, I.; Dobrzycki, Ł.; Staszewska-Krajewska, O.; Cyrański, M. K.; Jacquemin, D.; Gryko, D. T. Gold-Catalyzed 1,2-Aryl Shift and Double Alkyne Benzannulation. *Angew. Chem. Int. Ed.* **2023**, *62* (49), e202311123. DOI:10.1002/anie.202311123.

(3) **Sanil, G**.; Dobrzycki, Ł.; Cyrański, M. K.; Jacquemin, D.; Chaładaj, W.; Gryko, D. T. 1,4-Dihydropyrrolo[3,2-*b*]Pyrroles with Two Embedded Heptagons via Alkyne Annulation. *J. Org. Chem*. **2025,** *90* (1), 614–622. DOI:10.1021/acs.joc.4c02538.

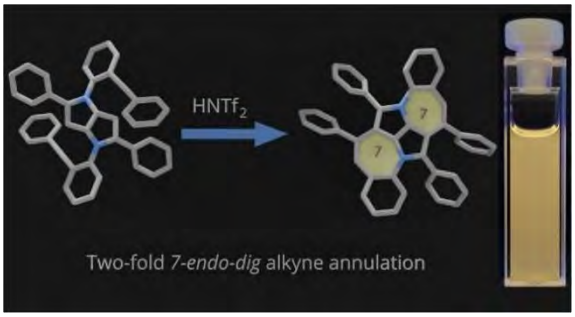

List of publications not included in the doctoral dissertation

(1) Kaplaneris, N.; Akdeniz, M.; Fillols, M.; Arrighi, F.; Raymenants, F.; **Sanil, G**.; Gryko, D. T.; Noël, T. Photocatalytic Functionalization of Dehydroalanine-Derived Peptides in Batch and Flow. *Angew. Chem. Int. Ed.* **2024**, *63* (19), e202403271. DOI:10.1002/anie.202403271.

(2) Govind, C.; Balanikas, E.; **Sanil, G**.; Gryko, D. T.; Vauthey, E. Structural and Solvent Modulation of Symmetry-Breaking Charge-Transfer Pathways in Molecular Triads. *Chem. Sci.* **2024**, *15* (42), 17362–17371. DOI:10.1039/d4sc05419a.

Participation in conferences and seminars

(1) 19th International Symposium on Novel Aromatic Compounds (ISNA 2022), 3–8 July, 2022, Warsaw, Poland. Poster title: “Unprecedented 1,2-aryl shift in tetraaryl pyrrolo[3,2-*b*]pyrroles triggered by alkyne activation catalyzed by a cationic gold complex ”

(2) CHAIR closing conference The “European Meeting on C-H Activation”, 23-24 January, 2024, Lisbon, Portugal. Title of talk “Gold-catalyzed 1,2-aryl shift and double alkyne benzannulation”

Short CV

I was born on 16th August 1996, at Kerala, India. In 2014, I started my integrated Bachelor-master's degree (BSMS) at Indian Institute of Science Education and Research, Thiruvananthapuram (IISER TVM). During the master's I did an internship on the "Synthesis and Characterization of Indeno [2,1-*a*] Indene Derivatives" under the supervision of Prof. S. Nagarajan, Central University of Tamilnadu. I completed my master's thesis on the topic "Unprecedented formation of hexathiadodecaphyrins bearing diheterole units" under the guidance of Prof. Gokulnath Sabapathi.

In 2020, I joined Prof. Daniel Gryko's group at the Institute of Organic Chemistry, Polish Academy of Sciences as the part of Marie Curie Innovative Training Nerwork (ITN), under CHAIR (C-H Activation for Industrial Renewal) consortium, EU Grant Agreement nr: 860762. My research was focused on the topic: Synthesis of polycyclic aromatic hydrocarbons built on 1,4-dihydropyrrolo[3,2-*b*]pyrroles via alkyne activation. This research has culminated into the publication of four Papers, one book chapter, a poster and an oral presentation.

1. Introduction

1.1 Planar and non-planar nanographenes (NGs)

Nanographenes (NGs) as well-defined cut-outs from graphene sheets, serve as an ideal bridge between the molecular and bulk carbon material realms.[1] The main advantages of such molecules is that their electronic and optical properties can be elegantly tuned by rationally designed bottom up synthesis, which in turn allows variety of NGs with varying shapes, size and functionality.[2], [3] Their potential applications span across various domains of material chemistry including electronic devices,[4] sensors,[5], biomedical analysis[6], polymer films[7] etc. NGs can be generally divided into two types, planar and non-planar. While completely fused planar systems possess all hexagonal rings (e.g. Coronene and hexabenzocoronene), introduction of non-benzenoid systems such as 5, 7 or 8 membered rings can induce curvature to the polycyclic system due to the geometric mismatch of adjacent rings. Embedding NGs with ring size less than 6 give rise to a positive Gaussian curvature as in the case of corannulene,[8],[9],[10] sumanene[11],[12] and their π-extended derivatives, while ring size larger than 6 can induce negative Gaussian curvature to have a saddle type geometry (e.g. isocoronene,[13] [7]circulene[14],[15]). The chemistry of such contorted NGs continues to evolve not only as a result of their aesthetic appeal, but also due to their unexpected redox, optical, charge transport and self-assembly properties which arises from the geometry.[16]

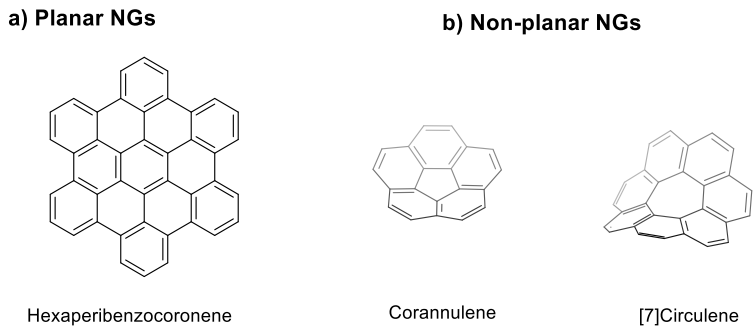

Figure 1. Representative examples of planar and non-planar NGs

1.2 Alkyne benzannulation towards nanographenes (NGs)

A comparatively simple and efficient method for the bottom-up synthesis of polycyclic systems is still a well-sought area in synthetic organic chemistry. Methods such as aryl-aryl oxidative coupling reaction (Scholl reaction),[17] transition-metal catalyzed[18] or light induced direct arylation reactions have been mostly used for such synthesis. Recently, there has been growing interest in exploring the ability of alkynes to act as versatile and efficient building blocks for the synthesis of carbon nano-structures. This is associated with the fact that a large thermodynamic gain act as a driving force enabling the formation of conjugated cyclic ring system from high energy alkyne precursors.[19] Historically, the first attempt of alkyne benzannulation towards PAHs was reported by Scott and co-workers in 1991 by utilizing Flash Vacuum Pyrolysis (FVP).[10] Under FVP conditions, two-fold alkyne benzannulation occurred smoothly to form curved nanographene, corannulene (**Scheme 1**). However, this method became more popular after the discovery of electrophilic activation of alkynes reported by Swager,[20],[21] which paved way to a variety of similar transformations involving Brønsted acids, π-Lewis acids, transition metals and radical reagents as catalysts.

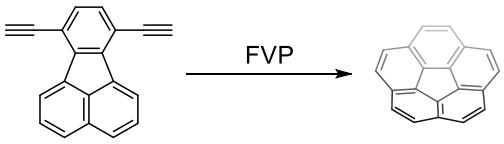

Scheme 1. FVP conditions towards corannulene [10]

1.2.1 Alkyne benzannulation mediated by electrophilic reagents.

1.2.1.1 Iodonium salt or iodine monochloride mediated alkyne benzannulation

Activation of alkynes using electrophilic reagents is a powerful tool to deliver access to a broad range of nanographenes with varying functionalities and complexities. Electrophilic iodine reagents were primarily used for this transformation where the iodine source was used either in the form of iodonium salt or iodine monochloride.[22] This approach offers an added value by creating a functional handle within the product,

allowing for post functional modifications. Barluenga and co-workers first developed this methodology using $I(py)_2BF_4$ as electrophilic reagent along with TfOH to undergo iodine substituted cyclohexene ring formation from corresponding alkyne bearing precursor (**Scheme 2a**).[23] Later, Swager group used the same conditions on terphenyl systems bearing internal alkynes to obtain completely fused halogenated analogues.[20] During the investigation, they observed that TfOH itself catalyzes the reaction quantitatively, which led to the invention of milder and more efficient conditions (**Scheme 2b**).

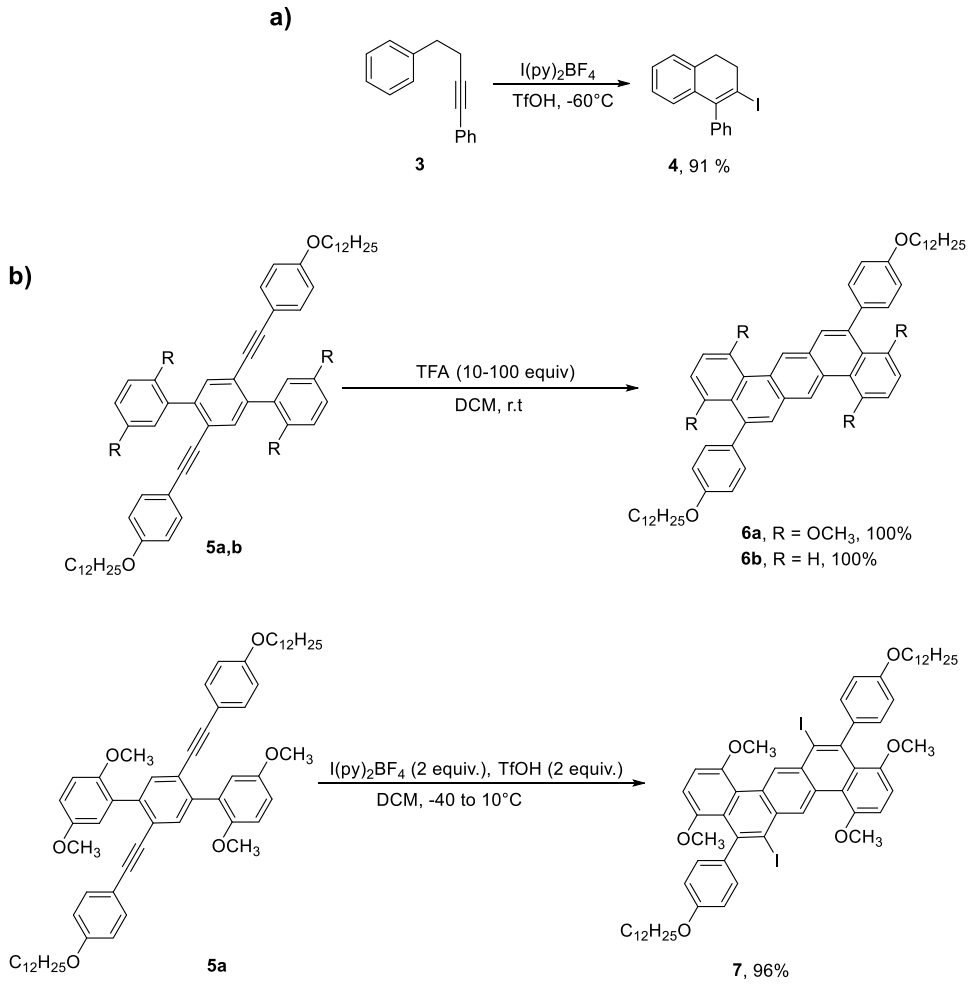

Scheme 2. a) Electrophilic benzannulation using iodonium salt in presence of TfOH. b) Electrophilic benzannulation using either TFA or iodonium salt.

A facile synthesis of differentially substituted dibenzo[*g,p*]chrysenes was reported by Liu group using ICl-induced alkyne benzannulation as the first step to synthesize 9-iodophenanthrene intermediate **9**.[24],[25] They took advantage of the iodine functionality to perform further Pd-catalyzed intramolecular direct arylation to form the

final product (**Scheme 3a**). Interestingly, in the case of substrates with *p*-methoxy group, the reaction exclusively underwent 5-*endo-dig* cyclisation to obtain corresponding spirocyclic product. This unique behavior of the substrate **11** to induce *ipso*-cyclisation is ascribed to the directing effect of *p*-methoxy group (**Scheme 3b**). They have also demonstrated the tunability of photophysical and electronic properties of dibenzo[*g,p*]chrysenes by varying the substituents to electron-rich and -deficient. While electron-withdrawing groups did not change the HOMO-LUMO energy gap from that of parent system, electron-rich substituents lowered the energy gap. Compounds with methoxy substituents also showed larger fluorescence quantum yields.[25]

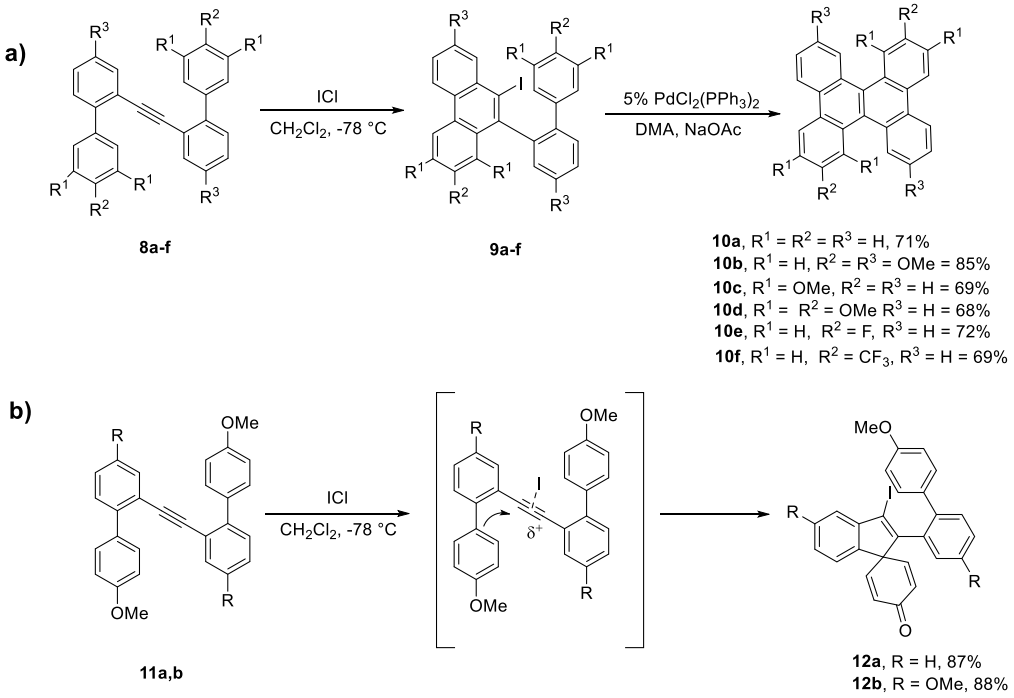

Scheme 3. a) Synthetic route toward dibenzo[*g,p*]chrysenes from bis(biaryl)acetylenes. **b)** ICl induced *ipso*-cyclisation of bis(biaryl)acetylenes with *p*-methoxy substituents.

Müllen and co-workers reported a novel synthetic route towards D_{2h} symmetric zigzag shaped nanographenes involving ICl catalyzed annulation as one among the key steps.[26] They showcased the cross-coupling versatility of the compound **13** by synthesizing intermediates **14,** which was then followed by Suzuki coupling and Scholl reaction leading to the final fused polycyclic system. This synthetic protocol allowed the strategical modification of symmetry and substitution pattern around aromatic core,

facilitating the control over molecular packing. Such alterations in packing arrangements for a system are anticipated to have distinct electronic device performance.

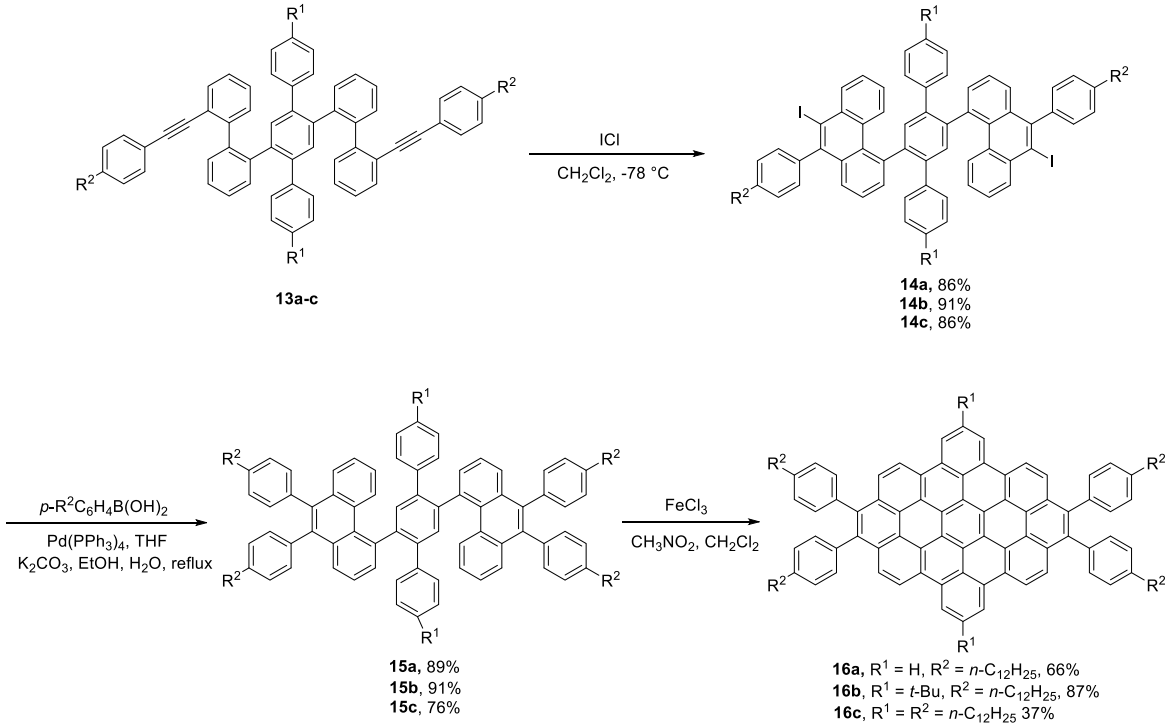

Scheme 4. Synthetic pathway towards zigzag nanographene.

Incorporation of curvature into aromatic compounds act as a novel design factor in regulating their packing arrangements in 3D crystal lattice.[27] As already mentioned before, by employing a non-planar core, aromatic systems can display unconventional behaviors that are not typical for planar molecules. Therefore, it is crucial to understand the impact of subtle modifications made on the molecular structure, on the photophysical and electrochemical properties of the bulk material. Alabugin group investigated the packing behavior of non-planar fused [5]helicenes obtained by a two-step synthetic route (**Scheme 5**).[28] The ICl catalyzed benzannulation reaction followed by photocatalyzed cyclisation and dehydroiodination. The X-ray crystallographic result showed that the crystal packing altered significantly based on the placement of functional group in [5]helicenes scaffold, while their HOMO/LUMO energy gap remained consistent.

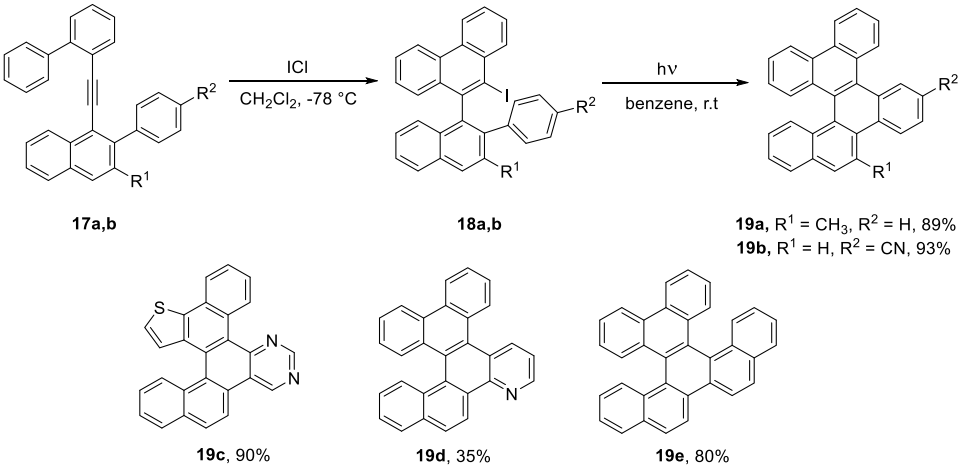

Scheme 5. Synthetic route towards fused [5]helicenes.

Larock and co-workers demonstrated the utility of this annulation reaction in heteroaromatic systems bearing oxygen or sulphur atoms (**Scheme 6**).[29] Although, the final products were obtained in high yields in most cases, the positioning of alkynyl moiety on heteroaromatic skeleton showed a marked effect on its reactivity. While 3-(2-(phenylethynyl)phenyl)benzofuran underwent the reaction smoothly, the regio-isomer with alkyne moiety substituted in furan ring gave only electrophile addition product. Evidently, the electron-withdrawing effect of adjacent oxygen atom inhibits the coordination of electrophile to the triple bond, thus preventing the cyclization.

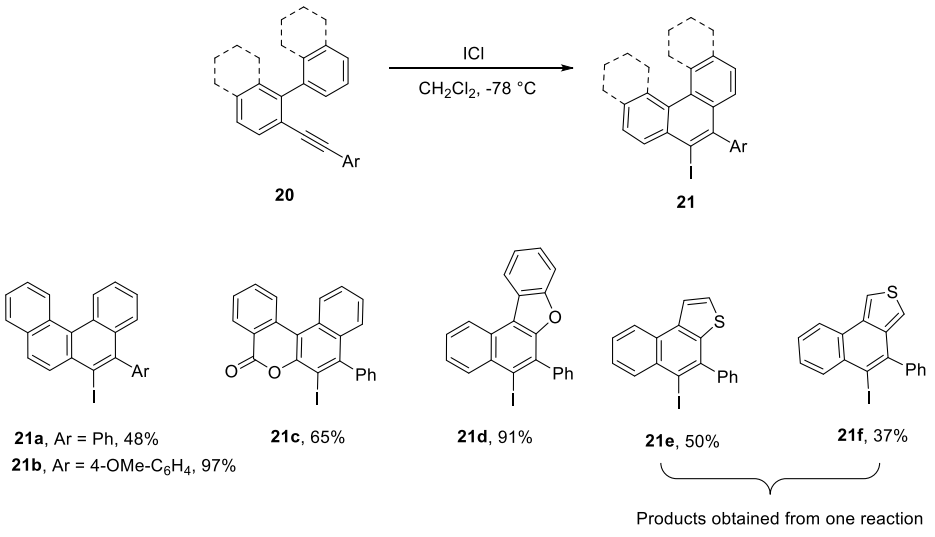

Scheme 6. Synthetic route towards polycyclic aromatics and hetero-analogues

Electrophilic iodine mediated benzannulation of alkynes have been demonstrated as a powerful method for the synthesis of planar or non-planar

nanographenes with various functionalities.[30],[31],[32] This methodology is typically high yielding and offers a convenient handle for further chemical modifications.

1.2.2 Alkyne benzannulation mediated by acids.

The ability of electrophilic reagents to induce *6-endo-dig* cyclization is highly valued in synthesizing nanographenes with heretofore unknown geometries. Acids are one among the commonly used reagents for alkyne activation reactions over the last three decades.

1.2.2.1 Brønsted acid catalyzed alkyne benzannulation.

Considering the previously mentioned benzannulations, iodine as electrophile always gets incorporated with the final cyclized product, where it requires multiple steps to obtain the protonated analogue. The simplest way to afford the protonated final product would be to use a proton source itself as the electrophilic reagent. The earliest work on benzannulation began with the discovery of Swager group in 1994. They noted the ability of TfOH or TFA to catalyze the annulation, while performing the iodonium-salt based cyclization reactions (**Scheme 2b**).[20] The hypothesized reaction mechanism involves the formation of carbocation as a result of the electrophilic attack of proton, which is resonance stabilized by the electron rich aryl ring attached to the alkyne moiety. Presence of electron rich arene ring was proven to be essential for this *6-endo-dig* pathway to occur.[21]

In 1997, the same group investigated the efficiency of two-fold alkyne benzannulation reactions by changing the substitution patterns of bis-ethynyl aryl moieties on terphenyl rings. The benzene rings involved in the annulation were placed *para, meta* and *ortho* to each other to obtain nanographenes **23**, **25** and **27** with varying architectures (**Scheme 7**).[21] While performing the reaction on more sterically demanding *ortho*-fused benzene rings, the general procedure led to only traces of final products. The authors had to rely on a more reactive form of I^+ source using iodine with silver triflate to obtain the desired product. Intriguingly, they did not observe iodine incorporation in the final cyclized system.

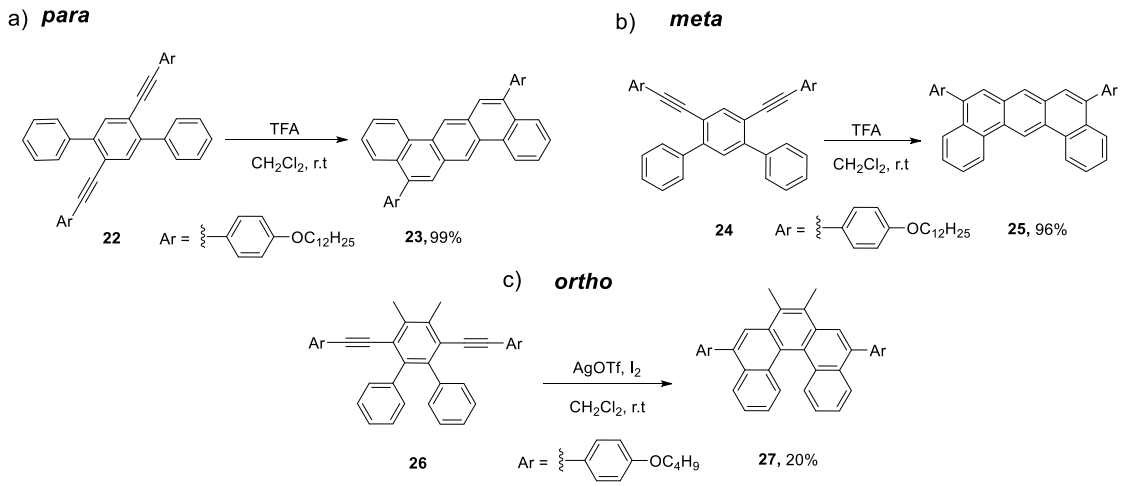

Scheme 7. TFA catalyzed two-fold alkyne benzannulation of a) *para* (**22**) b) *meta* (**24**) and iodonium induced annulation of c) *ortho* (**26**) substituted tri-phenyl systems.

Chalifoux and co-workers furthermore broadened the scope of this elegant method to synthesize pyrene and their π-extended trimeric and tetrameric analogues via a double or quadruple type alkyne benzannulation[33] Inspired by Swager's method, the key idea was to employ two-fold annulation of alkynyl moieties on the *ortho* positions of the same aryl ring to afford nanographene with extended lateral conjugation. Nonetheless, the standard conditions using TFA led to mono-annulation product **29** albeit quantitatively, with the triple bond intact (**Scheme 8**). Authors anticipated that the planarization caused by the first annulation to form the molecule **29** affects the efficacy of orbital overlapping between the alkyne and free *ortho* position of arene leading to higher activation energy. To overcome this, a stronger acid TfOH was used to afford pyrene derivative **30**. This method was then successfully employed on more elaborated derivatives to obtain peropyrenes and teropyrenes. As mentioned previously, electron-rich character of arene offered by alkoxy substituent is essential for the reaction to occur. In addition, thiophene rings are also tolerated.[34] All synthesized pyrene analogues displayed good solubility which made it possible to measure their photophysical properties. The UV/Vis absorption and emission spectra showed a gradual bathochromic shift owing to the π-extension. X-ray structure of both peropyrene and teropyrene showed slight twist from the molecular plane owing to the steric repulsion of hydrogens at the bay regions, which is thought to be the reason for their solubility. This twist made the peropyrene to exhibit axial chirality in solid-state, while teropyrene possesses a pseudo plane of symmetry. This method realized the synthesis of first ever soluble as well as functionalized pyreneacenes.

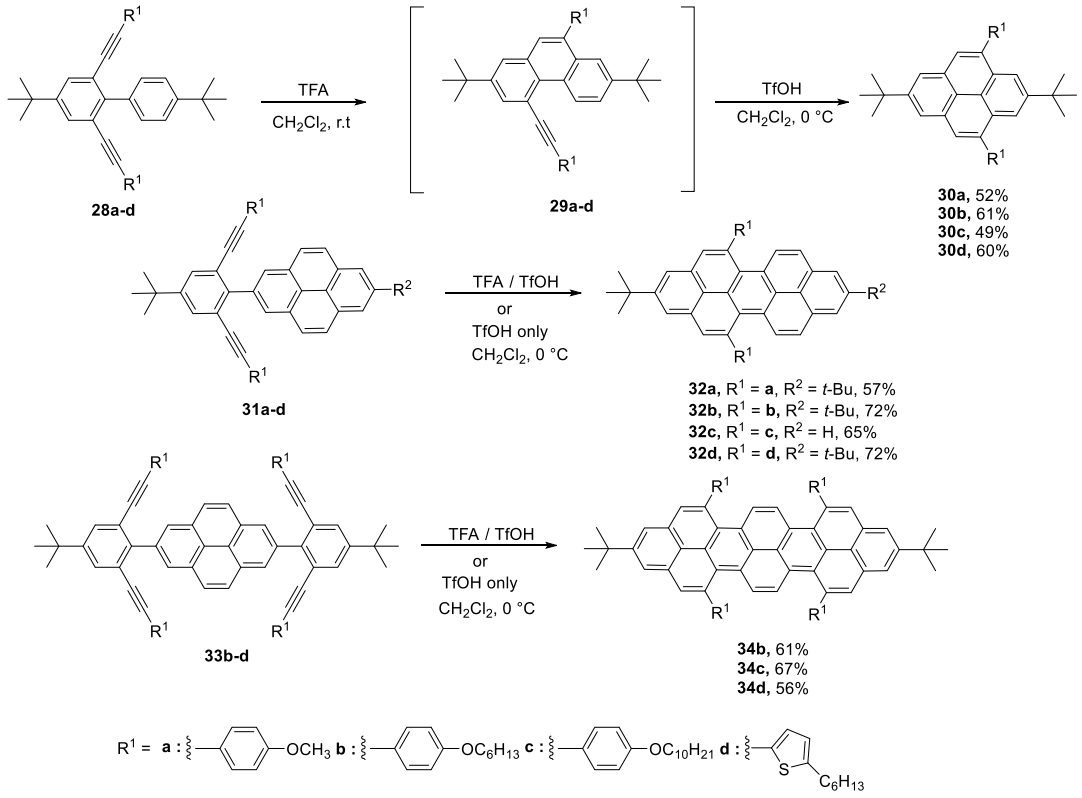

Scheme 8. TFA or TfOH catalysed two-fold and four-fold benzannulation for the rapid access to pyreneacenes.

The same group later took advantage of the twisting of peropyrene due to the steric repulsion at the bay region, via substitution to increase the barrier of inversion.[35] To explore the possibility of creating consistently chiral peropyrenes with larger inversion energies, they used tetrayne **35** as the precursor (**Scheme 9**). The subsequent TFA catalyzed two-fold alkyne annulation interestingly led to the formation of chiral picene intermediate **36**, via cyclization occurring on the same side. According to the calculations, authors report that this mode of cyclization is favored by a lower energy barrier 2 kcal/mol. Final step by treating the intermediate with TfOH led to the completely cyclized chiral peropyrene product **37**. The molecule possesses an end-to-end twist with an angle of 28° making it enantiomerically separable by chiral HPLC. The final peropyrene emits green light and display circularly polarized luminescent properties, similar to other chiral helical type nanographenes.[36]

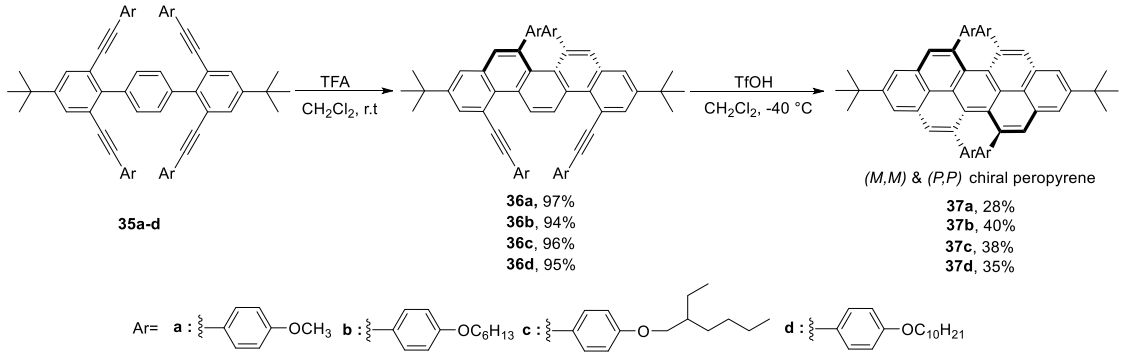

Scheme 9. Synthetic route towards chiral peropyrene **37.**

Graphene nanoribbons (GNRs) are fascinating category of quasi one-dimensional materials derived from definite termination of a graphene sheet possessing smooth edges.[37] Their intrinsic magnetic, electronic and conduction properties allow them for various device applicability via doping or functional modifications. Although, the first bottom-up synthesis towards GNRs are reported by Stille and co-workers early in 1970, the obtained ladder type polymeric structures exhibited significant solubility issues.[38] Further studies on these architectures were dormant until 1994 when Swager group made use of the Brønsted-acid based annulation to synthesize soluble and functionalized GNRs. The authors used strategically designed monomers by incorporating them with electron donating groups to allow efficient cyclization and placing alkyl groups on the scaffold for controlling the regioselectivity (**Scheme 10**).[20] The synthesized GNRs showed absorption band edge at 468 nm with maxima at 340 nm and large molecular weights ranging from Mn = 45000 – 55000 g/mol.

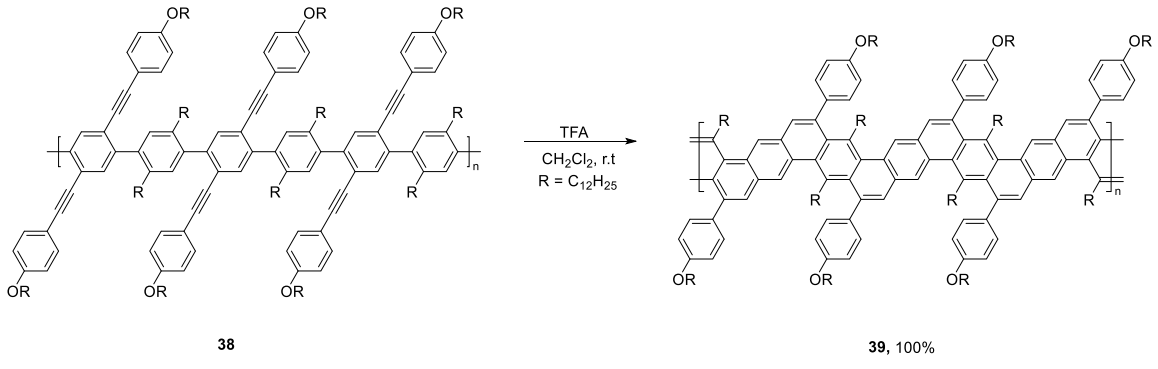

Scheme 10. Synthetic route towards GNRs via alkyne benzannulation**.**

Later in 2015, Wu, Zhao and colleagues reported the Brønsted-acid catalyzed synthesis of GNRs based on π-extended and rigid pyrene subunits (**Scheme**

11).[39] They exhibited the general features of the ladder type polymers, including the broad absorption band blue-green emission in solution state.

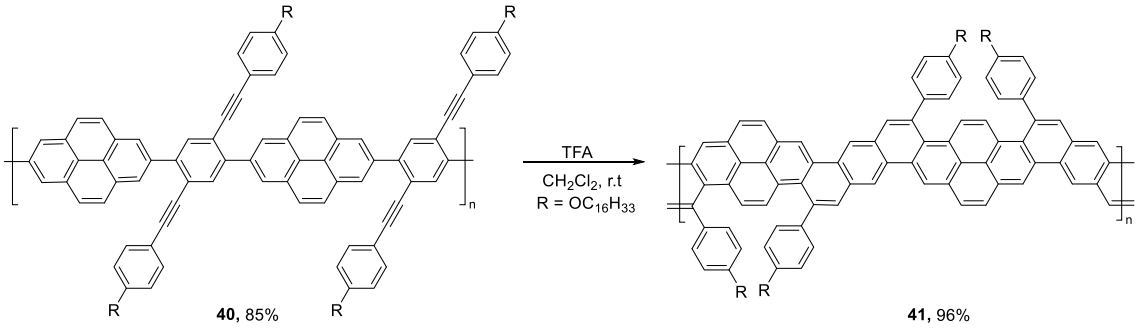

Scheme 11. Synthetic route towards GNRs possessing pyrene subunits via alkyne benzannulation

Chalifoux and co-workers expanded the potential of this reaction by designing the bottom-up approach towards very narrow (ca. 0.5 nm) and soluble GNRs via TFA / TfOH promoted benzannulation.[40] Authors used Suzuki reaction to obtain the poly(2,6-dialkynyl-*p*-phenylene) precursor followed by acid catalyzed cyclization which occurred efficiently on the side ethynylaryl chains (**Scheme 12**). The synthesized GNRs exhibited excellent solubility in common organic solvents, facilitating their characterization by IR, Raman, and UV/Vis/NIR spectroscopy. They displayed significant red shift in absorption compared to previously synthesized GNRs **39** and **40** and showed significant flexibility as proved by STM and TEM analysis.

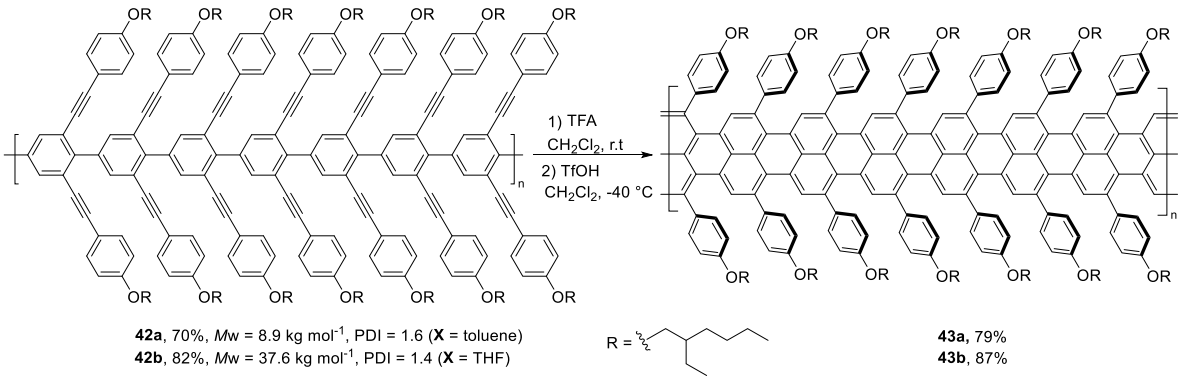

Scheme 12. Synthesis of soluble NGs by Chalifoux *et.al.*

The alkyne activation catalyzed by Brønsted acids has emerged as a convenient method to synthesize NGs and GNRs. However, in this case, the presence of electron-donating groups on the aryl ring connected to the triple bond is crucial for the *6-endo-dig* cyclization to occur. This factor narrows the scope of reactions catalyzed by

Brønsted-acids, thereby limiting the synthesis of polycyclic systems with diverse functional groups, which are important for tuning optical and electronic properties.

1.2.2.2 π-Lewis acid catalyzed alkyne benzannulation.

Over the years, the area of alkyne benzannulation reactions has evolved substantially fueled by thorough optimization trials leading to the invention of new reagents that are viable for obtaining cyclized product with high yields and complexity. As a result, several π-Lewis acids have been emerged as the potential candidates for such transformations.[41–45] Here, the *6-endo-dig* cyclization is reported to be initiated via the complexation of alkyne with the metal center to form η^2 -metal species followed by the nucleophilic attack of the adjacent arene ring.[44] In most instances, the electron-withdrawing groups directly attached to the alkyne unit favor *5-exo-dig* pathway while electron donating groups solely promote *6-endo-dig* type annulation.

1.2.2.2.1 Transition metal catalyzed alkyne benzannulation.

Ru-catalyst was the first metal-based catalyst reported in literature for alkyne annulation reaction. Merlic *et al*. discovered this method where the triple bond is initially activated through the formation of a vinylidene intermediate, followed by 6π-electrocyclization to afford the cyclized product (**Scheme 13**).[46] Consequently, this limits the scope of the reaction only to terminal alkynes. The efficiency of this transformation was found to be higher for substrates bearing external alkene as a part of heterocyclic ring to form polycyclic heteroaromatic system. Same catalytic conditions have been used to obtain nanographenes containing silicon and boron atoms.[47]

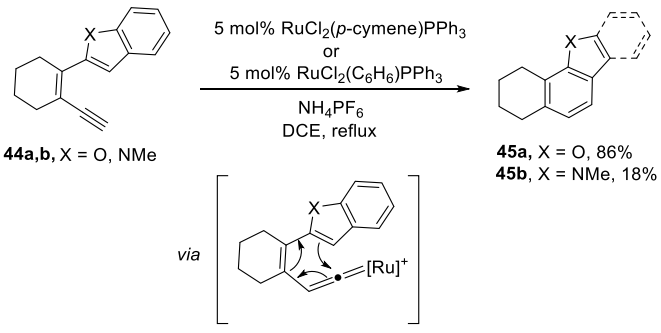

Scheme 13. Ru metal catalyzed alkyne annulation via vinylidene intermediates.

Scott and co-workers extended the utility of the Ru(II) catalytic system by performing two and four-fold cyclization reaction.[48] The reaction was performed on precursor **46** which was readily synthesized from anthraquinone via Corey-Fuchs

reaction followed by Sonogashira coupling and desilylation. This methodology provides an alternative synthetic pathway towards coronene (**Scheme 14**). Liu group later improved the reaction efficiency by using more active Ru(II) based catalyst.[49]

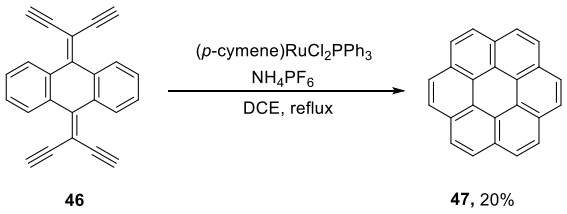

Scheme 14. Four-fold benzannulation reaction towards coronene.

Liu and co-workers made use of this approach to synthesize an array of GNRs with varying lengths.[50] Subsequently they demonstrated the compatibility of substrates possessing Ph_2N groups in this transformation to access second-generation ribbons possessing the fluorescence quantum yields as high as 96% (**Scheme 15**).[51] The trends observed in their optical properties including absorption values, photoluminescence and HOMO/LUMO gap were in accordance with extended π-conjugation.

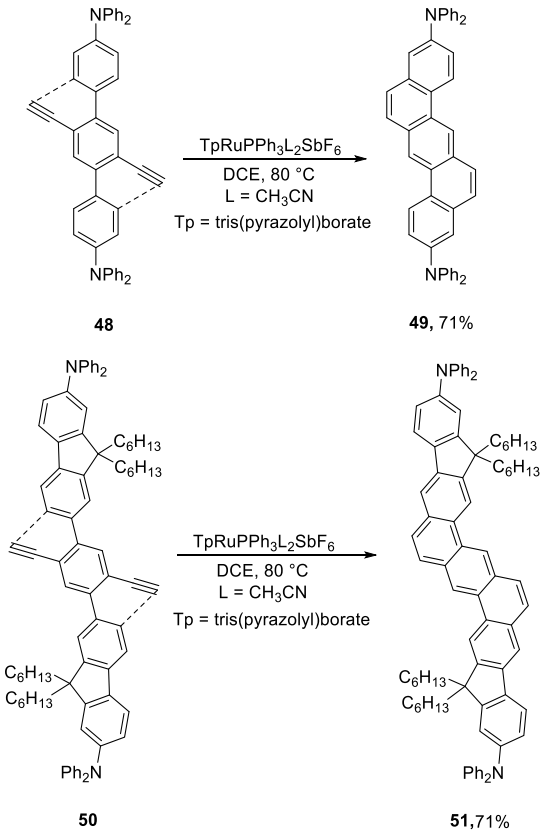

Scheme 15. Two-fold alkyne benzannulation towards GNRs bearing NPh_2 substituents.

Although Ru catalysis has contributed to the synthesis of NGs and their extended derivatives, the transformation is limited to only precursors possessing terminal alkynes. In broadening the scope and utility of polycyclic systems, it is essential to functionalize them to fine-tune their electronic properties and to incorporate groups which enhance solubility. The inability to attach any functional group or arenes to the alkyne moiety remains as the disadvantage of this reaction.

Pt(II)-catalysis has emerged as an efficient methodology to promote benzannulation of precursors bearing both terminal and internal alkynes. Fürstner and co-workers performed an extensive optimization study of the annulation process of *ortho*-ethynyl substituted biphenyl derivatives using variety of soft Lewis acids, in which $PtCl_2$ was found to be the most effective one (**Scheme 16**).[44] They expanded the scope to the heterocyclic systems including π-expanded indoles, carbazoles, thiophenes and bridgehead nitrogen heterocycles.

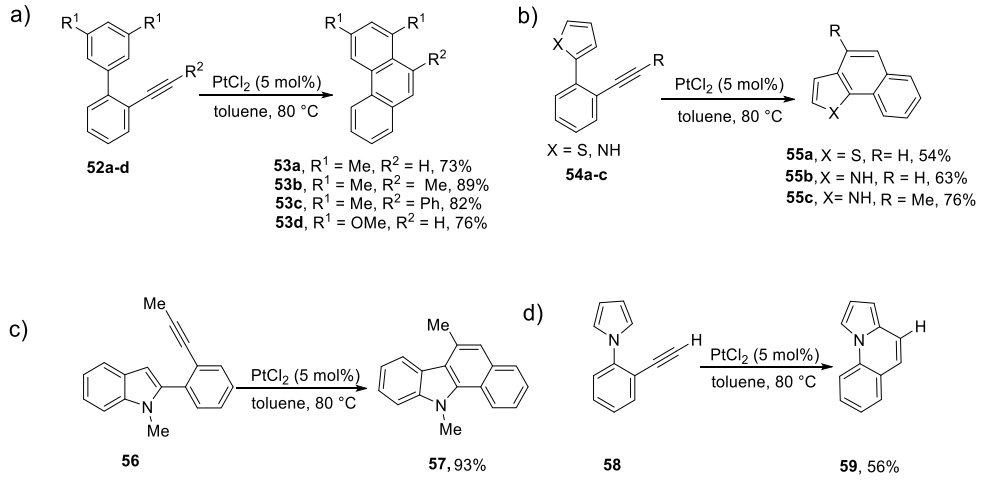

Scheme 16. Pt(II) catalyzed synthesis of a) phenanthrenes, b) and c) polycyclic heteroaromatics, d) bridge head aza-doped heterocycle.

Liu and co-workers later proved that the efficiency of this approach is comparable to that of Ru(II) catalyst, for the synthesis of GNRs possessing diverse lengths.[50][51] The same group exploited this method to develop an easier pathway towards unsubstituted chrysene from readily accessible starting materials.[52] The molecule was further functionalized via bromination followed by Suzuki, Buchwald-Hartwig or Sonogashira coupling to obtain the tetrasubstituted derivatives bearing aryl, amine or alkynyl groups (**Scheme 17**). The substitution gives rise to an increase in the fluorescence quantum yields along with bathochromic shift in both UV/Vis absorption and photoluminescence

spectra. The performance of diarylamino-substituted chrysene **62** was tested as a blue emitter in OLED, showing a remarkable external quantum efficiency accompanied by blue emission.

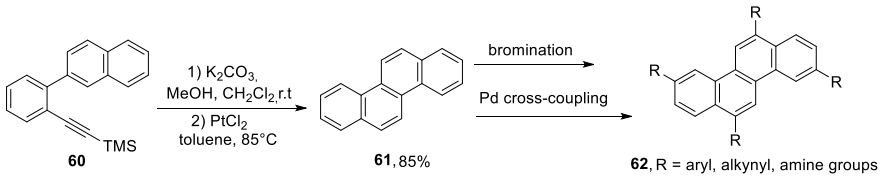

Scheme 17. Synthetic route towards tetrasubstituted chrysene.

A novel cove-edged type graphene nanoribbons were reported by Müllen and co-workers using 11,11′-dibromo-5,5′-bischrysene **64** as the key precursor which was synthesized via two-fold Pt(II)-catalyzed benzannulation (**Scheme 18**).[53] Subsequent Ullmann coupling followed by intramolecular oxidative cyclodehydrogenation led to the formation of GNRs which was predicted to have a low band gap value (Eg = 1.70 eV) and high charge carrier mobility of electrons and protons. However, in the case of hexamers and octamers, authors obtained only partially fused products after cyclodehydrogenation, which made it difficult for further purification. Such cove-type peripheral feature opens the possibility of further tuning by controlling their width through bottom-up synthesis.

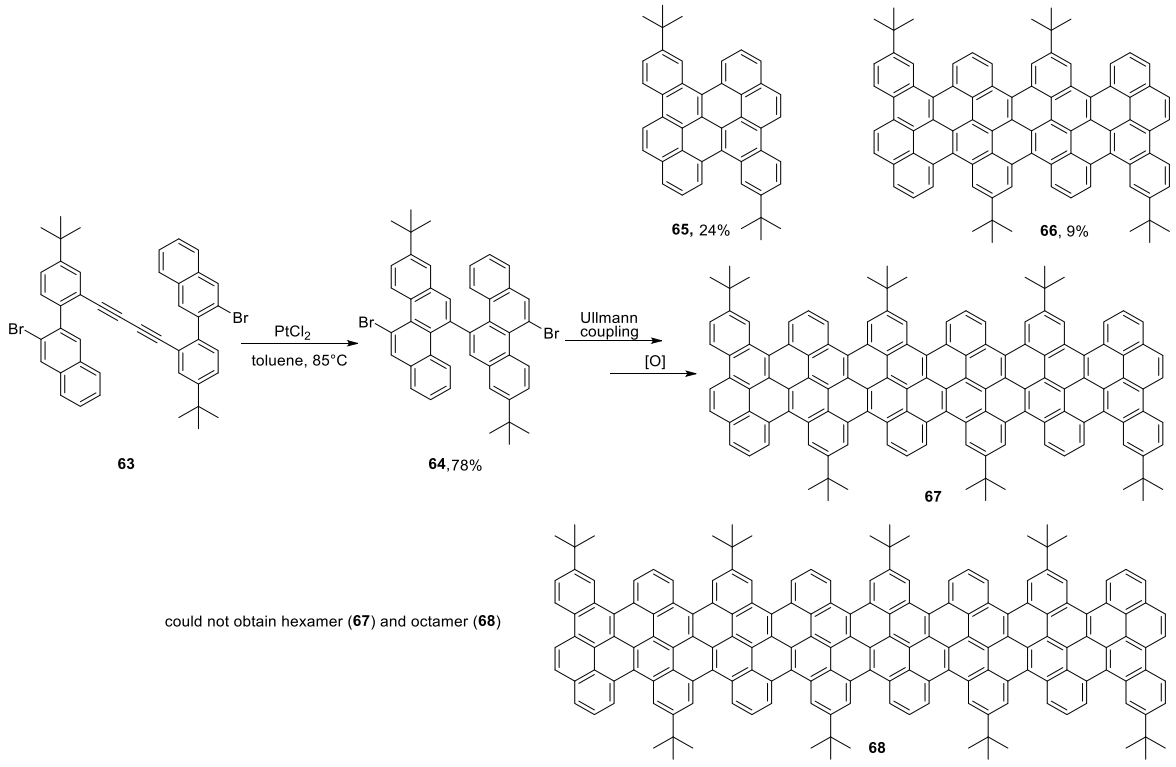

Scheme 18. Synthetic route towards cove-edged GNRs.

The applicability of platinum catalyzed benzannulation was explored in helicene synthesis by Storch *et al.* to afford [6]helicene from biphenyl-naphthalene derivatives (**Scheme 19a**).[54] In the case of aza-helicenes, the reaction required a combination of catalysts $InCl_3$ and $PtCl_4$ to facilitate the two-fold benzannulation.[55] While investigating the scope of this reaction, Fuchter and co-workers found these conditions to be inefficient to obtain the substituted aza[6]helicenes. Through systematic optimization by varying solvents and reaction temperature, the authors came up with much improved conditions without $InCl_3$ and lower catalyst loading. This condition realized the synthesis of an array of substituted [6]helicenes (**Scheme 19b**).[56] In addition, they could obtain enantiomerically pure non-cyclized precursor **71a** (R^1= R^2 = H) via semipreparative chiral HPLC, which underwent annulation to give **72a** with the same enantiomeric purity.

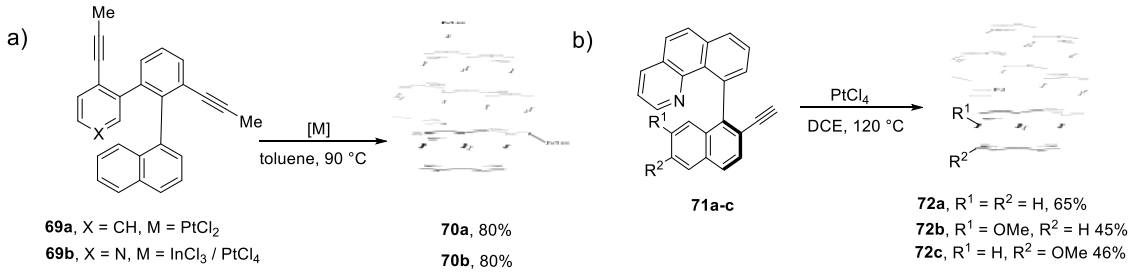

Scheme 19. a) Synthetic pathway towards [6]helicene and aza[6]helicene by Storch *et al*. b) aza[6]helicenes by Futcher and co-workers.

In contrast to Pt(II)-catalysts, Au-catalysis is less explored in synthesis of elaborated polycyclic aromatic systems via alkyne benzannulation. Although, its utility has been verified for nanographenes of relatively modest size. During the investigation of Fürstner group on the synthesis of phenanthrene derivatives using various π-Lewis acids, $AuCl_3$ and AuCl were found to be efficient alongside with $PtCl_2$.[57] While performing the annulation of biaryls bearing haloalkyne moiety, authors noted an intriguing behavior of gold catalyst to induce halide1,2 shift whereas $InCl_3$ led to halide retention (**Scheme 20**).[44] The generation of a metal vinylidene complex as the reactive intermediate was considered as the plausible explanation for this result.

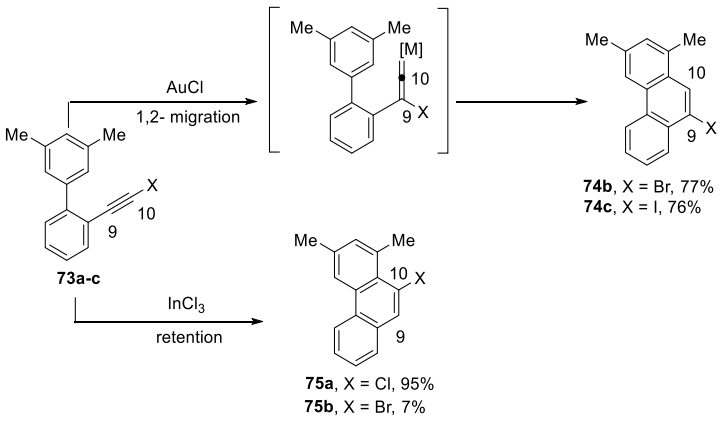

Scheme 20. Metal-catalyzed alkyne benzannulation of haloalkyne **73**.

Later, Müllen and co-workers utilized this methodology to synthesize di-iodo substituted pyrene which served as the key precursor for the synthesis of graphenic cutouts.[58] The crucial step during the cyclization involved the endo selective 6π-electrocyclization of metal vinylidene intermediate resulting in halogen 1,2 migration to 5,9 positions (**Scheme 21**). This halogen handle was further used to couple with two pyrenes to form terpyrenyl system which was then smoothly underwent oxidative cyclodehydrogenation catalyzed by $FeCl_3$.

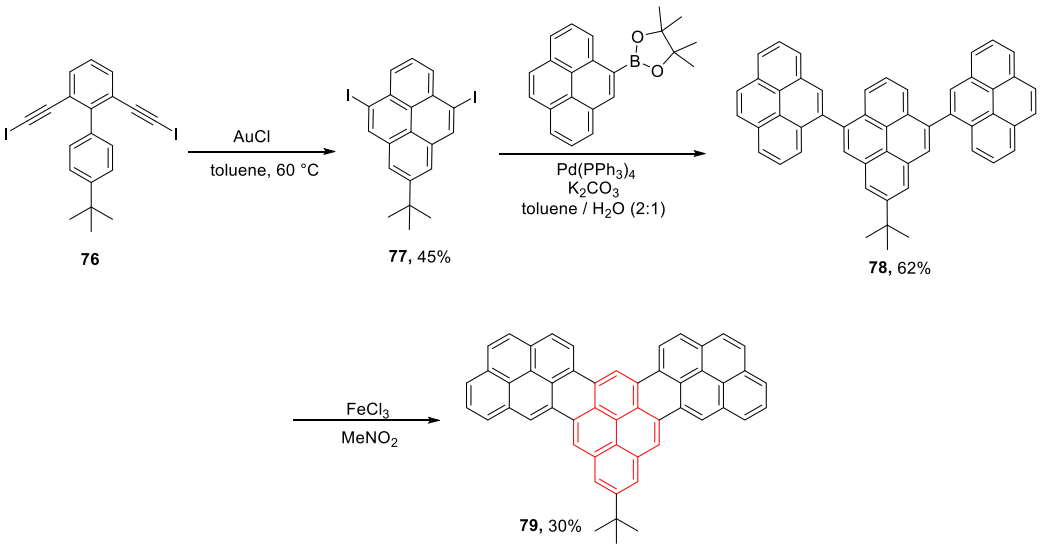

Scheme 21. Synthetic route towards graphenic cutouts.

Direct and selective substitution at 4,5,9 and 10 positions of pyrene is scarcely reported in literature. Murakami and co-workers used a slightly different approach towards 4,10-disubstituted pyrenes via cationic gold(I) catalyzed two-fold hydroarylation of 2,6-dialkynyl biphenyls (**Scheme 22**).[41] Authors reported that cationic gold catalysis is crucial for this reaction to occur as neutral chlorogold(I)

catalyst proved to be inefficient. They explored the impact of ligands by employing various Buchwald-type biaryl phosphine ligands, all of which exhibited equivalent efficacy. Significant electronic effects were also observed in this reaction where electron-rich aryl substituents gave higher reaction yields while electron deficient aryl rings and terminal alkynes lowered the yield.

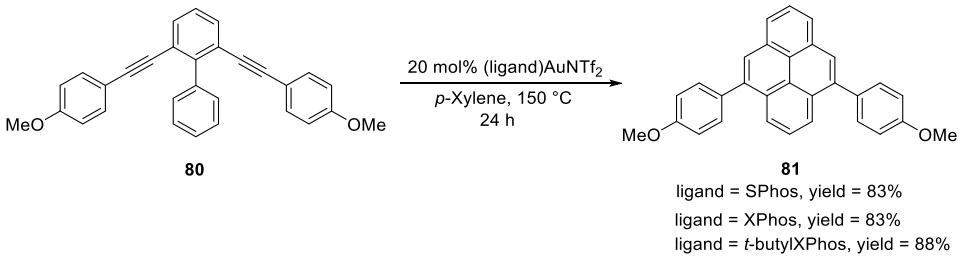

Scheme 22. Synthetic route towards 4,10-disubstituted pyrenes

The greater efficiency of cationic Au species in facilitating annulation processes can be attributed to their low-lying LUMO and limited back-donation capacity. Alcarazo and co-workers hypothesized that the inherent π-acidity of Au-catalysts can be substantially increased by incorporating dicationic phosphine ligands as strong π-acceptor ancillary ligands.[43] Bis(diisopropylaminocyclopropenium)-substituted phosphine was chosen as ligand which was prepared in two steps. The catalyst was used along with silver salts to substitute the chloride moiety in the gold complex. The authors demonstrated the efficacy of this catalytic system by performing alkyne benzannulation on an array of 2-ethynylbiphenyls with multiple substituents (**Scheme 23**).

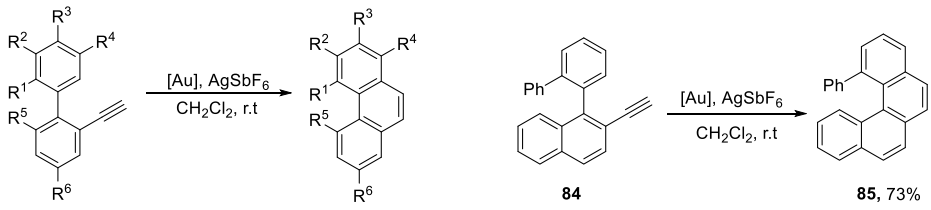

Scheme 23. Alkyne benzannulation reaction using gold catalyst with polycationic ligand.

Gold catalysis have also been applied in enantioselective synthesis of S-shaped double azahelicene.[59] The precursor molecule **86** was designed in such a way that the

first two-fold intramolecular hydroarylation of triple bonds occurs to form axially chiral intermediate bearing pyridone rings followed by second enantioselective annulation leading to helically chiral azahelicene **87** in one step using the same chiral gold catalyst (**Scheme 24**). Employing an excess of AgOTf with the Au complex was found to be crucial for the intended sequential hydroarylation. Remarkably, the circularly polarized luminescence (CPL) activity exhibited by the S-shaped double azahelicenes surpassed that of the regular azahelicenes.

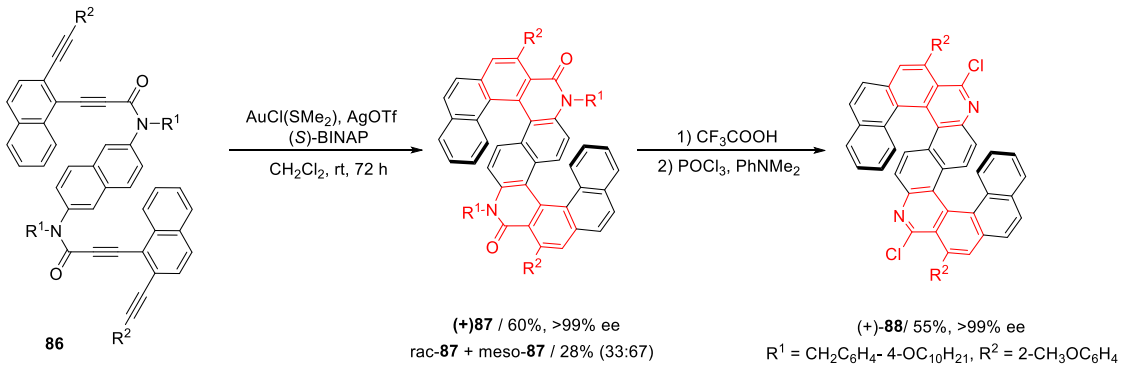

Scheme 24. Enantioselective sequential hydroarylation of alkynes towards double azahelicene.

1.2.2.2.2 Main group π-Lewis acid catalyzed alkyne benzannulation

The ability of main group element based π-Lewis acids to catalyze alkyne benzannulation have also been explored, especially after the extensive study by Fürstner *et al.*[57],[44] $InCl_3$, $GaCl_3$ and $SbCl_5$[60] are such examples out of which $InCl_3$ has been identified to be the best candidate to induce *6-endo-dig* cyclization for biphenyls bearing haloalkynes[44] and heteroaromatic substrates. Gryko and co-workers exploited this method to transform tetraarylpyrrolo[3,2-*b*]pyrroles to their π-expanded analogues indolo[3,2-*b*]indoles (**Scheme 25**).[45] This two-fold annulation reaction demonstrates high selectivity towards *6-endo* products and broad functional group tolerance including electron deficient ethynyl aryl group incorporated to pyrrolo[3,2-*b*]pyrrole core. The obtained chromophores showed notable enhancement in their two-photon absorption efficiency with increasing electron-withdrawing strength of peripheral substituents.

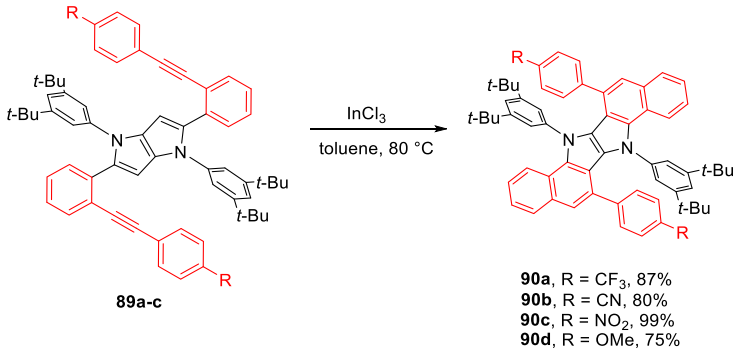

Scheme 25. $InCl_3$-catalyzed two-fold alkyne annulation towards π-expanded indolo[3,2-*b*]indoles

Inspired from the above mentioned work and Fürstner's study,[57],[44] Chalifoux and co-workers explored the possibility of using $InCl_3$ catalysis to broaden the scope of their previous work on the synthesis of peropyrenes and teropyrenes.[19] Interestingly, this method surpassed the limitations of Brønsted acid catalysis by realizing two-fold and four-fold cyclization of electron-rich, electron-poor and alkyl substituted alkynes to afford bay-region functionalized products (**Scheme 26**). This type of substitution at the bay region significantly influence both the chirality and crystal packing in the solid-state. The latter negligibly affects the absorption in the solid-state causing minor red shifts compared with planar analogues. The four-fold alkyne annulation was also demonstrated on differentially substituted substrate to obtain "push-pull" type system (**34h)**.

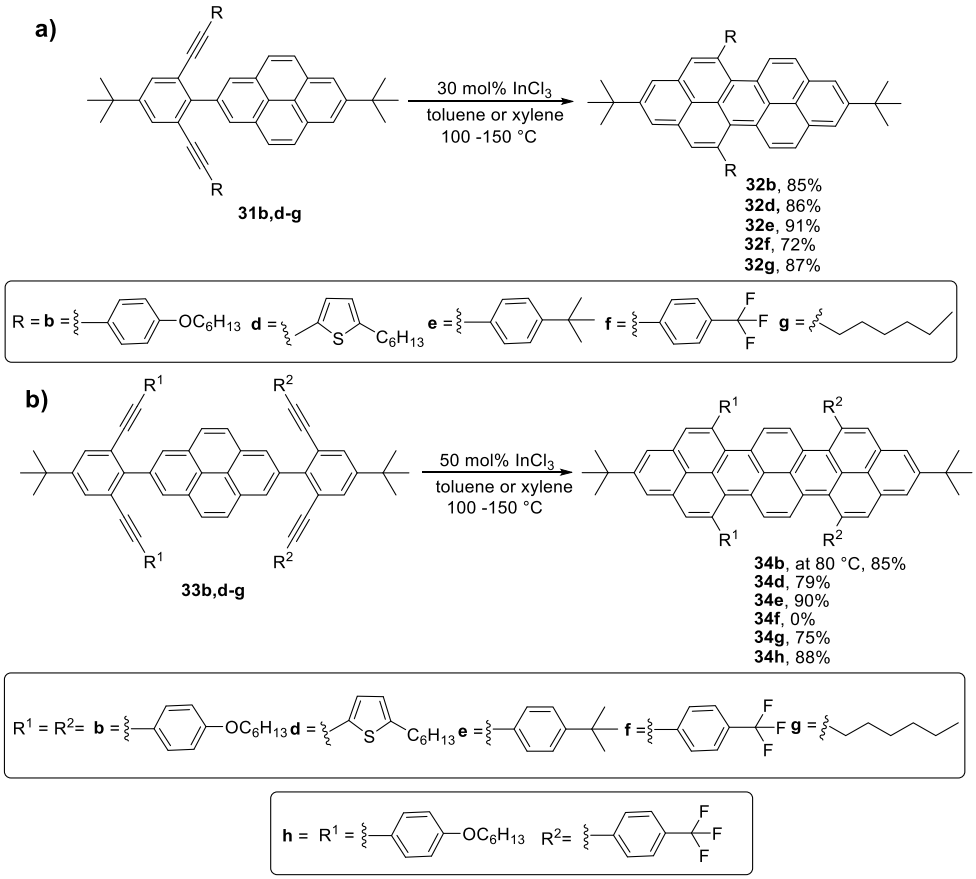

Scheme 26. $InCl_3$-catalyzed two-fold and four-fold alkyne annulation towards substituted a) peropyrenes and b) teropyrenes.

Later, the same group came up with the first case of domino benzannulation reaction of buta-1,3-diynes to synthesize irregular nanographenes (**Scheme 27a**).[61] $InCl_3$-$AgNTf_2$ catalytic system was found to be crucial for this reaction to occur as employing $InCl_3$ led to mono-annulation. The novel domino reaction demonstrates high regioselectivity towards carbon 1 over carbon 3 for first annulation, by allowing the formation of a new bay region in the intermediate. This serves as a site for the second annulation to form the final nanographenes in moderate to high yields. The substrate scope includes naphthalene, anthracene, and pyrene-based precursors to afford the corresponding irregular nanographenes. Authors expanded the utility of this reaction by performing four-fold alkyne annulation on dimethoxy substituted binaphthalene precursor to obtain chiral butterfly type cyclic system which can act as a chiral ligand in enantioselective synthesis (**Scheme 27b**). The same catalytic system was also used for the synthesis of benzodipyrenes via four-fold alkyne benzannulation reaction (**Scheme 27c**).[62] These π-extended analogues of pentacene showed blue-shifted absorption compared to pentacene even after the π-extension.

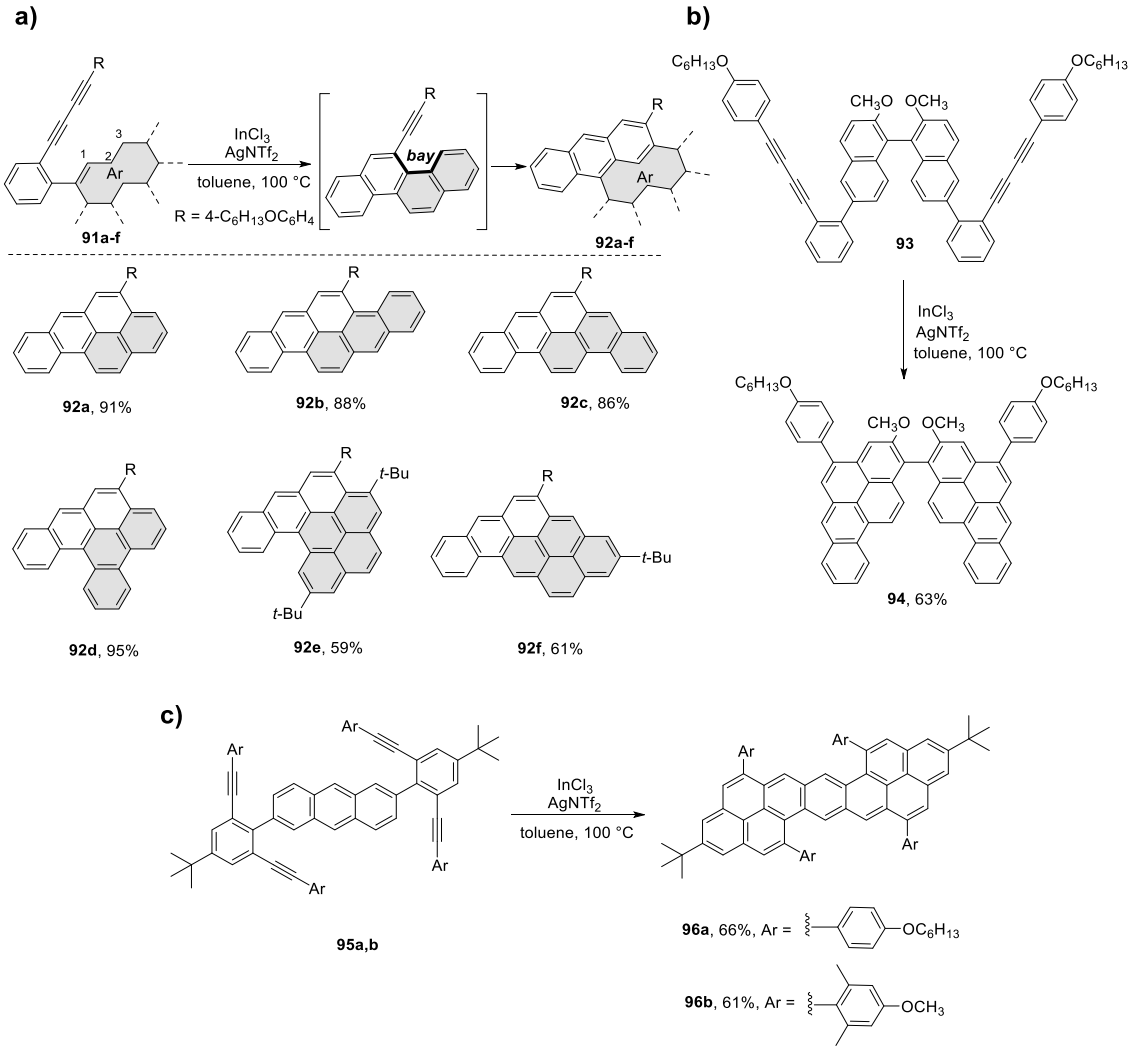

Scheme 27. $InCl_3$-$AgNTf_2$ catalyzed domino benzannulation towards a) irregular nanographenes b) butterfly type chiral nanographene and c) four-fold benzannulation towards benzodipyrenes.

As mentioned before, substituting bulkier aryl rings at the bay region of peropyrenes can create a barrier for racemization giving rise to chiral systems (section ***1.2.2.1***, **Scheme 9**).[35] Later, Chalifaux group reported laterally π-expanded [4]helicenes with substituents at the cove region via alkyne benzannulation. This modification serves to enhance the racemization barrier, facilitating the separation of enantiomers.[63],[64] They broadened this work by synthesizing fluorenone and dibenzoheterole centered nanographenes using $InCl_3$-$AgNTf_2$ catalyzed alkyne annulation (**Scheme 28**).[65] As the degree of steric congestion increases around the fjord region compared to bay region, chirality is induced which also twists the backbone. Authors noted a significant bathochromic shift for molecule **100** relative to **98** due to the reduction in the symmetry

thereby offering a novel approach to tune the optical and electronic characteristics of PAHs.

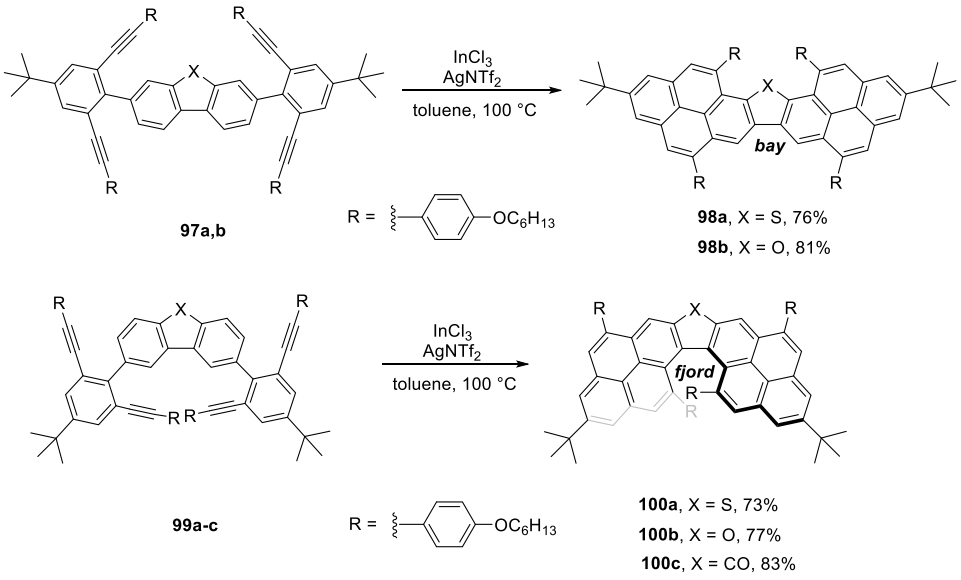

Scheme 28. In catalyzed four-fold benzannulation towards achiral and chiral dipyrenoheteroles.

1.2.3 Base-catalyzed alkyne benzannulation

Base-mediated alkyne annulations are majorly reported in the synthesis of coronene tetracarboxydiimides which can be seen as the π-extended version of perylene tetracarboxydiimides (PDI). Applications of PDIs and their analogues ranges from biological systems[66], supramolecular assemblies,[67] organo electronics etc.[68] Müllen and co-workers devised a synthetic route towards coronene tetracarboxydiimides by using alkyne benzannulation as a key step to expand the cyclic system around PDI core (**Scheme 29**).[69] They identified the requirement of base for the success of this reaction and non-nucleophilic base 1,8-diazabicyclo[5.4.0]undec-7-ene (DBU) was found to be the best one. This method was employed later on for other coronene tetracarboxydiimide derivatives.[70]

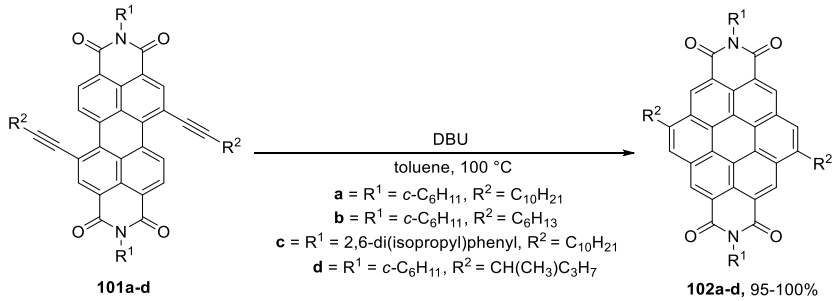

Scheme 29. DBU-mediated alkyne annulation towards coronene tetracarboxydiimides.

Later, DBU promoted cyclization reaction was successfully employed for π-expanded thienoacene synthesis (**Scheme 30**).[71] These acenes composed of alternating anthracene and thieno[3,2-*b*]thiophene units exhibited relatively low-lying HOMO-LUMO levels.

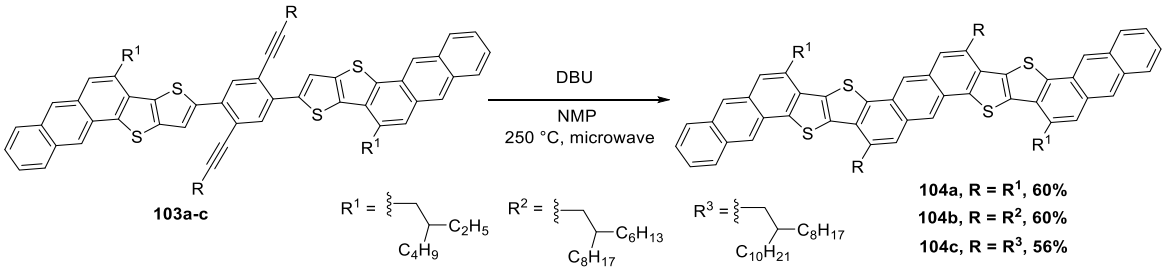

Scheme 30. DBU mediated alkyne benzannulation towards thienoacenes.

1.3 Aza-doped nanographenes (NGs)

A combined understanding of arenes and heteroarenes are crucial for gaining fundamental insights of aromatic compounds. Heteroatom-doped nanographene (NG) can be considered as a type of heteroarene that holds a prominent position in contemporary chemistry of aromatics and materials science.[72],[73] Introduction of a heteroatom into the sp^2-hybridized carbon framework is an elegant method to tune the electronic structure of NG, consequently resulting in optical and electrochemical properties that differ from those of undoped, all-carbon counterparts. However doping heteroatoms with higher precision and accuracy remains challenging.[74] Bottom-up organic synthesis has become a widely acknowledged method to overcome this challenge to have a precise control over the size and substituents of heteroatom-doped nanographene along with concentration and position of the dopant.[73] Nitrogen is considered as one among the primary element of choice as dopant, owing to the accessibility of synthetic methods and stability of the resulting nitrogen-containing polycyclic systems. Similar to their all-carbon analogues, nitrogen dopant enclosed by non-hexagonal rings acquires positive / concave or negative / saddle type geometries. Heterohelicenes are another type of non-planar aza-doped nanographenes with helical geometry arising from *ortho*-fused benzene rings.[75],[76] Although the non-planarity has a significant influence on the electronic and optical characteristics of the N-doped polycyclic system,[77],[74] the number of such examples are relatively scarce in literature (representative examples are shown in **Figure 2**).[59,76,78–82]

This can be attributed to the laborious and multi-step syntheses required for their preparation.

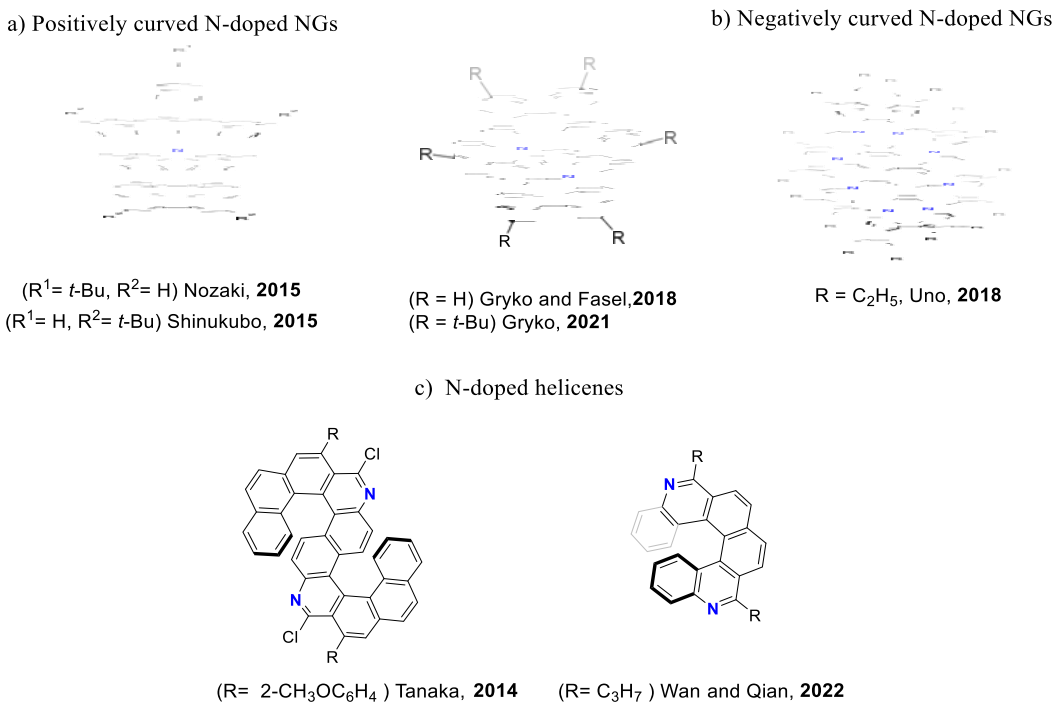

Figure 2. Representative examples for non-planar aza-doped nanographenes

1.3.1 Aza-doped nanographenes from tetraaryl pyrrolo[3,2-*b*]pyrrole precursor.

1,4-Dihydropyrrolo[3,2-*b*]pyrrole (DHPP) composed of two pyrrole rings fused in [3,2-*b*]-mode. Such type of fusion provides them exceptional characteristics such as high electron density, facile functionalization, and high symmetry. While synthetic approaches to DHPPs have been known since 1972, the real resurgence in this field began with the discovery of a one-pot multicomponent reaction that yields tetraaryl-1,4-dihydropyrrolo[3,2-*b*]pyrroles (TAPPs) (**Scheme 31**).[83] TAPPs exhibit remarkable optical properties including both strong absorption and intense emission tunable in a wide range. The discovery of this multicomponent synthesis made quite substantial contributions to the field of aza-doped nanographenes where TAPPs have been used as the potential precursors. In addition to their straightforward access, high functional compatibility, ability to obtain synthetic handles for post-functional modifications and presence of highly electron-dense 3 and 6 positions liable to electrophilic substitutions are the added values which makes them a perfect building block for nitrogen embedded

NGs. An extensive overview of their synthesis, reactivity, π-expansion and photophysical properties will be discussed in a separate chapter.

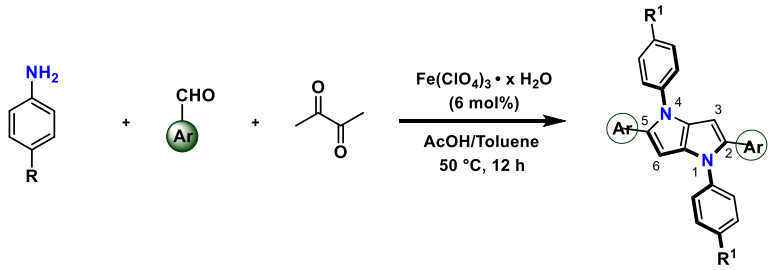

Scheme 31. Generic representation of the synthetic scheme towards TAPPs.

2. Aims and Objectives

The curiosity to explore new architectural patterns and topologies in polycyclic aromatic compounds is fueled by the potential of uncovering unique properties valuable for both material science and innovation. Particularly, precise design and bottom-up synthesis of non-planar architecture have gained growing attention as they offer several advantages over flat analogues. These benefits include increased solubility, structural and conformational dynamic character, varied chirality and aromaticity, tunability in electronic, magnetic, optical as well as conductive properties.[84],[85],[86] As I mentioned earlier, introduction of pentagons or heptagons into planar backbone forming bowl- or saddle-shaped structures were demonstrated to possess attractive functional properties.[80],[87],[88] However, the synthetic tool box towards such curved aza-doped architectures are still under development.

The main goal of my PhD-Thesis is to utilize the synthetic potential offered by TAPPs to explore the pathways leading to the synthesis of aza-doped non-planar polycyclic aromatic systems. TAPPs are superb substrates in this regard. Multicomponent reaction leading to their formation enables the assembly of large molecular skeletons from simple starting materials. These centrosymmetric architectures contain functional groups which are compatible with multicomponent reaction (vast majority are) in close proximity. Moreover positions 3 and 6 are free for functionalization and highly reactive. Although the properties of TAPPs as a platform for the synthesis of elaborated π-expanded systems were investigated,[89] their compatibility on alkyne annulation reactions are not completely known (The chemistry of 1,4-dihydro-pyrrolo[3,2-*b*]pyrroles, attached chapter). In addition to other factors mentioned earlier, adding two seven-membered rings seems to be a good strategy to induce non-planarity into the TAPP-based nanographene. Considering the versatility of alkyne activation reactions and their applicability, especially on the synthesis of polycyclic systems, I decided to investigate the utility of alkyne annulation using TAPPs in the synthesis of large N-doped polycyclic aromatic hydrocarbons.

3. Results and Discussion

3.1 Cationic gold-catalyzed 1,2-aryl shift and benzannulation towards S-shaped aza-doped polycyclic aromatic hydrocarbons

Alkyne benzannulations on pyrrolo[3,2-*b*]pyrrole precursors bearing alkynyl moieties have already been reported in our group. In that case, TAPP precursors possessing benzene rings bearing alkynyl moieties attached to positions 2 and 5 were used to obtain π-expanded indolo[3,2-*b*]indoles via $InCl_3$ catalyzed cyclization (section 1.2.2.2.2).[45] In the first phase of my PhD work, the synthetic approach was to incorporate the arylethynylaryl substituents at 1 and 4 positions of TAPP. Such rational design would allow the positioning of carbon-carbon triple bonds in a way that the final cyclization would lead to a unique 7-5-5-7 type ring system (**Scheme 33**). To evaluate this hypothesis, aniline precursors **105a-e** were synthesized by either Sonogashira or Sila Sonogashira coupling of corresponding substrates. Anilines were rationally chosen to

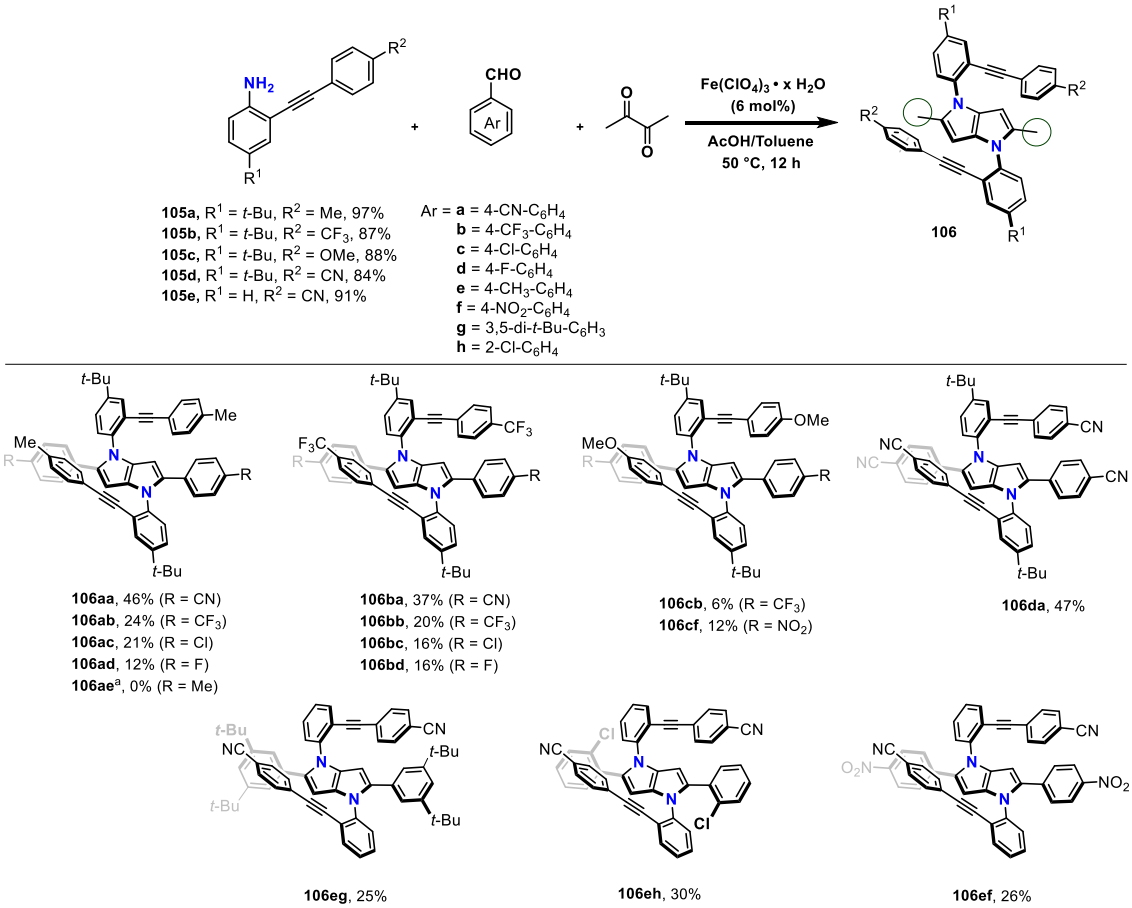

Scheme 32. Synthesis of precursor TAPPs **106aa-ef** bearing arylethynylaryl rings. [a] **106ae** not isolated.

have electronically different substituents at the *para* positions of benzene rings connected to the triple bond. The multicomponent synthesis of TAPPs were carried out using a library of differentially substituted aldehydes under reported conditions[90] to obtain the desired precursors **106aa** to **106ef** in moderate yields (**Scheme 32**).

With the precursors in hand, I attempted to perform the intramolecular hydroarylation reaction of alkynes by employing π-Lewis acids such as $InCl_3$, $GaCl_3$ and $PtCl_3$. These catalysts were predominantly used for alkyne activation reactions on polycyclic aromatic systems.[44],[53] However, none of these reactions led to any conversion. Alternatively, the usage of Brønsted acids (*p*-toluenesulfonic acid, trifluoroacetic acid) and neutral chlorogold(I) catalysts such as AuCl and $AuCl(PPh_3)$ gave the same result. While exploring the literature, I came across the double hydroarylation reaction to obtain aryl substituted pyrenes reported by Murakami and co-workers.[41] Authors stated that the use of cationic $SPhosAuNTf_2$ catalyst led the reaction to the final cyclized product, whereas the neutral chlorogold(I) catalysts were found to be ineffective. By performing the same reaction conditions on precursor molecule **106eg**, using electronically similar $IPrAuNTf_2$ catalyst led to the formation of a new product. Initial analysis of ^1H NMR (showing lower number of peaks corresponding to symmetric structure and absence of pyrrolic singlets at 6-6.5 ppm) and HRMS data confirming the mass appeared to support my hypothesis on the formation of new seven-membered rings. Surprisingly, X-ray crystallography contradicted the prediction (**Scheme 33[c]**). Apparently, two new six-membered rings are formed at the central DHPP core forming an S-shaped aza-doped non-planar polycyclic aromatic hydrocarbon. The 6-*endo* cyclisation has occurred at an already occupied C2 and C5 positions simultaneously inducing an aryl shift from C2 to C3 and C5 to C6.

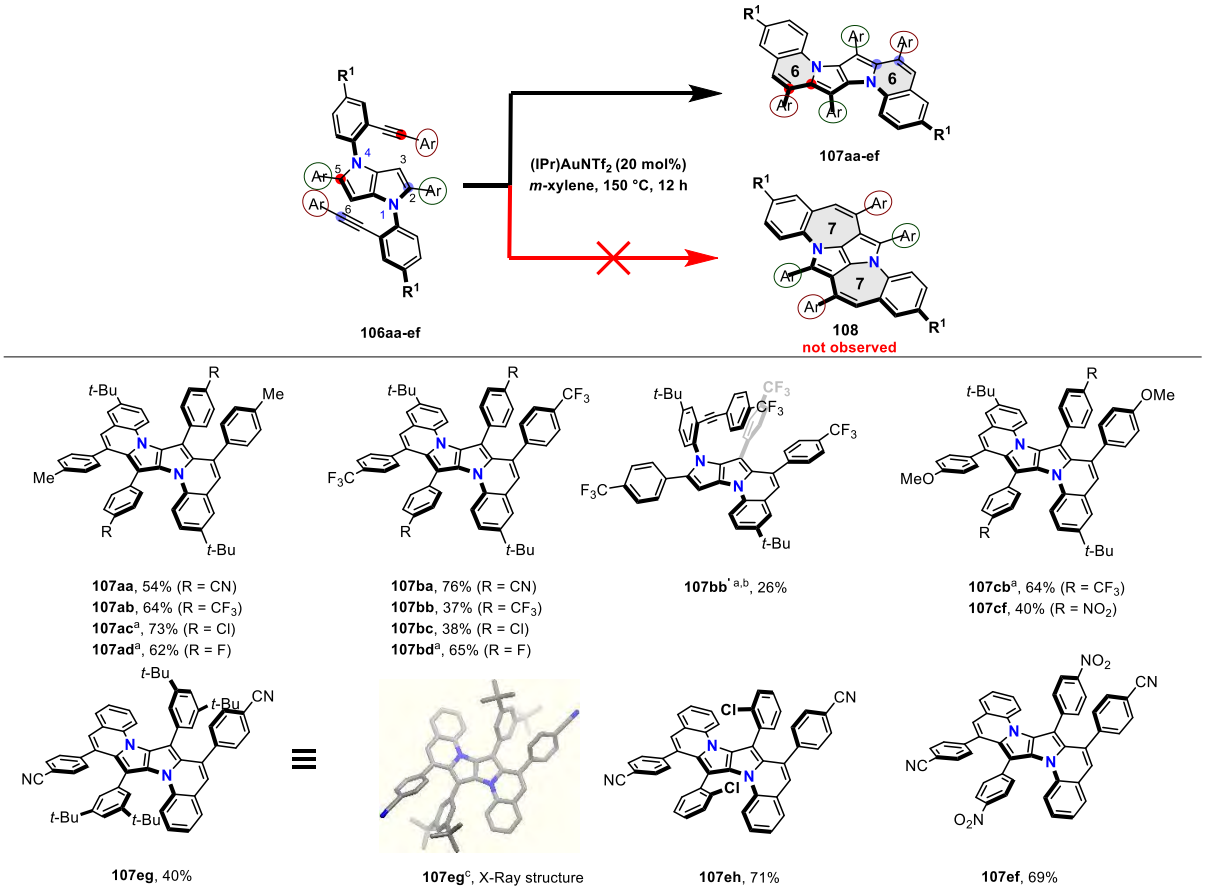

Scheme 33. Au-mediated double hydroarylation of alkyne-bearing TAPP **106,** accompanied by 1,2-aryl shift. [a] Reaction was completed in 4 hours. [b] One-fold hydroarylation leaving the other alkyne moiety intact. [c] Crystal structure of **107eg.**

To further showcase the functional group tolerance and synthetic utility of this established protocol, the reaction was carried out on a library of previously synthesized substrates possessing electronically different substituents (**Scheme 33**). In all cases, the reaction followed the same pathway leading to the rearranged products in moderate to good yields ranging from 37 to 76%. The only exception was the precursor with four cyano groups at the periphery (**106da)**, where the reaction did not lead to completion**.** A weakened nucleophilicity of the system caused by the cyano groups can be a reason for the low reactivity. When the reaction time was reduced to 4 hours, mono-annulated product was isolated denoting that the annulation occurs in a stepwise manner. The scope of this reaction was also tested on substrates possessing halogen handles *ortho* to the benzene rings attached to 2 and 5 positions. Interestingly, cyclisation followed by 1,2-aryl shift occurred smoothly to obtain **107eh** in 71% yield, showcasing the post-synthetic versatility and the efficiency of this reaction, even in the presence of steric hindrance

near the migrating center. Additional experiments to investigate the effect of Lewis acids and Brønsted acids as co-catalysts were carried out. Nevertheless, no significant effect was observed in the reaction outcome. Similarly, addition of inorganic base did not affect the reaction pathway, while the presence of an organic base slightly lowered the reaction conversion. Mechanistic computational studies performed by Dr. Wojciech Chaładaj (ICHO, PAN) revealed that the 6-*endo-dig* cyclisation accompanied by the 1,2-aryl shift is both kinetically and thermodynamically preferred over *7-endo-dig* type annulation, thereby corroborating the experimental results.

Considering the photophysical properties of the dyes **106**, TAPPs bearing electron-neutral substituents on 1 and 4 positions and electron-withdrawing substituents on 2 and 5 positions (**106aa, Figure 3**) showed a bathochromic shift in absorption and emission compared to the analogous TAPP with simple phenyl substituents (1,4-di(4-methylphenyl)-2,5-di(4-cyano phenyl)-1,4-dihydropyrrolo[3,2-*b*]pyrrole). At the same time, their absorption and emission maxima are insensitive to the change in polarity. An interesting observation was seen when the optical properties of **106da** with electron-withdrawing cyano groups on the rings at 1 and 4 positions was compared with **106aa** with methyl groups present on the rings at 1 and 4 positions**.** The molecule **106da** displayed bathochromic shift of emission around 20 nm in toluene compared to **106aa** and the shift is more pronounced in THF ≈ 80 nm (**Figure 3**). In addition, the fluorescence quantum yield (ϕ_{fl}) of **106da** is low (**Figure 3**). However, their $\lambda_{\text{abs}}^{\text{max}}$ are not affected by the solvent polarity. Theoretically, the large dihedral angle between N-aryl substituents and DHPP core limits the through bond electronic communication, meaning that changing the substituents on twisted aryl substituents should not affect their photophysical properties significantly. Therefore, the electronic communication is only possible via the *through-space* interaction. Computational studies performed by Prof. Denis Jacquemin (Nantes, France) revealed a significant difference in the topology of electron density difference (EDD) plots of **106aa** and **106da**, aligning with the experimental results and confirming the *through-space* charge transfer.

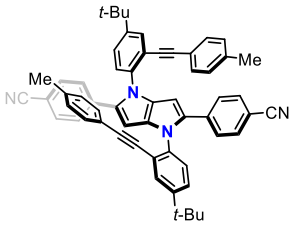

106aa

λ_{abs}^{max} = 410 nm λ_{em}^{max} = 450 nm

ϕ_{fl}= 0.74 (toluene)

λ_{abs}^{max} = 410 nm λ_{em}^{max}= 450 nm

ϕ_{fl}= 0.87 (THF)

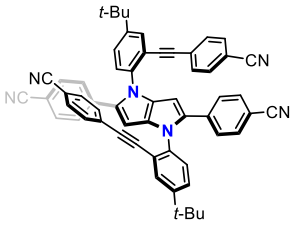

106da

λ_{abs}^{max} = 408 nm λ_{em}^{max} = 472 nm

ϕ_{fl} = 0.08 (toluene)

λ_{abs}^{max} = 410 nm λ_{em}^{max} = 531 nm

ϕ_{fl} = 0.02 (THF)

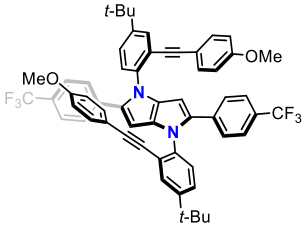

106cb

λ_{abs}^{max} = 378 nm λ_{abs}^{max} = 424 nm

ϕ_{fl}= 0.74 (toluene)

λ_{abs}^{max} = 382 nm λ_{abs}^{max} = 426 nm

ϕ_{fl}= 0.49 (THF)

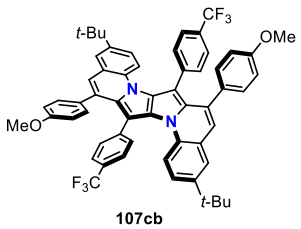

107cb

λ_{abs}^{max} = 484 nm λ_{abs}^{max} = 495;531 nm

ϕ_{fl} = 0.60 (toluene)

λ_{abs}^{max} = 480 nm λ_{abs}^{max} = 494;530 nm

ϕ_{fl} = 0.59 (THF)

Figure 3. Structure and optical properties of dyes **106aa,da,cb** and **107cb.**

The fused dyes **107** displayed bathochromic shift of absorption and emission compared to the precursors, as expected (**Figure 3**). Their absorption bands showing significant vibronic character are located in the blue region with maxima around 480 nm. These dyes display green emission with large fluorescence quantum yields typically around 75 %. The optical properties were not influenced by the substituents on the benzene rings attached to 3 and 6 positions. However, the only exception was the dye with NO_2 groups for which the fluorescence is quenched (below the detection limit) in both THF and toluene.

In conclusion, the combination of highly electron-rich DHPP core and cationic gold catalyst alters the reaction pathway of intramolecular hydroarylation. A new class of S-shaped nitrogen-doped polycyclic aromatic system has been synthesized with six

ortho-fused, conjugated aromatic rings. The 6-*endo-dig* cyclization occurred in already occupied positions, simultaneously inducing the migration of phenyl rings to adjacent positions. The functional group compatibility of this reaction was tested on a range of functional groups, especially those relevant to the field of optoelectronics. Optical properties of the precursor dyes bearing electron-withdrawing groups on arylethynyl rings were explained by *through-space* interaction. Despite a small substrate limitation, I believe this discovery will inspire further explorations on gold-catalyzed alkyne annulation reactions in the near future.

3.2 Contorted aza-doped polycyclic aromatic hydrocarbons with multiple odd-membered rings via alkyne annulation

PAHs possessing heptagons or larger rings are scarcely reported in literature compared to pentagons.[91],[92],[93] Incorporation of heptagonal ring creates geometrical strain caused by the warping of the graphenic system that may result in higher activation enthalpies. This can be a plausible reason behind the limited number of bottom-up approaches towards these architectures. Based on the findings from my prior work, altering the course of alkyne annulation opens up the possibility of introducing seven-membered rings to the system. During the follow-up investigations, alkyne annulation reaction was performed using Brønsted acid $HNTf_2$ on precursor TAPP **106aa**. This catalyst was specifically chosen as it is the conjugate acid of the gold catalyst's counter anion used in the previous work. A new product was formed, for which the ^1H NMR showed significantly different peak distribution as that of the 1,2-aryl shift product. X-ray crystallography confirmed that *7-endo-dig* cyclisation has occurred on C3 and C6 positions of the DHPP core to form a unique 7-5-5-7 type cyclic system (**Scheme 34**). This transformation turned out to be quite interesting as it could only be catalyzed by $HNTf_2$, while other Brønsted acids failed. I have performed the reaction using a broad range of catalysts, which were reported for alkyne annulation reaction. Nevertheless, none of them gave similar outcome.

To explore the functional group tolerance, the reaction was carried out on a library of electronically different substrates. The alkyne annulation was found to be limited to specific substrates in which the aryl ring connected to the triple bond had electron-donating groups (MeO or Me, see **Scheme 34(I)**). Additionally, substituents attached to

the benzene rings on 2 and 5 positions need to be electron-withdrawing to maintain the stability of the final structure (CN, CO_2Me or NO_2, see **Scheme 34(I)**). For substrates with other combinations of substituents, the reaction led to complex mixture of byproducts (**Scheme 34(II)**). Additionally, I carried out the reaction on substrate possessing halogen handles to demonstrate its post-synthetic utility (**Scheme 34(III)**). Annulation occurred efficiently to form the product **108ak**, followed by the final Pd-catalyzed intramolecular direct arylation leading to the formation of completely fused double-helical aza-nanographene **109ak**. Mechanistic computational studies conducted

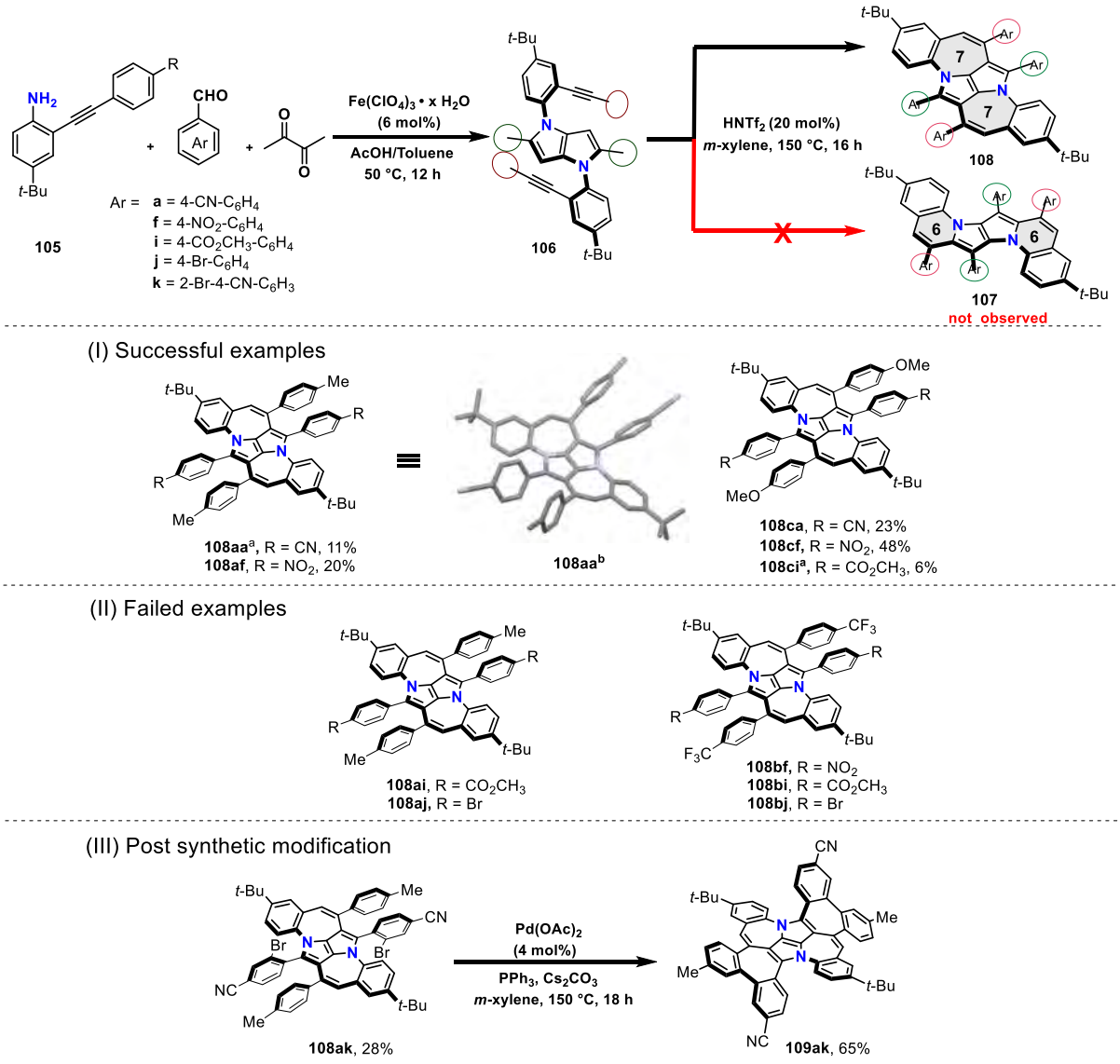

Scheme 34. $HNTf_2$-mediated double hydroarylation of alkyne-bearing TAPP **106.** [I] Successful examples [II] Failed examples. [III] Pd-catalyzed intramolecular direct arylation of **108ak**. [a] Reaction kept at 160 °C for 6 hours. [b] X-ray crystal structure of **108aa.**

by Dr. Wojciech Chaładaj (ICHO PAN) suggest that the formation of thermodynamically less stable 7-membered ring is favored by kinetically preferred attack of protonated alkyne at position 3a of the DHPP core over the intermediate leading to *6-endo-dig* cyclization.

The photophysical properties of fused dyes **108** clearly differs from that of usual TAPP systems.[94] These compounds display much lower fluorescence quantum yields typically ranged around 0.01. Compared to their regio isomers S-shaped π-expanded pyrrolo[3,2-*b*]pyrroles **107**, the molecule is characterized by an increased Stokes shift values which leads to a bathochromic shift of the emission. The substituents present on 2 and 5 positions have a significant impact on the absorption and emission maxima values. Changing the substituent from CN (**108aa**) to NO_2 (**108af**) caused red shift of ≈ 60 nm for both absorption and emission (**Figure 4**). The low radiative emission characteristic of the synthesized compounds was rationalized by computational studies performed by Prof. Denis Jacquemin (Nantes, France). The study revealed that the EDD plot upon excitation is delocalized on the DHPP core as well as the 7-membered rings, while the contribution from substituted phenyl rings on 2 and 5 positions are limited. This first excited state here is computationally dark, in contrast to all the reported TAPPs where the lowest transition is a bright quadrupolar charge transfer state, involving the pyrrolo[3,2-*b*]pyrrole core and substituents on benzene rings at 2 and 5 positions. Electrochemical properties of these compounds were also measured using cyclic voltammetry. The measurements revealed that the fused DHPPs possess a lower first oxidation potential compared to their non-fused parent counterparts, aligning with the general trend that an increased degree of conjugation results in a lower first oxidation potential. A similar pattern was observed for ionization potential as well. However, the fully fused molecule **109ak** exhibited a higher first oxidation potential than its precursor.

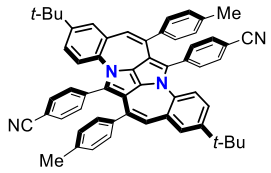

108aa

λ_{abs}^{max} = 450 nm λ_{em}^{max} = 618 nm

Stokes shift = 4800 cm^{-1}

ϕ_{fl}= 0.04 (toluene)

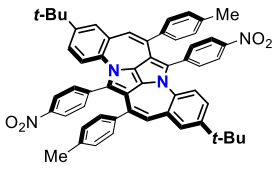

108af

λ_{abs}^{max} = 515 nm λ_{em}^{max} = 676 nm

Stokes shift = 4600 cm^{-1}

ϕ_{fl} = 0.02 (toluene)

Figure 4. Structure and optical properties of dyes **108aa** and **108af.**

To conclude, Brønsted acid $HNTf_2$ selectively catalyzes *7-endo-dig* alkyne annulation reaction of TAPPs bearing alkynyl moieties on N-aryl rings, resulted in a smooth formation of a unique non-alterant 7-5-5-7 type aza-doped polycyclic system. To the best of my knowledge, this methodology is one among the few examples of rare 7-membered ring alkyne annulation reaction reported till date in the area of alkyne activation.

4. Summary and Comparison

In the first part of my PhD, I developed and demonstrated intramolecular *6-endo-dig* alkyne annulation reaction accompanied by 1,2-aryl shift on TAPP substrates. Literature studies showed that the occurrence of such rearrangements during alkyne annulation is considerably higher for gold(I)-catalyzed reactions compared to other catalysts. The first case of 1,2-phenyl shift during alkyne annulation was reported in 1996 by Swager and co-workers while employing TFA as the catalyst during the synthesis of laterally fused polycyclic aromatic systems.[21] In this case, the rearrangement can be controlled, as the complete conversion to the rearranged product occurred only during harsh reaction conditions with high temperature and longer time. Additionally, annulation was specific to phenyl substituents bearing alkoxy groups. Similar rearrangement was observed recently by Chalifoux group during the TFA catalyzed benzannulation to synthesize pyreno[*a*]pyrene-based helicenes.[64] However, the 1,2-aryl shift product was obtained only in traces as byproduct and more likely occurred to release the steric strain. Considering the reaction involving cationic gold catalyst, similar type of migration of 1,2-alkyl or aryl group was demonstrated on allenyl ketones to obtain multisubstituted furans (**Scheme 35A**).[95] Analogous rearrangement was observed by Van der Eycken and co-workers during the enyne cycloisomerization of alkyne bearing precursors to synthesize pyrrolo[1,2-*b*]isoquinolines (**Scheme 35B**).[96] Nevertheless, the cyclization was assisted by heteronucleophiles in both cases. Current growing interest in this area has also led to the investigations on the effect of acidic co-catalysts on cationic gold catalysis.[97] The study performed by Xu group in collaboration with Hammond group found that the acid co-catalysts improve the turnover rate of many gold(I) catalyzed reactions including cyclization reactions, with lower catalyst loadings. However, in my work, the control experiments performed with the addition of Lewis or Brønsted acid along with the gold catalyst did not influence the reaction yield.

To conclude, my study explored the intramolecular hydroarylation of aza-doped precursors possessing alkyne moieties, leading to the synthesis of S-shaped polycyclic aromatic hydrocarbons. Although analogous instances of rearrangements have been reported in gold(I) catalyzed reactions, 1,2-aryl shift occurring during alkyne annulation reaction on such elaborated nitrogen-doped systems is scarce. Considering the alkyne activation reactions developed till date, only a few of them focus on heteroatom-doped

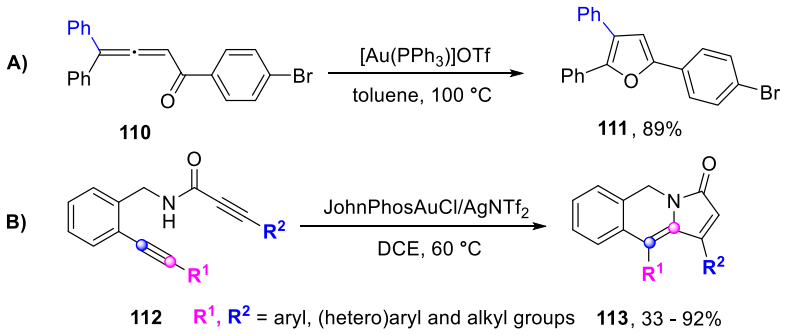

Scheme 35. A) 1,2-Aryl shift during the cyclization of allenyl ketones**. B)** 1,2-Aryl/(hetero)aryl/alkyl migration during cyclization to form pyrrolo[1,2-*b*]isoquinolines**.**

polycyclic systems (discussed in section 1.2). This study serves as a valuable reference for future research on alkyne annulation reactions on heteroatom-doped polycyclic aromatic systems.

In the second part of my work, I developed Brønsted acid catalyzed *7-endo-dig* type intramolecular alkyne annulation reaction on TAPP substrates to synthesize aza-doped polycyclic aromatic systems with two embedded heptagon rings. Literature reports indicate that the regioselectivity of alkyne annulation reaction is strongly influenced by the choice of substrates and the catalyst used.[98],[99] Regarding polycyclic aromatic systems, *6-endo-dig* cyclization is frequently reported, whereas *5-exo-dig, 6-exo-dig* and *7-endo-dig* type cyclization is rare. Shibata and co-workers utilized the synthetic potential of N-(2-alkynylphenyl)aniline derivatives to synthesize π-expanded dibenzazepines via *7-endo-dig* cyclization using cationic Au catalysis (**Scheme 36A**).[100] Later, the same group demonstrated selective cyclization of indoline derivatives to form 7-membered rings utilizing similar catalytic systems (**Scheme 36B**). Authors had to use indoline precursors instead of indoles so as to suppress the reactivity of C2 position and achieve selectivity.[101] In both cases, the increased nucleophilicity of aryl carbon attained by the resonance effect of lone pair from nitrogen is crucial for cyclization to occur. Alcarazo group did a comparative study on alkyne annulation catalyzed by Brønsted acid and gold catalyst (**Scheme 37**).[98] Authors demonstrated that the regioselectivity of cyclization catalyzed by Brønsted acid depends on the site of formation of stable vinyl cation after protonation. This can be tuned by making aryl rings connected to one side of

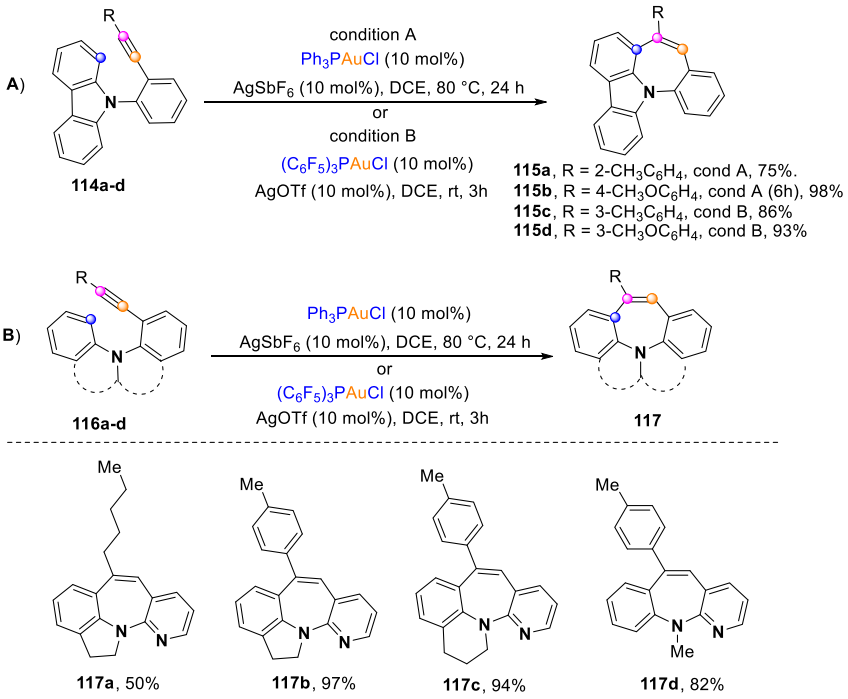

Scheme 36. Cationic Au(I) catalyzed *7-endo-dig* cyclization of N-heterocyclic precursors bearing alkyne moiety.

the triple bond electron-rich which favors carbocation formation selectively, followed by *7-endo-dig* cyclization. However, Au-catalysis activates both carbon atoms of the triple bond simultaneously which leads to the cyclization on less sterically hindered position, given that this position is not preferentially activated. Hence Au(I) catalysis leads to 7 membered ring formation in most of the cases. In a recent study, Langer and co- workers reported the regioselective alkyne annulation controlled by the choice of Brønsted acid and solvent (**Scheme 38**).[102] *6-endo-dig* type annulation of imidazo[1,2-*a*]pyridines possessing alkyne moiety was favored when TfOH was used in CH_2Cl_2 at lower temperatures (0-20 °C). At the same time, *p*-TsOH in toluene at elevated temperatures led to 7-membered ring formation. Although the exact reason behind the selectivity is not clear, authors hypothesize the cyclization of the protonated alkyne via benzene ring to be faster than the annulation through imidazole ring due to the protonation of nitrogen. At higher temperatures, this attack was assumed to become feasible.

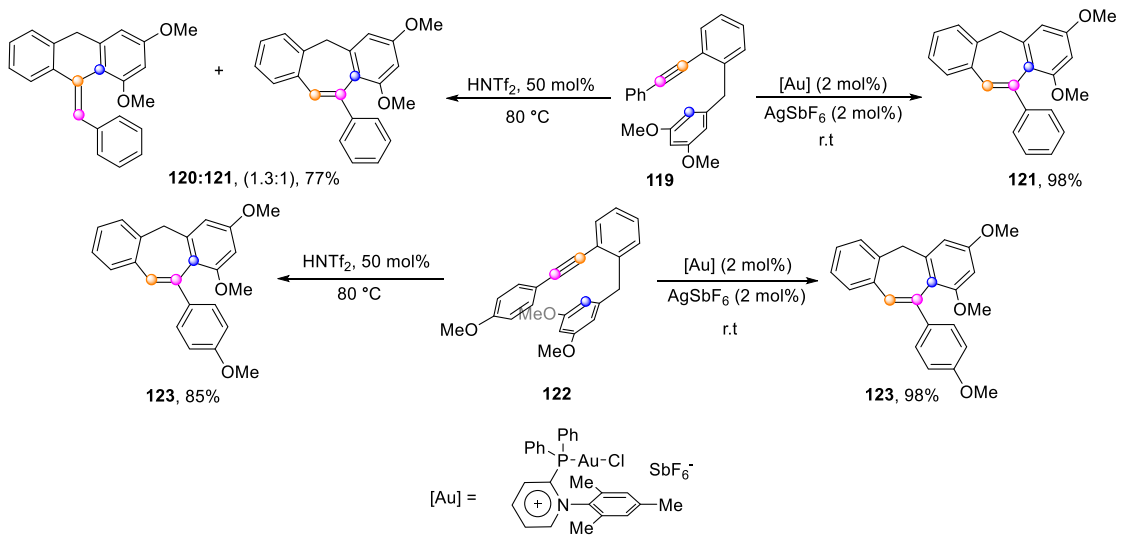

Scheme 37. Distribution of products of hydroarylation reaction on 1-(benzyl)-2-ethynylarylbenzenes under different reaction conditions.

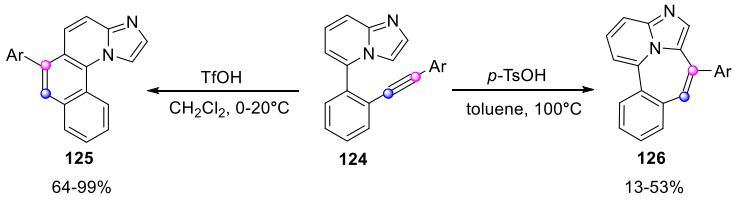

Scheme 38. Synthesis of benzo[*h*]imidazo[1,2-*a*]quinolines and 1,2a[1]-diazadibenzo[*cd*,*f*]azulenes via alkyne activation.

In conclusion, my study demonstrates that a change in the acidic character of acid catalysts can alter the course of benzannulation reaction towards *7-endo-dig* type cyclization in the case of 1,4-dihydropyrrolo[3,2-*b*]pyrroles. This is one of very few cases when alkynes' hydroarylation actually leads to the formation of seven-membered rings. Computational studies corroborate the unexpected course of this reaction and point towards the kinetic control as being responsible for it. The reaction is intriguing as it not catalyzed by cationic gold catalysts which are largely recognized for benzannulation.[99] Moreover, subsequent double intramolecular direct arylation leads to the N-doped nanographene possessing four seven-membered rings. The resulting nitrogen-doped twisted framework comprising of two five-membered and four seven-membered rings is unprecedented. In Alcarazo's work, the electron-donating group played a significant role in regioselectivity in the case of acid catalyzed cyclization. This study enabled me to investigate the relationship between the molecular architecture in such N-doped polycyclic aromatic hydrocarbons and their photophysics, discovering that the π-

conjugated materials possessing seven-membered rings exhibit weak red emission. This study has expanded our knowledge on alkyne benzannulation in complex heterocyclic π-systems. The discovered approach shows beyond a doubt that the constant growth of our synthetic toolbox allows scientists to fine-tune the structures and properties creating previously unimaginable organic materials.

5. References

[1] Z. Liu, S. Fu, X. Liu, A. Narita, P. Samorì, M. Bonn, H. I. Wang, *Adv. Sci.* **2022**, *9*, 2106055.

[2] S. Kumar, Y. T. Tao, *Org. Lett.* **2018**, *20*, 2320–2323.

[3] C. Aumaitre, J. F. Morin, *Chem. Rec.* **2019**, *19*, 1142–1154.

[4] L. Zhi, K. Müllen, *J. Mater. Chem.* **2008**, *18*, 1472–1484.

[5] J. Zhao, C. He, R. Yang, Z. Shi, M. Cheng, W. Yang, G. Xie, D. Wang, D. Shi, G. Zhang, *Appl. Phys. Lett.* **2012**, *101*, 063112.

[6] J. Lin, Y. Huang, P. Huang, *Biomed. Appl. Funct. Nanomater. Concepts, Dev. Clin. Transl.* **2018**, 247–287.

[7] L. Chen, Y. Hernandez, X. Feng, K. Müllen, *Angew. Chem. Int. Ed.* **2012**, *51*, 7640–7654.

[8] W. E. Barth, R. G. Lawton, *J. Am. Chem. Soc* **1971**, *93*, 1730–1745.

[9] M. M. Hashemi, M. S. Bratcher, L. T. Scott, *J. Am. Chem. Soc.* **1992**, *114*, 1920–1921.

[10] L. T. Scott, M. M. Hashemi, D. T. Meyer, H. B. Warren, *J. Am. Chem. Soc.* **1991**, *113*, 7082–7084.

[11] H. Sakurai, T. Daiko, T. Hirao, *Science* **2003**, *301*, 1878.

[12] S. Higashibayashi, H. Sakurai, *Chem. Lett.* **2011**, *40*, 122–128.

[13] D. Hellwinkel, T. Kosack, *Liebigs Ann.* **1985**, *1985*, 226–238.

[14] K. Yamamoto, T. Harada, M. Nakazaki, T. Naka, K. Yasushi., S. Harada, N. Kasai, *J. Am. Chem. Soc* **1983**, *105*, 7171–7172.

[15] S. H. Pun, Y. Wang, M. Chu, C. K. Chan, Y. Li, Z. Liu, Q. Miao, *J. Am. Chem. Soc.* **2019**, *141*, 9680–9686.

[16] W. S. Wong, M. Stępień, *Trends Chem.* **2022**, *4*, 573–576.

[17] M. Grzybowski, K. Skonieczny, H. Butenschön, D. T. Gryko, *Angew. Chem. Int. Ed.* **2013**, *52*, 9900–9930.

[18] W. Hagui, H. Doucet, J. F. Soulé, *Chem* **2019**, *5*, 2277.

[19] W. Yang, R. R. Kazemi, N. Karunathilake, V. J. Catalano, M. A. Alpuche-Aviles, W. A. Chalifoux, *Org. Chem. Front.* **2018**, *5*, 2288–2295.

[20] M. B. Goldfinger, T. M. Swager, *J. Am. Chem. Soc* **1994**, *116*, 7895–7896.

[21] M. B. Goldfinger, K. B. Crawford, T. M. Swager, *J. Am. Chem. Soc.* **1997**, *119*, 4578–4593.

[22] A. D. Senese, W. A. Chalifoux, *Molecules* **2019**, *24*, 118.

[23] J. Barluenga, J. M. González, P. J. Campos, G. Asensio, *Angew. Chem. Int. Ed.*

1988, *27*, 1546–1547.

[24] C. W. Li, C. I. Wang, H. Y. Liao, R. Chaudhuri, R. S. Liu, *J. Org. Chem.* **2007**, *72*, 9203–9207.

[25] R. Chaudhuri, M. Y. Hsu, C. W. Li, C. I. Wang, C. J. Chen, C. K. Lai, L. Y. Chen, S. H. Liu, C. C. Wu, R. S. Liu, *Org. Lett.* **2008**, *10*, 3053–3056.

[26] X. Feng, W. Pisula, K. Müllen, *J. Am. Chem. Soc.* **2007**, *129*, 14116–14117.

[27] S. Xiao, M. Myers, Q. Miao, S. Sanaur, K. Pang, M. L. Steigerwald, C. Nuckolls, *Angew. Chem. Int. Ed.* **2005**, *44*, 7390–7394.

[28] R. K. Mohamed, S. Mondal, J. V. Guerrera, T. M. Eaton, T. E. Albrecht-Schmitt, M. Shatruk, I. V. Alabugin, *Angew. Chem. Int. Ed.* **2016**, *55*, 12054–12058.

[29] T. Yao, M. A. Campo, R. C. Larock, *J. Org. Chem.* **2005**, *70*, 3511–3517.

[30] T. A. Chen, R. S. Liu, *Chem. Eur. J.* **2011**, *17*, 8023–8027.

[31] T. A. Chen, R. S. Liu, *Org. Lett.* **2011**, *13*, 4644–4647.

[32] Q. Yan, K. Cai, C. Zhang, D. Zhao, *Org. Lett.* **2012**, *14*, 4654–4657.

[33] W. Yang, J. H. S. K. Monteiro, A. de Bettencourt-Dias, V. J. Catalano, W. A. Chalifoux, *Angew. Chem. Int. Ed.* **2016**, *55*, 10427–10430.

[34] W. Yang, J. H. S. K. Monteiro, A. De Bettencourt-Dias, W. A. Chalifoux, *Can. J. Chem.* **2017**, *95*, 341–345.

[35] W. Yang, G. Longhi, S. Abbate, A. Lucotti, M. Tommasini, C. Villani, V. J. Catalano, A. O. Lykhin, S. A. Varganov, W. A. Chalifoux, *J. Am. Chem. Soc.* **2017**, *139*, 13102–13109.

[36] C. M. Cruz, I. R. Márquez, I. F. A. Mariz, V. Blanco, C. Sánchez-Sánchez, J. M. Sobrado, J. A. Martín-Gago, J. M. Cuerva, E. Maçôas, A. G. Campaña, *Chem. Sci.* **2018**, *9*, 3917–3924.

[37] S. Dutta, S. K. Pati, *J. Mater. Chem.* **2010**, *20*, 8207–8223.

[38] J. K. Stille, G. K. Noren, L. Green, *J. Polym. Sci. Part A-1 Polym. Chem.* **1970**, *8*, 2245–2254.

[39] X. Zhu, Y. Wu, L. Zhou, Y. Wang, H. Zhao, B. Gao, X. Ba, *Chinese J. Chem.* **2015**, *33*, 431–440.

[40] W. Yang, A. Lucotti, M. Tommasini, W. A. Chalifoux, *J. Am. Chem. Soc.* **2016**, *138*, 9137–9144.

[41] T. Matsuda, T. Moriya, T. Goya, M. Murakami, *Chem. Lett.* **2011**, *40*, 40–41.

[42] E. Aguilar, R. Sanz, M. A. Fernández-Rodríguez, P. García-García, *Chem. Rev.* **2016**, *116*, 8256–8311.

[43] J. Carreras, G. Gopakumar, L. Gu, A. Gimeno, P. Linowski, J. Petuškova, W. Thiel, M. Alcarazo, *J. Am. Chem. Soc.* **2013**, *135*, 18815–18823.

[44] V. Mamane, P. Hannen, A. Fürstner, *Chem. Eur. J.* **2004**, *10*, 4556–4575.

[45] R. Stępzycki, M. Grzybowski, G. Clermont, M. Blanchard-Desce, D. T. Gryko, *Chem. Eur. J.* **2016**, *22*, 5198–5203.

[46] C. A. Merlic, M. E. Pauly, *J. Am. Chem. Soc.* **1996**, *118*, 11319–11320.

[47] V. M Hertz, H.-W. Lerner, M. Wagner, *Org. Lett* **2015**, *17*, 5240–5243.

[48] P. M. Donovan, L. T. Scott, *J. Am. Chem. Soc.* **2004**, *126*, 3108–3112.

[49] H. C. Shen, J. M. Tang, H. K. Chang, C. W. Yang, R. S. Liu, *J. Org. Chem.* **2005**, *70*, 10113–10116.

[50] T. A. Chen, T. J. Lee, M. Y. Lin, S. M. A. Sohel, E. W. G. Diau, S. F. Lush, R. S. Liu, *Chem. Eur. J.* **2010**, *16*, 1826–1833.

[51] B. S. Shaibu, S. H. Lin, C. Y. Lin, K. T. Wong, R. S. Liu, *J. Org. Chem.* **2011**, *76*, 1054–1061.

[52] T. L. Wu, H. H. Chou, P. Y. Huang, C. H. Cheng, R. S. Liu, *J. Org. Chem.* **2014**, *79*, 267–274.

[53] J. Liu, B. W. Li, Y. Z. Tan, A. Giannakopoulos, C. Sanchez-Sanchez, D. Beljonne, P. Ruffieux, R. Fasel, X. Feng, K. Müllen, *J. Am. Chem. Soc.* **2015**, *137*, 6097–6103.

[54] J. Storch, J. Sýkora, J. Čermak, J. Karban, I. Císařová, A. Růžička, *J. Org. Chem.* **2009**, *74*, 3090–3093.

[55] J. Storch, J. Čermák, J. Karban, I. Císařová, J. Sýkora, *J. Org. Chem.* **2010**, *75*, 3137–3140.

[56] M. Weimar, R. Correa Da Costa, F. H. Lee, M. J. Fuchter, *Org. Lett.* **2013**, *15*, 1706–1709.

[57] A. Fürstner, V. Mamane, *J. Org. Chem.* **2002**, *67*, 6264–6267.

[58] D. Lorbach, M. Wagner, M. Baumgarten, K. Müllen, *Chem. Commun.* **2013**, *49*, 10578.

[59] K. Nakamura, S. Furumi, M. Takeuchi, T. Shibuya, K. Tanaka, *J. Am. Chem. Soc.* **2014**, *136*, 5555–5558.

[60] S. Yamaguchi, T. M. Swager, *J. Am. Chem. Soc.* **2001**, *123*, 12087–12088.

[61] W. Yang, R. Bam, V. J. Catalano, W. A. Chalifoux, *Angew. Chem. Int. Ed.* **2018**, *57*, 14773–14777.

[62] W. Yang, J. H. S. K. Monteiro, A. de Bettencourt-Dias, V. J. Catalano, W. A. Chalifoux, *Chem. Eur. J.* **2019**, *25*, 1441–1445.

[63] W. A. Chalifoux, P. Sitaula, R. J. Malone, G. Longhi, S. Abbate, E. Gualtieri, A. Lucotti, M. Tommasini, R. Franzini, C. Villani, V. J. Catalano, *Eur. J. Org. Chem.* **2022**, *2022*, e202101466.

[64] R. Bam, W. Yang, G. Longhi, S. Abbate, A. Lucotti, M. Tommasini, R. Franzini, C. Villani, V. J. Catalano, M. M. Olmstead, W. A. Chalifoux, *Org. Lett.* **2019**, *21*, 8652–8656.

[65] R. J. Malone, J. Spengler, R. A. Carmichael, K. Ngo, F. Würthner, W. A. Chalifoux, *Org. Lett.* **2023**, *25*, 226–230.

[66] M. Franceschin, A. Alvino, V. Casagrande, C. Mauriello, E. Pascucci, M. Savino, G. Ortaggi, A. Bianco, *Bioorg. Med. Chem.* **2007**, *15*, 1848–1858.

[67] X. Zhang, S. Rehm, M. M. Safont-Sempere, F. Würthner, *Nat. Chem.* **2009**, *1*, 623–629.

[68] X. Zhan, A. Facchetti, S. Barlow, T. J. Marks, M. A. Ratner, M. R. Wasielewski, S. R. Marder, *Adv. Mater.* **2011**, *23*, 268–284.

[69] U. Rohr, C. Kohl, K. Müllen, A. Van De Craats, J. Warman, *J. Mater. Chem.* **2001**, *11*, 1789–1799.

[70] Z. An, J. Yu, B. Domercq, S. C. Jones, S. Barlow, B. Kippelen, S. R. Marder, *J. Mater. Chem.* **2009**, *19*, 6688–6698.

[71] J. Shao, X. Zhao, L. Wang, Q. Tang, W. Li, H. Yu, H. Tian, X. Zhang, Y. Geng, F. Wang, *Tetrahedron Lett.* **2014**, *55*, 5663–5666.

[72] M. Stępień, E. Gońka, M. Żyła, N. Sprutta, *Chem. Rev.* **2017**, *117*, 3479–3716.

[73] A. Narita, X. Y. Wang, X. Feng, K. Müllen, *Chem. Soc. Rev.* **2015**, *44*, 6616–6643.

[74] M. Hirai, N. Tanaka, M. Sakai, S. Yamaguchi, *Chem. Rev.* **2019**, *119*, 8291–8331.

[75] Y. F. Wu, L. Zhang, Q. Zhang, S. Y. Xie, L. S. Zheng, *Org. Chem. Front.* **2022**, *9*, 4726–4743.

[76] X. Gong, C. Li, Z. Cai, X. Wan, H. Qian, G. Yang, *J. Org. Chem.* **2022**, *87*, 8406–8412.

[77] T. A. Schaub, K. Padberg, M. Kivala, *J. Phys. Org. Chem.* **2020**, *33*, e4022.

[78] S. Mishra, M. Krzeszewski, C. A. Pignedoli, P. Ruffieux, R. Fasel, D. T. Gryko, *Nat. Commun.* **2018**, *9*, 1714.

[79] K. Oki, M. Takase, S. Mori, A. Shiotari, Y. Sugimoto, K. Ohara, T. Okujima, H. Uno, *J. Am. Chem. Soc.* **2018**, *140*, 10430–10434.

[80] M. Krzeszewski, Ł. Dobrzycki, A. L. Sobolewski, M. K. Cyrański, D. T. Gryko, *Angew. Chem. Int. Ed.* **2021**, *60*, 14998–15005.

[81] H. Yokoi, Y. Hiraoka, S. Hiroto, D. Sakamaki, S. Seki, H. Shinokubo, *Nat. Commun.* **2015**, *6*, 8215.

[82] S. Ito, Y. Tokimaru, K. Nozaki, *Angew. Chem. Int. Ed.* **2015**, *54*, 7256–7260.

[83] A. Janiga, E. Glodkowska-Mrowka, T. Stoklosa, D. T. Gryko, *Asian J. Org. Chem.* **2013**, *2*, 411–415.

[84] C. Yuan, S. Saito, C. Camacho, S. Irle, I. Hisaki, S. Yamaguchi, *J. Am. Chem. Soc.* **2013**, *135*, 8842–8845.

[85] S. H. Pun, Q. Miao, *Acc. Chem. Res.* **2018**, *51*, 1630–1642.

[86] T. Yamakado, S. Takahashi, K. Watanabe, Y. Matsumoto, A. Osuka, S. Saito, *Angew. Chem. Int. Ed.* **2018**, *57*, 5438–5443.

[87] B. Liu, M. Chen, X. Liu, R. Fu, Y. Zhao, Y. Duan, L. Zhang, *J. Am. Chem. Soc.* **2023**, *145*, 28137–28145.

[88] J. Wagner, D. Kumar, M. A. Kochman, T. Gryber, M. Grzelak, A. Kubas, P. Data, M. Lindner, *ACS Appl. Mater. Interfaces* **2023**, *15*, 37728–37740.

[89] M. Krzeszewski, D. Gryko, D. T. Gryko, *Acc. Chem. Res.* **2017**, *50*, 2334–2345.

[90] M. Tasior, O. Vakuliuk, D. Koga, B. Koszarna, K. Górski, M. Grzybowski, Ł. Kielesiński, M. Krzeszewski, D. T. Gryko, *J. Org. Chem.* **2020**, *85*, 13529–13543.

[91] Q. Miao, *Chem. Rec.* **2015**, *15*, 1156–1159.

[92] Z. Qiu, S. Asako, Y. Hu, C. W. Ju, T. Liu, L. Rondin, D. Schollmeyer, J. S. Lauret, K. Müllen, A. Narita, *J. Am. Chem. Soc.* **2020**, *142*, 14814–14819.

[93] Chaolumen, I. A. Stepek, K. E. Yamada, H. Ito, K. Itami, *Angew. Chem. Int. Ed.* **2021**, *60*, 23508–23532.

[94] S. Stecko, D. T. Gryko, *JACS Au* **2022**, *2*, 1290–1305.

[95] A. S. Dudnik, V. Gevorgyan, *Angew. Chem. Int. Ed.* **2007**, *46*, 5195–5197.

[96] L. Song, G. Tian, L. Van Meervelt, E. V. Van Der Eycken, *Org. Lett.* **2020**, *22*, 6537–6542.

[97] P. Barrio, M. Kumar, Z. Lu, J. Han, B. Xu, G. B. Hammond, *Chem. Eur. J.* **2016**, *22*, 16410–16414.

[98] K. Sprenger, C. Golz, M. Alcarazo, *Eur. J. Org. Chem.* **2020**, *2020*, 6245–6254.

[99] C. Praveen, S. Szafert, *ChemPlusChem* **2023**, *88*, e202300202.

[100] M. Ito, R. Kawasaki, K. S. Kanyiva, T. Shibata, *Eur. J. Org. Chem.* **2016**, *2016*, 5234–5237.

[101] M. Ito, D. Inoue, R. Kawasaki, K. S. Kanyiva, T. Shibata, *Heterocycles* **2017**, *94*, 2229–2246.

[102] A. Khomutetckaia, P. Ehlers, A. Villinger, P. Langer, *J. Org. Chem.* **2023**, *88*, 7929–7939.

6. Original publications

CHAPTER FIVE

The chemistry of 1,4-dihydropyrrolo[3,2-*b*] pyrroles

Gana Sanil, Beata Koszarna, Yevgen M. Poronik, Olena Vakuliuk, Bartosz Szymański, Damian Kusy, and Daniel T. Gryko*

Institute of Organic Chemistry, Polish Academy of Sciences, Warsaw, Poland
*Corresponding author: e-mail address: dtgryko@icho.edu.pl

Contents

Abstract

1,4-Dihydropyrrolo[3,2-*b*]pyrrole (DHPP) skeleton is comprised of only two fused pyrrole rings and yet, in non-fused form, it had to wait for discovery until 1972. The [3,2-*b*]-mode of fusion leads to several important consequences such as exceptionally high electron-density, ease of functionalization and high symmetry. In this Chapter we provide a comprehensive overview of multiple synthetic methods leading to this aromatic, heterocyclic skeleton. Although older methods comprised of some truly spectacular transformations, it was the development of multicomponent reaction of aromatic aldehydes, aromatic primary amines and butane-2,3-dione leading directly to 1,2,4,5-tetraaryl-1,4-dihydropyrrolo[3,2-*b*]pyrroles, which triggered the intense exploration of chemical space. We concentrate on presenting the newest and the most spectacular synthetic approaches leading to heretofore unknown, ladder-type heterocyclic skeletons. The increased scientific activity has resulted in the preparation of planar, helical and bowl-shaped π-expanded 1,4-dihydropyrrolo[3,2-*b*]pyrroles and numerous research applications in, for example, optoelectronics. We provide a critical overview

Advances in Heterocyclic Chemistry, Volume 138
ISSN 0065-2725
https://doi.org/10.1016/bs.aihch.2022.04.002

of photophysical properties of DHPP and especially of its π-expanded analogs. 1,4-Dihydropyrrolo[3,2-*b*]pyrroles made a contribution into deepening of our understanding of excited-state symmetry breaking and fluorescence of nitroaromatics. The synthesis, reactivity, and photophysical properties are exhaustively presented.

Keywords: 1,4-dihydropyrrolo[3,2-*b*]pyrrole, Nitrogen heterocycles, Synthetic methods, Chromophores, Fused-ring systems, Acenes, Aromatic electrophilic substitution, Absorption, Fluorescence, Two-photon absorption

1. Introduction

1,4-Dihydropyrrolo[3,2-*b*]pyrroles (DHPP) belong to the heteropentalenes, the family of aromatic heterocycles comprised of two, fused, five-membered, aromatic rings (**1**, Fig. 1).[1–5] Although there are four distinct modes of fusion (i.e., [2,3-*b*], [2,3-*a*], [3,4-*b*] and [3,2-*b*]) we will focus herein only on the [3,2-*b*] pattern due to its importance reflected in its prevalence in the literature. Pyrrolo[3,2-*b*]pyrrole (PP) (**1a**, Fig. 1)[6] structurally related to 1,4-dihydropyrrolo[3,2-*b*]pyrrole will not be described here due to space limitations. In spite of the fact that 1,4-dihydropyrrolo[3,2-*b*]pyrroles do not exist in nature, they have attracted significant attention during the last couple of decades in relation to organic optoelectronics. As they consist of two fused electron-rich pyrrole moieties they maintain the electron-rich character. Indeed, in the case of unsubstituted 1,4-dihydropyrrolo[3,2-*b*]pyrrole the highest occupied molecular orbital (HOMO) is located at −4.88 eV which makes it more electron-rich than pyrrole or indole.[7]

Although some synthetic methodologies leading to DHPPs have existed since 1972, the true renaissance in this chemistry started after a one-pot multicomponent reaction leading to tetraaryl-1,4-dihydropyrrolo[3,2-*b*]pyrroles was discovered. This chapter starts with an extensive synthetic overview, followed by a description of photophysical properties and the final part focuses on applied research in the area. Although, we made an effort to include all results, we apologize to the respective authors in case we incidentally omitted some contributions.

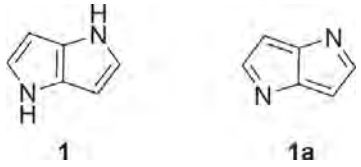

Fig. 1 General structure of 1,4-dihydropyrrolo[3,2-*b*]pyrrole (**1**, DHPP) and pyrrolo[3,2-*b*]pyrrole (**1a**, PP).

2. Synthesis

The first known method for the synthesis of heteropentalenes with a 1,4-dihydopyrrolo[3,2-*b*]pyrrole skeleton was discovered by Hemetsberger and Knittel in 1971.[8] These authors demonstrated the thermolysis of α-enazidoester **3** efficiently leading to corresponding pyrrolo[3,2-*b*]pyrrole. The method initiates with the preparation of the intermediate vinyl azide **3** via condensation of 2-formyl-1-methylpyrrole (2) with ethylazidoacetate (Scheme 1). The proposed mechanism includes the *in situ* formation of vinyl nitrene **4** under thermal conditions, which then undergoes 1,5-dipolar cyclization to form pyrrolo[3,2-*b*]pyrrole derivative **5**. Chemical companies including Sepracor Inc. and Zeneca Ltd. have used this method in the synthesis of compounds described in various patent applications.[9–11]

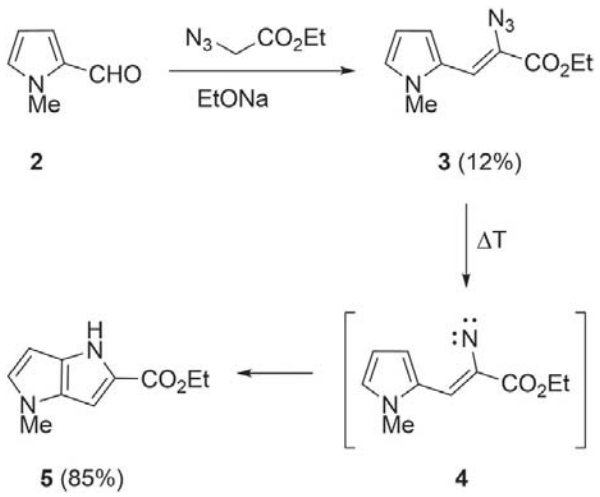

Scheme 1 Hemetsberger approach toward 1,4-dihydropyrrolo[3,2-*b*]pyrroles. *Adapted with permission from* Chem. Asian J. ***2014****, 9, 3036–3045.*

A few years later, Aratani and colleagues further explored the same method to come up with a modified synthetic strategy toward larger analogs of **1** (Scheme 2).[12] Introduction of a formyl group via Vilsmeier reaction on pyrrole derivative **3** paved a way to install one more pyrrole ring to the system. Compound **6** was thus prepared by formylation of azide **3**, which was the substrate in the synthesis of DHPP **7**. This molecule was then subjected to analogous sequence of Knoevenagel condensation followed by thermal cyclization. Finally, the resulting diester **8** underwent subsequent hydrolysis and decarboxylation to form dipyrrolo[3,2-*b*:2′,3′-*d*]pyrrole **9**. A similar

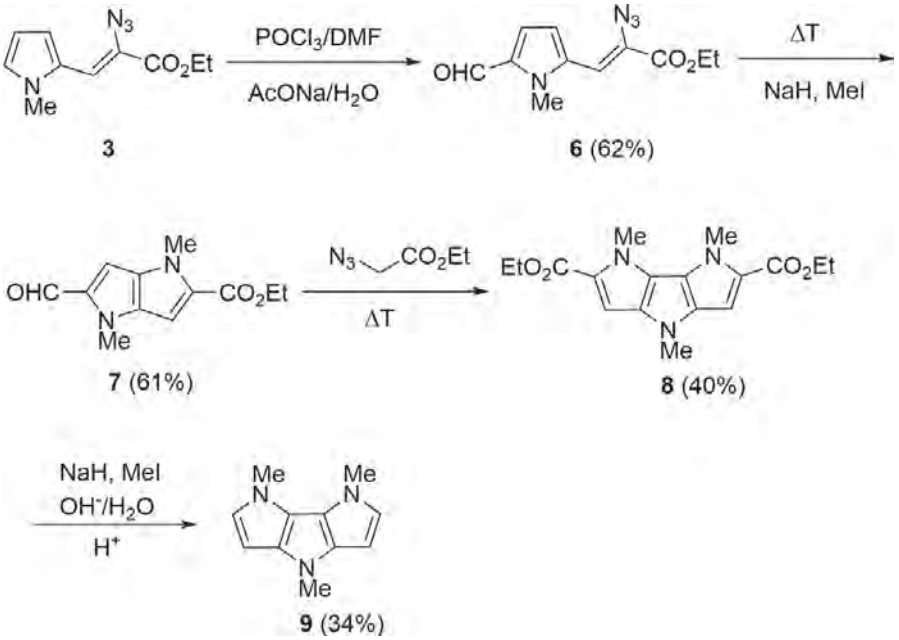

Scheme 2 The synthesis of dipyrrolo[3,2-*b*:2′,3′-*d*]pyrrole **9**. *Adapted with permission from* Chem. Asian J. ***2014**, 9, 3036–3045.*

method has been employed for the thiophene analogue dihydropyrrolo[3,2-*b*] thieno[2,3-*d*]pyrrole which was obtained in a higher overall yield of 79%.[12]

The applicability of α-azidoacrylates as a nitrene source in synthesizing nitrogen containing heterocycles have been further studied by Mukai's group, leading to the synthesis of tetrahydropyrrolo[3,2-*b*]pyrroles for the first time (Scheme 3).[13] This intriguing method involves an addition

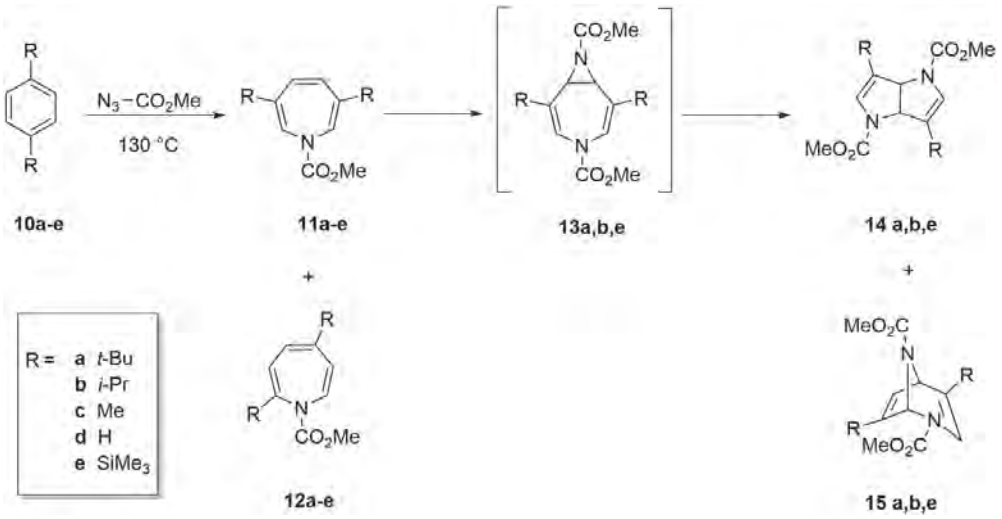

Scheme 3 Mukai approach toward 1,3a,4,6a-tetrahydropyrrolo[3,2-*b*]pyrroles. *Adapted with permission from* Chem. Asian J. ***2014**, 9, 3036–3045.*

of *in situ* formed nitrene to 1,4-disubstituted benzenes **10a–e** forming 1*H*-azepines **11a–e** and **12a–e**, and in the case of **10a**,**b**,**e** to form additional products **14a**,**b**,**e** and **15a,b,e**. The reaction mechanism was explained based on an intermediate diazabicyclooctadienes **13** formed after the sequential addition of the nitrene to 1*H*-azepines **11**. In fact, the bulky substituents in 1*H*-azepines **11a,b,e** activate the C4-C5 double bond for the further addition of the nitrene to form products **14a**,**b**,**e** and **15a**,**b**,**e**. Therefore DHPP **14a** was isolated in a yield of 18% accompanied by **15a** (9%) and two azepines **11a** and **12a** in 8% and 6%, respectively.

The preparation of unsubstituted 1,4-dihydropyrrolo[3,2-*b*]pyrrole (**1**) was first achieved by Mukai's group by introducing a slight modification on their earlier reported strategy (Scheme 3).[14] The presence of bulky trimethylsilyl groups at positions 1 and 4 of the benzene ring (derivative **10e**) led to the formation bicyclic system **14e**, as expected, by the stepwise addition of nitrene. Oxidation and desilylation was performed simultaneously using 2,3-dichloro-5,6-dicyano-1,4-benzoquinone (DDQ) to form **14d** which on further alkaline hydrolysis led to the desired molecule **1** (Scheme 4). 1,4-Dihydropyrrolo[3,2-*b*]pyrrole lacking any substituents was reported to be unstable and prone to polymerization under acidic conditions. This method has been patented by Sumitomo chemicals.[15]

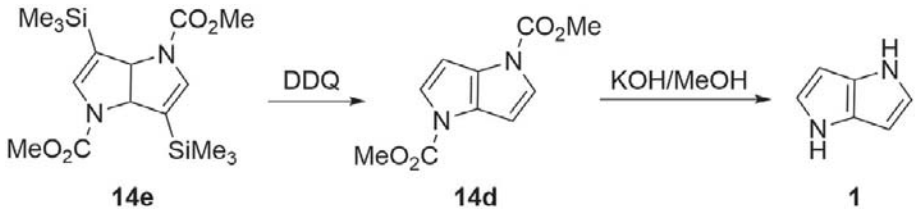

14e **14d** **1**

Scheme 4 The first synthesis of unsubstituted 1,4-dihydropyrrolo[3,2-*b*]pyrrole (**1**). *Adapted with permission from* Chem. Asian J. ***2014***, 9, *3036–3045.*

A recent discovery, made by Kubota et al in 2021, demonstrated a pathway toward unsymmetrical 1,4-dihydropyrrolo[3,2-*b*]pyrroles using 2-formyl-1-methylpyrrrole (**2**) as substrate.[16] To begin with, these authors used a similar synthetic route starting from the condensation reaction of **2** with ethyl azidoacetate followed by intramolecular cyclization through a nitrene intermediate to form pyrrolopyrrole **5** as described in the previous cases (Schemes 1 and 5). Bromination was performed on this compound at −40 °C using *N*-bromosuccinimide (NBS) to form two regioisomers **16** and **17** with 6-brominated compound **17** as the major product (1:7 ratio). The mixture of these highly reactive isomers was then directly subjected to

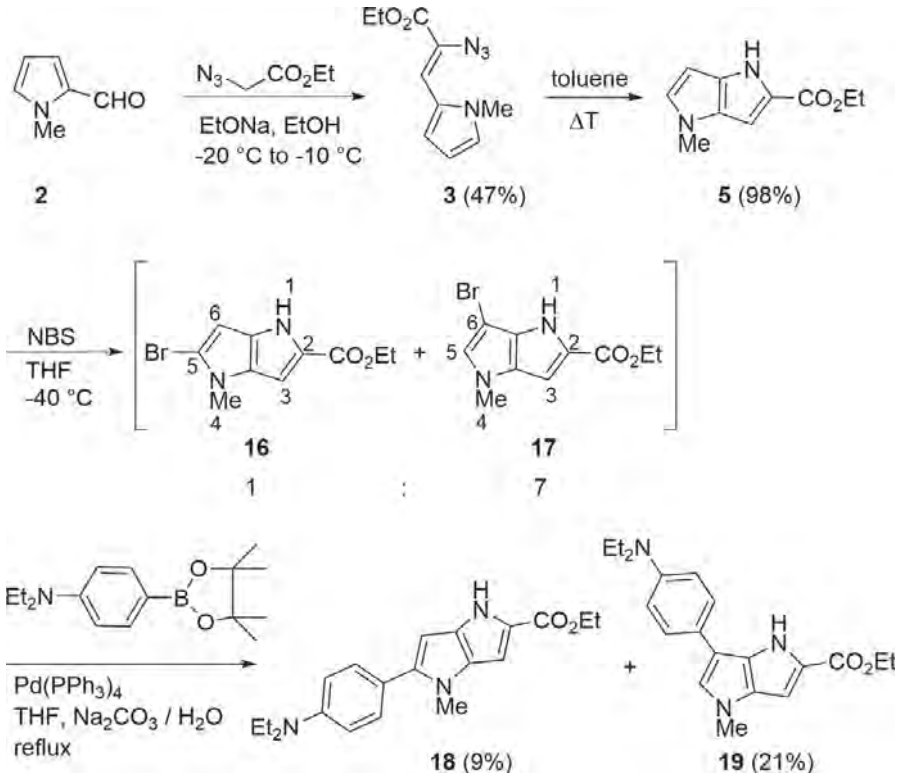

Scheme 5 Synthesis of 1,4-dihydropyrrolo[3,2-*b*]pyrroles with unsymmetric pattern of substituents.

Suzuki coupling to synthesize 1,4-dihydropyrrolo[3,2-*b*]pyrroles **18** and **19** with asymmetrical substitution of aryl group.

Metal-mediated nitrogen transfer reactions of azides can be considered as an improved alternative method for the nitrogen-containing heterocycles' synthesis. Although the production of nitrenes by thermolysis of azides is an effective method, the release of large amounts of nitrogen gas at high temperatures is always associated with an explosive hazard. Dirhodium(II) carboxylate ($Rh_2(O_2CC_3F_7)_4$) was identified as the catalyst of choice for such C—H amination reactions.[17] The proposed catalytic cycle is shown in Scheme 6. According to this mechanism, dirhodium(II) salt coordinates with azide **20** to generate metal complex **21**. Upon the release of nitrogen, the nitrene intermediate **22** undergoes C—N bond formation by stepwise electrophilic aromatic substitution via arenium cation **23**. Under optimal conditions, namely toluene as solvent at 40 °C, this reagent catalyzed several transformations of vinyl azides into pyrrole fused systems including thieno[3,2-*b*]pyrrole and furo[3,2-*b*]pyrrole.

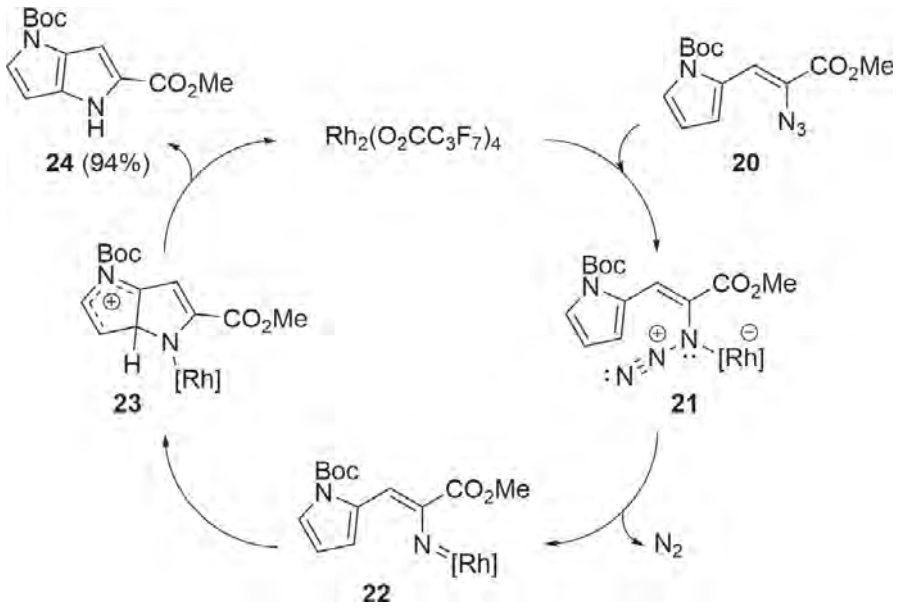

Scheme 6 Mechanism of rhodium-catalyzed 1,4-dihydropyrrolo[3,2-*b*]pyrrole synthesis. *Adapted with permission from* Chem. Asian J. ***2014**, 9, 3036–3045.*

An unexpected discovery of a thermal reaction leading to *N,N*-dimethyl-1,4-dihydropyrrolo[3,2-*b*]pyrrole occurred in Prinzbach group in 1975 (Scheme 7).[18] Authors studied the thermal isomerization of trimethyl-*cis*-triaza-tris-σ-homobenzene **25** to trimethyl-triazacyclo-octatriene **26**. When the compound **26** was heated up to 150 °C in benzene, they observed the formation of the DHPP **27** as the major product.

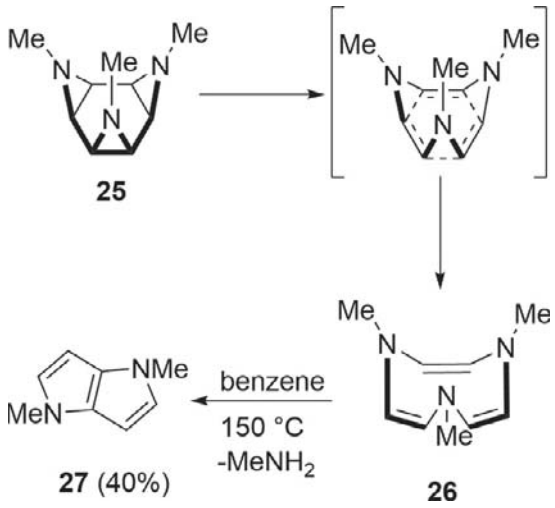

Scheme 7 Prinzbach discovery of the formation of pyrrolo[3,2-*b*]pyrrole **27**. *Adapted with permission from* Chem. Asian J. ***2014**, 9, 3036–3045.*

Fendesak and co-workers developed an interesting method involving alcoholysis of diazasilacyclopentene (**29**, Scheme 8).[19] Compound **29** was prepared by lithium metal reduction of 1,4-diaza-1,3-diene (**28**), followed by condensation with dichlorodimethylsilane. Silyl deprotection of diazasilacyclopentene was performed by dissolving in EtOH, leading to two tautomeric forms of **30**. The subsequent condensation step of **30** led to 3-aminopyrrole **31**. When tetrahydrofuran was used as solvent with simultaneous dropwise addition of EtOH, the 1,4-dihydropyrrolo[3,2-*b*] pyrrole **32** was formed as the major product.

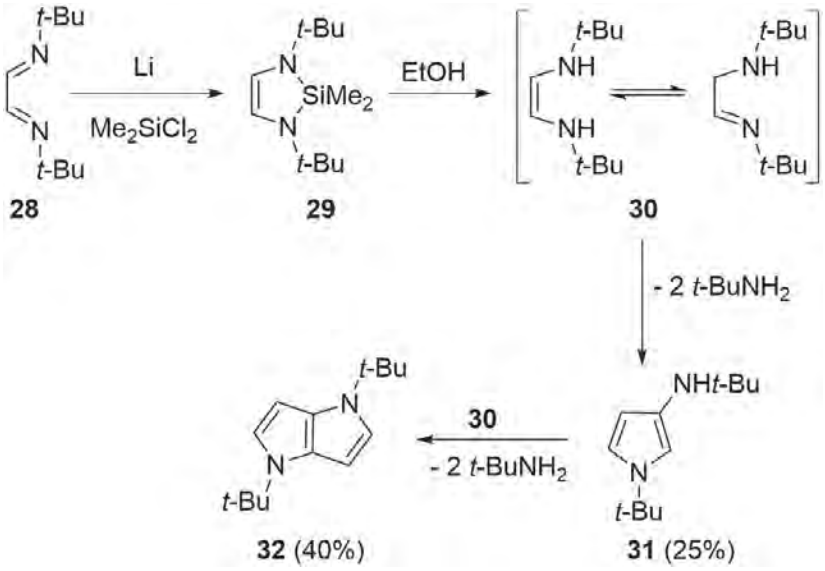

Scheme 8 Fendesak approach toward synthesis of DHPPs. *Adapted with permission from* Chem. Asian J. ***2014**, 9, 3036–3045.*

Borrowing hydrogen (BH) or hydrogen autotransfer (HA) reaction is an efficient and green method in alcohol activation.[20] Recent advances in this area made large contributions to the straightforward access to aza-heterocycles and their π-expanded analogs.[21] The Garrido group employed *ortho*- and *meta*- benzenediamine **33** to react with ethylene glycol using Pd/C or Pt/Al_2O_3 as the dehydrogenation catalyst and ZnO as co-catalyst which activates diol (Scheme 9).[22] Compounds **34** and **35** are formed from the respective diamines via acceptorless dehydrogenative condensation reaction (ADC). These authors later reported the same reaction using the *para* isomer as the substrate to form 1,4-tetrahydropyrrolo[3,2-*b*]pyrroles **36** from two units of benzene-1,4-diamine and three units of ethylene glycol.[22]

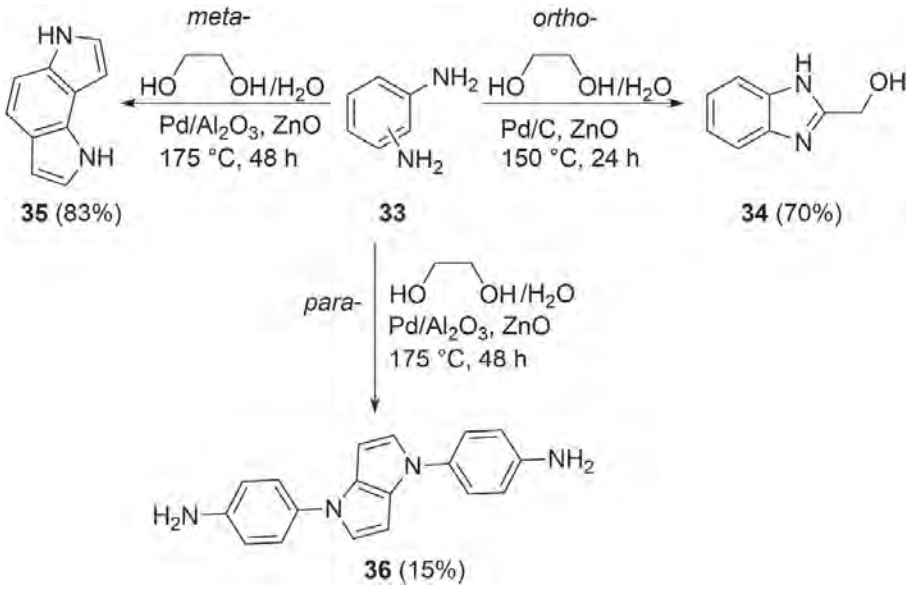

Scheme 9 Synthesis of aza-heterocycles via ADC reaction.

As a part of further studies to expand the substrate scope of this method, the same group performed this reaction using mono- and diaminopyridines as model substrates (Scheme 10).[23] Under the same conditions as before, 2,6-diaminopyridine (**37**) reacted with ethylene glycol to form azaindoles **38**. However, in the case of 2-aminopyridine (**39**), the formation of a pyridine-substituted DHPP **40a** was observed in 4% yield together with a byproduct **40b**. The drastic decrease in the electron density in the absence of second amino group, possibly prevents the electrophilic aromatic substitution on the pyridine ring in this case.

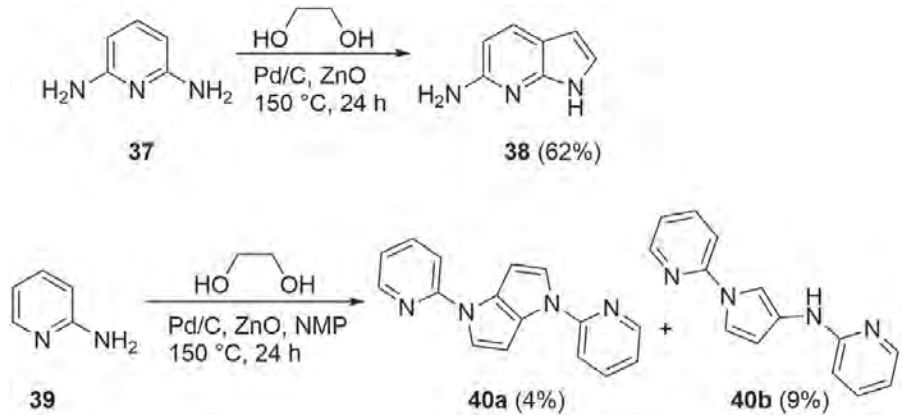

Scheme 10 Transformation of 2-aminopyridines into DHPP **40a** and other heterocycles.

Although discovered in 1972, DHPPs remained almost unknown for several decades. That was mainly due to the substantial drawbacks of the existing synthetic protocols. In general, low-yielding, extremely narrow in scope, multistep methodologies limited the utilization of these 10π-electron heterocycles in diverse fields of the research.

The studies on DHPPs significantly accelerated in 2013, as a consequence of the report on serendipitous transformation of simple building blocks into 1,2,4,5-tetraaryl-1,4-dihydropyrrolo[3,2-*b*]pyrroles (TAPPs).[24,25] Janiga et al. observed precipitation of a highly fluorescent compound whilst reacting 4-cyanobenzaldehyde **41** with *p*-toluidine **42** and butane-2,3-dione **43** under the conditions for Debus-Radziszewski imidazole synthesis. The comprehensive investigation of this side-product allowed for its structure assignment as 2,5-bis(4-cyanophenyl)-1,4-bis(4-methylphenyl)-1,4-dihydropyrrolo[3,2-*b*]pyrrole **45** (Scheme 11). The imidazole **44** is also formed in low yield.

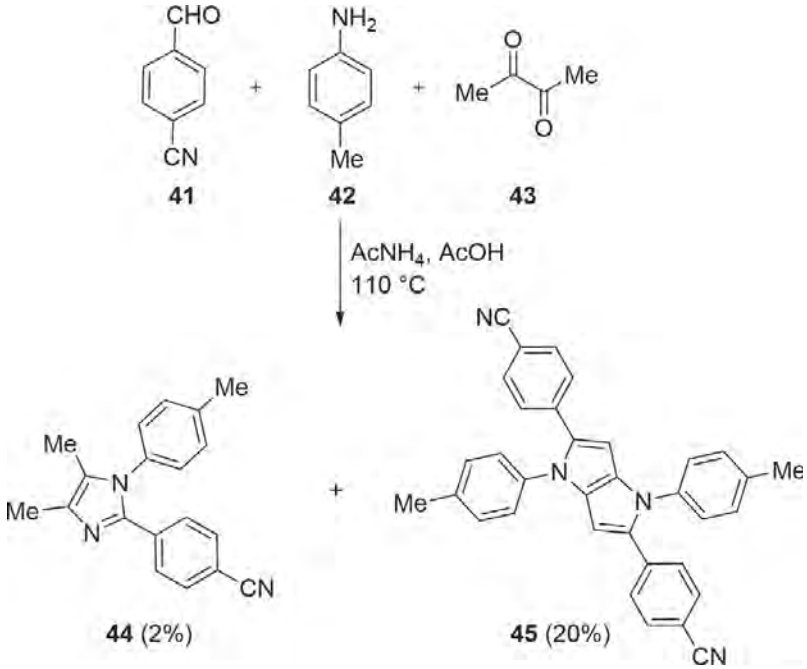

Scheme 11 The synthesis of 2,5-bis(4-cyanophenyl)-1,4-bis(4-methylphenyl)-1,4-dihydropyrrolo[3,2-*b*]pyrrole under Debus-Radziszewski conditions.

Intrigued by this novel multicomponent reaction, the Gryko group initiated studies toward its plausible mechanism. Two possible pathways were originally considered with the initial step proceeding through either formation of the Schiff base from parent aniline and aldehyde or alternatively the aldol condensation of the aldehyde with butane-2,3-dione.

Nevertheless, early-stage experiments have shown that both formed in situ and pre-prepared imine afforded the desired TAPPs. In contrast, subjecting α,β-unsaturated ketone obtained from 4-methoxybenzaldehyde and butane-2,3-dione to *p*-toluidine did not lead to the corresponding TAPP. This finding ruled out the pathway based on the aldol condensation of the aldehyde with butane-2,3-dione as the initial step.[24]

Thus, the reaction proceeds most likely through the formation of the Schiff base followed by Mannich-type addition of butane-2,3-dione to the imine. The next steps remain rather uncertain, probably being the sequence of cyclization with the five-membered ring formation, nucleophilic attack of the cyclic intermediate at the second molecule of Schiff base, followed by cyclization to give tetrahydropyrrolo[3,2-*b*]pyrrole and final dehydrogenation to the TAPP (Scheme 12).[26]

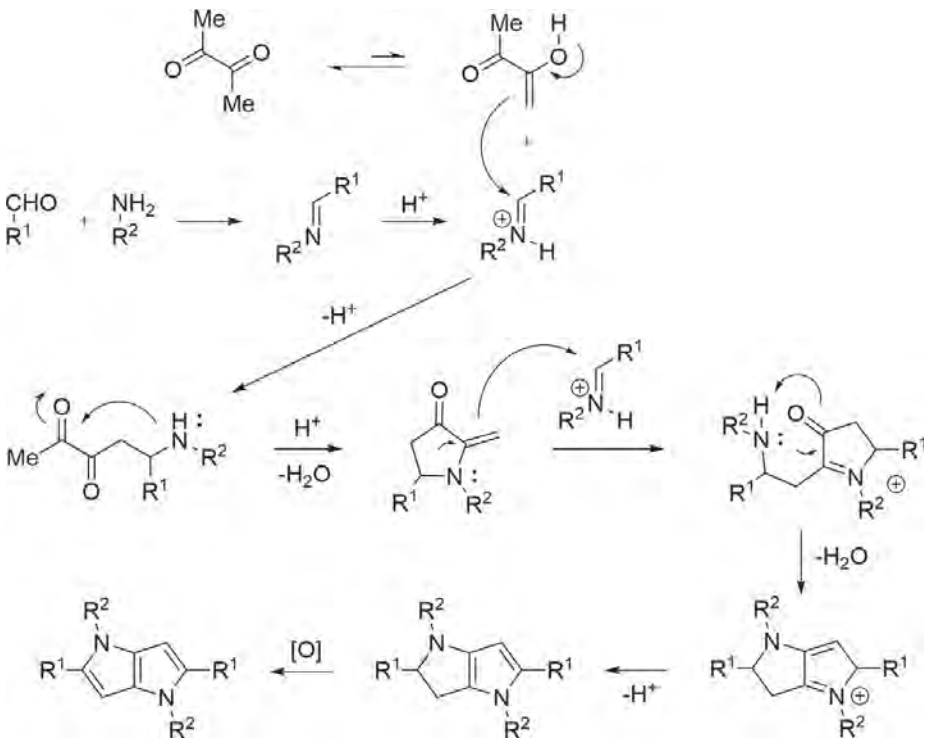

Scheme 12 Proposed mechanism of TAPP synthesis.

The clear evidence for final step came from the isolation of unoxidized tetrahydropyrrolo[3,2-*b*]pyrrole from the reaction of 2,6-dichlorobenzaldehyde with 4-*tert*-butylaniline and butane-2,3-dione;[27] as well as from the reactions performed under inert atmosphere. Nevertheless, the nature of oxidant is to date debatable. Most likely it is oxygen from air because reactions are

conducted without external oxidants in the open flask manner. All the efforts to improve the reaction outcomes under these originally developed reaction conditions by the addition of different oxidants (e.g., $Ce(NH_4)_2(NO_3)_6$, DDQ, *p*-chloranil, DMSO, $PhNO_2$, *etc.*) at various stages unfortunately failed.[26]

The studies toward scope and limitations of the developed methodology were performed under the optimal stoichiometry and conditions (aldehyde/amine/butane-2,3-dione ratio 2:2:1; in AcOH, 90 °C for 3 h, Fig. 2). The highest yield (34%) was observed for electron-neutral 4-methylbenzaldehyde and *p*-toluidine. In general, TAPPs were synthesized more efficiently from electron-neutral or electron-poor aldehydes than from electron-rich

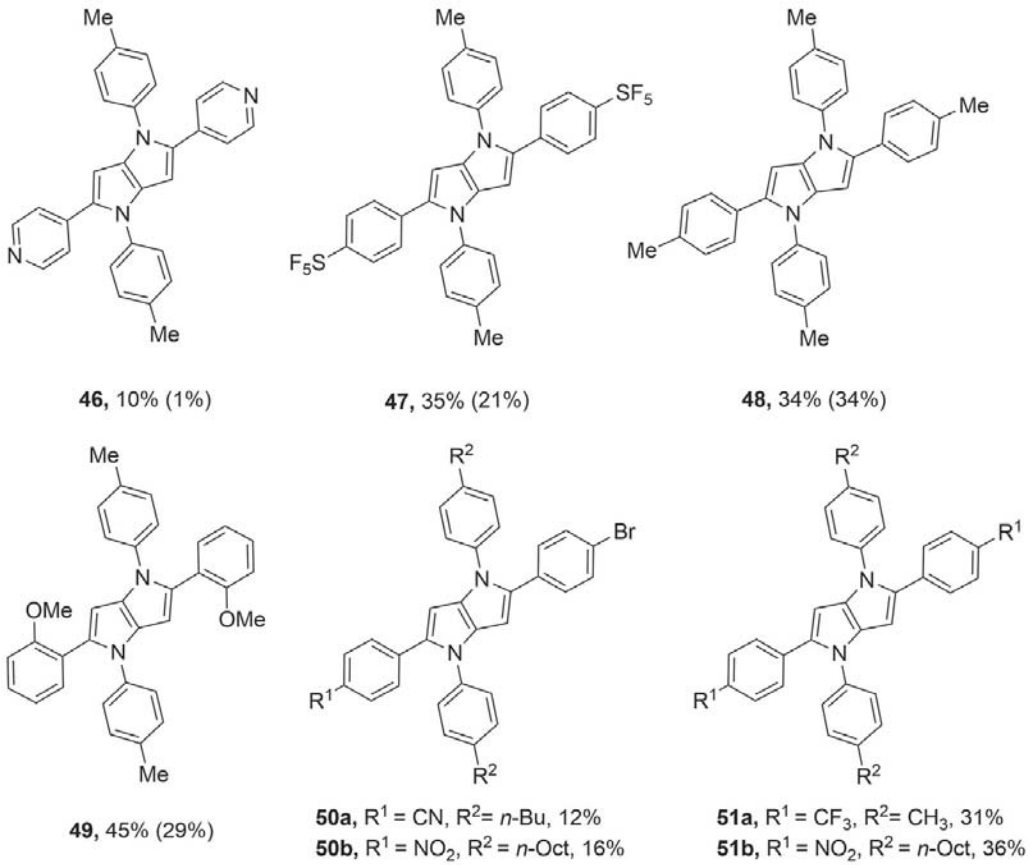

Fig. 2 Selected TAPPs prepared under TsOH-catalyzed conditions[25,28,29] (yields in parenthesis obtained with noncatalyzed protocol).

aromatic aldehydes. The reactivity of anilines with 4-methylbenzaldehyde and butane-2,3-dione was also contingent on their electronic character, increasing in the order: 4-NO_2 (11%) < 4-Br (15%) < 4-Me (34%). Noteworthy, in case both counterparts were electron rich, the corresponding TAPP suffered from the lack of stability that was mirrored in the reaction outcomes.[24]

Despite rather mediocre yields (up to 34%), this methodology possesses numerous advantages such as striking simplicity of the synthetic protocol (one-pot synthesis), good functional group tolerance and no need of tedious column chromatography.[24] Further attempts to increase the yield by changing solvent (EtOH, THF, DMF, acetonitrile, toluene) as well as by utilizing catalytic amounts of either Lewis or Brønsted acids proved that AcOH in a combination with *p*-toluenesulfonic acid was the most beneficial.[28] Modified reaction conditions allowed for the smooth reaction of aromatic aldehydes bearing electron-withdrawing and electron-donating groups with electron-rich or electron-neutral anilines (see products **46**–**51** in Fig. 2). In reaction with *p*-toluidine and butane-2,3-dione the best outcomes were observed for sterically demanding aldehydes (2-Br, 49% and 2-OMe, 45%) as well as for those bearing 4-CN and 4-SF_5 groups (37% and 35%, respectively). It is noteworthy that optimized conditions allowed for the introduction of heterocyclic units possessing basic nitrogen atoms (pyridyl and thiazolyl) as well as thienyl, benzothienyl and benzofuryl groups. Unsymmetrical TAPPs can also be obtained under TsOH-catalyzed conditions, however in a statistical manner, by mixing two aldehydes with similar reactivity (Fig. 2).[29, 30] Unfortunately, the scope of this methodology possesses several limitations. All the attempts with 1,4-dibromobutane-2,3-dione, hexane-3,4-dione as well as aliphatic amines and aldehydes gave no expected products. Moreover, the endeavors to introduce furyl, indolyl and pyrroyl substituents into positions 2 and 5 of the DHPP core were unsuccessful.[25]

Noteworthy, in the case of polycyclic aromatic substrates displaying miserable solubility in AcOH even at the elevated temperature, the use of toluene as a cosolvent considerably improved the reaction outcomes (Scheme 13).[31] Moreover, to enhance the solubility of the obtained TAPPs, aromatic amines with long alkyl chains (e.g., *n*-octyl, *n*-decyl or *n*-dodecyl) as well as *t*-butyl groups were chosen.

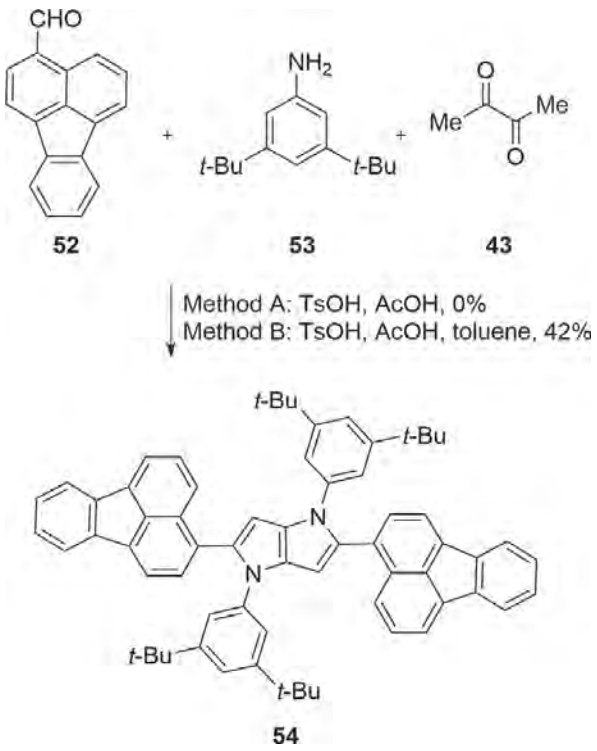

Scheme 13 Improved synthesis of TAPP **54** from polycyclic aromatic aldehyde **52** and amine **53**.

Prepared TAPPs were quickly perceived to have high potential due to their promising photophysical properties. Thus, moderately yielding synthetic protocols demanded further optimalization. The screening of various organic and inorganic catalysts (*L*-proline, TFA, TfOH, H_2SO_4, $AlCl_3$, $FeCl_3$, $Sc(OTf)_3$, $Eu(OTf)_3$, $Mn(OTf)_2$, $Bi(OTf)_3$, $Cu(OTf)_2$, $Zn(OTf)_2$, etc.) showed that catalytic amounts of iron(III) salts, such as $Fe(OTf)_3$ or $Fe(ClO_4)_3{\cdot}H_2O$, have significant influence on the reaction outcomes, affording up to two-fold yield improvement (77% versus 37% for the TsOH-catalyzed procedure in the case of 2,5-bis(4-cyanophenyl)-1,4-bis(4-methylphenyl)-1,4-dihydropyrrolopyrrole).[27] It is possible that iron(III) triflate and iron(III) perchlorate, in contrast to other tested salts, positively impacted not only on activation of imines but also on enhancement of the final oxidation step. However, taking into the consideration similar catalytic activity but significant price difference, iron(III) perchlorate was chosen for the further studies.

In general, reactivity of anilines under the $Fe(ClO_4)_3$-catalyzed protocol predominantly decreases with the increased electron-withdrawing character

of the substituent (4-Me (77%) > 4-Br (64%) > 4-CN (30%), in the reaction with 4-cyanobenzaldehyde and butane-2,3-dione). Steric effects also play an important role in the reactivity of the aniline counterpart. For example, 3,5-bis(*tert*-butyl)aniline led to the expected TAPP in significantly lower yield compared to *p*-toluidine in the reaction with 2-formylbenzothiophene (12% versus 46%). Noteworthy, this synthetic protocol allowed for first time to transform 3,5-bis(trifluoromethyl)aniline and 1-aminonaphthalene into the corresponding products in reaction with 4-cyanobenzaldehyde and butane-2,3-dione with 48% and 32% yield, respectively. It is also worth underlining that for the majority of aldehydes the relative yield increase was observed; however, for the electron deficient ones it was the most pronounced. The significant improvement of the reaction outcomes is particularly notable in case of five-membered aromatic aldehydes and their benzo analogues.[27]

The use of iron perchlorate as a catalyst also permitted the unprecedented transformation of hexane-3,4-dione **55**, leading to DHPP **56** possessing methyl groups at positions 3 and 6 in a single step (Scheme 14).[27]

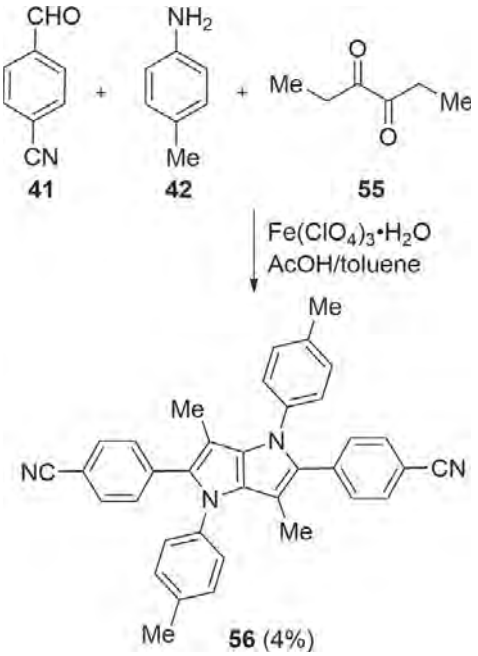

Scheme 14 Synthesis of 3,6-disubstituted TAPP.

Interestingly, niobium pentachloride was reported by Martins et al. to have superior catalytic activity in room temperature synthesis of various

TAPPs.[32,33] Reportedly good to excellent reaction outcomes were achieved in the presence of 25 mol% of $NbCl_5$ for a range of 4-substituted benzaldehydes and amines with a number of functional groups (Me, OMe, Hal, CO_2Me, etc.) being tolerated. Among others, *p*-toluidine displayed the highest reactivity with butane-2,3-dione and aromatic aldehydes bearing 4-OMe, 4-Cl, 4-Br and 4-SMe groups, yielding the corresponding TAPPs in 98%, 95%, 92% and 98% yield, respectively. All attempts by the Gryko group to repeat these multicomponent reactions with $NbCl_5$ in acetonitrile failed to give even trace quantities of TAPPs. We found however that $NbCl_5$ is reasonably good catalyst in AcOH/toluene mixture (vide infra).

It is noteworthy that TAPPs were also formed at ambient temperature in the $Fe(ClO_4)_3$-catalyzed reactions, albeit with somewhat lower yields (e.g., 52% versus 72% in case of the 2,5-bis(4-cyanophenyl)-1,4-bis(4-methylphenyl)-1,4-dihydropyrrolo[3,2-*b*]pyrrole). Interestingly, significant prolongation of the reaction time (up to 64 h) gave better outcomes, but at the same time decreased the synthetic utility of this methodology. Thus, elevated temperature (50 °C), allowing to minimize the loss of butane-2,3-dione (b.p. 88 °C) in the reaction course, proved to be optimal and led to the desired TAPPs in high yields within 16 h. Additional catalyst screening ($Fe(OTf)_2$, $Fe(OAc)_2$, $Fe(acac)_3$, $HClO_4$, $VO(acac)_2$, CeF_4, $NbCl_5$, $Mn(OTf)_2$) did not outperform the catalytic activity of $Fe(ClO_4)_3{\cdot}H_2O$.[34]

The above-mentioned synthetic protocol ($Fe(ClO_4)_3{\cdot}H_2O$, AcOH/toluene, 50 °C, 16 h) gave equal or higher outcomes for both electron-rich, neutral and deficient aldehydes and amines tested.[34] It is worth emphasizing that significant scope expansion was observed in this case. For the first time sterically demanding anilines (2-Cl, 2-Br and 2-CN) as well as electron-rich aromatic aldehydes (3-OH, 4-OH, 4-OMe, $4\text{-}NMe_2$, 4-OH-3,4-diMe) were converted into the corresponding TAPPs with up to 34% yields. The library of aldehydes was also expanded to pyrrole and quinoline derivatives, albeit the yields of the corresponding TAPPs were rather moderate (up to 32%). Nevertheless, one of the biggest breakthroughs was achieved with amine **58** and the 4-formyl-6,7-dimethoxycoumarin **57** – first formally nonaromatic aldehyde converted into the desired TAPP **59** in 39% yield (Scheme 15).

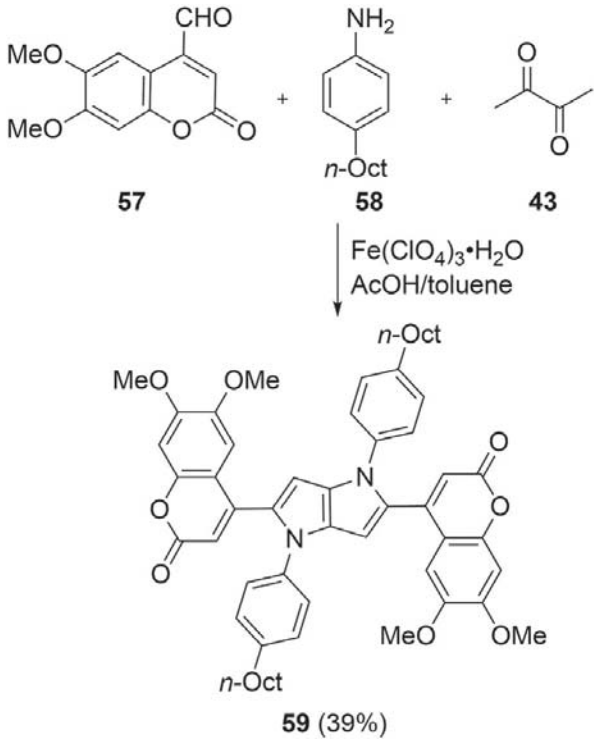

Scheme 15 Synthesis of first TAPP derived from formally nonaromatic aldehyde.

The progress in this methodology since 2013 has been tremendous and the scope of both aromatic amines and aromatic aldehydes has been expanded (Fig. 3). At the same time however, many challenges remain and various substrates, especially amines cannot be presently transformed into TAPPs (Fig. 3).

The synthetic utility of $Fe(ClO_4)_3$-catalyzed protocol has also been demonstrated for pyrrolo[3,2-*b*]pyrroles synthesized on a 40 mmol scale, e.g., **48**, **60**–**62** (Fig. 4). All performed experiments did not show significant loss of the substrates' reactivity and required no additional complex work up.[34,35]

The synthesis of 1,4-dihydropyrrolo[3,2-*b*]pyrroles has experienced rapid evolution during the last decade. The breakthrough discovery on the multicomponent reaction between butane-2,3-dione, aromatic aldehydes and anilines gave a new breath to this area of research.

3. Reactivity

3.1 Simple derivatization

The DHPP core possessing two fused pyrrole rings is the most electron-rich system of the 10π electron heteroaromatic compounds. Due to its electron-donating properties, 1,4-dihydropyrrolo[3,2-*b*]pyrrole has a strong

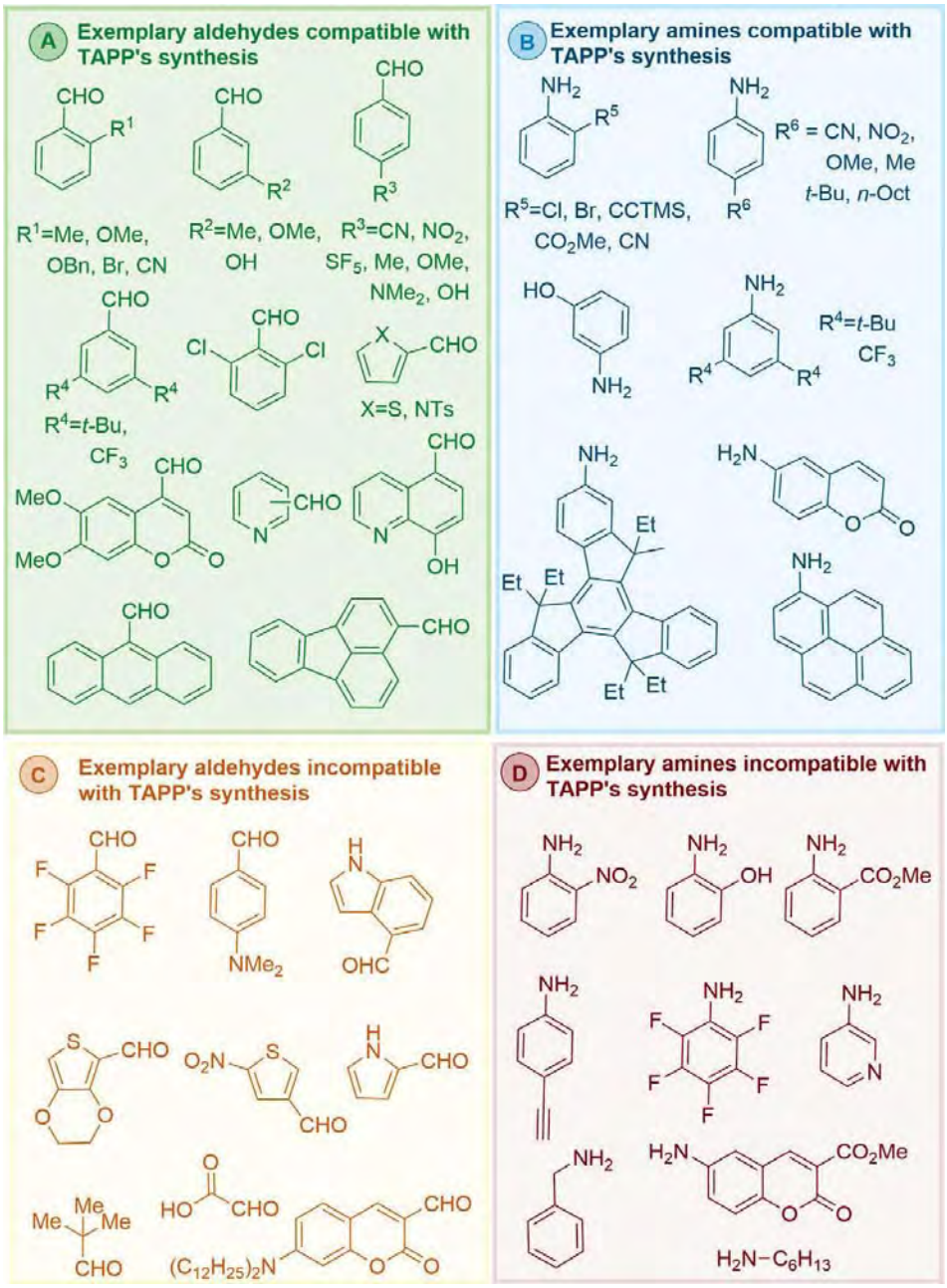

Fig. 3 The scope of aldehydes and amines compatible and incompatible with multicomponent reaction leading to TAPPs.

ability to undergo aromatic electrophilic substitution reactions especially in positions 3 and 6. Additionally, the DHPP skeleton allows the introduction of six peripheral substituents, which can be further modified to construct organic functional molecules. Unsubstituted DHPP is air sensitive and unstable, especially in acidic environments, decomposing to blue polymeric

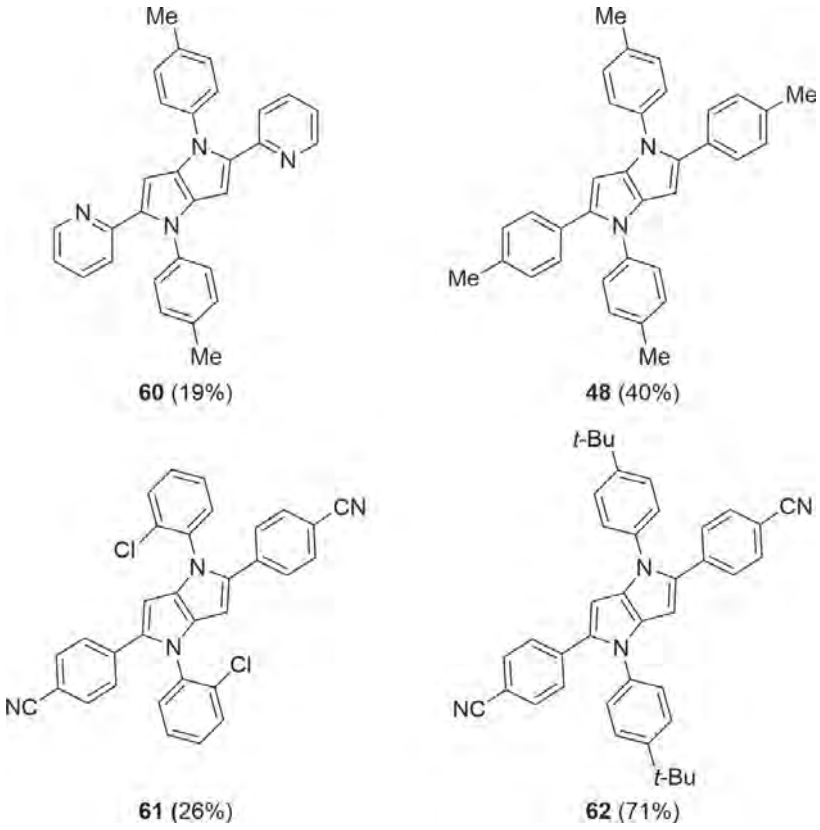

Fig. 4 Synthesis of selected TAPPs on the 40 mmol scale.

material.[36] Treatment of the 3,6-di-*tert*-butyl derivative **63a** with conc. HCl at 255–260 °C produces gold plates which most probably are the α-protonated form **63b** with a $pK_a = 3.6$ (determined by UV in H_2O, Scheme 16). This basicity is comparable to a pK_a of typical aromatic amines and it is much stronger than for pyrrole and indole. Additionally, the introduction of methyl groups on the nitrogen atom reduces the basicity.

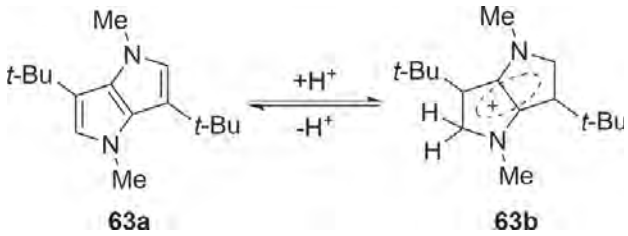

Scheme 16 The protonation of 1,4-dihydropyrrolo[3,2-*b*]pyrrole **63a**.

1,4-Dihydropyrrolo[3,2-*b*]pyrroles can undergo typical reactions of aromatic compounds, especially electrophilic aromatic substitution. The Gryko group has provided a few examples of electrophilic aromatic substitution

that takes place in positions 3 and 6 of 1,2,4,5-tetraaryl-1,4-dihydropyrrolo [3,2-*b*]pyrroles. Under mild conditions, compound **64** was subjected to nitration with a mixture of nitric acid and acetic anhydride to give the dinitro-product **65** (Scheme 17).[37]

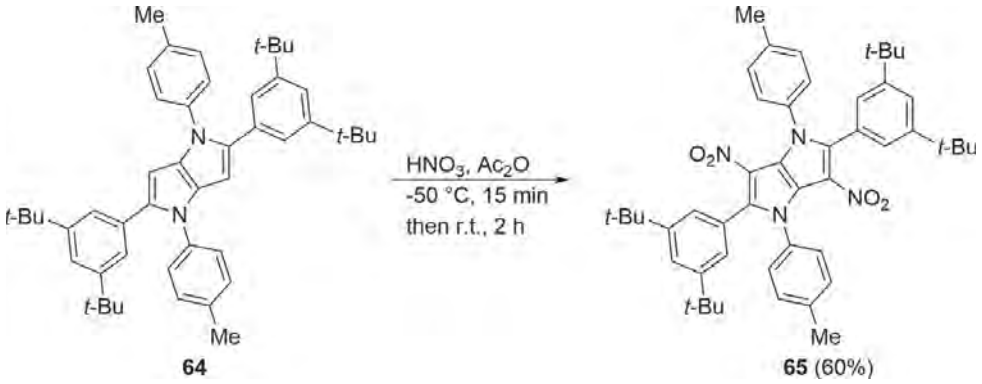

Scheme 17 The synthesis of 3,6-dinitro-TAPP **65**.

Tetraaryl-1,4-dihydropyrrolo[3,2-*b*]pyrroles, e.g., **62** and **67**, also react with Vilsmeier reagent ($POCl_3$/DMF) to give 3-formyl or 3,6-diformyl derivatives, e.g., **66** and **68**, depending on conditions and the character of the substituents (Scheme 18).[37, 38]

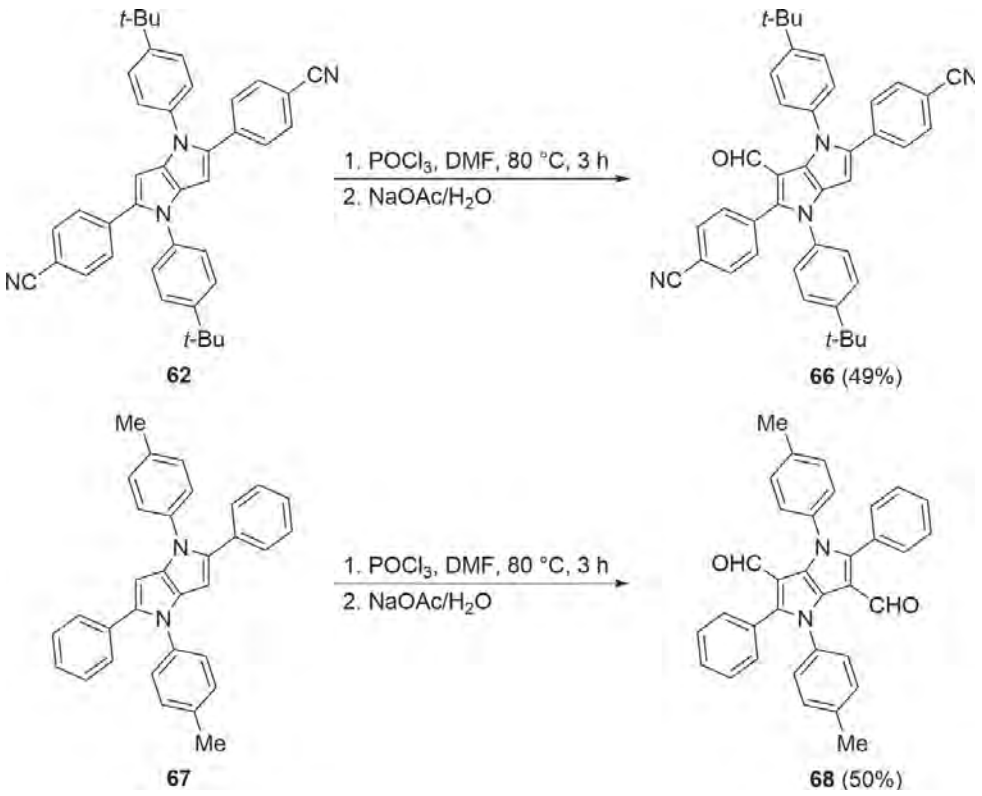

Scheme 18 Electrophilic aromatic substitution of TAPPs using Vilsmeier reagent.

In a manner similar to other pyrrole derivatives, direct cyanation of tetraaryl-1,4-dihydropyrrolo[3,2-*b*]pyrroles can be achieved using chlorosulfonyl isocyanate (CSI) followed by treatment with DMF. TAPP **67** reacts effectively with CSI in dichloromethane (DCM) followed by quenching with DMF to give 3,6-disubstituted TAPP **69** (Scheme 19).[37]

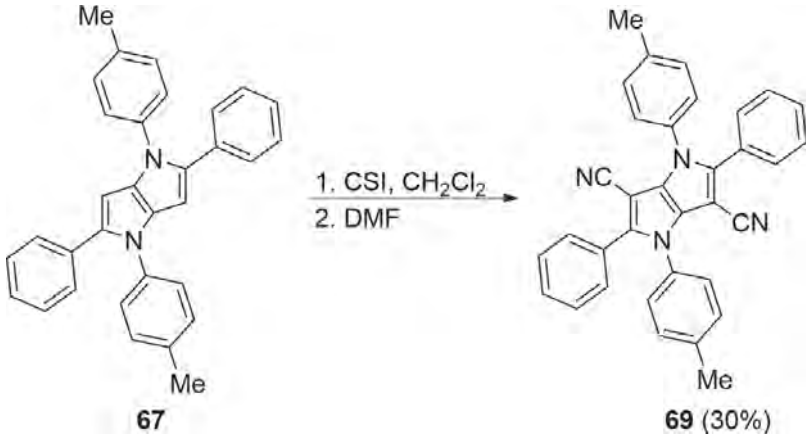

Scheme 19 The synthesis of 3,6-disubstituted TAPP **69**.

Satake and co-workers used 3,6-di-*tert*-butyl-1,4-dihydropyrrolo[3,2-*b*] pyrrole **70a** as substrate in the cyanation reaction to obtain the corresponding product **70b** with 50% yields (Scheme 20).[39]

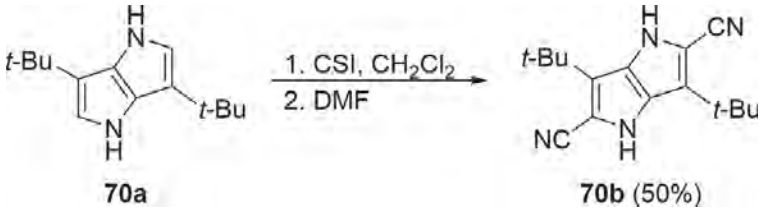

Scheme 20 The synthesis of 3,6-di-*tert*-butyl-1,4-dihydropyrrolo[3,2-*b*]pyrrole-2,5-dicarbonitrile (**70b**).

The *N*,*N*′-dimethoxycarbonyl derivative **14a** can also react with CSI under similar conditions, but it gives the anhydride **71**, the product of reaction between 2-chlorosulfonylcarbamoyl intermediate and a subsequent intramolecular elimination of *N*-methylsulfamoyl chloride (Scheme 21).[37] The solvolysis of this anhydride **71** in the presence of alcohol leads to the corresponding esters **72a** or **72b** in quantitative yields. Additionally, on heating in toluene compound **71** undergoes a self-condensation reaction to produce a pentacyclic product **73**.

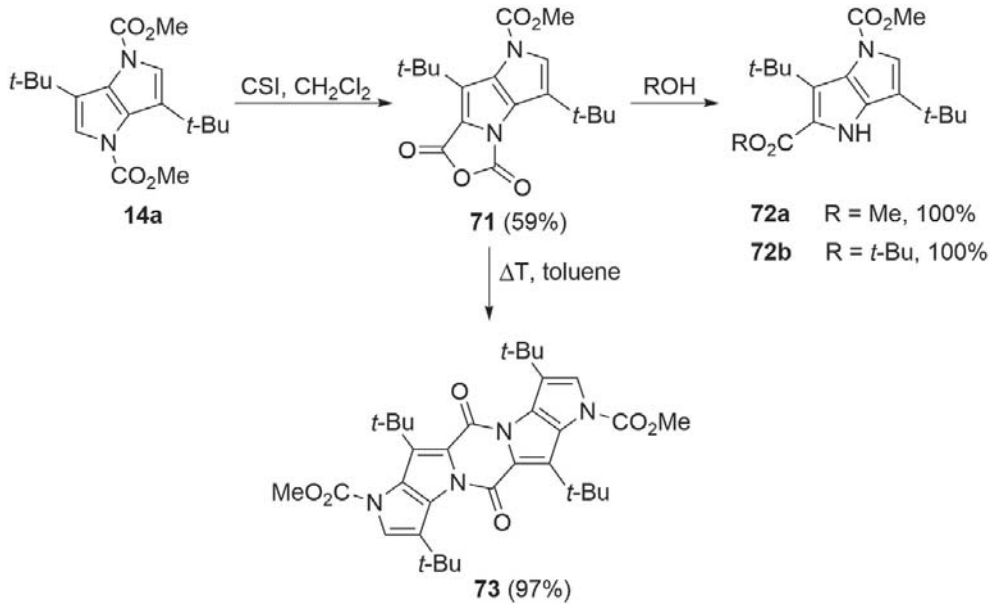

Scheme 21 Preparation of pentacyclic product **73**.

Gross and Wentrup obtained a similar product **75** using pyrolysis of 1,4-dihydropyrrolo[3,2-*b*]pyrrole carboxylic acid ester **74** at 850 °C followed by dimerization at a temperature below −80 °C (Scheme 22).[40]

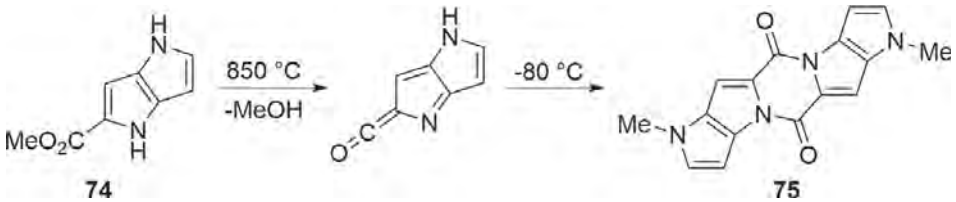

Scheme 22 Pyrolysis of 1,4-dihydropyrrolo[3,2-*b*]pyrrole carboxylic acid ester **74**.

1,2,4,5-Tetraaryl-1,4-dihydropyrrolo[3,2-*b*]pyrroles have been subjected to halogenation reactions which provide the corresponding 3,6-disubstituted derivatives with reasonable yields. There are many different methods for the iodination of heteroaromatic compounds. In the case of TAPP **67**, the preparation of the diiodo derivatives, e.g., **76**, was only possible with the use of *N*-iodosuccinimide (NIS) as an iodination agent (Scheme 23).[37]

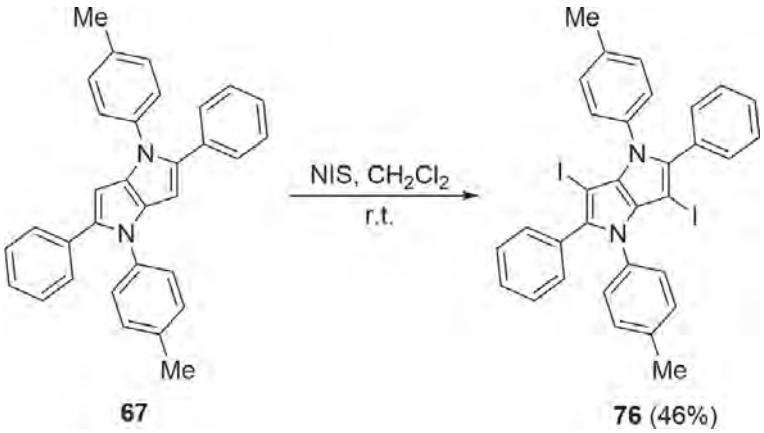

Scheme 23 Iodination of TAPP **67**.

Gryko and co-workers described regioselective chlorination at the 3 and 6 positions of the 1,2,4,5-tetraaryl-1,4-dihydropyrrolo[3,2-*b*]pyrroles **77**. A solution of *N*-chlorosuccinimide (NCS) in DCM was used as the chlorinating agent (Scheme 24).[41]

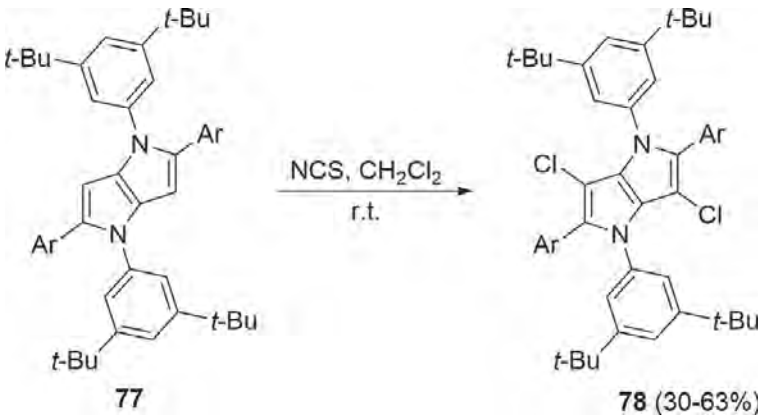

Scheme 24 Chlorination of TAPPs **77**.

Dibromosubstituted TAPP **79** can be obtained by treating TAPP **67** with *N*-bromosuccinimide in a mixture of DCM/MeOH in the presence of pyridine (Scheme 25).[37,42]

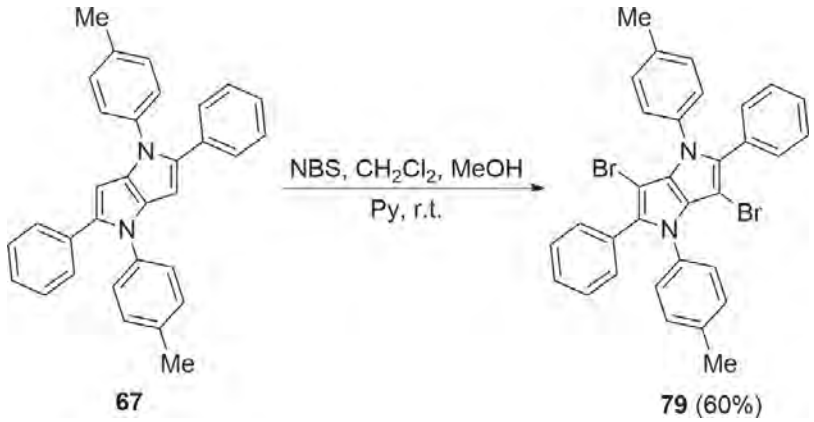

Scheme 25 Bromination of TAPP **67** (Py = pyridine).

The reactions of many pyrrole derivatives with the most reactive electrophilic reagents, such as trifluoroacetic anhydride (TFAA) or cyanuric chloride, proceed even without a catalyst. However, experiments conducted by Gryko and co-workers show that despite the electron-rich nature of the core, TAPPs do not react with these reagents.[37]

In 1985 Mukai and co-workers treated DHPP **14a** with two equivalents of NBS in dioxane containing 1% water for 1 h at room temperature, and the oxidized product **80** was obtained in excellent yield (90%).[43] Further addition of NBS (2 equiv.) leads to the formation of bicyclic lactam **81**. Hydrolysis and decarboxylation of **81** in a methanolic solution of KOH gave the deprotected compound **82** as yellow crystals with poor solubility in common organic solvents (Scheme 26).

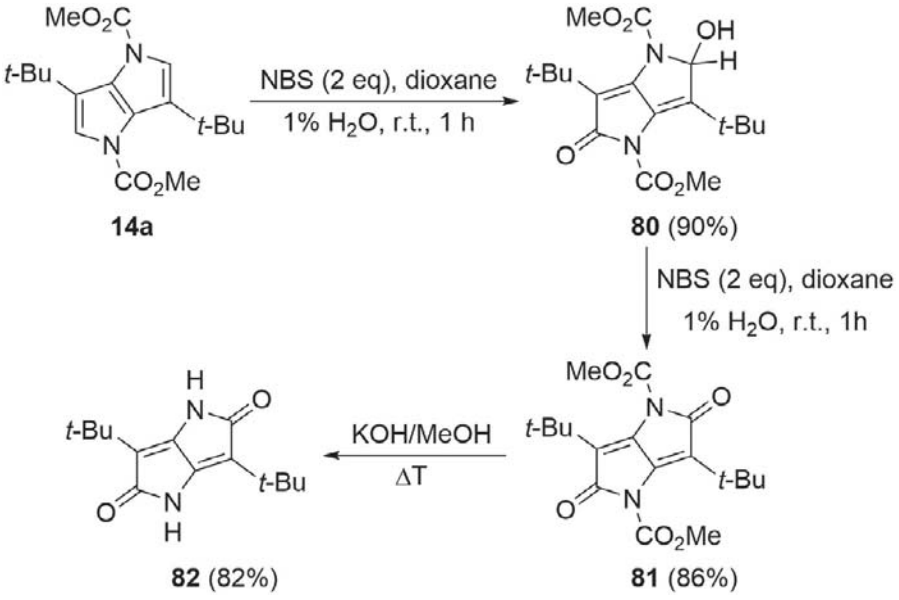

Scheme 26 Oxidation of DHPP **14a**.

Oxidation of 3,6-di-*tert*-butyl-1,4-dihydropyrrolo[3,2-*b*]pyrrole (**70a**) with NiO_2 easily gave 3,6-di-*tert*-butyl-1,4-diazapentalene (**70c**).[44] The product with 8 π-electrons exhibited anti-aromatic character and can be readily reduced back with hydroquinone (Scheme 27).

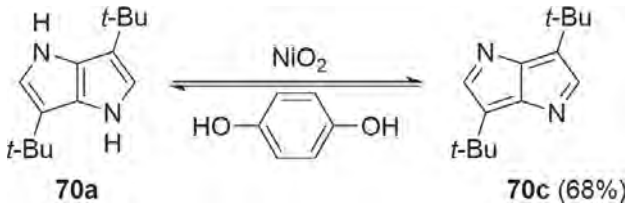

Scheme 27 Oxidation of DHPP **70a**.

Olivier and co-workers synthesized the ditungsten biscarbene complex of **83** with reasonable stability in the solid and solution under inert atmosphene.[45] Similar to thieno[3,2-*b*]thiophene, *N*-substituted derivatives of DHPP also undergo double lithiation with *n*-BuLi at positions 2 and 5. The dilithiated substrate was reacted with $W(CO)_6$ followed by alkylation with $Et_2O{\cdot}BF_3$ to obtain the ditungsten biscarbene product **83** in moderate yield. The complex was studied in terms of optoelectronics, charge transfer and communication between metal atoms. The methyl substituents on the nitrogen atoms play an important role in determining the molecular configurations (Scheme 28).

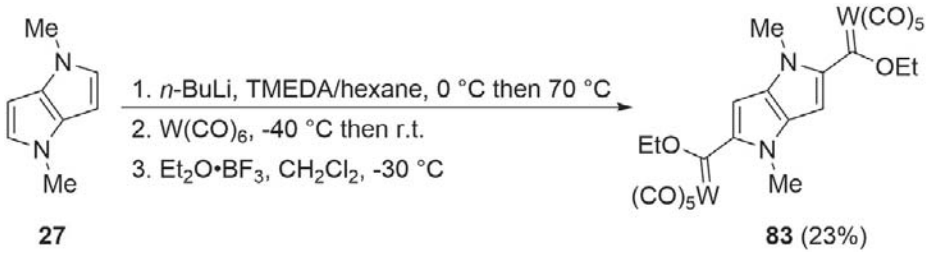

Scheme 28 Synthesis of ditungsten biscarbene **83**.

Satake and co-workers found that 3,6-disubstituted-1,4-dihydropyrrolo [3,2-*b*]pyrrole **63a** reacted with dimethyl acetylenedicarboxylate (DMAD) to form 2-vinyl-DHPP **84** together with 2,5-divinyl-1,4-dihydropyrrolo [3,2-*b*]pyrrole derivatives **85** (yields 31% and 5%, respectively).[46] The addition of excess of DMAD significantly improved the yield of the double-vinylated products (Scheme 29). The reaction indicates the strong electron-donating nature of DHPP, since both the indole and the pyrrole did not react with DMAD under similar conditions.

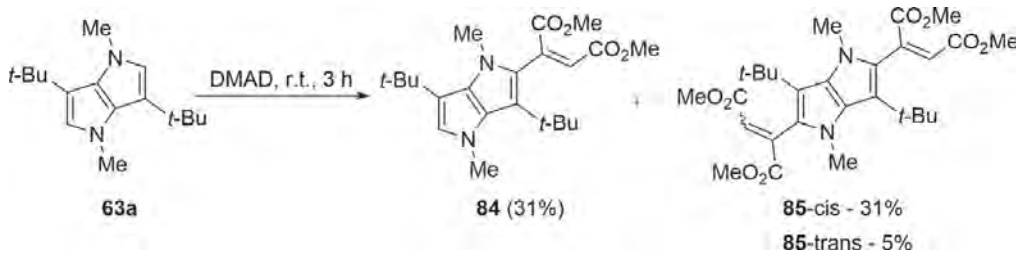

Scheme 29 Reaction of DHPP **63a** with DMAD.

Pd-catalyzed cross-coupling reactions are useful in the synthesis of TAPP-based chromophores. Suzuki reaction with organoboron compounds is an efficient method for the introduction of additional aryl substituents; however, it increases intramolecular steric repulsion, as evidenced by linear absorption and emission blue shift.[42] 3,6-Dibromo substituted TAPPs, e.g., **86**, react with various boronic acids in the presence of $Pd(PPh_3)_2Cl_2$ to give the corresponding hexaaryl-pyrrolo[3,2-*b*]pyrroles, e.g., **87**, in good yields (Scheme 30).

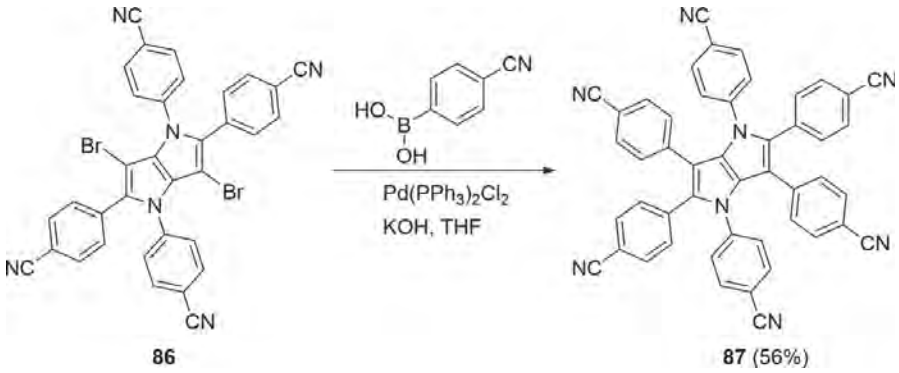

Scheme 30 Suzuki reaction of TAPP **86**.

Peripheral functional substituents on TAPPs can be used for further transformation leading to the expansion of the TAPP chromophore. Additionally, the electron-rich TAPP core can be utilized in the synthesis of A-D-A quadrupole systems, possessing interesting optical properties. In 2017, the first approach to obtain DHPP linked to two azulene moieties at positions 2 and 5 was developed (Scheme 31).[47] In the three-step synthesis (sequential N-arylation, ring-opening, and a reaction with cyclopentadiene), 2,5-bis(pyridyl)-1,4-dihydropyrrolo[3,2-*b*]pyrroles were transformed, via intermediates **89** and **92**, to the 2,5-bis(azulenyl)-1,4-dihydropyrrolo[3,2-*b*]pyrroles **90** and **93** characterized by bathochromically shifted absorption strongly dependent on the linkage position.

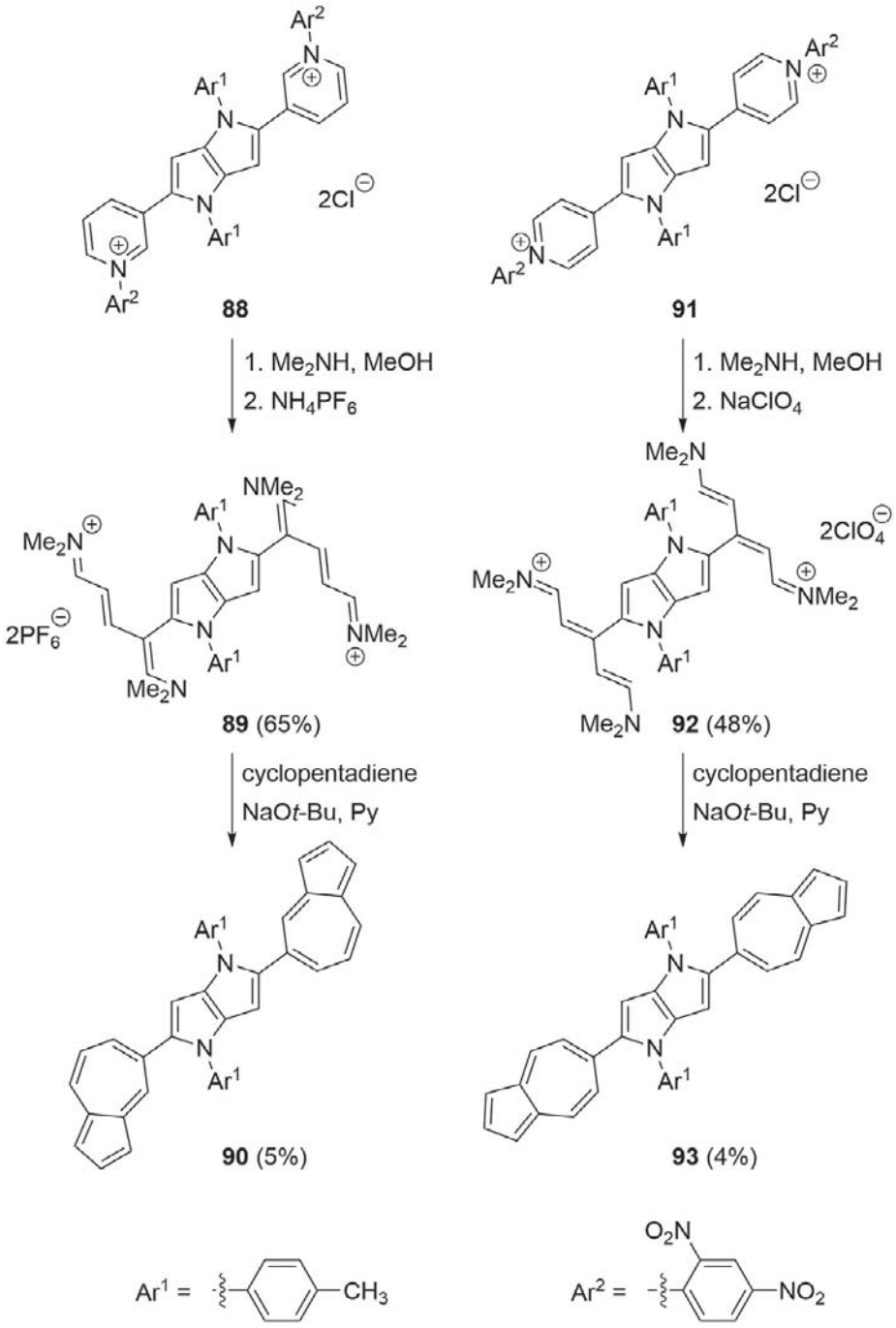

Scheme 31 Synthesis of 2,5-bis(azulenyl)-1,4-dihydropyrrolo[3,2-*b*]pyrroles **90** and **93**.

Ahn and co-workers utilized two pyridinium groups attached to the DHPP core (e.g., **94**–**97**) as both electron acceptors and water solubilizing groups (Scheme 32).[48] The introduction of such moieties on both sides of the electron-rich DHPP core changed the optical properties of the product.

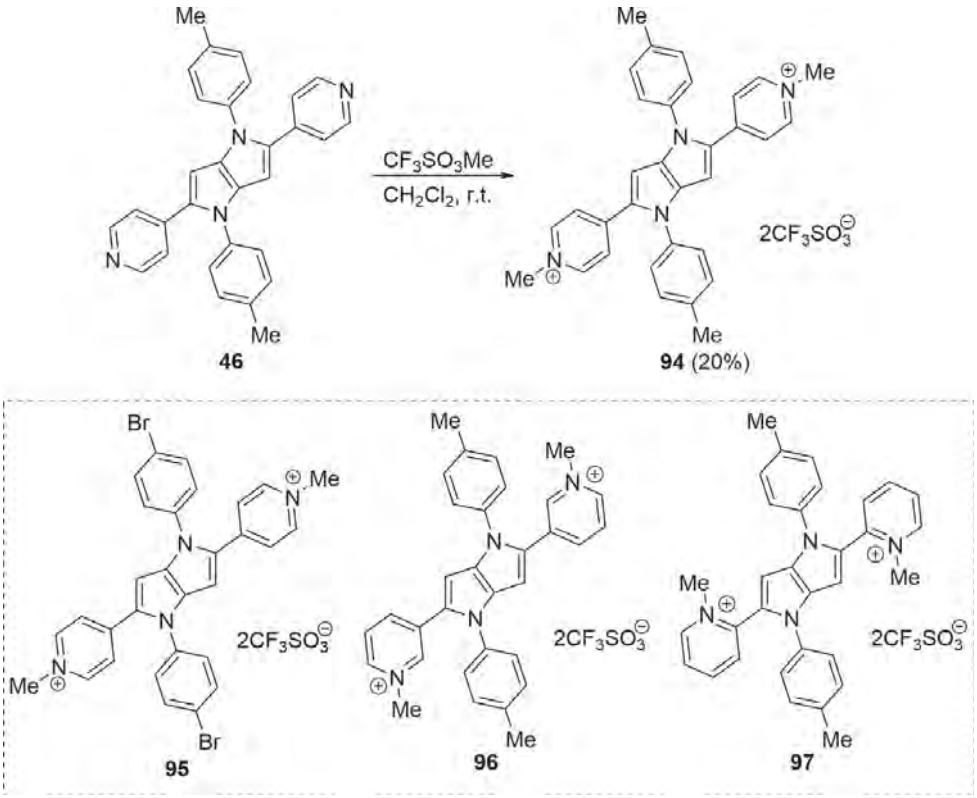

Scheme 32 Synthesis of TAPPs **94–97**.

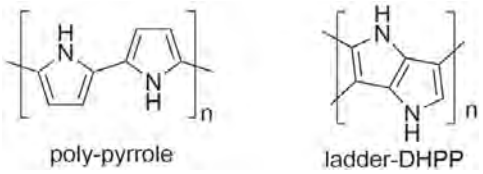

Fig. 5 Pyrrole-based polymers.

Conjugated polymers are of great interest due to their intriguing electronic properties that allow them to be applied in semiconducting devices. Oyama and *co*-workers reported that the electrooxidative polymerization of 1,4-dihydropyrrolo[3,2-*b*]pyrrole and its simple derivatives produced a polymeric form that was electroactive in both acetonitrile and water, but it was also sensitive to oxygen (Fig. 5).[49–51] Côté and *co*-workers performed a theoretical study of ladder-type DHPP polymers and compared them to poly-pyrrole polymers (Fig. 5).[52] The DFT calculations confirmed that the band gap in ladder-DHPP was lower than in poly-pyrrole. This phenomenon can be explained by the decrease of the bond length in the planar structure of the ladder-polymer, which causes a more favorable charge density distribution and guarantees better conductive properties.

3.2 Synthesis of π-expanded 1,4-dihydropyrrolo[3,2-*b*]pyrroles

3.2.1 Expansion via biaryl linkages and through carbon-carbon triple-triple bonds

One of the most modular strategies of π-expansion of a chromophore is by bridging it with another chromophore via a carbon-carbon triple bond. Such an increase in the molecular length of a chromophore is typically performed by a Sonogashira reaction. In the chemistry of TAPPs the positions 2 and 5 are already occupied with aryl substituents. This is an important factor since electronic communication is the strongest at these positions. Along these lines, it is perhaps not surprising that the decoration of the DHPP skeleton by introducing two arylethynylaryl substituents at positions 2 and 5 turned out to be an effective pathway toward novel chromophores (Scheme 33).[53] These dyes generally represent an A-D-A architecture where A is an electron-deficient aromatic ring connected via a triple bond and D as an electron-rich DHPP moiety.

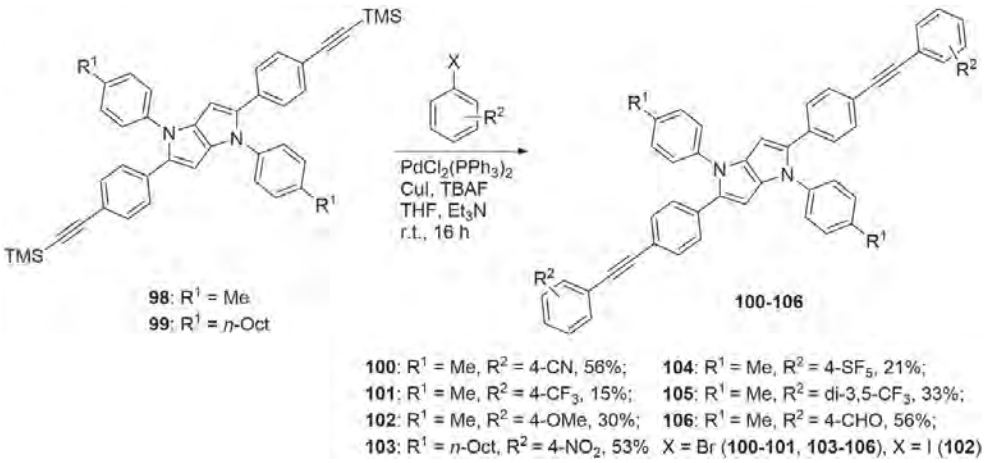

Scheme 33 One-pot sila-Sonogashira reaction toward peripherally π-expanded TAPPs.

TAPPs **98** and **99** possessing TMS ethynyl substituents at positions 2 and 5 were synthesized by multicomponent reaction. However, the Sonogashira coupling of these dyes performed after deprotection was found to be low yielding. In order to sort out this problem, Gryko group relied on the sila-Sonogashira reaction reported by Henze et al, combining both deprotection and coupling in one step.[54] Employing this method significantly shortened the reaction time along with an increase in the yield. Subsequent investigations on the scope of this synthetic route carried out using iodoarenes and bromoarenes bearing various substituents led to products **100–106** in yields ranging from 15% to 56%. The results apparently

proved bromoarenes as more compatible for the reaction with the exception of compound **102** which was obtained only from 4-iodoanisole.

As stated above, the best positions in the DHPP skeleton to bridge with an another π-system are positions 2 and 5. To date, however, all attempts to use cinnamaldehydes or arylpropargylaldehydes in the multicomponent reaction leading to TAPPs have failed. The use of formaldehyde was unsuccessful as well, limiting the possibilities of structural modification, e.g., via subsequent bromination. Very recently, in response to this problem, Gryko and co-workers have developed an original approach for the insertion of formyl substituents at positions 2 and 5 of 1,4-dihydropyrrolo[3,2-*b*]pyrroles by conversion of thiazol-2-yl substituents. The transformation of thiazoles into formyl group was developed by Altmann and Richheimer,[55] and then further refined by Corey and Boger[56] in the 1970s. The quaternization of 2,5-bis(thiazol-2-yl)-dihydropyrrolo[3,2-*b*]pyrrole **107** with methyl triflate followed by the reduction gave a bis-thiazolinyl derivative. Its hydrolysis using silver nitrate led to the final dialdehyde **108** in an acceptable 41% yield (Scheme 34). Further Knoevenagel condensation with malonitrile leading to dye **109** was achieved as well. Subsequently, the transformation of

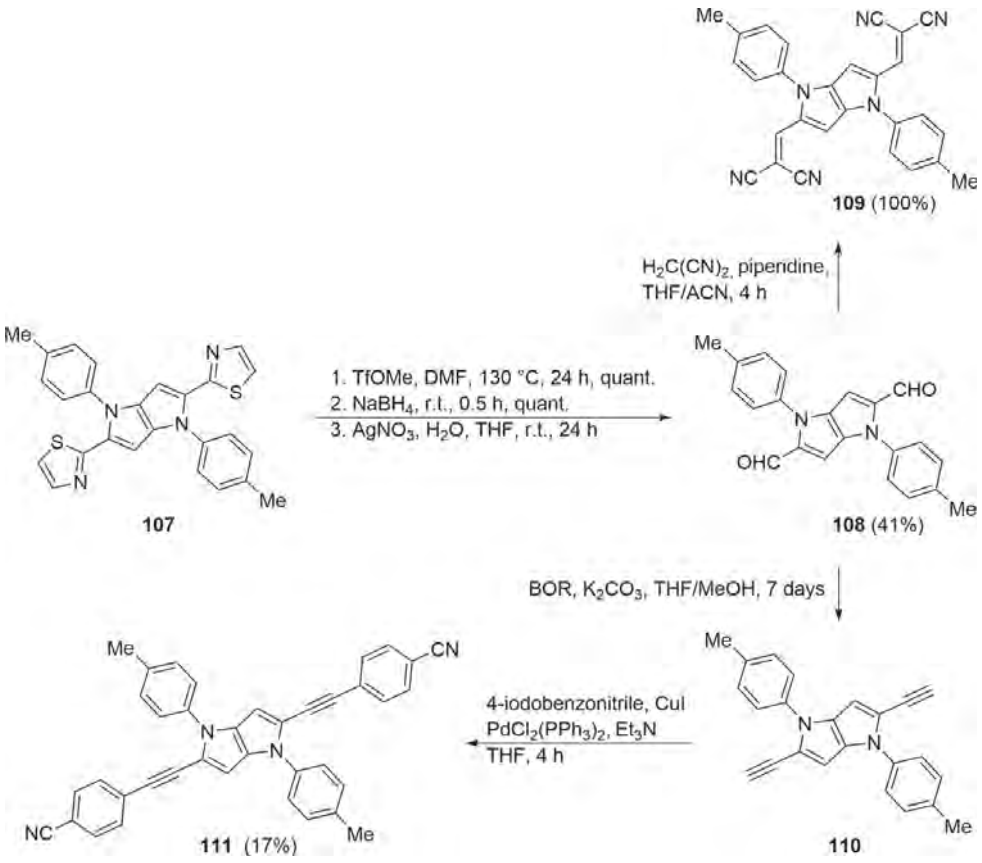

Scheme 34 Synthesis of aldehyde **108** and its further transformations.

dialdehyde **108** into 2,5-bis(ethynyl)-1,4-dihydropyrrolo[3,2-*b*]pyrrole **110** via reaction with the Bestmann-Ohira reagent (BOR), was successful. Due to the light sensitivity of this compound, it was used directly in the Sonogashira reaction to further expand the **π**-system leading to dye **111** (Scheme 34).[57]

The presence of inherently electron-rich free positions 3 and 6 in DHPPs renders the possibility of introducing a total of six different aryl substituents directly into the heterocyclic core. This linking allows a fine-tuning of optical properties of the desired compounds. However, as mentioned earlier, the low reactivity of the functional groups substituted at positions 3 and 6 limits the scope of such expansion enabled by them. To overcome this issue, Gryko and co-workers relied on direct arylation. The only reaction conditions that turned out to be feasible in this case was the one reported by Doucet for sterically congested pyrroles.[58] Hexaarylpyrrolopyrroles (HAPPs) derived from **45** were synthesized in a reasonable yield using various aryl and heteroaryl bromides (Scheme 35).[28,29] The aryl comprehensive

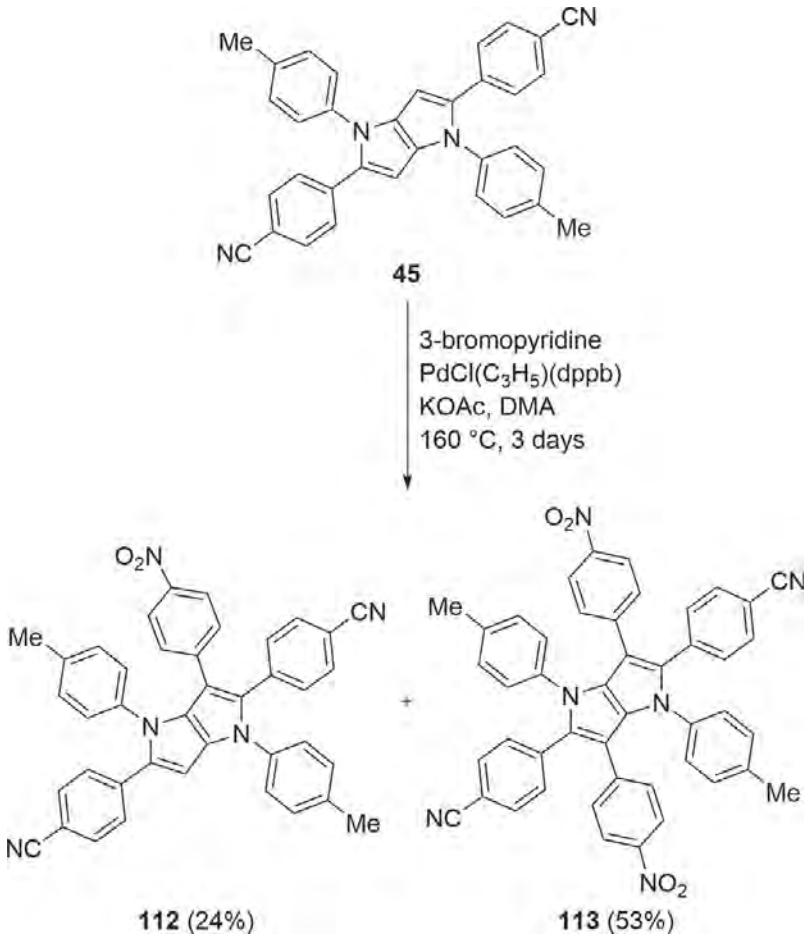

Scheme 35 Exemplary synthesis of penta- and hexaaryl-1,4-dihydropyrrolo[3,2-*b*]pyrroles by means of direct arylation.

scope investigation revealed the effect of electron density on bromoarene on the output of direct arylation. While electron-donating bromoarenes almost exclusively gave monoarylation product, electron-poor aryl bromides such as 4-nitrobromobenzene showed higher reactivity, affording hexaarylpyrrolo [3,2-*b*]pyrrole as the major product, e.g., **112**–**113**+, Scheme 35. The only exception in this case was 4-bromobenzonitrile which was transformed exclusively into pentaaryl-1,4-dihydropyrrolo[3,2-*b*]pyrrole.

The actual position of linkage of triple bonds has a pivotal role in modulating the optical properties of A-D-A type quadrupolar dyes. Linking aromatic substituents directly to the heterocyclic core through the carbon-carbon triple bond can lead to a new family of chromophores. As pointed out before, the inability of 3,6 dibrominated TAPPs to undergo the Sonogashira reaction led to an urge to obtain a synthetic route to perform alkynylation at the core. Based on the work done by the Waser group on gold-catalyzed alkynylation of electron-rich aromatics,[59] Gryko and co-workers proved that direct alkynylation is possible in the case of 1,4-dihydropyrrolo[3,2-*b*]pyrrole utilizing 1-{[tris-(1-methylethyl)silyl]ethynyl]}-1,2-benziodoxol-3(1*H*)-one (TIPS-EBX) as an alkynylating agent (Scheme 36).[60]

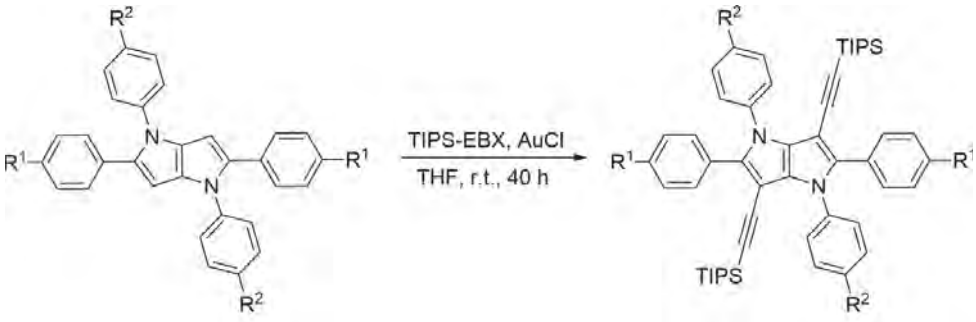

51b. $R^1 = NO_2$, R^2 = *n*-Oct
114. R^1 = Me, R^2 = *n*-Bu
115. R^1 = CN, R^2 = *n*-Oct

116. R^1 = Me, R^2 = *n*-Bu, 17%
117. R^1 = CN, R^2 = *n*-Oct, 31%
118. $R^1 = NO_2$, R^2 = *n*-Oct, 43%

Scheme 36 Synthesis of dyes **116–118**.

By following the Waser protocol, tetraarylpyrrolo[3,2-*b*]pyrroles **51b**, **114** and **115** were transformed to 3,6-bis(TIPS-ethynyl)tetraarylpyrrolo [3,2-*b*]pyrroles **116–118** using TIPS-EBX catalyzed by AuCl. These TIPS-ethynyl substituents can serve as a handle for further π-expansion by the removal of the TIPS group followed by the Sonogashira reaction forming bis(arylethynyl)pyrrolo[3,2-*b*]pyrroles, e.g., **119**, (Scheme 37).

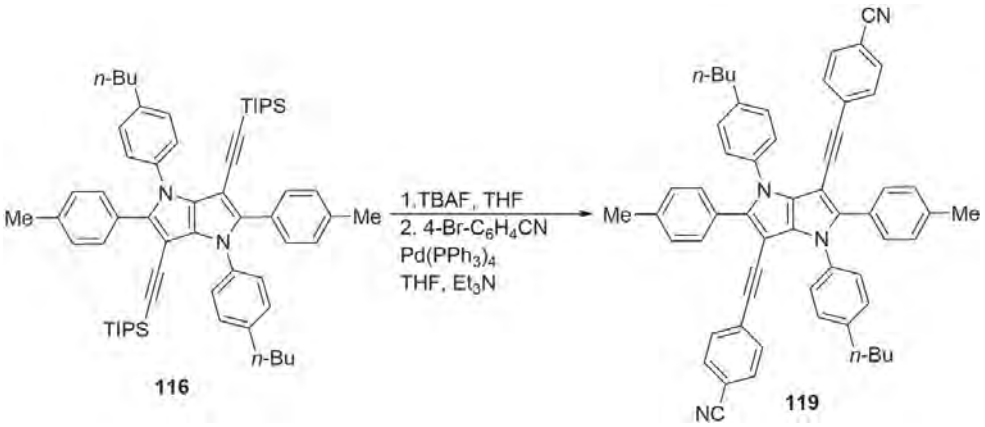

Scheme 37 Synthesis of bis(arylethynyl)pyrrolo[3,2-*b*]pyrrole.

The synthetic potential of this final step was established using bulky π-systems, such as anthracene, and electron-withdrawing naphthalene-1,8-imide substituents with excellent yields.

3.2.2 Synthesis of DHPPs fused with benzene rings

The synthesis of indolo[3,2-*b*]indole (**121**) was revealed for the first time in 1884, when Golubev reported a compound with formula $C_{14}H_{10}N_2$, as a product of reduction of 2,2′-dinitrobenzil with tin in HCl/EtOH.[61] Nevertheless, the exact structure of the compound was unknown and the authors gave it a simple name "diiminotolane."

Only thirty years later Kliegl and Hass showed the synthesis of 2,2′-dinitrobenzil (**120**) by oxidation of 2,2′-dinitrodiphenylacetylene with CrO_3 in acetic acid.[62] Then compound **120** was reduced with tin resulted in a substance identical with Golubev's "diiminotolane" **121**. However, the authors made further conclusions and they named this molecule as a doubly condensed indole (Scheme 38).

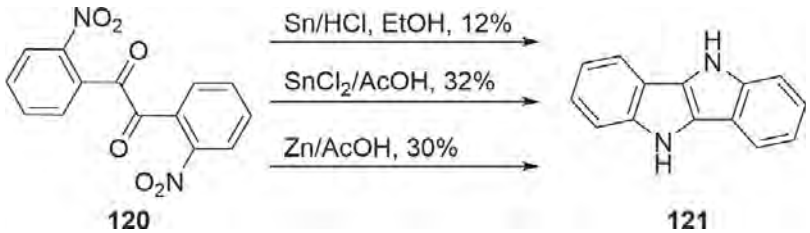

Scheme 38 Historical synthesis of indolo[3,2-*b*]indole **121**.

An improved synthesis of **121** was reported in 1917. Heller, Ruggli and Zaeslin described a method in which they used zinc powder or $SnCl_2$ instead

of tin, and they obtained the desired product in 30% and 32% yield, respectively (Scheme 38).[63–65] A new method of synthesis leading to indolo[3,2-*b*]indole (Scheme 39) was introduced by Ruggi in 1917.[63] The first stage is addition of Br_2 to 2,2′-dinitrodiphenylacetylene (**122**) resulted in dibromo derivative **123**, which was subsequently reduced with $SnCl_2$ in a HCl/AcOH mixture to give **124**, and cyclization to **125** led to indolo[3,2-*b*]indole (**121**) (Scheme 39).

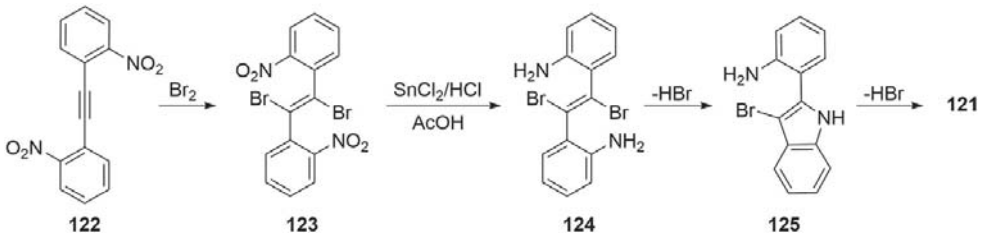

Scheme 39 Ruggli's route to indolo[3,2-*b*]indole **121**.

In 1935 Ruggli and Zaeslin described an even better method (Scheme 40).[65] In the first step 2,2′-dinitrodiphenylacetylene (**122**) was heated in aqueous solution of Na_2S leading to 2-(2-aminophenyl)-3*H*-indole-3-one (**126**). Then the reduction of this compound using a $SnCl_2$/HCl/AcOH system resulted in formation of indolo[3,2-*b*]indole **121** in 78% yield (Scheme 40).

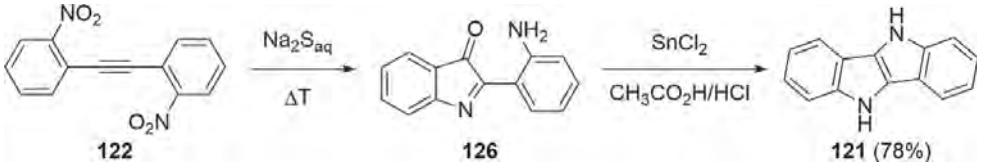

Scheme 40 Stepwise reduction of **122** to **121**.

Compound **121** can also be obtained via reduction of 2,2′-dinitrostilbene **128** (formed from **127**) with $P(OEt)_3$; however, the yield of this reaction is only 2% (Scheme 41, **A**).[66] Another method of synthesis was presented by Kaszynski and Dougherty.[67] A suitable stilbene was reduced to diethyl 2,2′-diaminostilbeno-4,4′-dicarboxylate with Fe/EtOH followed by diazotization. Afterwards, the bis-diazonium salt was turned into the bis-azide in 81% yield. Next step was double intramolecular cyclization of the latter compound to obtain diethyl 5*H*,10*H*-indolo[3,2-*b*]indole-2,7-dicarboxylate in 13% yield. Whereas, under Cadogan reaction conditions *N*-methyl-2-(2-nitrophenyl)indole **129** was transformed into *N*-methylindolo[3,2-*b*]indole **130** in good yield (Scheme 41, **B**).[68]

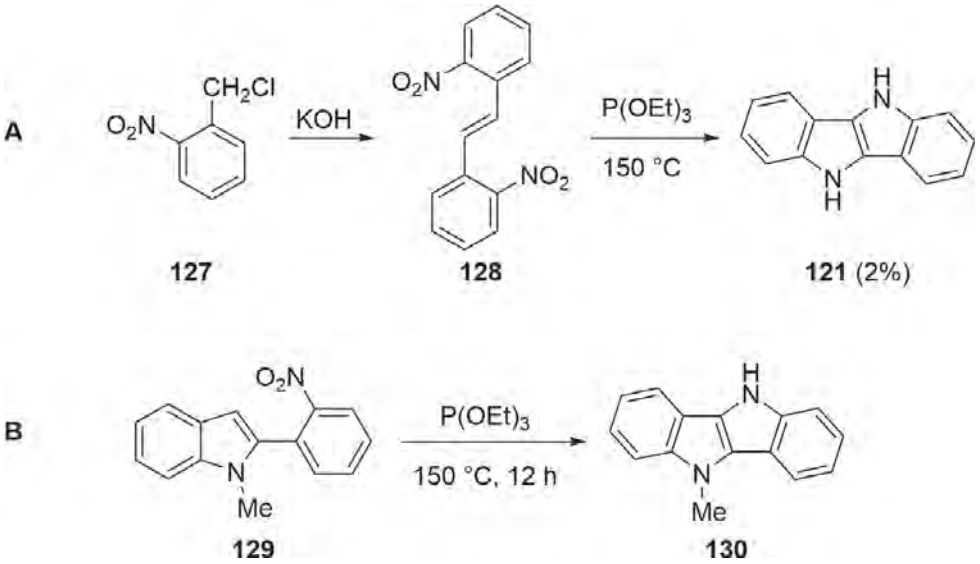

Scheme 41 Routes toward indolo[3,2-*b*]indole via Cadogan reaction.

The Fischer indole synthesis method has also been used starting with 2-indole-2-one and its derivatives. Their reaction with phenylhydrazine provided substituted indolo[3,2-*b*]indoles.[69–71]

On the grounds of previous research of Cooper and Partridge,[72] Wan and co-workers worked out a new method leading to compounds equipped with indolo[3,2-*b*]indole moiety (Scheme 42).[73] The first step was self-condensation of methyl 2-aminobenzoate (**131**) under basic conditions resulted in dibenzo[*b*,*f*][1,5]diazocine-6,12(5*H*,11*H*)-dione (**132**) in 75% yield. Reaction of this compound with PCl_5 gave 6,12-Dichlorodibenzo [*b*,*f*][1,5]diazocine (**133**) in 64% yield. Compound **133** was subjected to a reduction reaction in the presence of Zn under acidic conditions, giving indolo[3,2-*b*]indole **121** in 70% yield.[73] This approach has been further extended to embrace π-expanded indolo[3,2-*b*]indoles.[74]

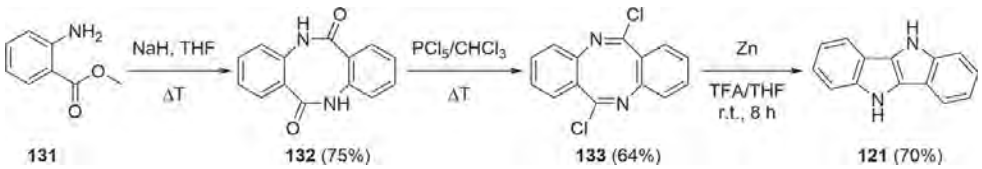

Scheme 42 The Wan-Cooper route toward 5*H*,10*H*-indolo[3,2-*b*]indole.

It has also been shown that the indolo[3,2-*b*]indole skeleton can be obtain in good yield using electrochemical reduction of dibenzodiazocines.[75,76] Previous literature data indicate that the same transformation can be

performed with Zn/AcOH.[77–79] On the other hand electrochemical oxidation of some indolo[3,2-*b*]indoles in CH_2Cl_2 in the presence of $Bu_4N^+ ClO_4^-$ gave dark green radical cation.[67]

Lan and Wan obtained stable unsubstituted 4π-electron acenes having the antiaromatic skeleton of 1,4-diazopentalene.[6] Analogue **134** was synthesized by oxidation with nickel(IV) oxide (Scheme 43). It has been shown that its π-expanded derivatives are less stable.

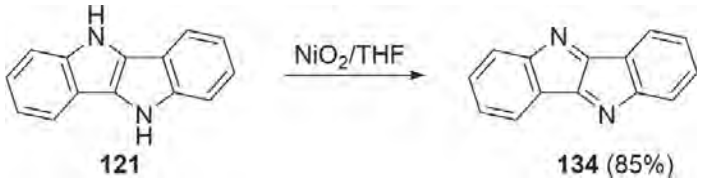

Scheme 43 Oxidation of indolo[3,2-*b*]indole **121**.

An another pathway toward indolo[3,2-*b*]indoles was developed by Langer and co-workers. 2-Aryl-3-bromoindoles, e.g., **135**, were subjected to Buchwald-Hartwig amination with both aromatic and aliphatic primary amines to afford *N*,*N*′-disubstituted heterocycles exemplified by the benzyl derivative **136** (Scheme 44).[80]

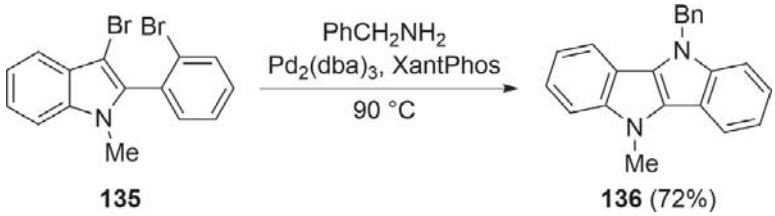

Scheme 44 Langer's method for the synthesis of indolo[3,2-*b*]indoles.

Very recently the Du and Jin groups have independently developed new copper-mediated strategies leading to these heterocycles, illustrated by formation of the derivatives **138** and **140** from the alkynes **137** and **139** (Scheme 45).[81, 82]

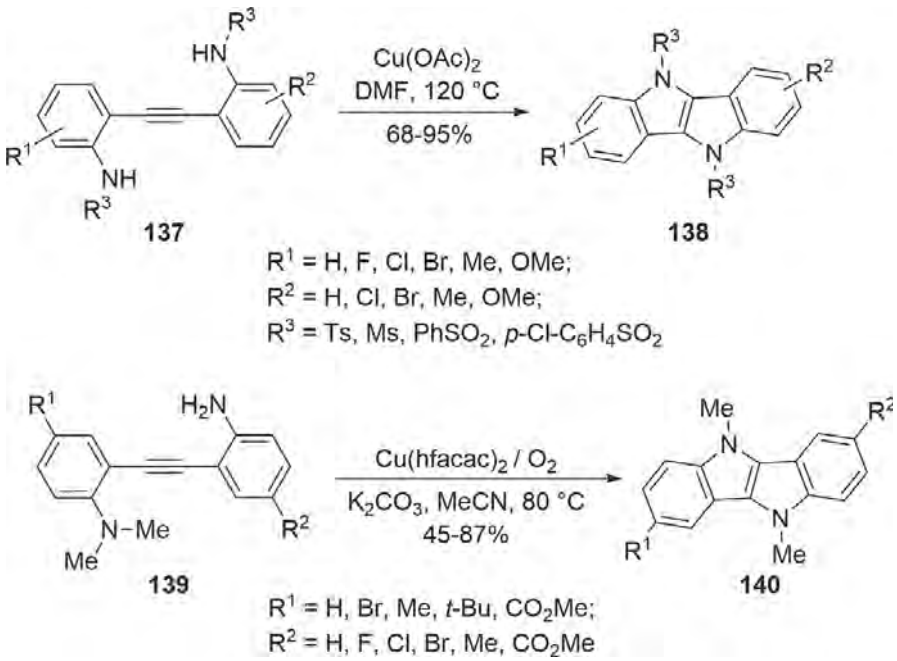

Scheme 45 The new copper-mediated strategies toward indolo[3,2-*b*]indoles.

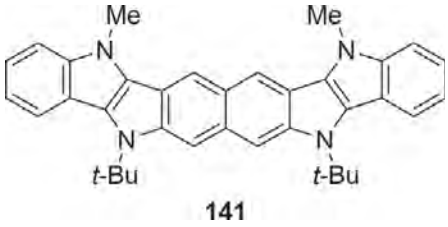

Fig. 6 Structure of a bisindolo[3,2-*b*]indole derivative.

A similar route has been published by Shi and co-workers to design and synthesize bisindolo[3,2-*b*]indole **141** (Fig. 6).[83]

The full potential of chemical space bearing DHPP cores was realized, however, once multicomponent reactions leading to TAPPs was discovered. The numerous functional groups present on substituents at either positions 2 and 5 or positions 3 and 6 combined with the free, electron-rich positions 3 and 6 offers a perfect recipe for a number of intramolecular transformations that may eventually lead to the expansion of π-system.

TAPPs with a carbon-carbon triple bond linked to the *ortho* position of the C-aryl substituent (**143**–**149**) can act as a precursor for π-expansion via intramolecular annulation reaction.[84] The parent TAPP **142** synthesized from the corresponding 2-trimethylsilylethynylbenzaldehyde and 3,5-bis(*tert*-butyl) aniline was subjected to sila-Sonogashira coupling with a rationally chosen set

of aryl iodides to form *Z*-shaped bisarylethynylpyrrolopyrroles. The strategic placement of bulky *tert*-butyl groups helps to prevent π-stacking of large aromatic systems ensuring good solubility. The final transformation relies on the double cyclization of TAPPs mediated by $InCl_3$ to form π-expanded indolo[3,2-*b*]indoles **150**–**156** (Scheme 46). It is noteworthy that in all these examples, 6-*endo*-*dig* cyclization products were solely formed even without a single trace of possible 5-*exo* isomers.

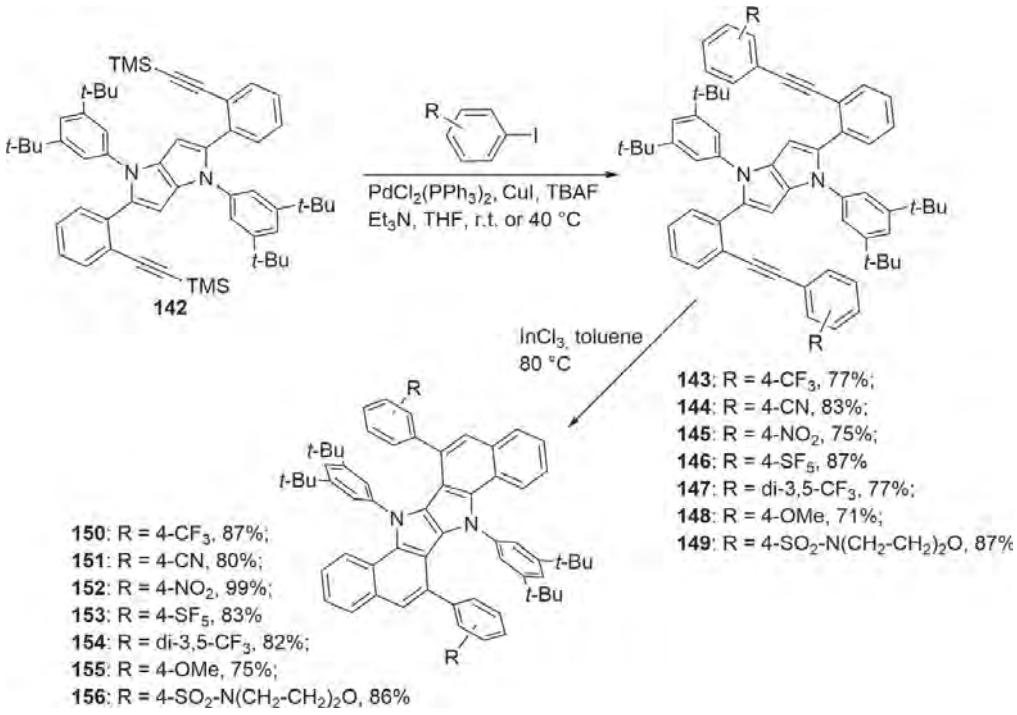

Scheme 46 $InCl_3$-mediated cyclization leading to π-expanded indolo[3,2-*b*]indoles **150–156**.

Interestingly, a similar strategy was used to synthesize dyes possessing seven-membered rings.[34] Such a methodology demands a TAPP precursor decorated with a triple bond located at the *ortho* position in the *N*-aryl ring. This type of cyclization significantly improves the conjugation between the core and substituents originating from aniline. The parent TAPP **157a**, was predominantly transformed into the 7-*endo*-*dig* product **158** by indium(III)

chloride catalyzed annulation (Scheme 47). It is anticipated that both the nature of the catalyst and the structure of the substrate plays key role in determining the preference of 7-*endo-dig* pathway over the 6-*exo-dig* pathway. Introduction of seven-membered ring to this polycyclic system can strongly alter the electronic distribution in the final molecule **158** compared to TAPP **157**. This substantial change might be the plausible reason that prevents double cyclization.

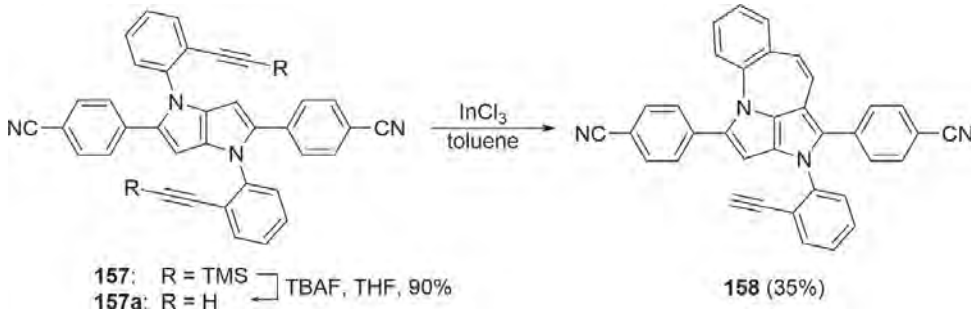

Scheme 47 Synthesis of dye **158** possessing a seven-membered ring.

Oxidative aromatic coupling (Scholl reaction) is among the most popular methods toward unprecedented polycyclic systems.[85,86] Since the presence of electron-rich substrates is crucial preconditions for oxidative aromatic coupling to occur,[87] an intrinsically electron-rich positions 3 and 6 of the TAPPs make them an ideal candidates for this transformation.

Indeed, a library of TAPPs bearing an additional aryl or heteroaryl ring in *ortho* position with respect to the central core (**159**, **161**) have been synthesized in moderate to high yields.[88] Parent aldehydes possessing heteroaromatic rings were synthesized by employing either direct arylation protocol using 2-bromobenzaldehyde or Suzuki coupling with the corresponding boronic acids. These TAPPs smoothly underwent oxidative aromatic coupling mediated by iron(III) chloride in nitromethane to form π-expanded ladder type dyes having an indolo[3,2-*b*]indole core (**160**, **162**) (Scheme 48). It is notable that in these cases, desired products were produced in 45% to 60% yields, once again demonstrating the synthetic potential of oxidative aromatic coupling.

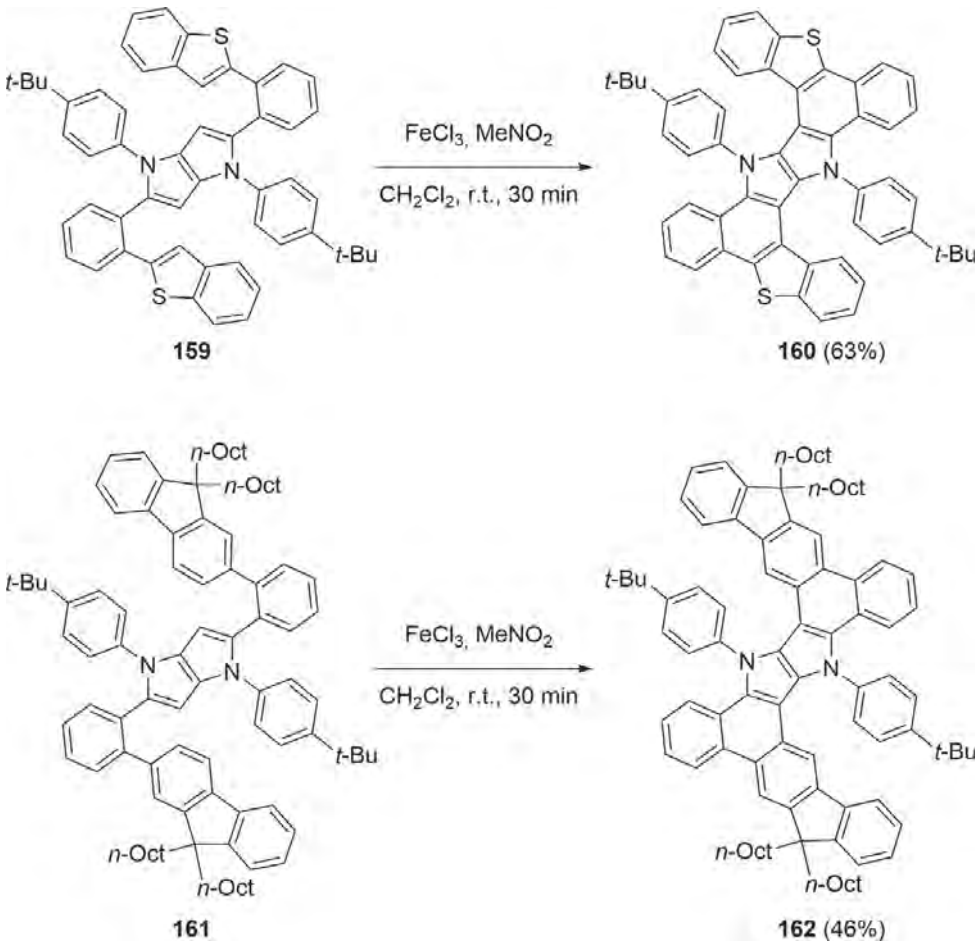

Scheme 48 Synthesis of π-expanded ladder-type dyes **160** and **162** possessing indolo[3,2-*b*]indole core.

During this study, the Gryko group made a surprising observation depicting the crucial relationship between steric effects and the mechanism of the oxidative aromatic coupling reactions of tetraarylpyrrolo[3,2-*b*]pyrroles, typically **163** → **164**.[89] The presence of larger steric congestion next to the oxidation site (e.g., **165**) significantly altered the reaction pathway. In this context, the attack of the intermediate radical cation occurs in an already occupied position to produce the pyrrolopyrrolium salt **166** bearing a new spiro carbon atom (Scheme 49). This experimental result was supported by quantum chemical calculations describing the formation of a spiro-5-membered ring to be preferred by both TS energy and relative energy of the product. The reaction seemed impossible to be termed as thermodynamically or kinetically controlled, since both thermodynamic and kinetic products turned out to be the same.

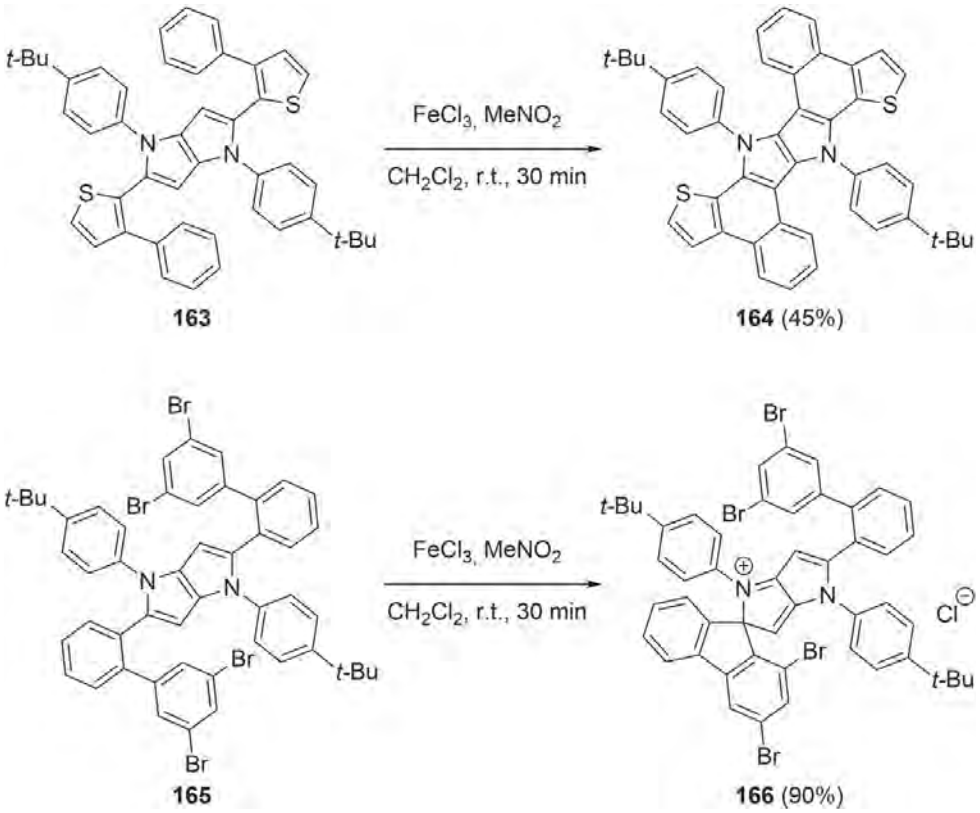

Scheme 49 Oxidative aromatic coupling of TAPPs **163** and **165.**

Another unprecedented discovery related to oxidative aromatic coupling was made while exploring the synthesis of π-expanded polycyclic systems utilizing TAPPs obtained from 2-phenylaniline (**167**).[90] However, the precursor compound **167** was obtained in a significantly lower yield compared to the analog TAPP possessing biphenyl units at 2 and 5 positions. Under Lewis acid catalyzed conditions, we expected the formation of compound **168** composed of seven-membered rings. Although a tentative analysis of ^{1}H NMR and HRMS-EI supported the formation of the expected product, X-ray crystallography result contradicted our assumption. Surprisingly, two hexagonal rings were formed via cyclization at already occupied positions 2 and 5 with subsequent 1,2-aryl shift from C2/C5 to C3/C6 (Scheme 50). X-ray diffraction analysis revealed that the rearrangement occurs in fact during dehydrogenation, as the XRD structure of **167** clearly showed the biphenyl moiety attached to the nitrogen. This rearrangement turned out to be general with respect to the functional group R and in all cases π-expanded TAPPs **169a–g** are formed in comparable yields ranging from 33% to 70%.

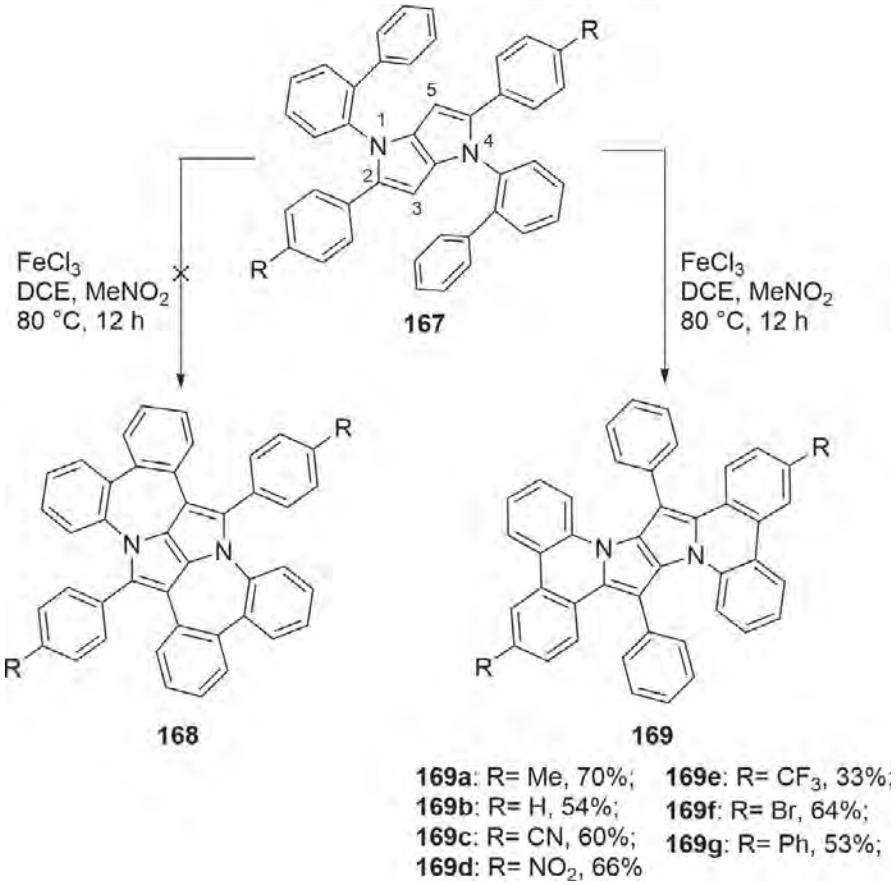

Scheme 50 1,2-Aryl shift triggered by oxidative aromatic coupling.

An alternative approach toward the synthesis of heteroanalogues of π-extended polycyclic systems similar to **169** was demonstrated employing the intramolecular direct arylation method.[34] TAPPs (e.g., **170**) obtained from 2-haloanilines are easily transformed to the fused derivative (e.g., **171**) via palladium-catalyzed direct arylation (Scheme 51). The reaction

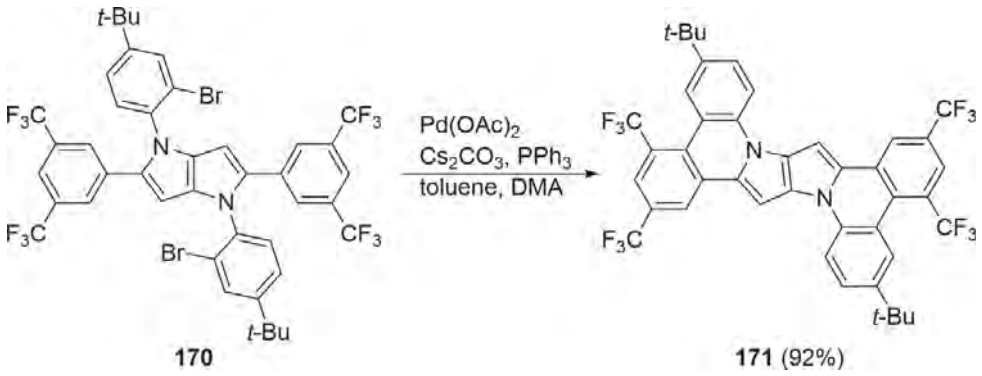

Scheme 51 Intramolecular direct arylation of TAPP **170**.

proceeds in a regioselective manner to form a new carbon–carbon bond *ortho* to the benzene rings attached to the 2 and 5 positions. This high yielding last step shows the remarkable influence of the DHPP core on the distribution of the electron density to the substituents, thus enhancing their reactivity. This simpler two-step method provides easy access to more elaborated heteropolycyclic aromatic systems.

Building upon our previous investigations on oxidative aromatic coupling, a new strategy was developed in combination with intramolecular direct arylation to synthesize a unique class of π-expanded DHPP **174** with large "wings" at the periphery.[91] A three-step protocol was developed for the preparation of this highly conjugated polycyclic system. TAPPs such as **172** synthesized in high yields (35–45%) starting from 2-bromo-6-arylbenzaldehydes in a multicomponent synthesis, once again proved the possibility of using sterically congested benzaldehydes as the perfect substrate for this reaction (Scheme 52). Deliberately placed bromine atom at the *ortho* positions allowed Pd-catalyzed intramolecular direct arylation to form planar derivatives **173** in the following step. The final intramolecular oxidative aromatic coupling successfully gave the desired butterfly-shaped compounds in very good yields (85–90%). As has been experienced in previous

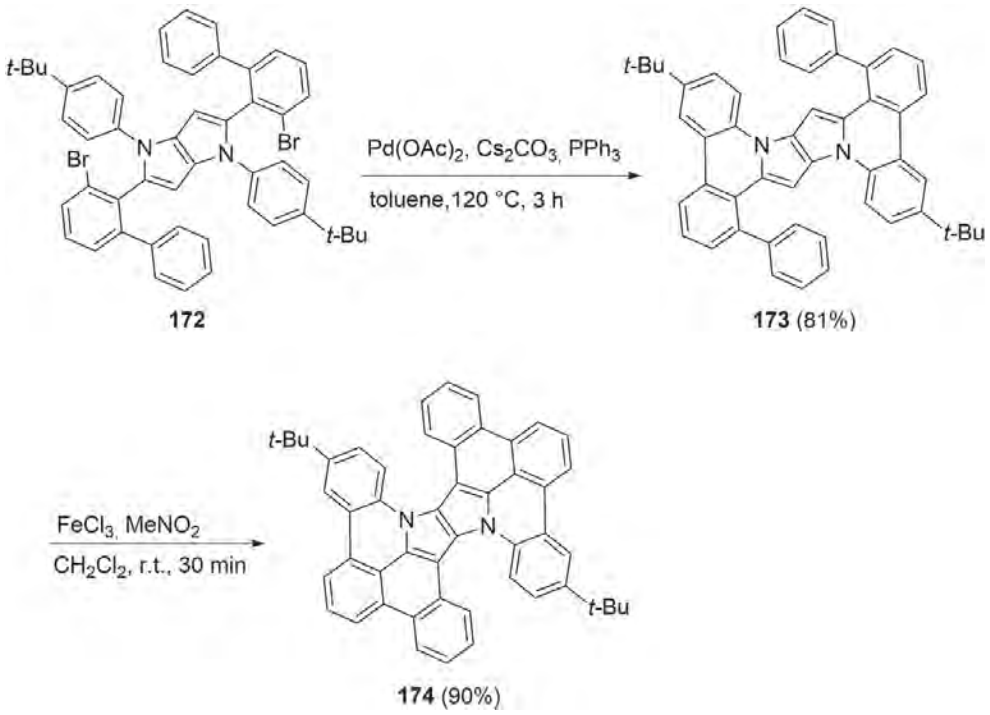

172 **173** (81%) **174** (90%)

Scheme 52 Exemplary pathway toward double helical π-expanded pyrrolo[3,2-*b*]pyrroles **174**.

work, the insolubility of the planar derivative **173** due to π-stacking was tackled by introducing bulky *tert*-butyl groups.

These compounds exhibit helicene-like architectures arising from the van der Waals radii overlaps between closely spaced hydrogen atoms of the adjacent aryl rings, preventing planarization. Dye **174** showed three different isomeric forms arising from its double-helicene-like structure: two twisted enantiomers (*P,P*) and (*M,M*) and one folded *meso* form (*P,M*). TD-NMR experiments and DFT calculations revealed the interconversion energy barrier between folded and twisted forms to be very low, making separation based on isomers impossible. However, X-ray crystallography undeniably confirmed their existence. In comparison with earlier literature reports on double helicenes,[92] this study reveals a pronounced effect on the interconversion barrier of such systems by replacing the central naphthalene units with fused heterocyclic pentagonal rings.

The synthesis of curved π-conjugated polycyclic hydrocarbons termed as buckybowls possessing a DHPP core was one of the most fascinating discoveries established by the Gryko group in collaboration with the Fasel research group.[93] A combined in-solution and on-surface synthetic strategy was performed to fabricate this bowl-shaped aza-nanographene constituting a non-hexagonal ring to provide unique structural features.

Based on our previous studies, a meticulous design of synthetic strategy allowed the formation of precursor molecule **177**, bearing preformed heptagonal rings (Scheme 53). Parent TAPP **175**, having bromine atoms and benzene rings in *ortho* position to the core, underwent palladium-catalyzed

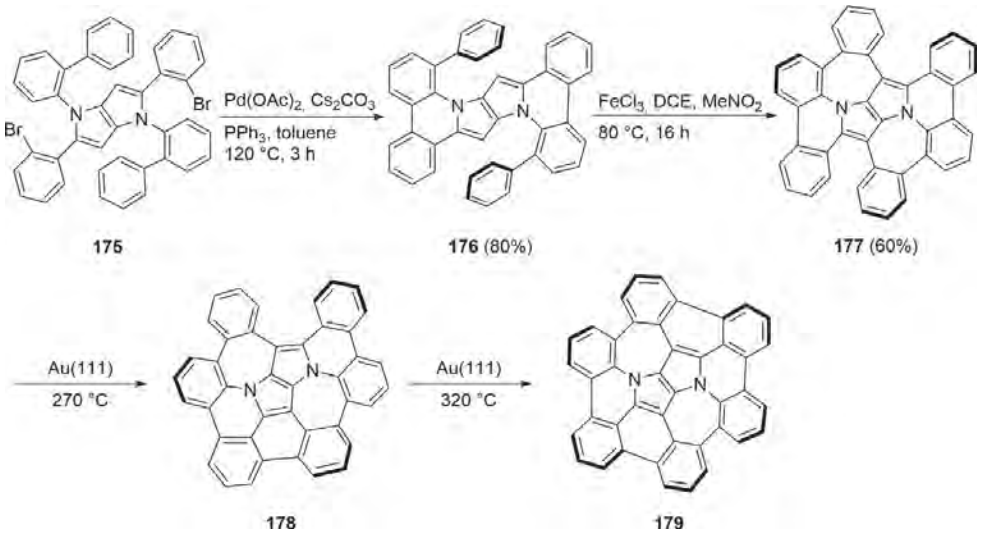

Scheme 53 Synthetic route toward nitrogen-embedded buckybowl **179**.

intramolecular direct arylation to give **176** followed by oxidation with iron(III) chloride forming compound **177** in high yield. Fortunately, this molecule was found to be viable for on-surface cyclodehydrogenation for the final closure of hexagonal rings giving initially **178**. Annealing this compound to 320 °C under ultra-high vacuum (UHV) conditions on an Au surface effectively led to the desired nitrogen-embedded bucky bowl **179**.

The molecule **179** was characterized by ultrahigh-resolution scanning tunneling microscopy and spectroscopy in combination with DFT calculations. Buckybowl **179** containing a unique combination of two fused non-hexagonal rings at its core was identified to possess the inverse Stone-Thrower-Wales topology (ISTW), exhibiting a distinctive bowl-opening-down conformation of the buckybowl on surface. This study remains as a perfect example of combining on-surface techniques with in-solution synthesis for the formation of unprecedented π-extended aza-analogues of carbon nanostructures with high atomic precision. It is worth mentioning that this is the first case of aza-nanographene in the literature to possess two fused pyrrole rings as a core possessing the unique ISTW topology.

Even though surface-assisted techniques have undeniably proven to be a powerful tool for constructing polycyclic aromatic systems, they have disadvantages because of the miniature scale, which makes it impossible to isolate product and to perform its fundamental physicochemical characterization. By critically modifying the synthetic strategy, a complete in-solution synthesis of azabuckybowls based on DHPP was achieved.[94] The idea behind this synthetic strategy stemmed from the X-ray analysis of the precursor molecule **177** for the previously reported on-surface dehydrogenation. The large distance between carbon atoms involved in the reaction (reaching 3.28 Å) was predicted to be the barrier for the final step. An alternative precursor was designed (**180**), possessing chlorine atoms attached to the corresponding carbon atoms located inside the helicene-like fjord regions, which was expected to undergo six-membered ring fusion via intramolecular direct arylation. In accordance with this information, the primary precursor molecule **180** was precisely designed constituting halogen atoms at *ortho* positions to the C-aryl ring and a biphenyl group attached to pyrrole nitrogen. The first intramolecular direct arylation proceeds selectively via palladium-catalyzed C—Br activation to give **181** followed by a double Scholl reaction leading to molecule **182** (Scheme 54). The order of these steps has more significance in preventing the occurrence of the 1,2-aryl shift that can result in the rearranged product. The final intramolecular direct arylation was carried out under the more stringent conditions reported by

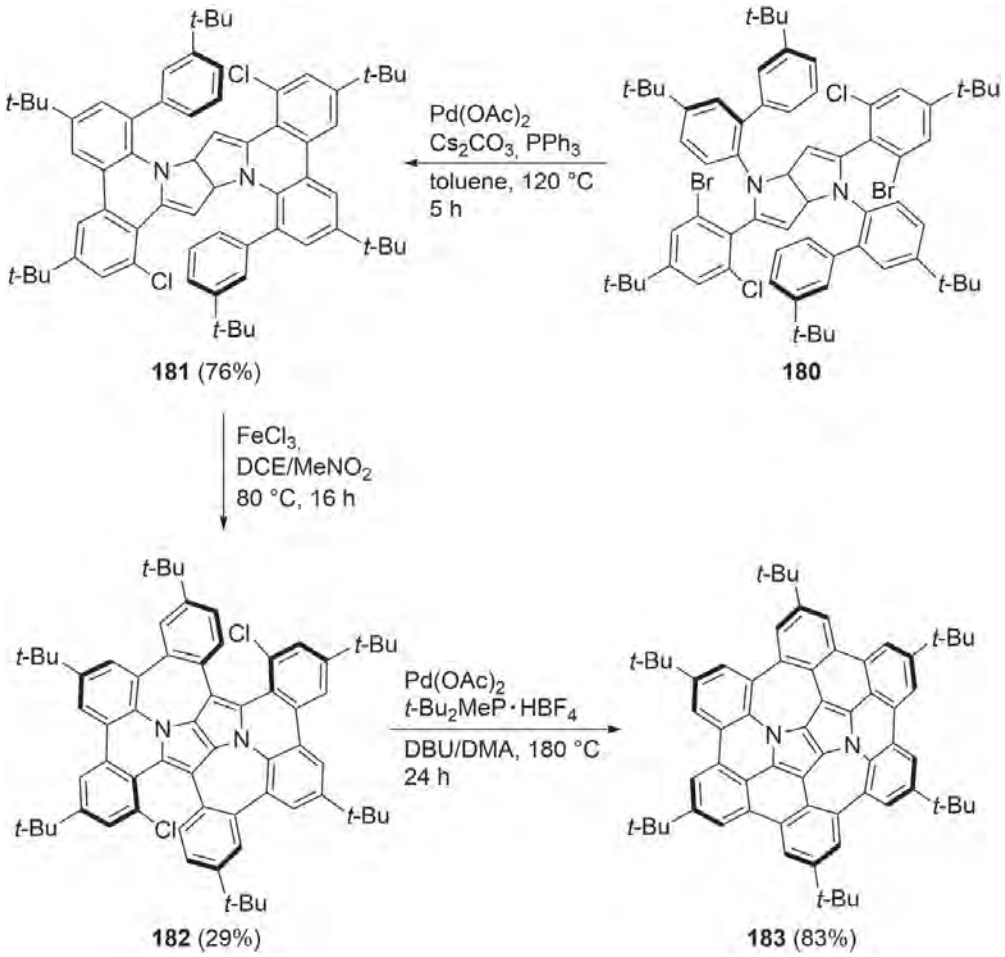

Scheme 54 Synthetic route to azabuckybowl **183**.

Nozaki et al,[95] allowing the formation of target nitrogen-doped curved nanographene **183**. The synthetic scheme represents the first case of programmed sequential intramolecular direct arylations based on the different reactivity of C—Br and C—Cl bonds.

An another example of taking an advantage of the presence of unsubstituted, highly electron-rich positions 3 and 6 within 1,4-dihydropyrrolo[3,2-*b*]pyrrole skeleton is the synthesis of bis-ketone **185**.[96] The initially synthesized TAPP **184** bearing 2-(methoxycarbonyl)phenyl substituents in positions 2 and 5 was subjected to hydrolysis under basic conditions, and the resulting bis-carboxylic acid underwent a ring closure reaction promoted by trifluoroacetic anhydride (TFAA), yielding the desired 1,4-dihydropyrrolo[3,2-*b*]pyrrole-dione **185** (Scheme 55).

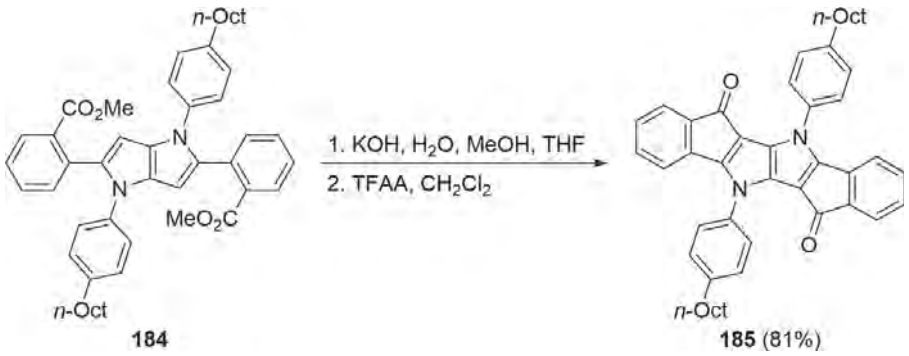

Scheme 55 Synthesis of pyrrolo[3,2-*b*]pyrrole-dione.

3.2.3 N-doped π-expanded DHPPs

Recently, there has been an explosion of research interest in heteroatom-doped polycyclic aromatic systems, in particular thiophene and furan-based heterocycles.[2,97] Still, compared with them, pyrrole-based heterocycles exhibit several advantages over the others. Specifically (1) pyrrole is more electron-donating which can improve the π-conjugation and electron density, (2) functionalization of nitrogen facilitates the addition of different groups, which helps to modulate solubility and polarity. The multicomponent synthesis of TAPPs opened up numerous possibilities toward π-expanded nitrogen-doped polycyclic systems with four or more N-heterocyclic rings.[26]

A versatile library of π-expanded nitrogen-doped ladder type acenes have been synthesized using the corresponding TAPPs **186–194** bearing 2-nitrophenyl substituents at positions 2 and 5 (Scheme 56). Performing a Cadogan reaction on these molecules using triethyl phosphite led to the formation of diindolo[2,3-*b*:2′,3′-*f*]pyrrolo[3,2-*b*]pyrrole (DIPP) comprising four consecutive fused pyrrole rings.[98] As the molecule possess highly electron-rich backbone, photochemically driven decomposition was observed in chlorinated solvents. The stability was significantly improved for the molecules bearing electron-withdrawing substituents such as a CF_3 group and by protecting pyrrolic nitrogen using Boc_2O to give rise to the target compounds **195–199**. Scope studies revealed the reaction to be promising with a set of diversely substituted benzaldehydes in yields ranging from 24% to 35% (Table 1).

Another approach toward similar heteroacene incorporated with hexacyclic nitrogen was carried out from the same substrate. Reduction of the nitro group using $NaBH_4$ in combination with $Ni(OAc)_2$ (*in situ* formation of nickel boride) followed by condensation with the corresponding aldehyde led to diquinolinopyrrolo[3,2-*b*]pyrroles **204–210**.[99] Both electron-rich and electron-poor aldehydes efficiently participated in the final step

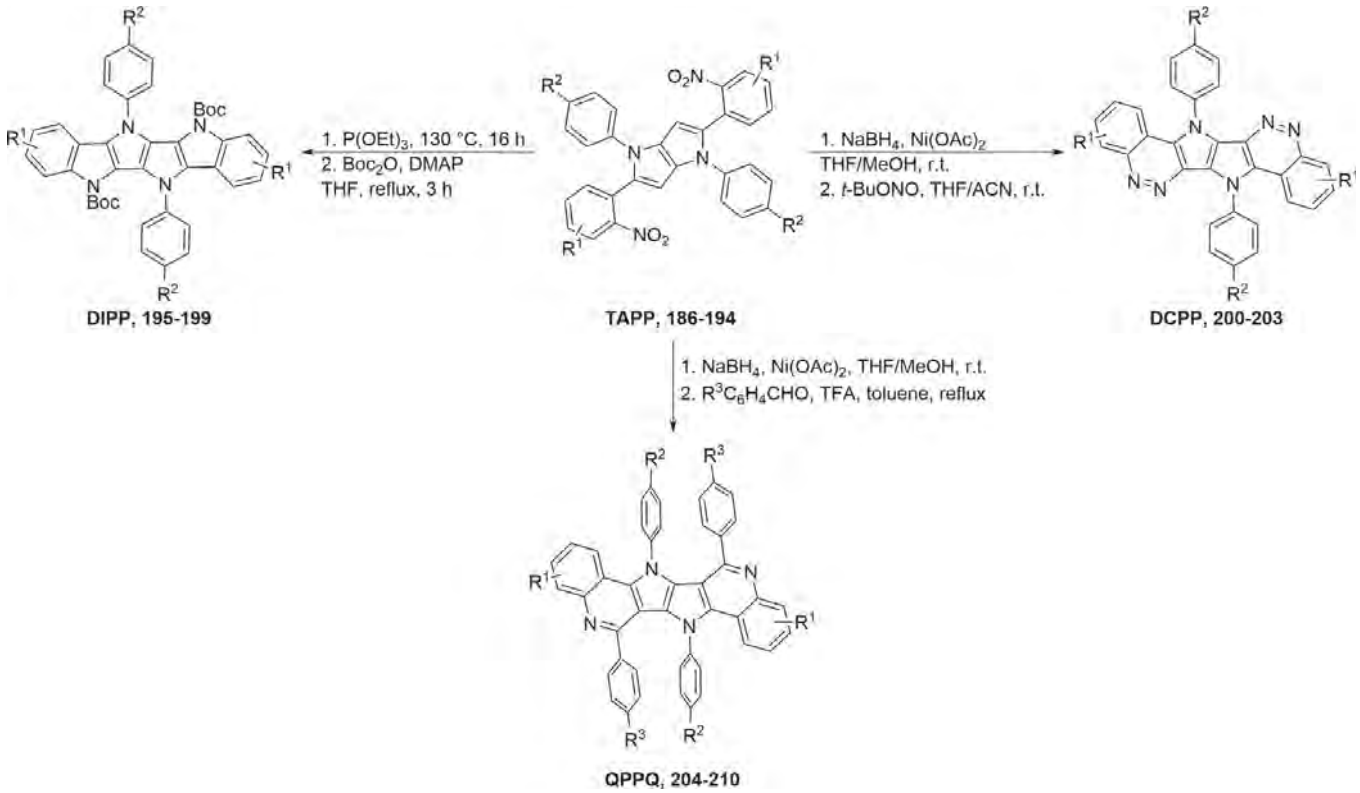

Scheme 56 Synthetic methods toward N-doped π-expanded DHPPs. *Adapted with permission from* Acc.Chem. Res. *2017,* 50*, 2334–2345.*

Table 1 Different approaches toward N-doped π-expanded DHPPs.

TAPP	R^1	R^2	DIPP	Yield (%)	DCPP	Yield (%)	QPPQ	R^3	Yield (%)
186	H	*n*-Dec	**195**	34	–	–	–	–	–
187	4-Br	*n*-Hex	**196**	42	–	–	–	–	–
188	4,5-OCH_2O	*n*-Hex	**197**	61	–	–	–	–	–
189	4-F	*n*-Bu	**198**	34	–	–	–	–	–
190	4-CF_3	*n*-Bu	**199**	50	**200**	45	**204**	CN	63
191	H	*n*-Oct	–	–	**201**	37	**205**	CN	38
192	5-F	*n*-Bu	–	–	**202**	71	**206**	OMe	88
193	3-OMe	*n*-Hex	–	–	**203**	57	**207**	CN	54
193	3-OMe	*n*-Hex	–	–	**–**	–	**208**	Me	65
193	3-OMe	*n*-Hex	–	–	**–**	–	**209**	OMe	42
194	H	OMe	–	–	–	–	**210**	CN	60

Adapted with permission from *Acc.Chem. Res.* 2017, *50*, 2334–2345.

of this reaction, enabling the fine-tuning of the structural and optical properties. X-ray crystallography unambiguously proved the structure describing the azaindolo[3,2-*b*]azaindole core as perfectly planar with external benzene rings twisted from the plane of the molecule.

The synthetic potential of *in situ* formed 2,5-bis(2-aminophenyl)DHPPs was again showcased by the preparation of previously unknown ladder-type dicinnolino[3,4-*b*:3′4′-*f*]pyrrolo[3,2-*b*]pyrroles (DCPP) **200–203**.[100] The substrates react with *tert*-butylnitrite in a modified Sandmeyer reaction via the intramolecular cyclisation of the diazonium group generated from aniline.

3.2.4 B-doped π-expanded DHPPs

Incorporation of other heteroatoms directly connecting to the core of 1,4-dihydropyrrolo[3,2-*b*]pyrroles has proven to be effective in modulating the electronic properties and molecular geometries of the π-conjugated backbone, creating a new type of heteroacenes.[26,100] Doping with three-coordinate, sp^2-hybridized boron atom has been discovered to have a greater effect on aromatic systems among other main group elements.

BN-embedded ladder-type acenes were synthesized from the previously described TAPP precursors **190–193**, which possess 2-nitrophenyl substituents

at positions 2 and 5. Ni(II)-catalyzed reduction of these compounds led to relatively unstable amines, which were directly used for the following step even without purification (Scheme 57).[100] The final reaction with dichlorophenylborane resulted in the products **211–214** in good overall yields. Although these BNPPs were stable as crystals and as solution in most organic solvents, comparatively faster decomposition was observed in chlorinated solvents. X-ray analysis of the molecule demonstrated C_{2h} symmetry with an almost perfectly planar pyrrolopyrrole core.

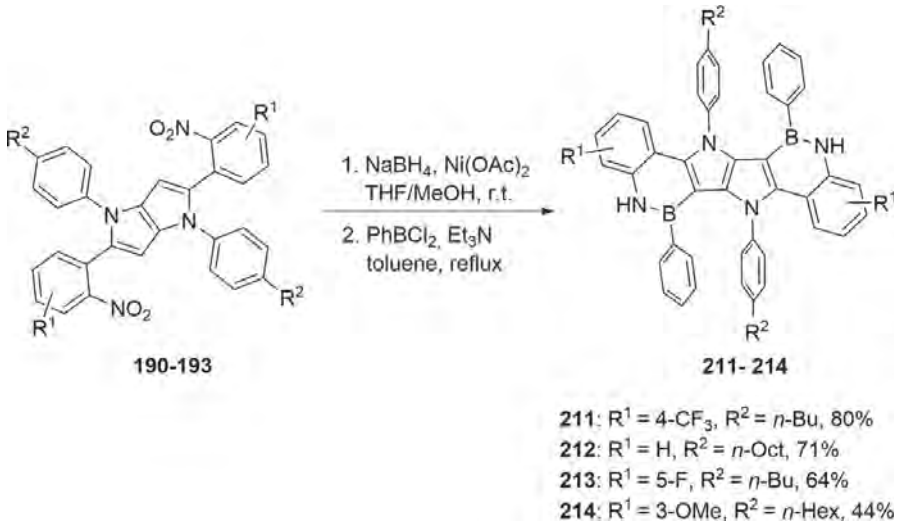

Scheme 57 Synthesis of BNPPs **211–214**.

Further exploration in BN-embedded polycyclic systems led to an interesting discovery of a new family of BN-doped dyes containing four coordinated boron.[101] This approach exploits the intrinsically reactive positions 3 and 6 of DHPP and the direct access to derivatives bearing *N*-heteroaryl substituents at positions 2 and 5. These C═N bonds in *N*-heteroaromatic rings can act as an efficient donor in coordinating with the boron moiety and an appropriate boron source has to be used in the next step. A straightforward cascade B—Cl/C—B cross-metathesis and C—H borylation procedure reported by Song and co-workers,[102] turned out to be the successful strategy (Scheme 58). The process involving the cross

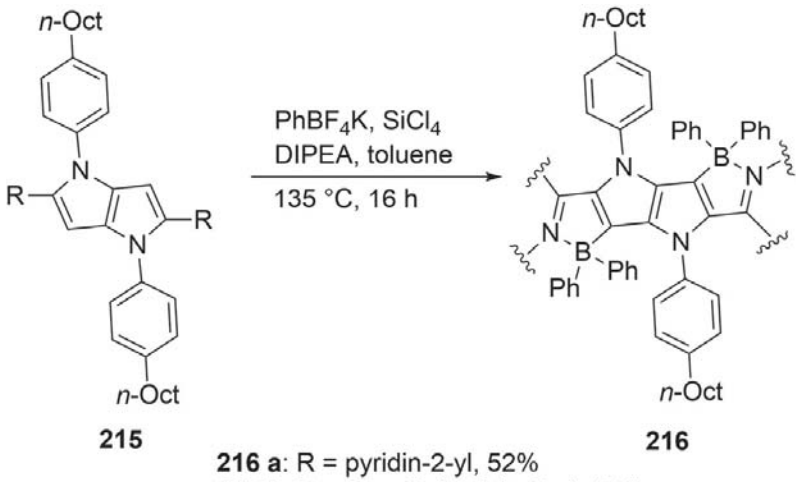

215 **216**

216 a: R = pyridin-2-yl, 52%
216 b: R = 6-methylpyridin-2-yl, 15%
216 c: R = 5-bromopyridin-2-yl, 20%
216 d: R = 4-bromopyridin-2-yl, 29%
216 e: R = 5-fluoropyridin-2-yl, 42%
216 f: R = quinolin-2-yl, 18%
216 g: R = 6-chloroquinolin-2-yl, 24%
216 h: R = isoquinolin-3-yl, 8%

Scheme 58 Synthesis of 1,4-dihydropyrrolo[3,2-*b*]pyrroles **216** containing four-coordinate borons.

metathesis of B—Cl/C—B would take place between the arylchloroborane generated *in situ* by the reaction of aryltrifluoroborate with $SiCl_4$ and another aryltrifluoroborate to give diphenylchloroborane. This molecule undergoes pyridine-directed electrophilic aromatic borylation of the precursors **215**, leading to the target BN-embedded heteroacenes. The sterically bulkier base plays a role in improving the yield of this step to a large extent. The resultant C═N → B five-membered chelate ring fuses pyrrolopyrrole and heteroaryl substituent together, maintaining the π-conjugation in a coplanar fashion, forming this unique chromophore (**216a–h**). According to X-ray analysis, **216a** adopts planar structure at the core with peripheral pyridine rings twisted by 5° from the plane.

This simple and convenient method can be applied to starting materials like TAPPs bearing *N*-heteroaromatic rings. The reaction also tolerates the presence of halogens in the precursor molecule, allowing the post-functional modification. Accordingly, a few BN-embedded TAPPs substituted with halogens were submitted to Sonogashira or Buchwald-Hartwig cross-

couplings to further expand the π-system (Scheme 59). Although the presence of reactive boron atoms makes the outcome of the reaction unpredictable, the desired compounds **216i** and **216j** were isolated in comparable yield.

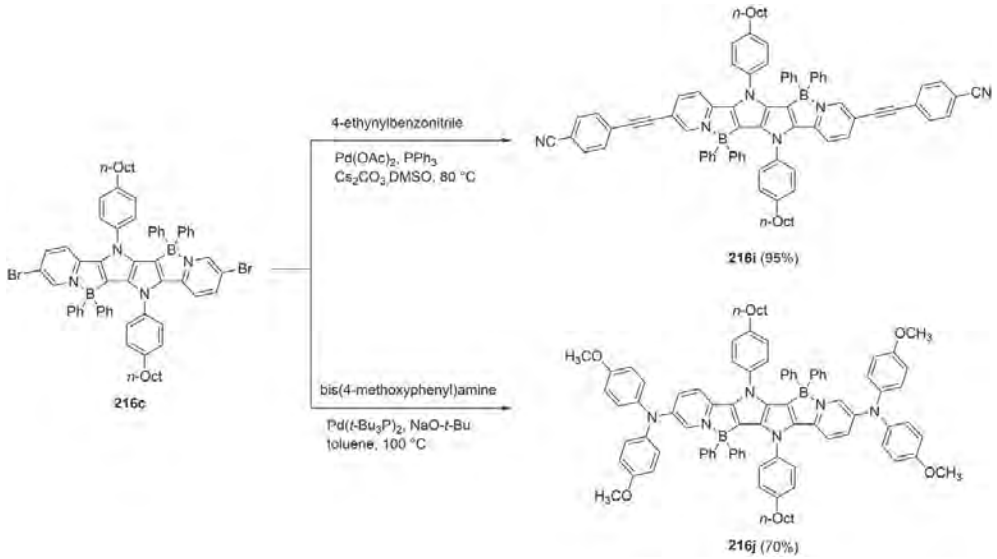

Scheme 59 Post functionalization of BN-TAPP **216c** leading to dyes **216i** and **216j.**

3.2.5 P-doped π-expanded DHPPs

As a result of extensive investigations on heteroatom doping in polycyclic systems, Mathey's group recently reported the first case of phosphorous embedded ladder-type heteroacenes possessing a DHPP core.[103] The classical dilithiobiaryl method was adopted to introduce phosphorous atom into the system. This was achieved by synthesizing TAPPs with bromine atoms at the *ortho* position (**217**) which can undergo the lithium-halogen exchange reaction using *n*-BuLi (Scheme 60). The organolithium intermediates react with dichlorophenylphosphine to form TAPPs **218**, which then experience the cyclization to give the bisphosphindol-pyrrolo[3,2-*b*]pyrrole derivatives **219** (BPhosPPs). The synthesized compounds was further oxidized with H_2O_2 or S_8 to obtain phosphole oxides (**220a-b**) and sulfide (**220c**), respectively. Phosphindol-pyrrolo[3,2-*b*]pyrroles (PhosPP) composed of a single phosphole ring have also been prepared by the same method using one equivalence of *n*-BuLi and dichlorophenylphosphine.

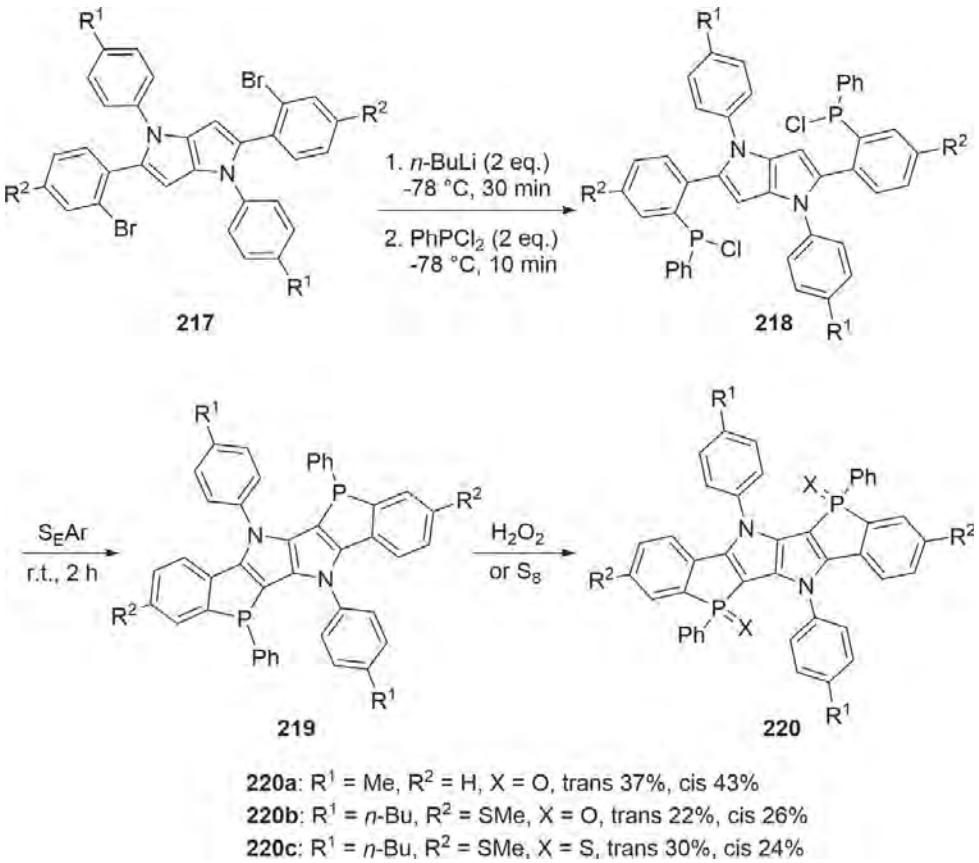

Scheme 60 Synthesis of BPhosPPs **219** and **220**.

The synthesized compounds **220** exhibit two isomeric *trans* and *cis* forms depending on the relative conformation of the phenyl substituent attached to the phosphine moiety. These isomers were separated easily by the classical purification method and showed a significant difference in their physicochemical properties.[103]

3.2.6 S-doped π-expanded DHPPs

Several examples of structurally interesting heteroacenes consisting of thiophene rings have been reported in the literature.[104–106] However, thienoacenes bearing a DHPP core became possible only after the discovery of the multicomponent synthesis of tetraarylpyrrolo[3,2-*b*]pyrrole.[107] TAPP precursor **221**, was synthesized with 2-(methylsulfinyl)phenyl substituents at 2 and 5 positions (Scheme 61). The subsequent ring closure step involves intramolecular electrophilic substitution in the presence of trifluoroacetic acid (TFA) and P_2O_5 followed by demethylation of the sulfonium salt intermediates. Further oxidation of dye **222** was achieved by treating with

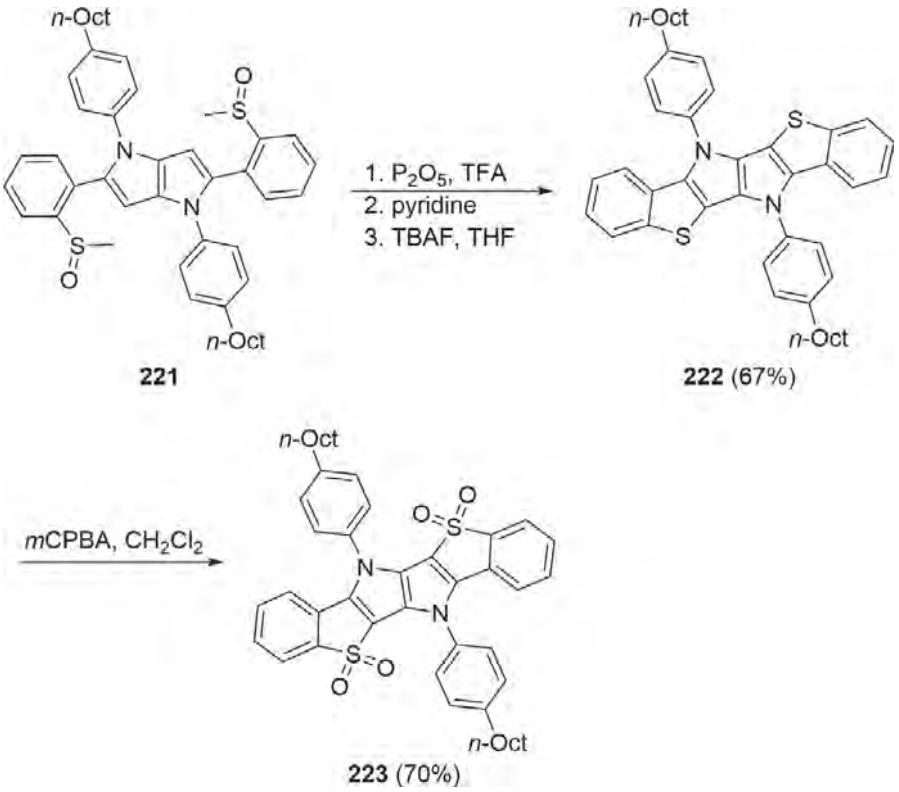

Scheme 61 Synthesis of dibenzothienopyrrolo[3,2-*b*]pyrroles **222** and **223**.

m-chloroperbenzoic acid (*m*CPBA) to form the corresponding *S,S,S′,S′*-tetraoxide **223**. Crystallization of compound **223** was successfully achieved and X-ray data showed a C_{2h} symmetric molecule with a planar pyrrolopyrrole core.

4. Photophysical properties

During the last decade a large number of TAPPs have been synthesized. This allowed for studying the influence of different substituents on the spectroscopic properties of the TAPP chromophores (Fig. 7, Table 2). Both unsubstituted DHPP and indolo[3,2-*b*]indole (**121**) has an absorption still in the ultraviolet region of the electromagnetic spectrum and a rather weak emission since it possesses a relatively small chromophore system.[73] Adding substituents or π-expansion gives rise to bathochromic shifts of both absorption and emission as it increases the conjugation chain.

One of the heavily studied phenomenon of 1,4-dihydropyrrolo[3,2-*b*]pyrroles is the particularly strong electronic communication effect through positions 2 and 5. In the case of **51b** (Fig. 2), the corresponding dihedral

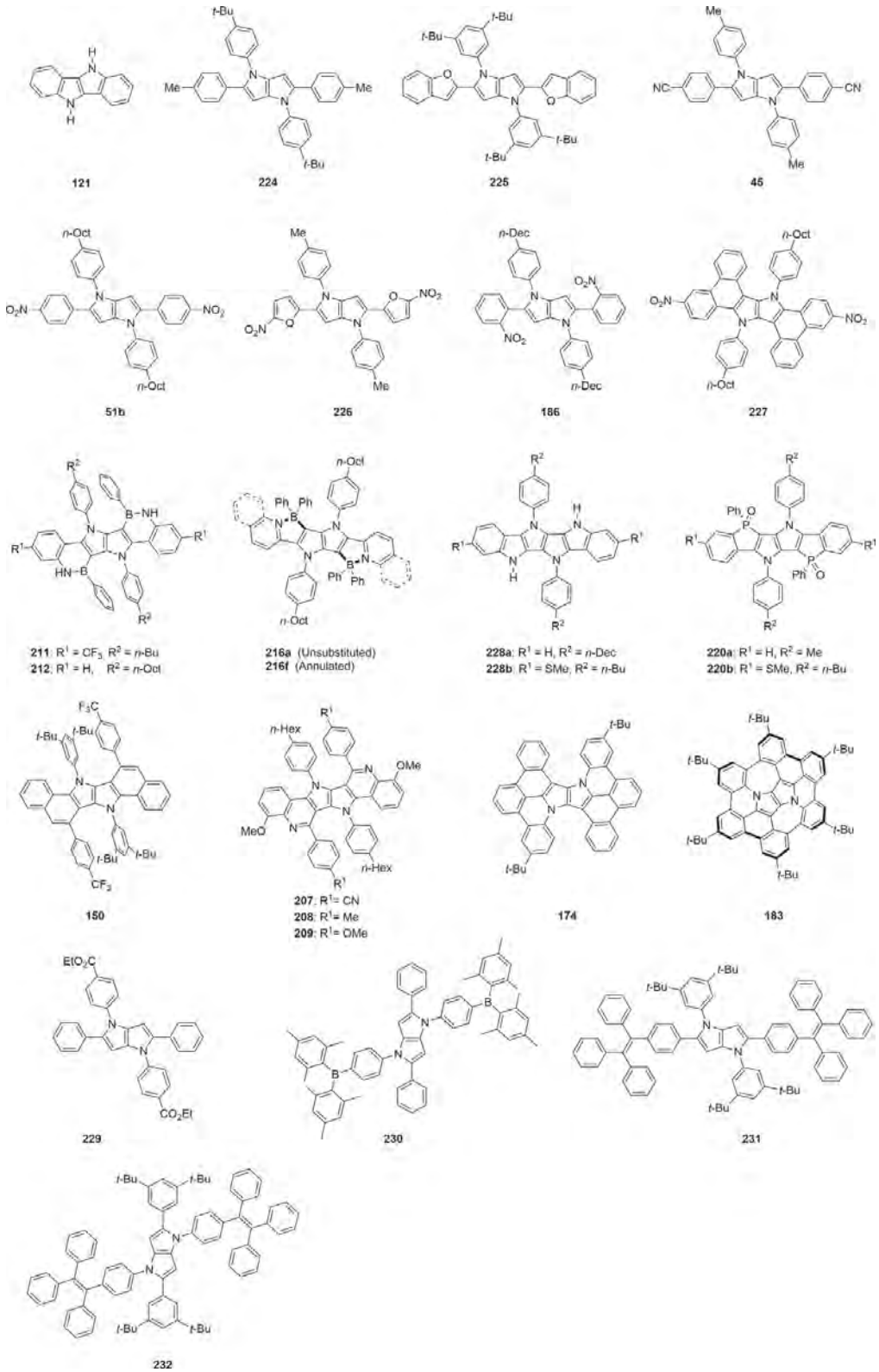

Fig. 7 Structures of exemplary TAPPs and π-expanded DHPPs.

Table 2 Photophysical properties of exemplary π-expanded DHPPs.

Compound	λ_{abs} (nm)	λ_{em} (nm)	$\Delta\bar{\nu}$ (cm^{-1})	Φ_{fl}	References
45[c]	403	450	2600	0.76	
51b[c]	465	552	3400	0.70	108
51b[d]	471	610	4800	0.03	
121[a]	360	400	2800	nd	73
150[c]	379	465	4900	0.26	84
174[c]	430	470	2000	0.13	91
174[b]	428	498	3300	0.18	
183[c]	530	593	2000	0.027	94
183[b]	530	615	2600	0.016	
186[c]	428	nd		nd	108
207[e]	322	504	11200	0.13	
208[e]	315	464, CT band appears	10200	0.02	
209[e]	317	453	9500	0.042	99
211[c]	402	413	660	0.78	
212[c]	387	400	840	0.70	100
216a[c]	502	521	730	0.78	101
216f[c]	583	601	510	0.78	
220a[b]	416	487	3500	0.55	103
220b[b]	439	513	3300	0.49	
224[c]	352	408	3900	0.66	24, 27
225[c]	420	438	1000	0.72	
226[c]	506	580	2500	0.28	27
227[c]	480	518	1500	0.72	29
228a[c]	394	407	810	0.52	98
228b[c]	406	419	760	0.82	
229[d]	322	488	10500	0.012	109
230[d]	395	479 (537)[f]		nd	110

[a]Absorption and fluorescence in DMF.
[b]Absorption and fluorescence in CH_2Cl_2.
[c]Absorption and fluorescence in toluene.
[d]Absorption and fluorescence in THF.
[e]Absorption and fluorescence in $CHCl_3$.
[f]In THF:water 5:95
nd – not determined.

angles are ca. 38° in the ground state and ≈26° in the S_1 state. The angles can vary but the general tendency is that TAPP molecules planarize in the excited state so that the aryl substituents in these positions become more strongly coupled with the central framework.[29]

The TAPP **224** (Fig. 7) lacking EDG/EWG shows absorption merely reaching the visible spectral range (λ_{abs} 352 nm) with the visible blue emission (λ_{em} 408 nm). Because aryl substituents lay out of a DHPP plane and the system somewhat planarizes in the excited state TAPP molecules tend to demonstrate moderate Stokes shift, e.g., 3900 cm^{-1} for compound **224**. In the case of 5-membered rings at positions 2 and 5 the geometry of the chromophore is more planar; in fact compound **225** shows the fluorescence maximum with the lower Stokes shifted compared with **224**. On the other hand modulation of the acceptor strength of substituents at the positions 2 and 5 adjusts the charge distribution between the DHPP framework and the terminal moieties. In fact, an increase of the electron-withdrawing properties of terminal moieties can lead to formation of charge transfer states with red-shifted both absorption and emission. Indeed, increasing the electron-acceptor strength of the aryl moieties (**45** vs. **224**) gives rise to a bathochromic shift of the absorption maximum with a smaller Stokes shift that indicate more efficient conjugation with aryls at positions 2 and 5 (Fig. 7, Table 2).[24,27]

The thorough study of TAPP **45** (Fig. 7) by means of the time-resolved IR (TRIR) spectroscopy reveals that the molecule experiences the processes caused by the excited-state symmetry-breaking (ES-SB).[111,112] The use of ultrafast time-resolved infrared spectroscopy enables the visualization of ES-SB. The study of the CN stretching modes on the electron-withdrawing moiety in real time enables monitoring this photophysical phenomenon. In polar solvents the IR spectrum shows two CN bands. The latter suggests that the ES-SB occurs within ca. 100 fs. Conversely, in apolar solvents the presence of a single CN band suggests that the S_1 state remains symmetric. On the other hand, in protic solvents the presence of H-bonds tends to amplify the ES-SB. Based on these studies Ivanov proposed a new model for ES-SB.[113]

An interesting observation resulted from studying highly polarized, quadrupolar bis-coumarins possessing an electron-rich DHPP bridging unit. It turned out that in analogy to the classical 7-dialkylaminocoumarins, bis-coumarin with a DHPP unit at the seventh position possesses strong and moderately bathochromically shifted fluorescence. Shifting the bridge to the position 6 has a profound effect as it results in a weakly emitting dye with λ_{em}^{max} at 650 nm.[114]

The thorough photophysical studies on TAPPs led to two important discoveries. TAPP **51b**, possessing two 4-nitrophenyl substituents at positions 2 and 5, has almost quantitative fluorescence quantum yield in cyclohexane. [115] Being an unusual example of an efficient fluorophore with nitro groups, compound **51b** was thoroughly studied in terms of the processes occurring in the excited state. It revealed an important role of planar CT states for the fluorescence response. In the excited state the chromophore experiences a fast transition from ^{1}LE* into the charge transfer state with the torsional angles reduced compared with the steady state.[29,108,116] The growth of the solvent polarity gives rise to the second CT state with one nitroaryl substituent twisted with respect to the rest of the chromophore (ES-SB), the latter causes fluorescence quenching.

A special case is the 5-nitrofuran-2-yl substituted TAPP **226** since less sterically hindered five-membered rings with the electron-withdrawing NO_2 group are more efficiently conjugated with the core, forming a strongly polarized quadrupolar system. This leads to significant shifts in both absorption and fluorescence compared to the analogous TAPP **51b** that possess 4-nitrophenyl substituents.

The strong electron-donating central framework and the terminal electron-withdrawing moieties form a strongly polarized A-D-A structure. In fact, quadrupolar chromophores tend to show stronger two-photon absorption (TPA) compared with dipolar chromophores. Compounds **45** and **51b** were studied in terms of the TPA properties. The two-photon absorption cross-section (σ_2) for compounds **45** and **51b** were measured as 530 and 420 GM, respectively.[115] Computational results show the calculated TPA of these compounds as 1650 and 1180 GM, respectively.

If substituents at positions 2 and 5 of the DHPP core are strongly electron-withdrawing the centrosymmetric, quadrupolar systems are created with markedly bathochromically shifted absorption and emission. Recent studies have revealed that if particularly strong electron-withdrawing groups are present the emission maxima of TAPPs reaches 600 nm.[117] Conversely the combination of too strong electron acceptors and highly polar media can lead to configurations with the twisted geometry and the quenched fluorescence.

The planarity of the structures ensures a spatial overlap between the orbitals carrying the positive charge of the oxidized donor (DHPP core) and the negative charge of the reduced acceptor (nitrophenyl substituent) even for polarized CT states. Such orbital overlap, indeed, translates to large radiative-decay rates and strong fluorescence, while the CT character of the excited states reduces the propensity for intersystem crossing (ISC) leading to triplet formation. Torsional degrees of freedom allow conformations with

orthogonality between the rings of the donor and the acceptor breaking the delocalization of the frontier orbitals and diminishing orbital overlap. Therefore, such twisted intramolecular charge-transfer (TICT) excited states are dark. Furthermore, the orthogonal geometry of the TICT states enhances ISC. Solvent polarity stabilizes such TICT states with relatively well separated charges localized on the donor and the acceptor. The steric hindrance between the NO_2 groups and the pyrrolopyrrole core maintains orthogonality in the 2-nitrophenyl TAPP **186**, which is consistent with the lack of detectable fluorescence and the sub-picosecond excited-state lifetimes.[108] These paradigms bring us closer to electron-deficient nitroaromatics that, in addition to their characteristics as n-type conjugates, also have attractive optical properties.[118]

In compound **227**, on the other hand, two carbon bridges secure the planar configuration the TAPP chromophore with the dihedral angles ca. 6.7°. It shows an intense light absorption in the spectral range as for **51b**. The fluorescence of **227** is also sensitive to the solvent polarity; however due to the fixed geometry, it demonstrates a much smoother decrease of the fluorescence response while bridging inhibits a fully twisted CT state (Fig. 7, Table 2).[29]

In the case of π-expanded DHPPs, the range of skeletons studied during the last decade is overwhelming, which reflects the availability of the TAPPs possessing suitable synthetic handles. The fusion of parent chromophores with additional moieties such as indole (**228a**, **228b**), phosphoxole (**220a**, **220b**), quinoline (**207**, **208**, **209**), etc. leads to skeletons possessing eight, ten, twelve or even fourteen conjugated rings with planar or curved geometry. In most cases, the λ_{abs} is located at approximately 400–500 nm and emission is moderately bathochromically shifted which leads to rather small Stokes shifts (Table 2). Emission intensity depends on the particular heteroatoms involved in N-doping. The general trend is that with carbon-only analogs (**207–209**) the Φ_{fl} is in the range of 0.1–0.2 whereas it considerably increases when a B—N bond is present C (**211**, **212**).

A bridging approach often rigidifies planar geometry of TAPP and prevents twisted CT states. On the other hand, if the bridge moiety features an additional electronic effect, it can significantly change the charge distribution within the chromophore. In compounds **211**, **212** bridging occurs by means of an azaborine fragment. This modification does not change the chromophore in terms of the electronic structure as there is no new conjugation chain and the electron donor and the acceptor parts interact the same way as in a generic TAPP chromophore. Indeed compounds **211** and **212** show the absorption maxima in the same range compared with **225**. At the

same time compound **211** bearing electron-withdrawing terminal moieties shows somewhat red-shifted absorption compared with **212**. Furthermore, compounds **211** and **212** demonstrate a strong emission response with the small Stokes shift indicating a small geometry change in the excitation-emission process. The structures of compounds 216a,f possess strong similarities with **211** and **212** as the former possess boron bridges bound with the pyridine-type nitrogen atoms by means of donor-acceptor bonds, partially withdrawing the electron density from the pyridine ring. Consequently, the absorption band of compound **216a** is red-shifted in comparison with compounds **212**. In turn **216f** shows the absorption red-shifted in relation with **216a** due to a larger conjugation system. Both compounds 216a,f demonstrate strong fluorescence and small Stokes shifts because of a stable planar geometry. The spectroscopic properties of DHPP fused with indole systems **228a,b** resemble generic TAPPs **224**, **225** and **45** as well as compounds **211** and **212**. They show small deviation in the absorption maxima as rigid geometry is much less prone to the change of the terminal moiety character, so that **228b** is only a 12 nm red-shifted related to **228a**. Both compounds 228a,b show strong emission with a small Stokes shift. Dyes 220a,b bridged with a phosphorus atom demonstrate absorption maxima at the range 415–440 nm with the strong fluorescence, but in contrast to other DHPPs fused with heteroatoms the Stokes shifts are much higher. Though this comparison is not accurate enough as spectral data for 220a,b were collected only in CH_2Cl_2.

Despite the superficial similarity, the spectroscopic properties of compounds **150** and **207–209** are different from described above **211**, **212**, **216a,f** and **228a,b** series. The former demonstrate by a weak or a moderate fluorescence response with a large Stokes shift. The specific orientation of polarized substituents in **207–209** leads to a different model of a charge distribution than that for other TAPPs. Changing the electron-donor moiety (**209**) to the neutral substituent **208** results in the fluorescence from two states (1: similar to **209** and 2: new CT state). Introducing the electron-acceptor moiety (**207**) instead of neutral leads to the fluorescence exclusively from the CT state (Fig. 7, Table 2).[99]

Further chromophore annulation leads to a partial planarity distortion. The compound **174** has a π-extended system with fused benzene rings. The comparison with TAPP **224** shows that the annulation by itself leads to about 80 nm red-shift. The geometry of compound **174** is twisted according to both X-ray and computation data that cause lower fluorescence quantum yield related with other DHPPs (Fig. 7, Table 2).[91] Another consequence of the curved geometry is the solvatochromism of the fluorescence because the geometry in the excited state depends on the solvent polarity.

Fully fused DHPP analogue **183** demonstrates as high as 100 nm red-shifted absorption maximum compared with partially fused **174**. However, the curved geometry causes the fluorescence to be significantly quenched in any solvents with a noticeable solvatochromism of the fluorescence.[94]

Conversely, the electronic properties of substituents at the positions 1 and 4 barely affect the location of both absorption and fluorescence maxima as the electronic communication is weaker through the nitrogen atoms. Consequently, owing to a large bond alternation in the substituents aryl rings experience free rotation around the C—N bond (Fig. 8). Introducing

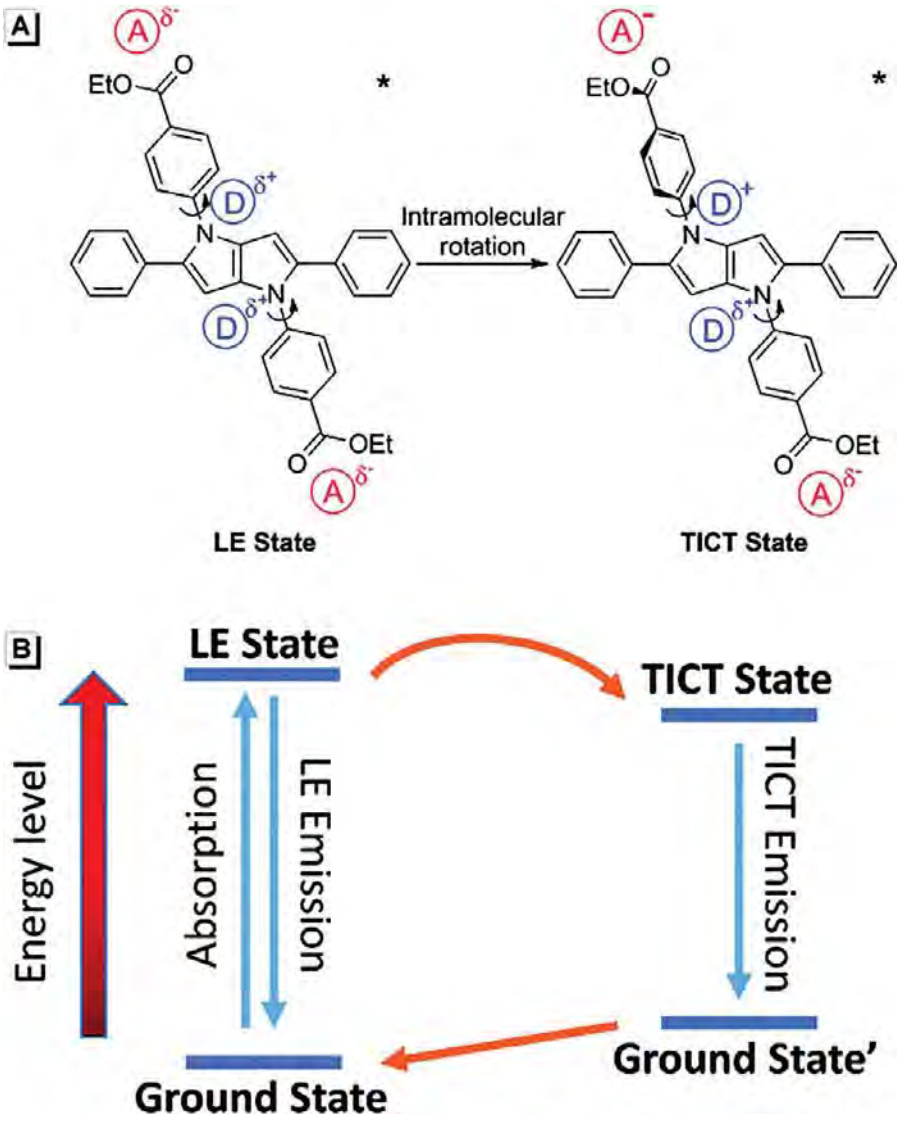

Fig. 8 (A) Transition from the LE state of **229** to the TICT state through intramolecular rotation of its donor and acceptor units at the excited state. (B) Energy diagram of the TICT process. *Reproduced from* Chem. Sci., ***2017***, 8, *7258–7267 with permission from the Royal Society of Chemistry.*

electron-acceptor groups at those aryls can even facilitate the rotation as it induces stable CT states (**229**). The control of the rotation around C—N bond is crucial to govern the fluorescence properties for this system as it allows formation of fluorescent aggregates (AIE).[119] The authors claim that the restricted intramolecular rotation (RIR) is the key mechanism responsible for the AIE character displayed by TAPP **229**. Compound **229** possessing a hydrophobic character, in a THF-water solvent system shows fluorescence growth by increasing the water content in the mixture as this promotes the aggregation (AIE). In THF solution TAPP **229** shows temperature dependent behavior since the fluorescence response exhibits a twofold increase in the course of a temperature rise from 10 °C to 60 °C. The authors claim that the underlying reason is the stabilization of the TICT state.[109] Due to the RIR mechanism, TAPP **229** shows high selectivity toward Cd(II) displaying a rapid growth of the fluorescence signal. Compound **230** is the analogue of TAPP **229**, though, it consists of boron acceptor centers. The addition of water to a THF solution of **230** leads to a significant red-shift of the fluorescence maximum along with an increase of the fluorescence efficiency.[110] TAPPs **231** and **232** consist of tetraphenylethylene (TPE) moieties.[120] Indeed, both compounds shows a weak fluorescence response in solution. Diversely, a bulky TPE moiety prevents the close mutual orientation of the π-systems of the adjacent molecules in the crystal lattice thus blocking aggregation caused quenching (ACQ). Compounds **231** and **232** demonstrate the strong fluorescence response in the solid state (λ_{em} 516 nm, Φ_{fl} 0.77 and λ_{em} 468 nm, Φ_{fl} 0.16, respectively), which is another example of the AIE.

The fluorescence efficiency vs. the absorption and emission wavelengths of selected DHPP-based dyes is collected in Fig. 9.

5. Applications

5.1 Optoelectronic applications

Linearly π-conjugated acenes are considered to be a workhorse in research directed toward field-effect transistors (OFETs), organic light-emitting diodes (OLEDs), and organic solar cells. Among them, pentacene is the most explored but at the same time, due to the high HOMO level, it is unstable. [121] In the light of this problem the more stable, ladder-type compounds possessing condensed thiophene rings became very popular in the literature related to optoelectronics.[5,97,122,123] Along these lines heteroacenes possessing a DHPP moiety are the obvious object for extensive studies, which indeed

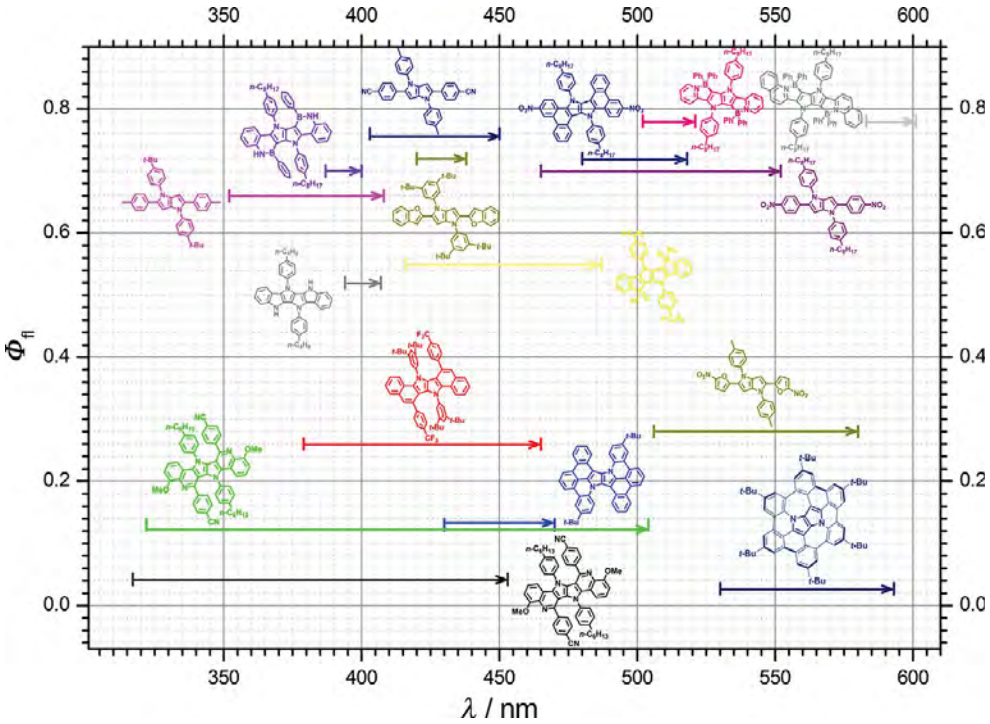

Fig. 9 The fluorescence efficiency of DHPP-based dyes vs. absorption and emission wavelengths.

took place in the last two decades. OFET-related properties for DHPPs have been reported only in a few patents.[124–126]

On the other hand both indolo[3,2-*b*]indole[127] and DHPPs were applied in advanced investigations directed toward high-spin organic polymers and OLEDs.[128] As early as in 1994 linear polymers prepared from indolo[3,2-*b*] indole were investigated as high-spin polymers or photoluminescent diodes.[129] As later reported by Suh and co-workers, optical and electrochemical properties of polymers containing exclusively indolo[3,2-*b*]indoles were excellent, but low molecular mass precluded formation of a high quality of film, which excluded practical applications.[128] More recently TAPPs possessing 4-cyanophenyl substituents in positions 2 and 5 were successfully investigated as light-emitting layer in OLEDs.[130] A similar line of research was conducted in China revealing that structurally complex DHPPs can be used to construct blue OLEDs devices with a high efficiency, high brightness and high stability.[131, 132] Red-emitting OLEDs based on DHPPs possessing strongly electron-accepting substituents were reported to have external quantum efficiency 3.4%.[117]

Solution-processed organic photovoltaics (OPVs) have the superiorities of light weight, low cost, easy fabrication, high mechanical flexibility and good semitransparency, enabling great potential in next-generation photovoltaic technology.[133] TAPPs were also investigated as donors in bulk heterojunction solar cells. Unfortunately, due to the overall low charge mobility for holes (10^{-9} cm^2/Vs), the overall performance of the blend of π-expanded DHPP **233** and C70, was measured to be rather poor.[134] An another π-expanded DHPP **234** (Fig. 10) was investigated as photosensitizer in DSSCs.[135] A multistep synthesis has afforded quadrupolar TAPP **235** designed to be a non-fullerene acceptor in bulk-heterojunction organic solar cells. It was revealed that dye **235** has high stability, adequate energy level,

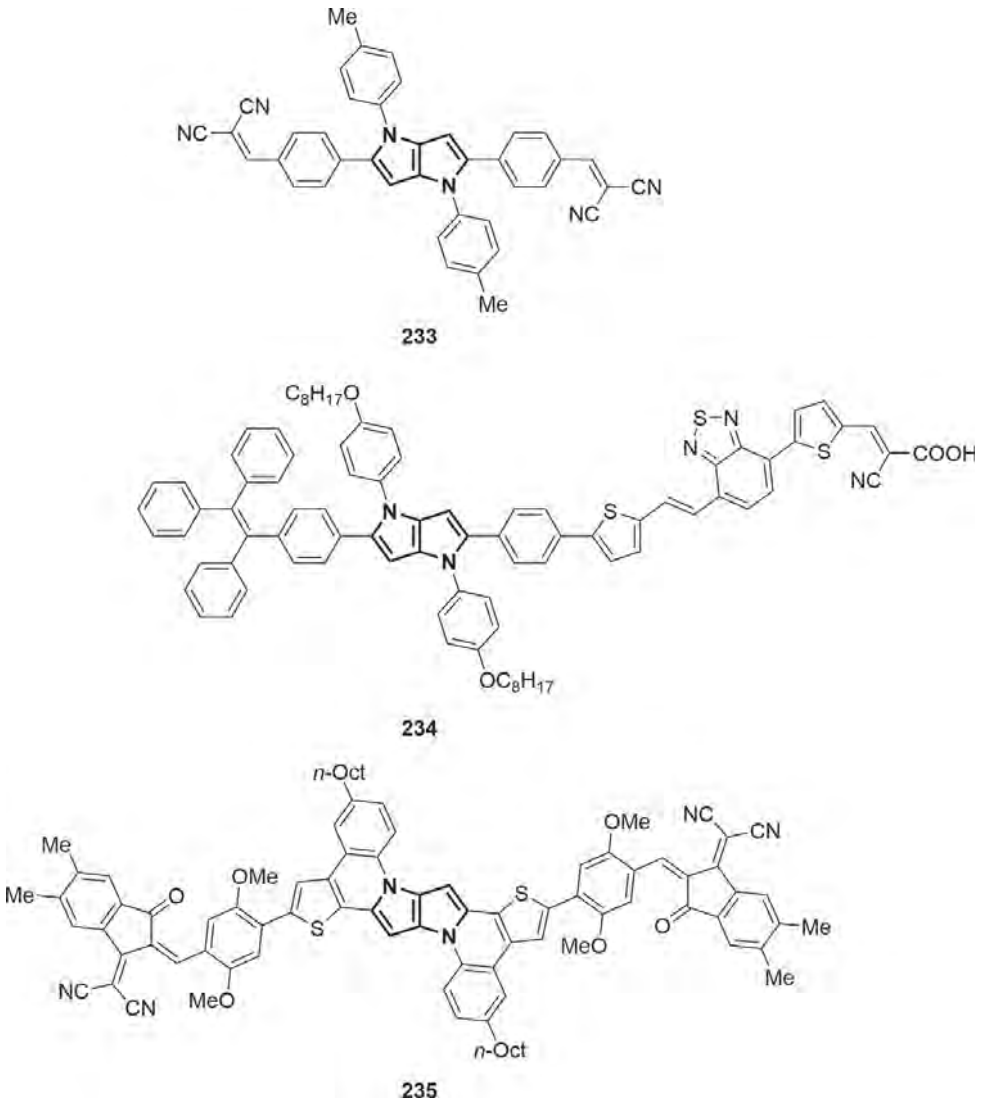

Fig. 10 Structures of DHPPs applied in OPV-related research.

high carrier mobility, good solubility and film formation, which makes it a potential acceptor material in organic solar cell devices.[136,137]

5.2 Metal-organic frameworks and related applications

Gunnlaugson was the first to present an example of crystalline coordination polymers containing TAPPs. The design was based on derivatives bearing nitrile, carboxylate and mixed imidazole-carboxylate donor functionality.[138] More recently Mukherjee and co-workers described the use of a TAPP as a trifacial nanobarrel (Fig. 11).[139] The Pd-barrel was composed of three 1,4-dihydropyrrolo[3,2-*b*]pyrrole panels, clipped through six cis-Pd(II) acceptors. The tetra-imidazole ligand **L** was synthesized via a copper-catalyzed Ullmann coupling reaction of 1,2,4,5-tetrakis(4-bromophenyl)-1,4-dihydropyrrolo[3,2-*b*]pyrrole with imidazole. The ligand was reacted with *cis*-(TMEDA)Pd$(NO_3)_2$ in a water/methanol mixture (1:1) at 65 °C in 1:2 M ratio. In the next stage the solution was treated with excess KPF_6 to afford the targeted compound as a yellow precipitate in quantitative yield (Fig. 11).

Unfortunately, the authors failed to obtain a crystallographic structure of this complex. In order to analyze the geometry of this trifacial barrel, they used the PM6 method. Investigation of its energy-optimized molecular structure has revealed that three tetraimidazole ligands (L) are paneled to the three faces horizontally and 90° *cis*-(TMEDA)Pd$(NO_3)_2$ acceptors are clipped at the six corners of the barrel (Fig. 12A and B). Research showed that the presence of a concave cavity with an internal diameter of 13.8 Å

Fig. 11 Schematic representation of the synthesis of the Pd-barrel. *Copied with permission from* Angew. Chem. Int. Ed. ***2021***, 60, *14109.*

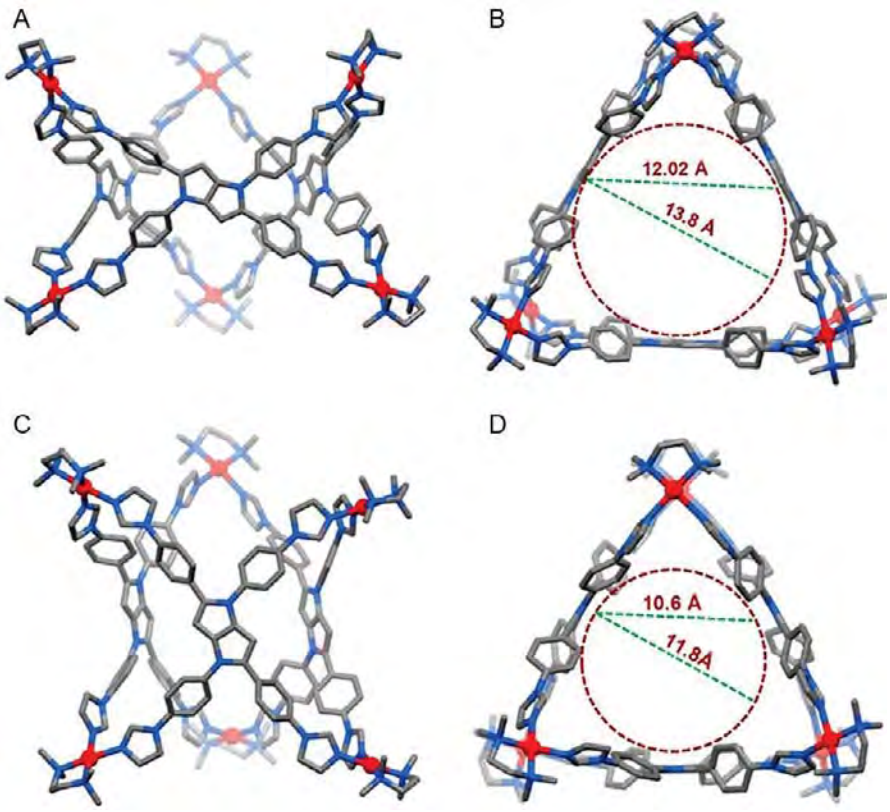

Fig. 12 Optimized structure of trifacial barrel: (A) Side view and (B) top view where ligands are horizontally oriented; (C) Side view and (D) top view of the other expected geometry where ligands are vertically oriented. Color codes: carbon (gray), nitrogen (blue), palladium (red). H-atoms are omitted for clarity. *Copied with permission from* Angew. Chem. Int. Ed. ***2021***, 60, *14109.*

with an open window size of 13.6 Å makes the barrel an ideal host to accommodate curved-surfaced fullerenes C_{60} and C_{70}.

In 2019 Zang and co-workers reported the synthesis of new luminescent three-dimensional stable silver cluster-assembled materials (SCAM) Ag_{12}CPPP.[140] The SCAM of Ag_{12}CPPP was easily synthesized using a one-pot method from DHPP possessing two pyridine moieties, in a mixed solvent dimethylacetamide (DMAc), $CHCl_3$ and CH_3OH. SCXRD analysis of Ag_{12}CPPP has shown that it has a trigonal l2/m space group and two-fold self-interpenetrated 3D framework (Fig. 13).

Two CF_3COO^- ligands are connected with Ag^+ in a monocoordinate mode, and the other four CF_3COO^- ligands are chelated with Ag^+ in tricoordinate mode. The SBUs are linked with eight CPPP ligands; four of them coordinate with the silver cluster through pyridine groups, and the other four ligands coordinate with the silver cluster through nitrile groups (Fig. 13C).

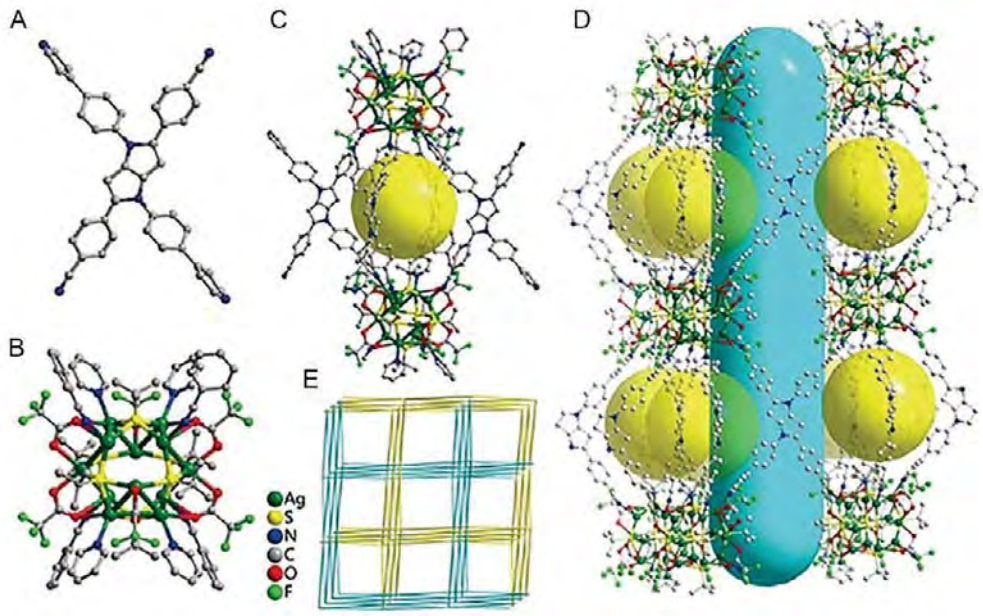

Fig. 13 Crystal structure of Ag_{12}CPPP: (A) CPPP ligand; (B) Silver–chalcogenolate cluster node; (C) Cage in Ag_{12}CPPP; (D) Distribution of the cages in Ag_{12}CPPP; (E)Topological representation of Ag_{12}CPPP. All hydrogen atoms and guest solvent molecules are omitted for clarity. *Copied with permission from* Chem. Eur. J. ***2019***, 25, *2750–2756.*

Photochemical research has shown that the emission intensity of Ag_{12}CPPP is much stronger than that in CPPP regardless of whether it is being measured in the solid or in solution. Additionally, Ag_{12}CPPP shows high photostability. The authors performed a number of experiments to understand this phenomenon. Mechanistic studies have shown that the matrix coordination induced emission (MCIE) effect in Ag_{12}CPPP is responsible for this appearance. The stiffening tactic not only enhances the fluorescence of the ACQ molecule in the aggregated state, but also improves the silver cluster in the unstable state.

An another group reported the use of DHPP-based organic linkers in construction of metal−organic frameworks (MOFs).[141] In the first stage DHPP-based tetracarboxylate linkers were obtained by the reaction of corresponding benzaldehyde and arylamine followed by a hydrolysis reaction (Fig. 14). The final stage was a solvothermal reaction of $ZrCl_4$ with H_4L_1 in *N,N*-dimethylformamide (DMF) in the presence of formic acid as the modulator which a gave colorless single crystals of IAM-7. In an analogous procedure IAM-8 was obtained.

On account of unequal lengths of the branch arms, the H_4L_1 linker has the largest aspect ratio 1.29, compared to H_4L_2 which contains four branch arms with equal lengths with a smaller aspect ratio of 1.08 (Fig. 14).

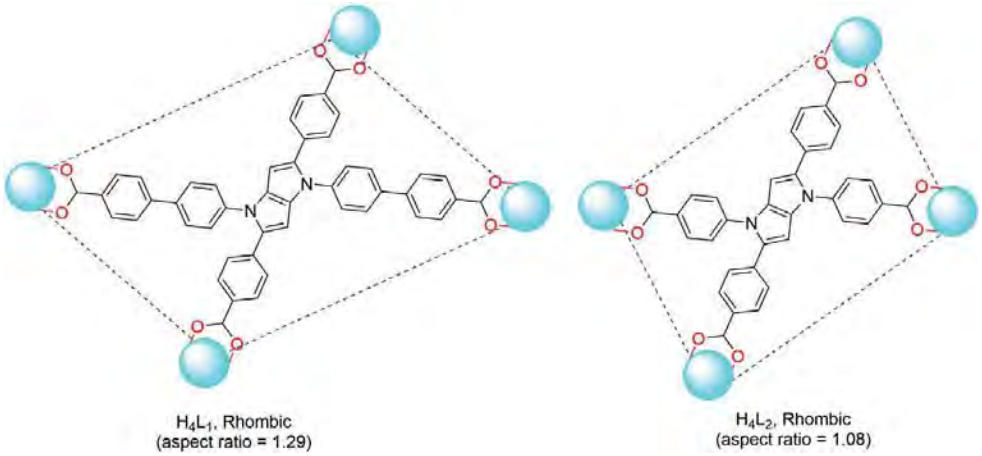

Fig. 14 Illustration of the different shapes of planar tetratopic linkers observed in Zr-MOFs. *Adapted with permission from* Inorg. Chem. ***2021***, 60, *12129 – 12135.*

IAM-7 can be regarded as the result of the self-installation of the linear "spacer" $H_2L_1^{2-}$ into the rhombic channels of the 4,8-connected structure from which the connectivity of the Zr_6 clusters increased from 8 to 10. The authors emphasize that this is the first construction of 10-connected Zr-MOFs from one single type of tetratopic linker (Fig. 15).

It needs to be highlighted that IAM-7 displays a high proton conductivity of $1.43 \times 10^{-2}\,Scm^{-1}$ at 95% RH and 90 °C, which is among one of the highest for conductive Zr-MOFs. IAM-8 exhibits a much lower proton conductivity from $5.33 \times 10^{-6}\,Scm^{-1}$ at 30 °C to $3.00 \times 10^{-5}\,Scm^{-1}$ at 90 °C. Such high proton conductivity may be due to high hydrophilicity and the presence of a carboxylic acid functionality in IAM**–7**. It turns out that the asymmetric pyrrole-pyrrole unit can be an excellent basis for the design of organic linkers with new functionalities and geometries which can contribute to the development of MOF materials in many applications.

5.3 Other applications

The strong charge-transfer characteristics of A-D-A type TAPPs have been exploited in other areas of research. Basak and co-workers discovered that organic resistive memory devices (ORMs) can be prepared from TAPPs possessing 4-nitrophenyl and 3-nitrophenyl substituents at positions 2 and 5.[142] Interestingly, the 2,5-bis(4-nitrophenyl)DHPP fitted characteristics of "write-once-read-many" type of memory device, whereas 2,5-bis (3-nitrophenyl)DHPP behaved like "write-read-erase-read" (typical for FLASH memory devices). This research was later extended to achieve the encoding of nano "bits" with temporary remanence.[143]

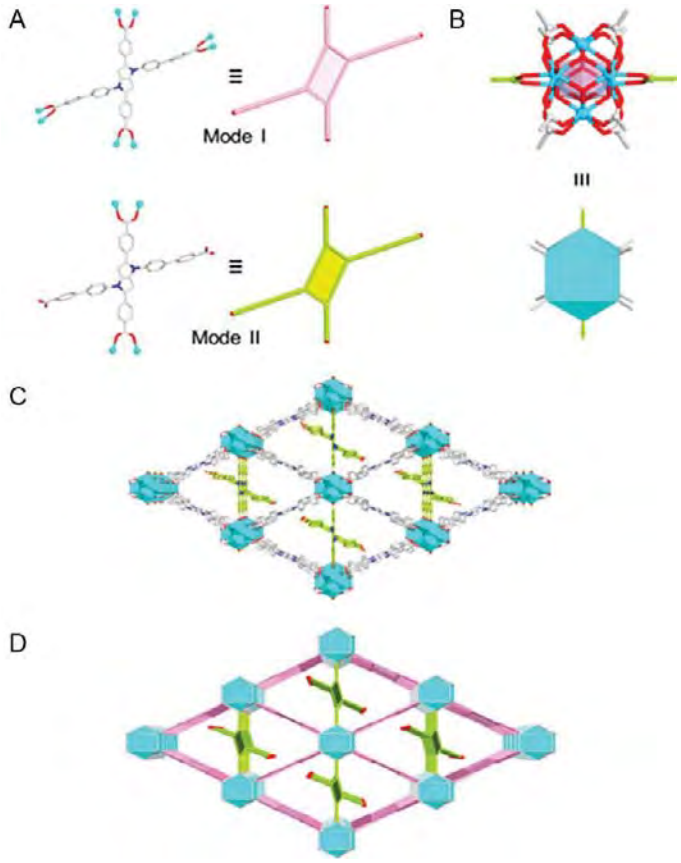

Fig. 15 Structure and topology of IAM-7: (A) Coordination modes I and II of the L_1^{4-} linker; (B) The 10-connected Zr_6 node; (C and D) 3D structure and topology of IAM-**7** viewed along the c-axis (Zr, turquoise; O, red; and C, gray). *Copied with permission from* Inorg. Chem. ***2021***, 60, *12129–12135.*

A different area was targeted with DHPPs bearing substituents with electron-donating character. Leung and co-workers discovered that 2,5-bis(triphenylamine)-substituted DHPP enables quick detection of $CHCl_3$ with the naked eye via reaction with halocarbons leading to deeply colored species.[144] The authors concluded that, since the photochromic responses differ in color, the mechanism of photodecomposition must follow electron transfer from electron-rich dye to chlorinated compound. The chlorination, bromination or iodination at positions 3 and 6 are followed by further oxidation of these products to highly colored species. An another approach toward chloroform detection was based on change of emission of thin films of TAPPs in the presence of chloroform and light.[145] Very recent application targets selective detection of Ti^{3+} cations.[38]

6. Summary and outlook

1,4-Dihydropyrrolo[3,2-*b*]pyrrole, a non-natural aromatic scaffold, is isoelectronic with indole. In contrast to indole and pyrrole however, this aromatic skeleton was practically unknown until the 1970s and its chemistry remained rather dormant until 2013 when multicomponent condensation leading to tetraaryl-1,4-dihydropyrrolo[3,2-*b*]pyrroles was developed. The latter was transformative not only because of straightforward access to these heterocycles but also due to the simultaneous presence of the following factors: (i) functional group compatibility is superb; (ii) the reaction gives rise to DHPPs possessing synthetic handles ready for further transformations; (iii) the presence of highly reactive, electron-rich positions 3 and 6 prone to electrophilic aromatic substitutions. Combination of these factors is responsible for releasing the unprecedented stream of activity which resulted thus far in the preparation of at least 15 novel heterocyclic skeletons possessing up to 14 conjugated rings. Eventually it turned out to be possible to link all six substituents present at positions 1–6, creating an oval-shaped π-expanded system possessing a bowl shape.

The exploration of DHPPs has embraced such areas as MOFs, optoelectronics, detection of chloroform, etc. It has also contributed to our understanding of excited-state symmetry-breaking and to the renaissance in popularity of fluorescence of nitro-aromatics as a research topic. The electron-rich nature of 1,4-dihydropyrrolo[3,2-*b*]pyrroles has attracted scientists' attention which coincided with the rise of optoelectronics. The combination of superb physicochemical features and straightforward synthesis has contributed to their popularity in various research applications, as it makes them an ideal platform for many photonics-oriented challenges of modern technology-driven society.

We envision that the next stage of DHPP's development will be focused mostly on organic light-emitting diodes. Indeed, the never ending quest for more stable blue emitters can one day focus on one of the derivatives of DHPP. However, a lot of research is still required to reach this goal. In spite of the fact that many combinations have been reported in recent years for various OPV-related applications, the potential of DHPP as the most electron-rich small aromatic heterocycle has not been yet fully realized. This will be, in our opinion, one of the most promising directions of research during the next decade. In the near future, both structures and applications of 1,4-dihydropyrrolo[3,2-*b*]pyrroles will be limited only by our imagination.

References

1. Mishra, A.; Ma, C. Q.; Bäuerle, P. *Chem. Rev.* **2009**, *109*, 1141–1176.
2. Cinar, M. E.; Ozturk, T. *Chem. Rev.* **2015**, *115*, 3036–3140.
3. Heteropentalenes, T. In *Special Topics in Heterocyclic Chemistry*; Potts, K., Weissberger, A., Taylor, E. C., Eds.; Wiley, 2009; pp. 317–380.
4. Bulumulla, C.; Gunawardhana, R.; Gamage, P. L.; Miller, J. T.; Kularatne, R. N.; Biewer, M. C.; Stefan, M. C. *ACS Appl. Mater. Interfaces* **2020**, *12*, 32209–32232.
5. Wang, C.; Dong, H.; Hu, W.; Liu, Y.; Zhu, D. *Chem. Rev.* **2012**, *112*, 2208–2267.
6. Qiu, L.; Zhuang, X.; Zhao, N.; Wang, X.; An, Z.; Lan, Z.; Wan, X. *Chem. Commun.* **2014**, *50*, 3324–3327.
7. Janiga, A.; Gryko, D. T. *Chem. Asian J.* **2014**, *9*, 3036–3045.
8. Hemetsberger, H.; Knittel, D. *Monatsh. Chem.* **1972**, *103*, 194–204.
9. Heffernan, M. L. R.; Dorsey, J. M.; Fang, Q. K.; Foglesong, R. J.; Hopkins, S. C.; Jones, M. L.; Jones, S. W.; Ogbu, C. O.; Perales, J. B.; Soukri, M.; et al. *Fused Heterocyclic Inhibitors of D-Amino Acid Oxidase for Treatment of Neurological Disorders, Pain, Ataxia, and Convulsion*; US20080058395 A1, 2008.
10. Barker, A. J.; Kettle, J. G.; Faull, A. W. *Bicyclic Pyrrole Derivatives as MCP-1 Inhibitors*; WO 9940914 A1, 1999.
11. Murphy, B. P.; Glenn, R. W. J.; Lim, M.; Gardlik, J. M.; Jones, S. D.; Laidig, W. D.; David, S. J. *Keratin Dyeing Compounds, Keratin Dyeing Compositions Containing Them, and Use Thereof*; WO 2005077324 A1, 2005.
12. Aratani, T.; Yoshihara, H.; Suzukamo, G. *Tetrahedron Lett.* **1989**, *30*, 1655–1656.
13. Kumagai, T.; Satake, K.; Kidoura, K.; Mukai, T. *Tetrahedron Lett.* **1983**, *24*, 2275–2278.
14. Kumagai, T.; Tanaka, S.; Mukai, T. *Tetrahedron Lett.* **1984**, *25*, 5669–5672.
15. Mukai, T.; Kumagai, T.; Tanaka, S. *N-Alkyldihydropyrrolopyrrole Compound and Production Thereof*; JPS62212389A, 1987.
16. Kubota, Y.; Koide, K.; Mizuno, Y.; Nakazawa, M.; Inuzuka, T.; Funabiki, K.; Sato, H.; Matsui, M. *New J. Chem.* **2022**, *46*, 1533–1542.
17. Stokes, B. J.; Dong, H.; Leslie, B. E.; Pumphrey, A. L.; Driver, T. G. J. *Am. Chem. Soc.* **2007**, *129*, 7500–7501.
18. Prinzbach, H.; Breuninger, M.; Gallenkamp, B.; Schwesinger, R.; Hunkler, D. *Angew. Chemie* **1975**, *87*, 350–351.
19. Dieck, H. T.; Verfürth, U.; Diblitz, K.; Ehlers, J.; Fendesak, G. *Chem. Ber.* **1989**, *122*, 129–131.
20. Watson, A. J. A.; Williams, J. M. J. *Science* **2010**, *329*, 635–636.
21. Llabres-Campaner, P. J.; Ballesteros-Garrido, R.; Ballesteros, R.; Abarca, B. J. *Org. Chem.* **2018**, *83*, 521–526.
22. Giordano, L.; Ballesteros, R.; Ballesteros-Garrido, R. *Mol. Ther.* **2020**, *2020*, 1–4.
23. Bou-Puerto, A.; Bellezza, D.; Martinez-Morro, C.; Gonzalez-Sanchis, N.; Ballesteros, R.; Cuñat, A. C.; Ballesteros-Garrido, R. *Tetrahedron Lett.* **2021**, *84*, 153460.
24. Janiga, A.; Glodkowska-Mrowka, E.; Stoklosa, T.; Gryko, D. T. *Asian J. Org. Chem.* **2013**, *2*, 411–415.
25. Janiga, A.; Krzeszewski, M.; Gryko, D. T. *Strongly Fluorescent Heterocycles and a Method for Their Synthesis*; WO2014070029A8, 2013.
26. Krzeszewski, M.; Gryko, D.; Gryko, D. T. *Acc. Chem. Res.* **2017**, *50*, 2334–2345.
27. Tasior, M.; Koszarna, B.; Young, D. C.; Bernard, B.; Jacquemin, D.; Gryko, D.; Gryko, D. T. *Org. Chem. Front.* **2019**, *6*, 2939–2948.
28. Krzeszewski, M.; Thorsted, B.; Brewer, J.; Gryko, D. T. *J. Org. Chem.* **2014**, *79*, 3119–3128.

29. Łukasiewicz, Ł. G.; Ryu, H. G.; Mikhaylov, A.; Azarias, C.; Banasiewicz, M.; Kozankiewicz, B.; Ahn, K. H.; Jacquemin, D.; Rebane, A.; Gryko, D. T. *Chem. Asian J.* **2017**, *12*, 1736–1748.
30. Orłowski, R.; Banasiewicz, M.; Clermont, G.; Castet, F.; Nazir, R.; Blanchard-Desce, M.; Gryko, D. T. *Phys. Chem. Chem. Phys.* **2015**, *17*, 23724–23731.
31. Banasiewicz, M.; Stężycki, R.; Kumar, G. D.; Krzeszewski, M.; Tasior, M.; Koszarna, B.; Janiga, A.; Vakuliuk, O.; Sadowski, B.; Gryko, D. T.; et al. *Eur. J. Org. Chem.* **2019**, *2019*, 5247–5253.
32. Martins, L. M.; de Faria Vieira, S.; Baldacim, G. B.; Bregadiolli, B. A.; Caraschi, J. C.; Batagin-Neto, A.; da Silva-Filho, L. C. *Dyes Pigm.* **2018**, *148*, 81–90.
33. Martins, L. M.; Bregadiolli, B. A.; Augusto, L. C.; Carvalho, J. H. L.d.; Zaghete, M. A.; Silva Filho, L. C.d. *Mater. Res.* **2021**, 24. https://doi.org/10.1590/1980-5373-mr-2021-0008.
34. Tasior, M.; Vakuliuk, O.; Koga, D.; Koszarna, B.; Górski, K.; Grzybowski, M.; Kielesiński, Ł.; Krzeszewski, M.; Gryko, D. T. *J. Org. Chem.* **2020**, *85*, 13529–13543.
35. Krzeszewski, M.; Tasior, M.; Marek, G.; Gryko, D. T. *Organic Synth.* **2021**, *98*, 242–262.
36. Kumagai, T.; Tanaka, S.; Satake, K.; Mukai, T. *Heterocycles* **1985**, *23*, 183.
37. Janiga, A. *Derivatives of Pyrrolo[3,2-b]Pyrrole Exhibiting High Two-Photon Cross Section*; Polish Academy of Sciences, 2014.
38. Tong, B.; Xin, W.; Shuangxiong, D.; Peng, Z.; Dong, Y.; Jianbing, S.; Zhengxu, C. *Novel Compound, Preparing Method Thereof and Application of Compound in Detecting* Ti^{3+}; CN109608469B, 2020.
39. Satake, K.; Yano, K.; Fujiwara, M.; Kimura, M. *Heterocycles* **1996**, *43*, 2361–2365.
40. Gross, G.; Wentrup, C. *J. Chem. Soc. Chem. Commun.* **1982**, 360–361.
41. Stezycki, R.; Reger, D.; Hoelzel, H.; Jux, N.; Gryko, D. T. *Synlett* **2018**, *29*, 2529–2534.
42. Liu, H.; Ye, J.; Zhou, Y.; Fu, L.; Lu, Q.; Zhang, C. *Tetrahedron Lett.* **2017**, *58*, 4841–4844.
43. Mukai, T.; Konno, A.; Kumagai, T.; Satake, K. *Chem. Lett.* **1985**, *14*, 1809–1812.
44. Tanaka, S.; Satake, K.; Kiyomine, A.; Kumagai, T.; Mukai, T. *Angew. Chem. Int. Ed.* **1988**, 1061–1062.
45. Lotz, S.; Landman, M.; Görls, H.; Crause, C.; Nienaber, H.; Olivier, A. *Zeitschrift fur Naturforsch. - Sect. B J. Chem. Sci.* **2007**, *62*, 419–426.
46. Satake, K.; Nakogc, D.; Kimura, M. *Stable Antiaromatic 1,4-Diazapentalenes: Synthesis and Oxidation Reaction of 2-Vinyl- and 2,5-Divinyl-1,4-Dihydropyrrolo[3,2-b]Pyrrole Derivatives*, Vol. 48; 1998.
47. Poronik, Y. M.; Mazur, L. M.; Samoć, M.; Jacquemin, D.; Gryko, D. T. *J. Mater. Chem. C* **2017**, *5*, 2620–2628.
48. Santra, M.; Jun, Y. W.; Bae, J.; Sarkar, S.; Choi, W.; Gryko, D. T.; Ahn, K. H. *Asian J. Org. Chem.* **2017**, *6*, 278–281.
49. Oyama, N.; Ohsaka, T.; Chiba, K.; Miyamoto, H.; Mukai, T.; Tanaka, S.; Tsutomu, K. *Synth. Met.* **1987**, *20*, 245–258.
50. Miyamoto, H.; Oyama, N.; Ohsaka, T.; Tanaka, S.; Miyashi, T. *J. Electrochem. Soc.* **1991**, No. 138, 2003–2008.
51. Oyama, N.; Ohsaka, T.; Miyamoto, H.; Chiba, K.; Mukai, T.; Tanaka, S.; Kumagai, T.; Aratani, T.; Yoshihara, H. *J. Chem. Soc., Perkin Trans.* 1988, *2*, 833–838.
52. Pesant, S.; Boulanger, P.; Côté, M.; Ernzerhof, M. *Chem. Phys. Lett.* **2008**, *450*, 329–334.
53. Janiga, A.; Bednarska, D.; Thorsted, B.; Brewer, J.; Gryko, D. T. *Org. Biomol. Chem.* **2014**, *12*, 2874–2881.

54. Zhou, Z. L.; Zhao, L.; Zhang, S.; Vincent, K.; Lam, S.; Henze, D. *Synth. Commun.* **2012**, *42*, 1622–1631.
55. Altman, L. J.; Richheimer, S. L. *Tetrahedron Lett.* **1971**, *12*, 4709–4711.
56. Corey, E. J.; Boger, D. L. *Tetrahedron Lett.* **1978**, *19*, 5–8.
57. Kowalczyk, P.; Tasior, M.; Ozaki, S.; Kamada, K.; Gryko, D. T. *Org. Lett.* **2022**, *24*, 2551–2555.
58. Xu, Y.; Zhao, L.; Li, Y.; Doucet, H. *Adv. Synth. Catal.* **2013**, *355*, 1423–1432.
59. Li, Y.; Brand, J. P.; Waser, J. *Angew. Chem. Int. Ed.* **2013**, *52*, 6743–6747.
60. Tasior, M.; Clermont, G.; Blanchard-Desce, M.; Jacquemin, D.; Gryko, D. T. *Chem. A Eur. J.* **2019**, *25*, 598–608.
61. Golubev, P. *Ber. Dtsch. Chem. Ges.* **1884**, *17*, A581–A582.
62. Kliegl, A.; Haas, K. *Berichte der Dtsch. Chem. Gesellschaft* **1911**, *44*, 1209–1218.
63. Ruggli, P. *Berichte der Dtsch. Chem. Gesellschaft* **1917**, *50*, 883–893.
64. Heller, G. *Berichte der Dtsch. Chem. Gesellschaft* **1917**, *50*, 1202–1203.
65. Ruggli, P.; Zaeslin, H. *Helv. Chim. Acta* **1935**, *18*, 845–852.
66. Cadogan, J. I. G.; Cameron-Wood, M.; MacKie, R. K.; Searle, R. J. G. *J. Chem. Soc.* **1965**, 4831–4837.
67. Kaszynski, P.; Dougherty, D. A. *J. Org. Chem.* **1993**, *58*, 5209–5220.
68. Jackson, A. H.; Johnston, D. N.; Shannon, P. V. R. *J. Chem. Soc. Chem. Commun.* **1975**, 911–912.
69. Grinev, A. N.; Ryabova, S. Y. *Chem. Heterocycl. Compd.* **1982**, *18*, 153–154.
70. Mérour, J. Y.; Savelon, L. *Heterocycles* **1991**, *32*, 849–853.
71. Grinev, A. N.; Lomanova, E. V.; Trofimkin, Y. I. *Chem. Heterocycl. Compd.* **1983**, *19*, 959–961.
72. Cooper, F. C.; Partridge, M. W. *J. Chem. Soc.* **1955**, 991–994.
73. Qiu, L.; Yu, C.; Zhao, N.; Chen, W.; Guo, Y.; Wan, X.; Yang, R.; Liu, Y. *Chem. Commun.* **2012**, *48*, 12225.
74. Qiu, L.; Wang, X.; Zhao, N.; Xu, S.; An, Z.; Zhuang, X.; Lan, Z.; Wen, L.; Wan, X. *J. Org. Chem.* **2014**, *79*, 11339–11348.
75. Koch, R. W.; Dessy, R. E. *J. Org. Chem.* **1982**, *47*, 4452–4459.
76. Metlesics, W.; Resnick, T.; Silverman, G.; Tavares, R.; Sternbach, L. H. *J. Med. Chem.* **1966**, *9*, 633–634.
77. Metlesics, W.; Sternbach, L. H. *J. Am. Chem. Soc.* **1966**, *88*, 1077.
78. Metlesics, W.; Tavares, R.; Sternbach, L. H. *J. Org. Chem.* **1966**, *31*, 3356–3362.
79. Metlesics, W.; Sternbach, L. H. *Derivatives of 4b, 5, 9b, 10 Tetrahydro-4b, 9b-Diphenylindolo-[3, 2-b] Indole and Process for Their Preparation*; US P. 3282958, 1966.
80. Hung, T. Q.; Hancker, S.; Villinger, A.; Lochbrunner, S.; Dang, T. T.; Friedrich, A.; Breitsprecher, W.; Langer, P. *Org. Biomol. Chem.* **2015**, *13*, 583–591.
81. Ho, H. E.; Oniwa, K.; Yamamoto, Y.; Jin, T. *Org. Lett.* **2016**, *18*, 2487–2490.
82. Yu, J.; Zhang-Negrerie, D.; Du, Y. *Org. Lett.* **2016**, *18*, 3322–3325.
83. Debnath, S.; Liang, L.; Lu, M.; Shi, Y. *Org. Lett.* **2021**, *23*, 3237–3242.
84. Stężycki, R.; Grzybowski, M.; Clermont, G.; Blanchard-Desce, M.; Gryko, D. T. *Chem. A Eur. J.* **2016**, *22*, 5198–5203.
85. Grzybowski, M.; Skonieczny, K.; Butenschön, H.; Gryko, D. T. *Angew. Chem. Int. Ed.* **2013**, *52*, 9900–9930.
86. Tsuda, A.; Osuka, A. *Science* **2001**, *293*, 79–82.
87. Narita, A.; Feng, X.; Hernandez, Y.; Jensen, S. A.; Bonn, M.; Yang, H.; Verzhbitskiy, I. A.; Casiraghi, C.; Hansen, M. R.; Koch, A. H. R.; et al. *Nat. Chem.* **2014**, *6*, 126–132.
88. Krzeszewski, M.; Gryko, D. T. *J. Org. Chem.* **2015**, *80*, 2893–2899.
89. Krzeszewski, M.; Świder, P.; Dobrzycki, Ł.; Cyrański, M. K.; Danikiewicz, W.; Gryko, D. T. *Chem. Commun.* **2016**, *52*, 11539–11542.

90. Krzeszewski, M.; Sahara, K.; Poronik, Y. M.; Kubo, T.; Gryko, D. T. *Org. Lett.* **2018**, *20*, 1517–1520.
91. Krzeszewski, M.; Kodama, T.; Espinoza, E. M.; Vullev, V. I.; Kubo, T.; Gryko, D. T. *Chem. A Eur. J.* **2016**, *22*, 16478–16488.
92. Fujikawa, T.; Segawa, Y.; Itami, K. *J. Am. Chem. Soc.* **2015**, *137*, 7763–7768.
93. Mishra, S.; Krzeszewski, M.; Pignedoli, C. A.; Ruffieux, P.; Fasel, R.; Gryko, D. T. *Nat. Commun.* **2018**, *9*, 1714.
94. Krzeszewski, M.; Dobrzycki, Ł.; Sobolewski, A. L.; Cyrański, M. K.; Gryko, D. T. *Angew. Chem. Int. Ed.* **2021**, *60*, 14998–15005.
95. Tokimaru, Y.; Ito, S.; Nozaki, K. *Angew. Chem. Int. Ed.* **2018**, *57*, 9818–9822.
96. Tasior, M.; Hassanein, K.; Mazur, L. M.; Sakellari, I.; Gray, D.; Farsari, M.; Samoć, M.; Santoro, F.; Ventura, B.; Gryko, D. T. *Phys. Chem. Chem. Phys.* **2018**, *20*, 22260–22271.
97. Dong, H.; Wang, C.; Hu, W. *Chem. Commun.* **2010**, *46*, 5211–5222.
98. Janiga, A.; Krzeszewski, M.; Gryko, D. T. *Chem. Asian J.* **2015**, *10*, 212–218.
99. Tasior, M.; Chotkowski, M.; Gryko, D. T. *Org. Lett.* **2015**, *17*, 6106–6109.
100. Tasior, M.; Gryko, D. T. *J. Org. Chem.* **2016**, *81*, 6580–6586.
101. Tasior, M.; Kowalczyk, P.; Przybył, M.; Czichy, M.; Janasik, P.; Bousquet, M. H. E.; Łapkowski, M.; Rammo, M.; Rebane, A.; Jacquemin, D.; et al. *Chem. Sci.* **2021**, *12*, 15935–15946.
102. Yang, K.; Zhang, G.; Song, Q. *Chem. Sci.* **2018**, *9*, 7666–7672.
103. Wu, D.; Zheng, J.; Xu, C.; Kang, D.; Hong, W.; Duan, Z.; Mathey, F. *Dalton Trans.* **2019**, *48*, 6347–6352.
104. Wang, Z.; Liang, M.; Tan, Y.; Ouyang, L.; Sun, Z.; Xue, S. *J. Mater. Chem. A* **2015**, *3*, 4865–4874.
105. Chen, L.; Baumgarten, M.; Guo, X.; Li, M.; Marszalek, T.; Alsewailem, F. D.; Pisula, W.; Müllen, K. *J. Mater. Chem. C* **2014**, *2*, 3625–3630.
106. Park, J. I. L.; Chung, J. W.; Kim, J. Y.; Lee, J.; Jung, J. Y.; Koo, B.; Lee, B. L.; Lee, S. W.; Jin, Y. W.; Lee, S. Y. *J. Am. Chem. Soc.* 2015, *137*, 12175–12178.
107. Tasior, M.; Czichy, M.; Łapkowski, M.; Gryko, D. T. *Chem. Asian J.* **2018**, *13*, 449–456.
108. Poronik, Y. M.; Baryshnikov, G. V.; Deperasińska, I.; Espinoza, E. M.; Clark, J. A.; Ågren, H.; Gryko, D. T.; Vullev, V. I. *Commun. Chem.* **2020**, *3*, 190.
109. Li, K.; Liu, Y.; Li, Y.; Feng, Q.; Hou, H.; Tang, B. Z. *Chem. Sci.* **2017**, *8*, 7258–7267.
110. Wang, H.; Huo, J.; Tong, H.; Wei, X.; Zhang, Y.; Li, Y.; Chen, S.; Shi, H.; Tang, B. Z. *J. Mater. Chem. C* **2020**, *8*, 14208–14218.
111. Dereka, B.; Rosspeintner, A.; Krzeszewski, M.; Gryko, D. T.; Vauthey, E. *Angew. Chem. Int. Ed.* **2016**, *55*, 15624–15628.
112. Dereka, B.; Vauthey, E. *Chem. Sci.* **2017**, *8*, 5057–5066.
113. Ivanov, A. I. *J. Phys. Chem. C* **2018**, *122*, 29165–29172.
114. Górski, K.; Deperasińska, I.; Baryshnikov, G. V.; Ozaki, S.; Kamada, K.; Ågren, H.; Gryko, D. T. *Org. Lett.* **2021**, *23*, 6770–6774.
115. Friese, D. H.; Mikhaylov, A.; Krzeszewski, M.; Poronik, Y. M.; Rebane, A.; Ruud, K.; Gryko, D. T. *Chem. Eur. J.* **2015**, *21*, 18364–18374.
116. Łukasiewicz, Ł. G.; Rammo, M.; Stark, C.; Krzeszewski, M.; Jacquemin, D.; Rebane, A.; Gryko, D. T. *ChemPhotoChem* **2020**, *4*, 508–519.
117. Zhou, Y.; Zhang, M.; Ye, J.; Liu, H.; Wang, K.; Yuan, Y.; Du, Y. Q.; Zhang, C.; Zheng, C. J.; Zhang, X. H. *Org. Electron.* **2019**, *65*, 110–115.
118. Poronik, Y. M.; Sadowski, B.; Szychta, K.; Quina, F. H.; Vullev, V. I.; Gryko, D. T. *J. Mater. Chem. C* **2022**, *10*, 2870–2904.
119. Ji, Y.; Peng, Z.; Tong, B.; Shi, J.; Zhi, J.; Dong, Y. *Dyes Pigm.* **2017**, *139*, 664–671.

120. Sadowski, B.; Hassanein, K.; Ventura, B.; Gryko, D. T. *Org. Lett.* **2018**, *20*, 3183–3186.
121. Anthony, J. E.; Eaton, D. L.; Parkin, S. R. *Org. Lett.* **2002**, *4*, 15–18.
122. Shinamura, S.; Osaka, I.; Miyazaki, E.; Nakao, A.; Yamagishi, M.; Takeya, J.; Takimiya, K. *J. Am. Chem. Soc.* **2011**, *133*, 5024–5035.
123. Yuan, Y.; Giri, G.; Ayzner, A. L.; Zoombelt, A. P.; Mannsfeld, S. C. B.; Chen, J.; Nordlund, D.; Toney, M. F.; Huang, J.; Bao, Z. *Nat. Commun.* **2014**, *5*, 3005.
124. Nakatsuka, M. *Organic Transistor. JP2009054809*; 2009.
125. Nakatsuka, M. *Organic Transistor. JP2009182034*; 2009.
126. Nakatsuka, M. *Organic Transistor. JP2009218335*; 2009.
127. Samsoniya, S. A.; Trapaidze, M. V. *Russ. Chem. Rev.* **2007**, *76*, 313–326.
128. Yeong-Eup, J.; Kwang-hyun, K.; Su-hee, S.; Jin-woo, K.; Jae-hong, K.; Sung-Heum, P.; Kwang-hee, L.; Hong-suk, S. *Bull. Korean Chem. Soc.* **2006**, *27*, 1043–1047.
129. Murray, M. M.; Kaszynski, P.; Kaisaki, D. A.; Chang, W.; Dougherty, D. A. *J. Am. Chem. Soc.* **1994**, *116*, 8152–8161.
130. Hayama, T.; Kawamura, M.; Mizuki, Y.; Ito, H.; Haketa, T.; Gryko, D. T.; Janiga, A.; Krzeszewski, M. *Material for Organic Electroluminescent Element, Organic Electroluminescent Element and Electronic Apparatus*; JP2016127083A, 2016.
131. Ye, J.; Liu, H.; Zhang, M. *A Kind of Blue Emission Luminous Organic Material and Preparation Method Thereof*; CN106977519A, 2017.
132. Pan, J.; Shi, C. *Fused Pyrrole Derivative and Application Thereof in Organic Electronic Device*; WO2017118237A1, 2017.
133. Xu, C.; Zhao, Z.; Yang, K.; Niu, L.; Ma, X.; Zhou, Z.; Zhang, X.; Zhang, F. *J. Mater. Chem. A* **2022**, *10*, 6291–6329.
134. Domínguez, R.; Montcada, N. F.; de la Cruz, P.; Palomares, E.; Langa, F. *ChemPlusChem* **2017**, *82*, 1096–1104.
135. Wang, J.; Chai, Z.; Liu, S.; Fang, M.; Chang, K.; Han, M.; Hong, L.; Han, H.; Li, Q.; Li, Z. *Chem. Eur. J.* **2018**, *24*, 18032–18042.
136. Zhao, B.; Xu, Y.; Liu, S.; Li, C.; Fu, N.; Wang, L. *Non-Fullerene Receptor Material Based on Tetra-Aryl Pyrrole, and Application Thereof*; CN108912125A, 2018.
137. Yang, Z. *Synthesis Method of Poly-Thiophene-Fullerene-Polylactic Acid Triblock Copolymer*; CN102391481A, 2012.
138. Hawes, C. S.; Ó Máille, G. M.; Byrne, K.; Schmitt, W.; Gunnlaugsson, T. *Dalton Trans.* **2018**, *47*, 10080–10092.
139. Purba, P. C.; Maity, M.; Bhattacharyya, S.; Mukherjee, P. S. *Angew. Chem. Int. Ed.* **2021**, *60*, 14109–14116.
140. Wei, Z.; Wu, X.-H.; Luo, P.; Wang, J.-Y.; Li, K.; Zang, S.-Q. *Chem. Eur. J.* **2019**, *25*, 2750–2756.
141. Li, Y.; Li, X.; Jia, S.; Zhang, C.; Luo, Y.; Lin, Z.; Zhao, Y.; Huang, W. *Inorg. Chem.* **2021**, *60*, 12129–12135.
142. Canjeevaram Balasubramanyam, R. K.; Kumar, R.; Ippolito, S. J.; Bhargava, S. K.; Periasamy, S. R.; Narayan, R.; Basak, P. *J. Phys. Chem. C* **2016**, *120*, 11313–11323.
143. CB, R. K.; Kandjani, A.; Jones, L.; Periasamy, S.; Wong, S.; Narayan, R.; Bhargava, S.; Ippolito, S.; Basak, P. *Adv. Electron. Mater.* **2018**, *4*, 1–11.
144. Wu, J.-Y.; Yu, C.-H.; Wen, J.-J.; Chang, C.-L.; Leung, M. *Anal. Chem.* **2016**, *88*, 1195–1201.
145. Peng, Z.; Feng, X.; Tong, B.; Chen, D.; Shi, J.; Zhi, J.; Dong, Y. *Sens. Actuators B Chem.* **2016**, *232*, 264–268.

How to cite: Angew. Chem. Int. Ed. 2023, 62, e202311123
doi.org/10.1002/anie.202311123

Polycycles

Gold-Catalyzed 1,2-Aryl Shift and Double Alkyne Benzannulation

Gana Sanil, Maciej Krzeszewski, Wojciech Chaładaj, Witold Danikiewicz, Iryna Knysh, Łukasz Dobrzycki, Olga Staszewska-Krajewska, Michał K. Cyrański, Denis Jacquemin,* and Daniel T. Gryko**

Dedicated to prof. Harry B. Gray on occasion of his 88th birthday

Abstract: The tandem intramolecular hydroarylation of alkynes accompanied by a 1,2-aryl shift is described. Harnessing the unique electron-rich character of 1,4-dihydropyrrolo[3,2-*b*]pyrrole scaffold, we demonstrate that the hydroarylation of alkynes proceeds at the already occupied positions 2 and 5 leading to a 1,2-aryl shift. Remarkably, the reaction proceeds only in the presence of cationic gold catalyst, and it leads to heretofore unknown π-expanded, centrosymmetric pyrrolo[3,2-*b*]pyrroles. The utility is verified in the preparation of 13 products that bear six conjugated rings. The observed compatibility with various functional groups allows for increased tunability with regard to the photophysical properties as well as providing sites for further functionalization. Computational studies of the reaction mechanism revealed that the formation of the six-membered rings accompanied with a 1,2-aryl shift is both kinetically and thermodynamically favourable over plausible formation of products containing 7-membered rings. Steady-state UV/Visible spectroscopy reveals that upon photoexcitation, the prepared S-shaped N-doped nanographenes undergo mostly radiative relaxation leading to large fluorescence quantum yields. Their optical properties are rationalized through time-dependent density functional theory calculations. We anticipate that this chemistry will empower the creation of new materials with various functionalities.

Introduction

The venerable polycyclic aromatic hydrocarbons (PAHs) and their heterocyclic analogs have garnered exceptional attention from the scientific community during the last decade.[1–12] Among dozens of key reactions which are employed to assemble these dyes, alkyne benzannulation (intramolecular hydroarylation of alkynes) discovered by Swager in 1994[13,14] is one of the most universal approaches. Over the years a panel of different catalysts belonging to either Brønsted acids or Lewis acids were introduced. As a result, alkyne benzannulation has been used to form various nanographenes.[15–20] Among several emblematic examples, a spectacular illustration concerns the synthesis of a polymeric graphene nanoribbon by Chalifoux and co-workers.[21] This reaction has also been used to assemble S-doped[22,23] and N-doped nanographenes,[24] and, more recently, for the construction of helicenes.[25–28] Alkyne benzannulation occurs at the free position adjacent to the biaryl linkage leading to the formation of new rings of various sizes. Depending on the conditions and the catalyst used in the reaction, 5-, 6- and 7-membered rings can be formed through 5-*exo*-dig, 6-*endo*/*exo*-*dig* and 7-*endo*-*dig* ring closure mechanisms, respectively (Figure 1a).[17,19,23,25,28,29]

Double 6-*endo*-*dig* cyclizations are also known, including impressive domino twofold cyclization reported by Chalifoux (Figure 1b),[19] or our previous work where two six-membered rings were fused to the central pyrrolopyrrole core (Figure 1c).[30] Tetraarylpyrrolo[3,2-*b*]pyrroles (TAPPs)[31,32] are being applied as scaffolds to prepare numerous *N*-doped nanographenes, owing to the intrinsic reactivity of positions 3 and 6, the ability to introduce sterically hindered substituents and its high amenability to

[*] G. Sanil, Dr. M. Krzeszewski, Dr. W. Chaładaj, Prof. W. Danikiewicz, Dr. O. Staszewska-Krajewska, Prof. D. T. Gryko
Institute of Organic Chemistry, Polish Academy of Sciences
Kasprzaka 44/52, 01-224 Warsaw (Poland)
E-mail: mkc@chem.uw.edu.pl
dtrgyko@icho.edu.pl
I. Knysh, Prof. D. Jacquemin
Nantes Université, CNRS, CEISAM UMR 6230,
F-44000 Nantes (France)
E-mail: denis.jacquemin@univ-nantes.fr
Dr. Ł. Dobrzycki, Prof. M. K. Cyrański
Faculty of Chemistry, University of Warsaw,
Pasteura 1, 02-093 Warsaw (Poland)
Prof. D. Jacquemin
Institut Universitaire de France (IUF), F-75005 Paris (France)
E-mail: denis.jacquemin@univ-nantes.fr

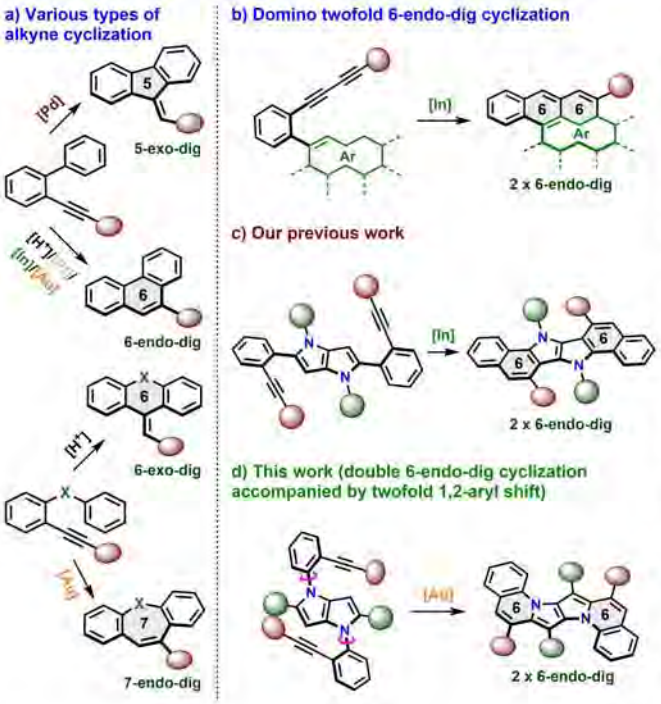

Figure 1. Intramolecular cyclization of alkynes under various conditions leading to the formation of one new 5-,6- or 7-membered rings or two 6-membered rings at once.

chemical modifications.[33–35] Taking advantage of this new chemical space, enabled by a multicomponent reaction leading to 1,4-dihydropyrrolo[3,2-*b*]pyrroles (DHPPs)[36,37] we hypothesized that it could be possible to obtain π-expanded DHPPs possessing fused five- and seven-membered rings.[38–40] Assessing this hypothesis requires DHPPs possessing arylethynylaryl substituents at positions 1 and 4 which could undergo double alkyne benzannulation forming two 7-membered rings (Figure 1d, Figure 2).

It turned out, however, that the obtained compounds comprised of two six-membered rings fused to the central core. Herein we present the double intramolecular cyclization of alkynes via cyclization at the already occupied positions C2/C5 with a consequent double aryl shift from position C2/C5 to C3/C6.

Results and Discussion

Design and Synthesis

A two-step strategy comprising of a multicomponent reaction affording TAPPs followed by double alkyne benzannulation was thought to present an ideal synthetic platform for modular access to the envisioned dyes (Figure 2). Our synthetic approach capitalizes on the inherently electron-rich positions 3 and 6 of DHPPs and the direct access to TAPPs possessing diphenylethyne moieties at positions 1 and 4 (Figure 2). This enables to position the carbon-carbon triple bond in proximity to the free positions 3 and 6, thus facilitating the formation of seven-membered rings during the hydroarylation. The designed protocol initiates with the synthesis of 2-(phenylethynyl)anilines **1a–e**. Amines **1a–d** were synthesized via Sonogashira reaction using the corresponding 4-*tert* butyl-2-iodoaniline and rationally chosen ethynylbenzenes possessing both electron-donating and electron-withdrawing substituents in the *para*-position. For the synthesis of amine **1e**, however we resort to the sila-Sonogashira variant, namely, 2-((trimethylsilyl)ethynyl)aniline and 4-bromobenzonitrile as a coupling partner. In light of our previous experiences, the introduction of alkyl groups such as *tert*-butyl has a significant impact on increasing the solubility of extended aromatic systems by preventing π-stacking.[30] With the amines **1a–e** in hand, by employing our multicomponent reaction[41] we readily prepared a library of tetraarylpyrrolo[3,2-*b*]pyrroles (TAPPs) **4aa–4ec** in yields ranging from 6 to 47 %. In most of the cases, the products were precipitated in the reaction mixture and further purified by recrystallization (see the ESI for details).

In order to perform the envisioned double intramolecular hydroarylation, we initially relied on the use of π-Lewis acids such as $PtCl_2$,[42,43] $InCl_3$, and $GaCl_3$, primarily used for 6-*endo* annulation reported by Fürstner and co-workers.[42,44] The choice of catalysts was based on the literature and our previous reports of successful hydroarylation strategies on structurally similar TAPPs.[30] Unfortunately, none of the attempts led to any conversion. Subsequent studies involving Brønsted acids (i.e. trifluoroacetic acid and *p*-toluenesulfonic acid) and neutral chlorogold(I) catalysts (e.g., AuCl-(PPh_3))[45–48] were also unsuccessful. Even increasing the temperature to 150 °C did not result in any conversion of TAPP **4aa** (see the ESI). Steric hindrance around the reaction center may account for the failure of this reaction. Murakami and co-workers reported hydroarylation of dialkynylbiphenyls for the synthesis of aryl substituted pyrenes using cationic (SPhos)$AuNTf_2$ catalyst.[49] By employing the same conditions with electronically analogous $IPrAuNTf_2$ as the catalyst, the transformation of substrate **4ea** into a new substance was observed. The primary analysis of ^1H NMR (showing small number of peaks denoting the symmetry and the absence of pyrrolic singlet around 6.0–6.5 ppm) and matching HRMS-EI (Calculated for $C_{64}H_{60}N_4^{+\bullet}$: $[M]^{+\bullet}$ = 884.4812, found = 884.4840) of the obtained compound apparently supported our assumption of the formation of seven membered ring. Surprisingly, X-ray crystallography analysis disproved our prediction (Figure 2).[50] It became clear that two new six-membered rings were formed at the central core of the compound **4ea** leading to an S-shaped non-planar π-expanded DHPP. 6-*Endo* cyclization occurs at the already occupied C2/C5 positions simultaneously inducing the double aryl shift from positions C2/C5 to C3/C6.

It is pivotal to emphasize that already in 1997 Swager and co-workers reported rearrangements during alkyne hydroarylations.[13] Recently Chalifoux and co-workers revealed the 1,2-shift occurring during four-fold alkyne benzannulation leading to pyreno[*a*]pyrene-based helicene hybrids.[51] Processes reported by Swager and Chalifoux are most probably the proton-mediated reactions rather than an

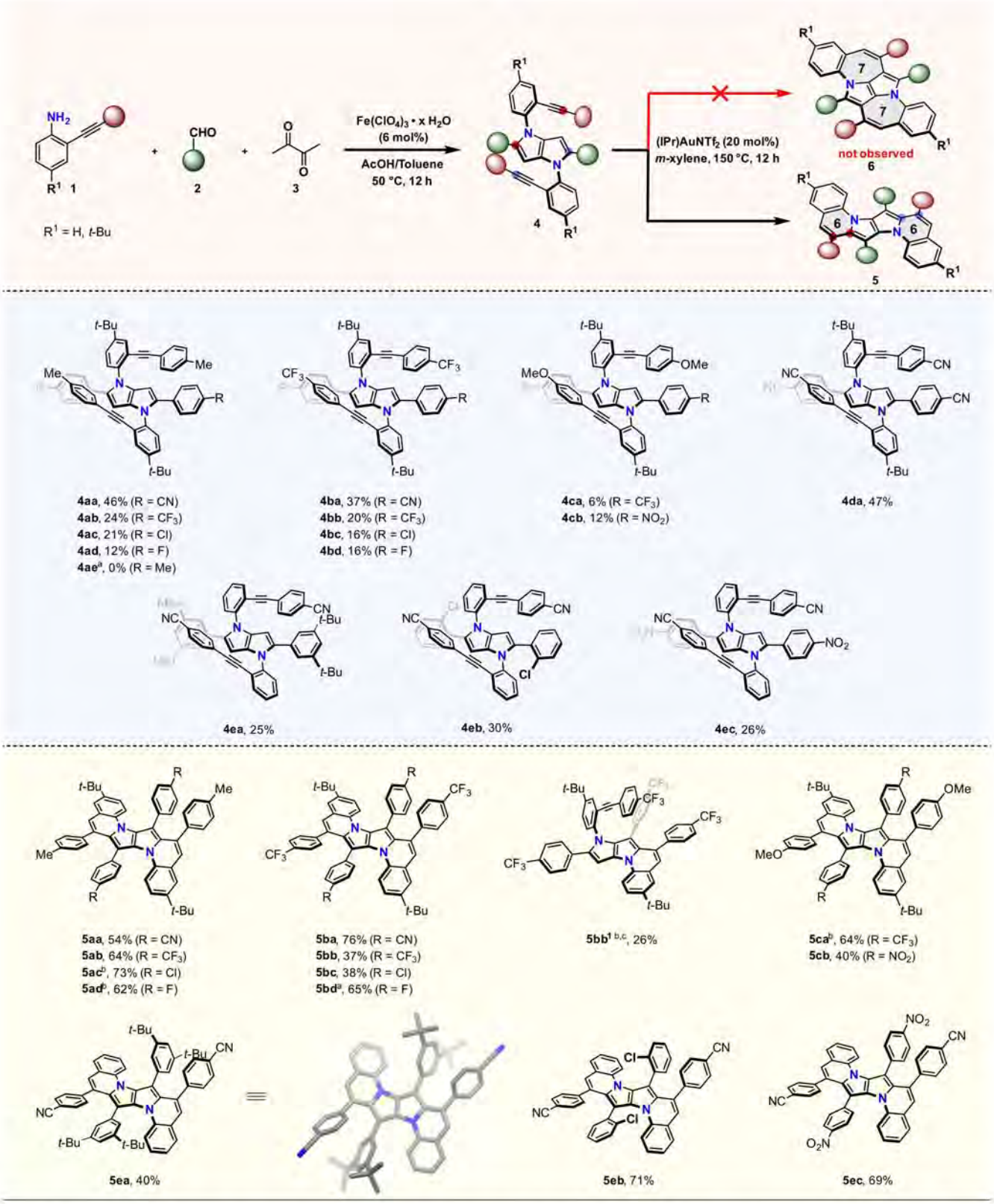

Figure 2. The synthesis of π-extended pyrrolopyrroles **5** through Au-mediated double hydroarylation of alkyne-containing TAPPs **4** accompanied by twofold 1,2-aryl migration. [a] Expected product **4ae** was not isolated, most likely due to decomposition caused by the extreme electron-rich character of the TAPP lacking any electron-withdrawing group. [b] Reaction completed in 4 hours. [c] Reaction took place on the one side of the molecule only giving the product of mono-hydroarylation leaving the other alkyne intact. [d] X-Ray crystal structure of **5ea**, solvent molecule and hydrogen atoms were omitted for clarity (CCDC 2285219)./Analogical compound **5da** was not obtained due to lack of reactivity of **4da** in the final step.

in situ rearrangement. An analogous 1,2-migration of alkyl or aryl groups was observed in the gold-catalyzed intramolecular cascade cyclization assisted by heteronucleophiles.[29,52] In broader context, one has to point out that 1,2-aryl shift of halides were reported multiple times by the groups of Fürstner, Müllen, Davis etc.[42,53–55] The recent revival of interest in gold catalysis led to important findings which reveal that gold(I) complexes are prone to induce various rearrangements[56] and that the interplay between gold catalysis and protic acids catalysis is rather complex.[57,58]

To further demonstrate functional group compatibility and synthetic utilization, after establishing the protocol, the reaction was performed on the previously synthesized TAPPs bearing various substituents at the periphery. The reaction turned out to be general in most of the cases and the rearranged products **5aa–ec** were formed in reasonable yields ranging from 27–76 % (Figure 2). The only case where the reaction did not proceed to completion was that of TAPP **4da** bearing four cyano groups at the periphery. The presence of highly electron withdrawing groups in the *para*-position to the carbon atom attached to the alkyne and on the migrating aryl substituents might affect the nucleophilicity of the system by preventing the reaction from proceeding towards completion. The reaction mixture showed the presence of parent TAPP even after 48 hours of reaction time. The extremely low solubility of both the product and reactant in common organic solvents made the purification process impossible. Interestingly, for the compound **4bb**, we could obtain the mono-fused unsymmetrical DHPP **5bb′** by lowering the reaction time to 4 hours. This shows the tunability of the reaction by time and confirms that the aryl-shift occurs in a stepwise manner. It is worth mentioning that the formation of the product **5eb** bearing *ortho*-chlorine substituents in high yield (71 %) depicts the efficiency of this reaction even with the steric hindrance close to the migration center. This also broadens its synthetic potential for further transformations. If two arylethynyl groups differing in an electronic effect (i.e. 4-$CF_3C_6H_4$ and 4-$MeOC_6H_4$) are present in the starting TAPP, double benzannulation occurs smoothly leading to expected rearranged product, with no apparent regio- and chemoselectivity. Shortening the reaction time to 2 h did not enable to isolate any intermediate products (see the ESI for details).

No other identifiable products have been detected in any of these reactions. In our opinion the key reason responsible for the low yields of the products is that double alkyne benzannulation accompanied by 1,2-aryl shift is very demanding. Indeed it does not occur with any other Brønsted or Lewis acid employed (ESI, Table S1), even at very high temperature. The only exception is the prolonged heating of TAPP **4aa** with $HNTf_2$ at 150 °C which led to approx. 10 % of conversion. Control experiments when both $IPrAuNTf_2$ and several Brønsted or Lewis acid were simultaneously employed led to the same results as with gold-based catalyst only (Table S2). On the other hand the addition of $NaHCO_3$ has no effect and the addition of organic base has marginal effect on the reaction conversion (Table S3).

Computational Studies—Mechanism

To rationalize observed *6-endo-dig* benzannulation merged with aryl shift, ultimately providing **5**, rather than expected *7-endo-dig* cyclization leading to **6**, both mechanistic scenarios were investigated computationally (Figure 3, black and grey paths, respectively). The calculations were performed on model substrate **7**, bearing no substituents on benzene rings, and full structure of gold catalyst ($IPrAuNTf_2$).

Both paths start form endoergic displacement of triflimide anion by alkyne moiety of **7** giving rise to the corresponding π-complex **8** or **8a**. Coordination of cationic gold motif to C–C triple bond triggers intramolecular nucleophilic attack of electron-rich pyrrolopyrrole system on the activated alkyne moiety of **8** through a *6-endo-dig* manifold. The process leading to the formation of intermediate **9** proceed through a transition state **TS1** ($\Delta G^{\ddagger} = 159.6$ kJ/mol, from **7**). The subsequent 1,2-aryl shift delivers **10** via **TS2** with Gibbs free energy of activation of 74.3 kJ/mol. Finally, abstraction of proton from the position 3 of the pyrrolopyrrole scaffold followed by protodeauration liberates catalyst and compound **11**, product of single *6-endo-dig* benzanulation of **7**. Analogical sequence of reactions triggered by coordination of cationic gold complex to the alkyne motif in **11** delivers final product **12**. Noticeably, the overall transformation of **7** involving one or two sequences of hydroarylation of alkynes accompanied by a 1,2-aryl shift, leading to **11** and **12** is highly exergonic ($\Delta G = -165.2$ and -301.3 kJ/mol, respectively).

Alternatively, *7-endo-dig* cyclization of **8a** (conformer of **8**) towards intermediate **10a** proceeds through a transition state **TS3** ($\Delta G^{\ddagger} = 177.6$ kJ/mol, from **7**) lying 18 kJ/mol higher than **TS1** (leading to **10** via *6-exo-dig* process). Such a difference in the reaction barriers correspond to selectivity higher than 160:1 at 150 °C. Moreover, due to strain and steric hindrance of intermediate **10a** bearing 7-membered ring is also considerably less thermodynamically stable than both **9** and **10**. The hypothetical product **11a** is liberated through a sequence of deprotonation followed by protodeauration, and can enter a second event of *7-endo-dig* benzannulation giving rise to **12a**. Noticeably, formation of **11a** and **12a** is not only kinetically unfavourable compared to **11** and **12**, but also thermodynamically less preferred ($\Delta G = -80.2$ and -166.2 kJ/mol for **11a** and **12a** *vs* -165.2 and -301.3 kJ/mol for **11** and **12**, respectively).

Photophysical Properties

For TAPPs possessing electron-withdrawing substituents at positions 2 and 5 and electron-neutral arylethynylaryl substituents at positions 1 and 4 the absorption and emission characteristics are different than for analogs bearing simple phenyl substituents at positions 1 and 4. The direct comparison of TAPP **4aa** ($\lambda_{abs}^{max} = 410$ nm and $\lambda_{em}^{max} = 450$ nm in

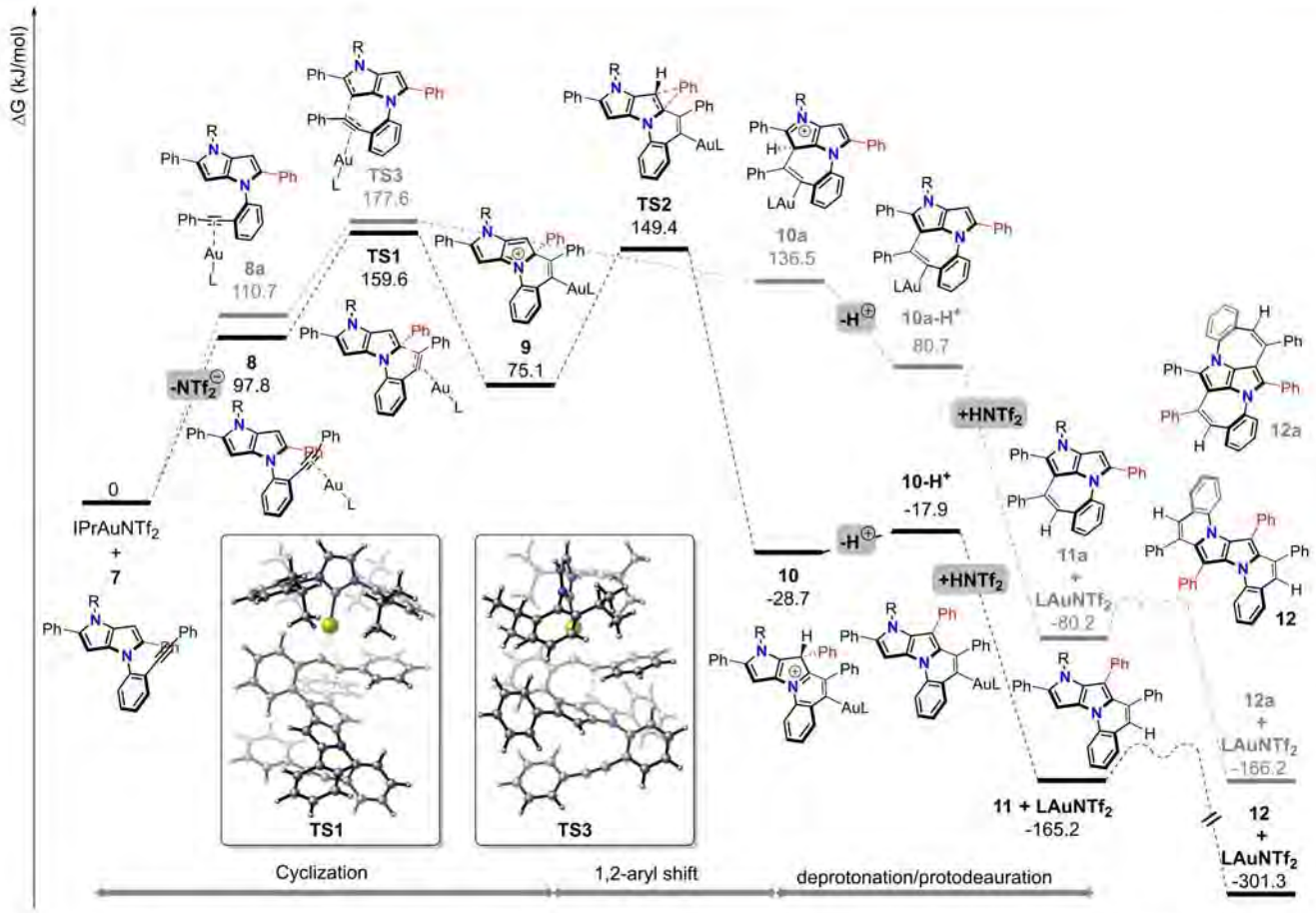

Figure 3. Gibbs free energy profiles for two plausible *6-endo-dig* and *7-endo-dig* benzannulations of **7** catalyzed by the IPrAuNTf$_2$. Calculated at SMD(*m*-xylene)/M06/def2-TZVPP//B3LYP-D3/def2-SVP level of theory.

toluene) with model 1,4-di(4-methylphenyl)-2,5-di(4-cyanophenyl)-1,4-dihydropyrrolo[3,2-*b*]pyrrole[59] reveals that both absorption and emission are bathochromically shifted, by 20 nm and 50 nm respectively (Table S5, Figure 4). In analogy with parent TAPP, both emission maximum and fluorescence quantum yield (ϕ_{fl}) for TAPP **4aa** are insensitive to solvent polarity change.[60] An analogous observation can be performed for **4ab**. Strikingly a different situation occurs when 4-cyanophenyl substituents are present at position 1 and 4. In the case of TAPP **4da** whereas λ_{abs}^{max} is located at the same position (408 nm), λ_{em}^{max} is already bathochromically shifted in toluene to 472 nm and this effect becomes pronounced in THF (531 nm, see Table S5 and Figure 4). At the same time ϕ_{fl} decreases in polar THF > 10-fold unlike in the case of **4aa**. Close examination of the remaining TAPPs (e.g. **4bb**, **4bc**, **4bd**, etc.) shows that the presence of electron-withdrawing substituents (4-CNC$_6$H$_4$ and 4-CF$_3$C$_6$H$_4$) at positions 1 and 4 always induces large bathochromic shift of fluorescence in polar solvents (THF). Since through-bond electronic communication cannot be too strong due to the large dihedral angle, this indicates a through-space interaction, as confirmed by theoretical calculations (see below). Intriguingly, in some of these cases, ϕ_{fl} is very small which again does not resemble many parent analogs.[59] Yet different observations are noted in the case of TAPPs **4cb** and **4ec** bearing 4-nitrophenyl substituents at position 2 and 5. Regardless of the electronic character of substituents present at positions 1 and 4 the fluorescence is essentially quantitative in toluene and very weak in THF.[61]

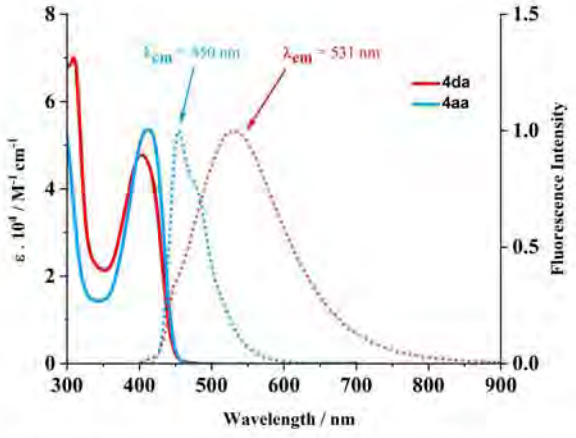

Figure 4. UV/Vis absorption spectra (solid lines) and fluorescence spectra (dotted lines) of compounds **4da** and **4aa** measured in THF.

Needless to say, the fused dyes **5** possess a more rigid structure and they can be considered analogs of π-expanded

DHPPs synthesized in 2015.[62] For these fused architectures, the low energy absorption band is located at ca. 480 nm and it has a pronounced vibronic structure and very small Stokes shifts (Table S5, Figure 5). Dyes **5** are generally characterized by strong green emission with ϕ_{fl} typically above 0.75. The substituents at positions 3 and 6 do not strongly influence the photophysical properties (**5aa** vs. **5ad**). The presence of 4-nitrophenyl substituent at these positions (**5cb** vs. **5ec**) leads to the quenching of emission (ϕ_{fl} below the detection limit), whereas 4-cyanophenyl substituent at positions 3 and 6 (**5ba**, **5aa**) have negligible effect on the photophysics. Compared with X-shaped π-expanded pyrrolopyrroles,[62] dyes **5** are ≈100 nm bathochromically shifted for both absorption and emission.

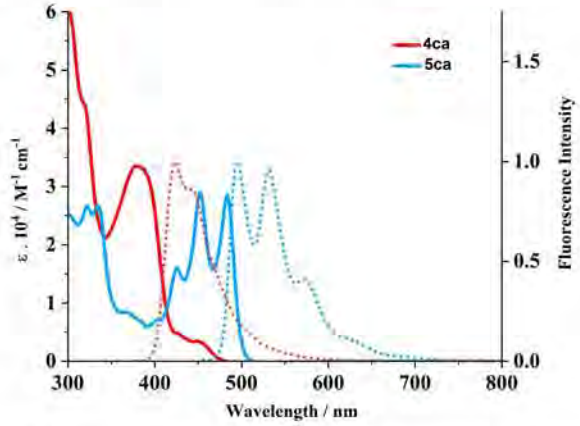

Figure 5. UV/Vis absorption spectra (solid lines) and fluorescence spectra (dotted lines) of compounds **4ca** and **5ca** measured in toluene.

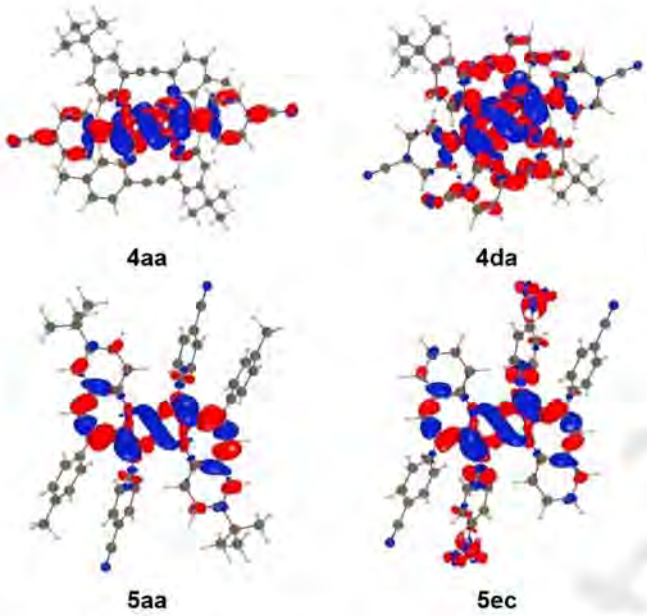

Figure 6. EDD plots for selected compounds. Navy blue and crimson red are regions of decrease and increase of density upon excitation. See the ESI for additional examples.

Computational Studies—Photophysics

We have used time-dependent density functional theory (TD-DFT)[63] and second-order coupled-cluster (CC2)[64] to model the photophysical properties of the selected compounds, accounting for solvent effects are the cLR^2-PCM level[65] (see the ESI). Figure 6 provides electron density difference (EDD) plots for **4aa** and **4da**. Both compounds show a large twist (56°) between the benzene rings at position 1 and 4, and the DHPP core preventing strong conjugation, yet their EDDs differ. In **4aa**, the excited state is delocalized on the central unit, the DHPP acting as the donor group and the benzonitrile moieties acting as acceptors, leading to the expected quadrupolar CT. This is consistent with the experimental findings that **4aa** essentially behaves like a standard quadrupolar centrosymmetric TAPP. In contrast in **4da**, one clearly notices a change of topology, the CT occurring *through-space*, from the DHPP moiety towards the 4-CNC$_6$H$_4$ groups attached through position 1 and 4, rather than the groups at position 2 and 5. According to Le Bahers' metric, the amount of charge transferred also increases from 0.67 e in **4aa** to 0.86 e in **4da**.

As expected, the hydroarylation leads to a strong decrease of the twist between the *N*-substituent and the core (ca. 15° instead of ca. 56°), with the excited states delocalized along the longer quasi-planar π-conjugated path (Figure 6). Interestingly, the EDDs show that the cyano group at positions 3 and 6 are not strong enough (as electron-withdrawing groups) to influence the topology of the electron distribution, whereas nitro groups do alter the photophysics of π-expanded DHPPs (**5aa** versus **5ec**). The significant contributions of the nitro groups in the excited state are consistent with the quenching of the emission in **5ec** (Table S5).

More quantitative comparisons between theory and experiments can be obtained by using 0–0 energies and band topologies. For the former, our calculations report values of ca. 2.5 eV for **4aa** and **4ba** but values around 2.2 eV for compounds of series **5** (**5aa**, **5ea**, **5eb**, and **5ec**, see Table S6 in the ESI). In particular, the **4aa** to **5aa** redshift is −0.38 eV, which perfectly fits the measurements of −0.36 eV. This redshift is a clear consequence of the planarization of the system. On the other hand, for **4da**, theory overshoots the experimental redshift of the emission due to the CT nature, but yields a fluorescence associated with a small oscillator strength, consistent with the decrease of emission yield noticed experimentally. Figure 7 shows the computed band shapes for the analogous **4aa** and **5aa**, and the more pronounced vibronic progression in the latter also appears clearly, as in Figure 5. In **5aa**, the vibronic shapes are mainly related to vibrations at ca. 1500–1600 cm^{-1} involving changes in the alternation of single and double CC bonds (see the ESI), as expected for a π-conjugated dye. Interestingly for **5ea**, the fact that the absorption spectrum is more resolved than its fluorescence counterpart is well reproduced by the calculations (see the ESI), an outcome that we attribute to the loss of symmetry taking place in the excited state of **5ea** (and not in **5aa**).

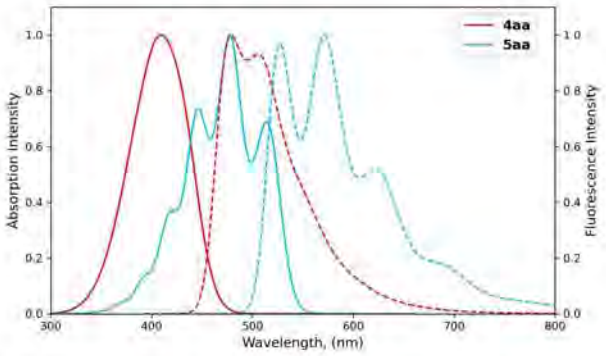

Figure 7. Vibrationally resolved spectra in toluene of **4aa** and **5aa** determined using the VG PES model on the basis of TD-DFT vibrations and CC2-corrected adiabatic energies.

Conclusion

The presence of a 1,4-dihydropyrrolo[3,2-*b*]pyrrole core alters the course of intramolecular hydroarylation of alkynes. Reactions leading to the anticipated formation of two seven-membered rings, instead, proceeds via a 1,2-aryl shift and six-membered rings are formed. Substituents present initially at positions 2 and 5 migrate to positions 3 and 6. In addition to uncovering the special example of a 1,2-aryl shift during the hydroarylation of alkynes, we identified that this reaction is tolerant to many functional groups, in particular those that are viable in the area of optoelectronics. This reaction leads to heretofore unknown heterocyclic skeletons, the structure of which consists of six conjugated aromatic rings. These results, combined with earlier examples of the Scholl reaction occurring with concomitant 1,2-aryl shift,[66,67] suggests that the exceptional electron-rich character of DHPP core is responsible for this reaction course. Moreover, in all cases, the reaction led exclusively to the formation of 6-*endo-dig* cyclization products, and the possible 5-*exo* isomers were not detected. Importantly we successfully deciphered the mechanistic rationale behind the reaction, via computational studies. Critically, the properties of the benzannulation substrates i.e. sterically congested tetraaryl-1,4-dihydropyrrolo[3,2-*b*]pyrroles are controlled by both the strongly conjugated substituents at positions 2 and 5 and by weakly conjugated substituents at positions 1 and 4. We showed that the fluorescence of TAPPs possessing electron-withdrawing arylethynyl substituents at positions 1 and 4 could plausibly be rationalized by a through-space interaction. Although certain substrate limitations exist, the findings will provide impetus for future explorations that use alkyne benzannulation. Collectively these results highlight the compatibility of exceptionally electron-rich heterocycles with Au(I)-catalyzed alkynyl hydroarylation.

Supporting Information

The authors have cited additional references within the Supporting Information.[68-89]

Author Contributions

The manuscript was written through contributions of all authors. All authors have given approval to the final version of the manuscript.

Acknowledgements

This project has received funding from EU's Horizon 2020 research and innovation programme under Grant Agreement No 860762. The work was financially supported by the Polish National Science Centre, Poland (HARMONIA 2018/30/M/ST5/00460), the Foundation for Polish Science (TEAM POIR.04.04.00-00-3CF4/16-00 and START scholarship no. 039.2017 to M.K.). M.K. is a recipient of a scholarship awarded by the Polish Ministry of Education and Science to outstanding young scientists. I.K. and D.J. thank the French *Agence Nationale de la Recherche* (ANR) for support under contract No. ANR-20-CE29-0005 (BSE-Forces). This work used the computational resources of the CCIPL/GliciD mesocenter installed in Nantes. DFT calculations were carried out using resources provided by Wroclaw Centre for Networking and Supercomputing (grant no. 518). The authors thank Joseph Milton for proofreading the manuscript.

Conflict of Interest

The authors declare no conflict of interest.

Data Availability Statement

The data that support the findings of this study are available in the supplementary material of this article.

Keywords: Alkynes · Biaryls · Dyes/Pigments · Fluorescence · Heterocycles

[1] K. P. Kawahara, W. Matsuoka, H. Ito, K. Itami, *Angew. Chem. Int. Ed.* **2020**, *59*, 6383–6388.
[2] K. Oki, M. Takase, S. Mori, H. Uno, *J. Am. Chem. Soc.* **2019**, *141*, 16255–16259.
[3] A. Caruso, J. D. Tovar, *Org. Lett.* **2011**, *13*, 3106–3109.
[4] A. Fukazawa, S. Yamaguchi, *Chem. Asian J.* **2009**, *4*, 1386–1400.
[5] M. Navakouski, H. Zhylitskaya, P. J. Chmielewski, T. Lis, J. Cybińska, M. Stępień, *Angew. Chem. Int. Ed.* **2019**, *58*, 4929–4933.
[6] S. Mishra, M. Krzeszewski, C. A. Pignedoli, P. Ruffieux, R. Fasel, D. T. Gryko, *Nat. Commun.* **2018**, *9*, 1714.
[7] M. Stępień, E. Gońka, M. Żyła, N. Sprutta, *Chem. Rev.* **2017**, *117*, 3479–3716.
[8] T. Hensel, N. N. Andersen, M. Plesner, M. Pittelkow, *Synlett* **2016**, *27*, 498–525.
[9] E. Gońka, P. J. Chmielewski, T. Lis, M. Stępień, *J. Am. Chem. Soc.* **2014**, *136*, 16399–16410.

[10] G. E. Rudebusch, A. G. Fix, H. A. Henthorn, C. L. Vonnegut, L. N. Zakharov, M. M. Haley, *Chem. Sci.* **2014**, *5*, 3627–3633.
[11] G. Li, Y. Wu, J. Gao, J. Li, Y. Zhao, Q. Zhang, *Chem. Asian J.* **2013**, *8*, 1574–1578.
[12] J. Fan, L. Zhang, A. L. Briseno, F. Wudl, *Org. Lett.* **2012**, *14*, 1024–1026.
[13] M. B. Goldfinger, K. B. Crawford, T. M. Swager, *J. Am. Chem. Soc.* **1997**, *119*, 4578–4593.
[14] M. B. Goldfinger, T. M. Swager, *J. Am. Chem. Soc.* **1994**, *116*, 7895–7896.
[15] N. K. Saha, T. H. Barnes, L. J. Wilson, B. L. Merner, *Org. Lett.* **2022**, *24*, 1038–1042.
[16] Y. Gu, V. Vega-Mayoral, S. Garcia-Orrit, D. Schollmeyer, A. Narita, J. Cabanillas-González, Z. Qiu, K. Müllen, *Angew. Chem. Int. Ed.* **2022**, *61*, e202201088.
[17] K. M. Magierа, V. Aryal, W. A. Chalifoux, *Org. Biomol. Chem.* **2020**, *18*, 2372–2386.
[18] J. Gicquiaud, A. Hacıhasanoğlu, P. Hermange, J. M. Sotiropoulos, P. Y. Toullec, *Adv. Synth. Catal.* **2019**, *361*, 2025–2030.
[19] W. Yang, R. Bam, V. J. Catalano, W. A. Chalifoux, *Angew. Chem. Int. Ed.* **2018**, *57*, 14773–14777.
[20] W. Yang, R. R. Kazemi, N. Karunathilake, V. J. Catalano, M. A. Alpuche-Aviles, W. A. Chalifoux, *Org. Chem. Front.* **2018**, *5*, 2288–2295.
[21] W. Yang, A. Lucotti, M. Tommasini, W. A. Chalifoux, *J. Am. Chem. Soc.* **2016**, *138*, 9137–9144.
[22] Y. Li, A. Concellón, C. J. Lin, N. A. Romero, S. Lin, T. M. Swager, *Chem. Sci.* **2020**, *11*, 4695–4701.
[23] K. Sprenger, C. Golz, M. Alcarazo, *Eur. J. Org. Chem.* **2020**, 6245–6254.
[24] J. Labella, G. Durán-Sampedro, S. Krishna, M. V. Martínez-Díaz, D. M. Guldi, T. Torres, *Angew. Chem. Int. Ed.* **2023**, *62*, e202214543.
[25] E. González-Fernández, L. D. M. Nicholls, L. D. Schaaf, C. Farès, C. W. Lehmann, M. Alcarazo, *J. Am. Chem. Soc.* **2017**, *139*, 1428–1431.
[26] M. Satoh, Y. Shibata, K. Tanaka, *Chem. Eur. J.* **2018**, *24*, 5434–5438.
[27] T. Ikai, K. Oki, S. Yamakawa, E. Yashima, *Angew. Chem. Int. Ed.* **2023**, *62*, e202301836.
[28] L. D. M. Nicholls, M. Marx, T. Hartung, E. González-Fernández, C. Golz, M. Alcarazo, *ACS Catal.* **2018**, *8*, 6079–6085.
[29] A. S. Dudnik, V. Gevorgyan, *Angew. Chem. Int. Ed.* **2007**, *46*, 5195–5197.
[30] R. Stężycki, M. Grzybowski, G. Clermont, M. Blanchard-Desce, D. T. Gryko, *Chem. Eur. J.* **2016**, *22*, 5198–5203.
[31] G. Sanil, B. Koszarna, Y. M. Poronik, O. Vakuliuk, B. Szymański, D. Kusy, D. T. Gryko, *Adv. Heterocycl. Chem.* **2022**, *138*, 335–409.
[32] S. Stecko, D. T. Gryko, *JACS Au* **2022**, *2*, 1290–1305.
[33] M. Krzeszewski, Ł. Dobrzycki, A. L. Sobolewski, M. K. Cyrański, D. T. Gryko, *Angew. Chem. Int. Ed.* **2021**, *60*, 14998–15005.
[34] M. Tasior, M. Chotkowski, D. T. Gryko, *Org. Lett.* **2015**, *17*, 6106–6109.
[35] M. Tasior, P. Kowalczyk, M. Przybył, M. Czichy, P. Janasik, M. H. E. Bousquet, M. Łapkowski, M. Rammo, A. Rebane, D. Jacquemin, D. T. Gryko, *Chem. Sci.* **2021**, *12*, 15935–15946.
[36] M. Krzeszewski, M. Tasior, M. Grzybowski, D. T. Gryko, *Org. Synth.* **2021**, *98*, 242–262.
[37] A. Janiga, E. Glodkowska-Mrowka, T. Stoklosa, D. T. Gryko, *Asian J. Org. Chem.* **2013**, *2*, 411–415.
[38] H. Luo, J. Liu, *Angew. Chem. Int. Ed.* **2023**, *62*, e202302761.
[39] C. Wang, Z. Deng, D. L. Phillips, J. Liu, *Angew. Chem. Int. Ed.* **2023**, *62*, e202306890.
[40] Chaolumen, I. A. Stepek, K. E. Yamada, H. Ito, K. Itami, *Angew. Chem. Int. Ed.* **2021**, *60*, 23508–23532.
[41] M. Tasior, O. Vakuliuk, D. Koga, B. Koszarna, K. Górski, M. Grzybowski, Ł. Kielesiński, M. Krzeszewski, D. T. Gryko, *J. Org. Chem.* **2020**, *85*, 13529–13543.
[42] V. Mamane, P. Hannen, A. Fürstner, *Chem. Eur. J.* **2004**, *10*, 4556–4575.
[43] G. Wu, A. L. Rheingold, S. J. Geib, R. F. Heck, *Organometallics* **1987**, *6*, 1941–1946.
[44] A. Fürstner, V. Mamane, *J. Org. Chem.* **2002**, *67*, 6264–6267.
[45] T. Ghosh, J. Chatterjee, S. Bhakta, *Org. Biomol. Chem.* **2022**, *20*, 7151–7187.
[46] C. M. Hendrich, K. Sekine, T. Koshikawa, K. Tanaka, A. S. K. Hashmi, *Chem. Rev.* **2021**, *121*, 9113–9163.
[47] M. Kumar, K. Kaliya, S. K. Maurya, *Org. Biomol. Chem.* **2023**, *21*, 3276–3295.
[48] J. Labella, G. Durán-Sampedro, M. V. Martínez-Díaz, T. Torres, *Chem. Sci.* **2020**, *11*, 10778–10785.
[49] T. Matsuda, T. Moriya, T. Goya, M. Murakami, *Chem. Lett.* **2011**, *40*, 40–41.
[50] Deposition number 2285219 contains the supplementary crystallographic data for this paper. These data are provided free of charge by the joint Cambridge Crystallographic Data Centre and Fachinformationszentrum Karlsruhe Access Structures service.
[51] R. Bam, W. Yang, G. Longhi, S. Abbate, A. Lucotti, M. Tommasini, R. Franzini, C. Villani, V. J. Catalano, M. M. Olmstead, W. A. Chalifoux, *Org. Lett.* **2019**, *21*, 8652–8656.
[52] L. Song, G. Tian, L. Van Meervelt, E. V. Van Der Eycken, *Org. Lett.* **2020**, *22*, 6537–6542.
[53] D. B. Walker, J. Howgego, A. P. Davis, *Synthesis* **2010**, 3686–3692.
[54] T. Nakae, R. Ohnishi, Y. Kitahata, T. Soukawa, H. Sato, S. Mori, T. Okujima, H. Uno, H. Sakaguchi, *Tetrahedron Lett.* **2012**, *53*, 1617–1619.
[55] D. Lorbach, M. Wagner, M. Baumgarten, K. Müllen, *Chem. Commun.* **2013**, *49*, 10578–10580.
[56] A. Suárez, S. Suárez-Pantiga, O. Nieto-Faza, R. Sanz, *Org. Lett.* **2017**, *19*, 5074–5077.
[57] D. Garayalde, G. Rusconi, C. Nevado, *Helv. Chim. Acta* **2017**, *100*, e1600333.
[58] P. Barrio, M. Kumar, Z. Lu, J. Han, B. Xu, G. B. Hammond, *Chem. Eur. J.* **2016**, *22*, 16410–16414.
[59] M. Tasior, B. Koszarna, D. C. Young, B. Bernard, D. Jacquemin, D. Gryko, D. T. Gryko, *Org. Chem. Front.* **2019**, *6*, 2939–2948.
[60] B. Dereka, A. Rosspeintner, M. Krzeszewski, D. T. Gryko, E. Vauthey, *Angew. Chem. Int. Ed.* **2016**, *55*, 15624–15628.
[61] Y. M. Poronik, G. V. Baryshnikov, I. Deperasińska, E. M. Espinoza, J. A. Clark, H. Ågren, D. T. Gryko, V. I. Vullev, *Commun. Chem.* **2020**, *3*, 190.
[62] M. Krzeszewski, D. T. Gryko, *J. Org. Chem.* **2015**, *80*, 2893–2899.
[63] C. Adamo, D. Jacquemin, *Chem. Soc. Rev.* **2013**, *42*, 845–856.
[64] O. Christiansen, H. Koch, P. Jørgensen, *Chem. Phys. Lett.* **1995**, *243*, 409–418.
[65] C. A. Guido, A. Chrayteh, G. Scalmani, B. Mennucci, D. Jacquemin, *J. Chem. Theory Comput.* **2021**, *17*, 5155–5164.
[66] M. Krzeszewski, P. Świder, Ł. Dobrzycki, M. K. Cyrański, W. Danikiewicz, D. T. Gryko, *Chem. Commun.* **2016**, *52*, 11539–11542.
[67] M. Krzeszewski, K. Sahara, Y. M. Poronik, T. Kubo, D. T. Gryko, *Org. Lett.* **2018**, *20*, 1517–1520.
[68] C. L. Deng, J. P. Bard, J. A. Lohrman, J. E. Barker, L. N. Zakharov, D. W. Johnson, M. M. Haley, *Angew. Chem. Int. Ed.* **2019**, *58*, 3934–3938.
[69] APEX3 V2019, Bruker Nano, Inc, Program for the Solution of Crystal Structures, Madison, WI, USA **2019**.

[70] SAINT V8.40 A, Bruker Nano, Inc, Software package for the Solution of Crystal Structures, Madison, WI, USA **2019**.
[71] SADABS V2016/2, Bruker Nano, Inc, Program for the solution of Crystal Structures **2019**.
[72] G. M. Sheldrick, *Acta Crystallogr. Sect. A* **2015**, *71*, 3–8.
[73] G. M. Sheldrick, *Acta Crystallogr. Sect. C* **2015**, *71*, 3–8.
[74] D. C. Creagh, W. J. McAuley, *International Tables for Crystallography*, Vol C (Ed.: A. J. C. Wilson), Kluwer: Dordrecht **1992**, pp. 200–206.
[75] C. F. Macrae, I. J. Bruno, J. A. Chisholm, P. R. Edgington, P. McCabe, E. Pidcock, L. Rodriguez-Monge, R. Taylor, J. van de Streek, P. A. Wood, *J. Appl. Crystallogr.* **2008**, *41*, 466–470.
[76] M. J. Frisch, et al., *Gaussian 16, revision C.01*, Gaussian Inc.: Wallingford, CT **2019**.
[77] F. Weigend, R. Ahlrichs, *Phys. Chem. Chem. Phys.* **2005**, *7*, 3297–3305.
[78] S. Grimme, J. Antony, S. Ehrlich, H. Krieg, *J. Chem. Phys.* **2010**, *132*, 154104.
[79] Y. Zhao, D. G. Truhlar *Theor. Chem. Acc.* **2008**, *120*, 215–241.
[80] A. V. Marenich, C. J. Cramer, D. G. Truhlar, *J. Phys. Chem. B* **2009**, *113*, 6378–6396.
[81] CYLview20, C. Y. Legault, *Visualization and analysis software for Computational chemistry*, Université de Sherbrooke **2020** (http://www.cylview.org).
[82] M. J. Frisch, et al., *Gaussian 16, revision A.03*, Gaussian Inc.: Wallingford, CT **2016**.
[83] J. Tomasi, B. Mennucci, R. Cammi, *Chem. Rev.* **2005**, *105*, 2999–3094.
[84] A. D. Laurent, D. Jacquemin, *Int. J. Quantum Chem.* **2013**, *113*, 2019–2039.
[85] TURBOMOLE V7.3/V7.5, a development of University of Karlsruhe and Forschungszentrum Karlsruhe GmbH, **1989–2007**; TURBOMOLE GmbH, can be found under http://www.turbomole.com.
[86] D. Jacquemin, I. Duchemin, X. Blase, *J. Chem. Theory Comput.* **2015**, *11*, 5340–5359.
[87] J. Cerezo, F. Santoro, FCClasses 3.0, can be found under http://www.pi.iccom.cnr.it/fcclasses.
[88] J. Cerezo, F. Santoro, *J. Comput. Chem.* **2023**, *44*, 626–643.
[89] F. Santoro, D. Jacquemin, *WIREs Comput. Mol. Sci.* **2016**, *6*, 460–486.

Manuscript received: August 2, 2023
Accepted manuscript online: October 12, 2023
Version of record online: November 2, 2023

JOC The Journal of Organic Chemistry

pubs.acs.org/joc Article

1,4-Dihydropyrrolo[3,2-*b*]pyrroles with Two Embedded Heptagons via Alkyne Annulation

Gana Sanil, Łukasz Dobrzycki, Michał K. Cyrański,* Denis Jacquemin,* Wojciech Chaładaj,* and Daniel T. Gryko*

Cite This: *J. Org. Chem.* 2025, 90, 614–622 Read Online

ACCESS | Metrics & More | Article Recommendations | Supporting Information

ABSTRACT: Drastic changes to the character of the acidic catalyst enable the reversal of the double alkyne benzannulation reaction output. In the presence of a strong Brønsted acid, 1,4-dihydropyrrolopyrroles undergo transformation which results in the formation of two 7-membered rings. Computational studies imply that the thermodynamically unfavored 7-membered ring is forged via the kinetically favored *6-endo-dig* attack of a protonated alkyne at the position 3a of pyrrolopyrrole followed by a 1,2-vinyl shift.

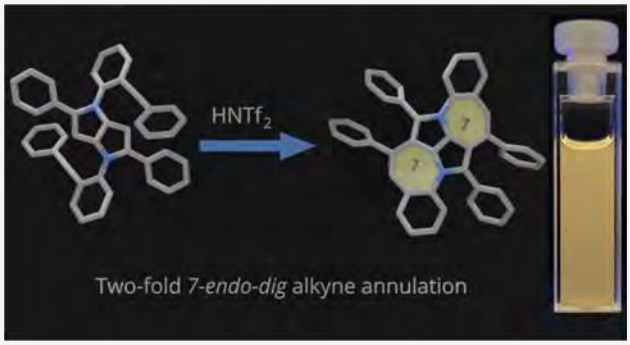

INTRODUCTION

The incorporation of seven-membered rings into the structure of polycyclic aromatic hydrocarbons and their heterocyclic analogues offers an unprecedented strategy to modify their physicochemical characteristics.[1−5] In particular, introduction of heptagons leads to nonplanar architectures with bowl shape or negative curvature, which translates to distinct electronic structures and unique intermolecular stacking in the solid state.[6−12] As a result, electronic, magnetic, and mechanical properties are entirely different from classical alternant systems. As far as purely benzenoid structures are concerned, intramolecular alkyne benzannulation was employed as one of the key reactions used to make new C−C bonds. Although the first case of alkyne benzannulation was reported by Scott et al., who used flash vacuum pyrolysis (FVP),[13] the method only became popular after the discovery of electrophilic activation of alkyne using Brønsted acid which was reported by Goldfinger and Swager.[14] Over the last 20 years, the reaction has evolved significantly—novel catalysts were introduced such as π-Lewis acids based on either transition metals or main group elements, radical reagents, and non-nucleophilic bases.[15−17] Significant examples involve the 2-fold alkyne annulation utilized to synthesize a bis-chrysene precursor of graphene nanoribbon (GNR),[18] reported by Müllen and co-workers as well as Chalifoux group's work on multifold cyclization to make narrow and soluble GNRs.[19] The scope of this reaction was also demonstrated on geometrically strained nonplanar nanographenes, namely, tetrasubstituted chiral peropyrenes[20] and helicenes.[21−23] Impressively, this reaction shows tolerance toward sulfur-,[24−26] oxygen-, and nitrogen-doped[23,27] polycyclic systems as well.

The regioselectivity of alkyne annulation reactions heavily depends on the substrates and catalyst employed (Figure 1a).[15−17,28] In terms of polycyclic aromatic systems, *6-endo-dig*-type cyclization is majorly reported, while *5-exo-dig*, *6-exo-dig* and 7-endo-dig are less common. Formation of nonhexagonal rings induces a warping of the graphenic system, causing a geometrical strain, which can lead to higher activation enthalpies.[29−33]

Tetraarylpyrrolo[3,2-*b*]pyrroles (TAPPs) have proven to be an excellent platform for the synthesis of aza-doped polycyclic aromatic hydrocarbons.[34,35] Although in most cases dyes comprising exclusively six-membered and five-membered rings were synthesized, a limited number of architectures bearing seven-membered rings were reported as well.[36,37] The presence of highly electron-rich positions 3 and 6 makes TAPPs a potent precursor for intramolecular C−H activation, leading to the introduction of π-extension and curvature. Herein, we report the double intramolecular alkyne annulation via Brønsted acid catalysis toward nonplanar aromatic heterocycle bearing multiple odd rings (Figure 1c).

Received: October 14, 2024
Revised: December 7, 2024
Accepted: December 16, 2024
Published: December 31, 2024

https://doi.org/10.1021/acs.joc.4c02538
J. Org. Chem. 2025, 90, 614−622

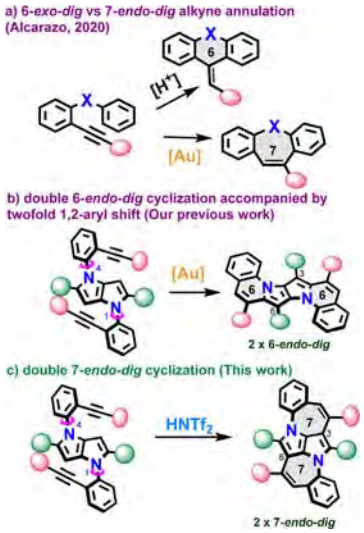

Figure 1. Intramolecular alkyne annulation reactions performed under different conditions leading to the incorporation of one or two new 6- or 7-membered rings.

RESULTS AND DISCUSSION

Design and Synthesis. Recently, we reported the synthesis of aza-doped S-shaped nanographenes via a cationic gold-catalyzed alkyne benzannulation reaction (Figure 1b).[38] The work capitalized on the modular access to tetraarylpyrrolo[3,2-*b*]pyrroles (TAPPs) bearing *ortho*-diphenylethyne moieties at positions 1 and 4, where the triple bonds are placed in close proximity to the electron-rich positions 3 and 6. We envisioned that this design would allow for the formation of two new seven-membered rings leading to a unique (7−5−5−7)-type cyclic system. Interestingly, however, the gold catalyst ($IPrAuNTf_2$) induced a *6-endo-dig* annulation with a subsequent 1,2-aryl shift leading to a 6−5−5−6 ring system. During the additional investigations, we performed the reaction, under the same temperature and using the same solvent on the precursor **4aa**, with bistriflimidic acid ($HNTf_2$)[39]—the conjugate acid of the gold catalyst's counteranion employed in our prior work. Both triflic acid and bistriflimidic acid were employed in alkyne benzannulation for various substrates.[40,41] To our surprise, we observed the formation of a new product with a different color and R_f than

Scheme 1. Gibbs Free Energy Profile for Benzannulation of Model TAPP I Catalyzed by $HNTf_2$[a]

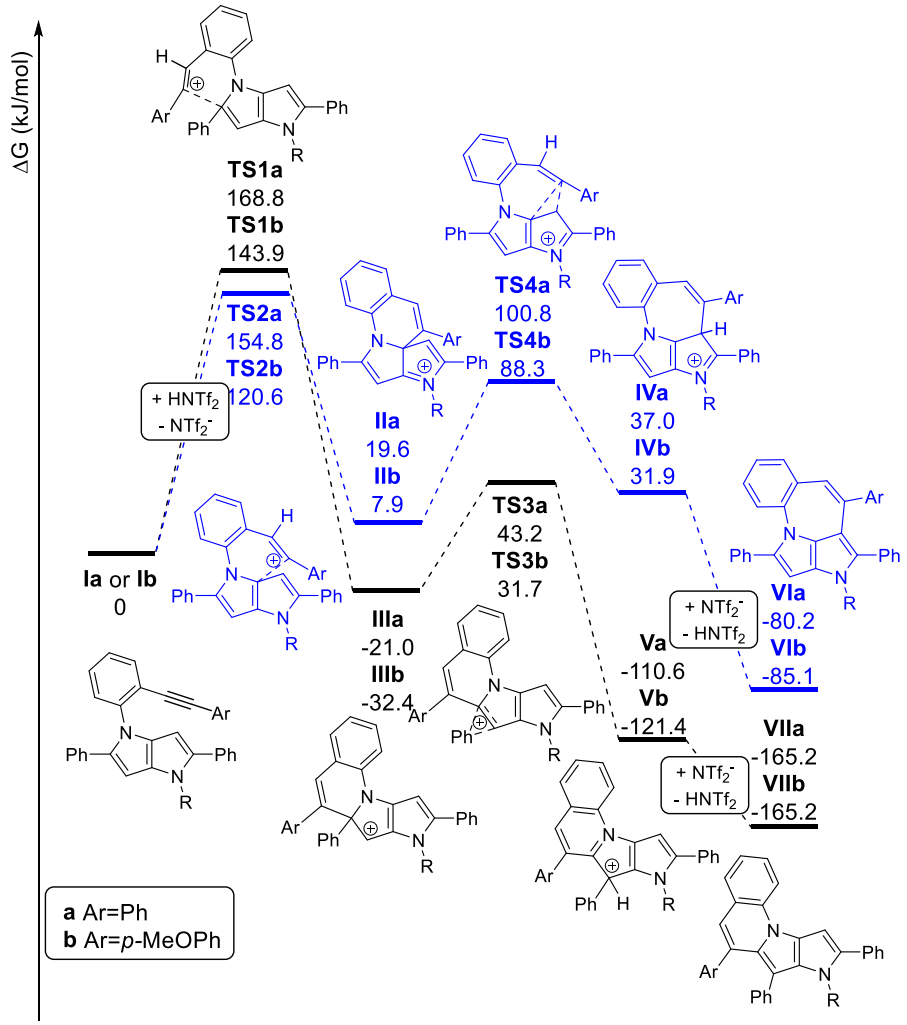

[a]Calculated at the SMD(*m*-xylene)/M06/def2-TZVPP//B3LYP-D3/def2-SVP level of theory. Structures marked with (a,b) correspond to Ar = Ph and *p*-MeOPh, respectively.

https://doi.org/10.1021/acs.joc.4c02538
J. Org. Chem. 2025, 90, 614−622

Scheme 2. Synthesis of π-Extended Pyrrolo[3,2-*b*]pyrroles with Two Embedded Heptagons 5aa via $HNTf_2$-Mediated Two-fold Alkyne Annulation of Alkyne-Bearing TAPP 4aa

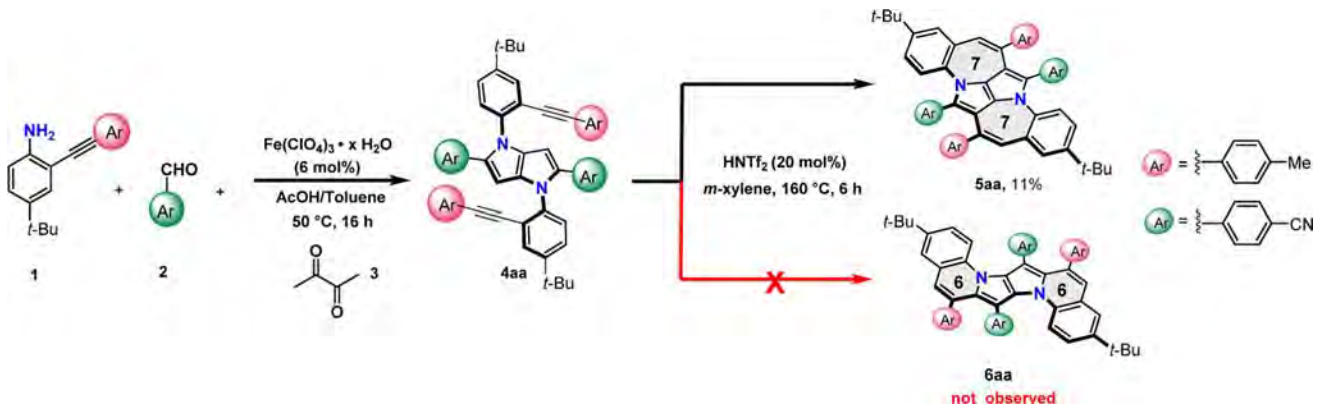

that of both 1,2-aryl shift product **6aa** and starting material **4aa** (Scheme 2). However, the reaction mixture showed the presence of additional spots with similar R_f values, which made isolation of the major spot difficult. We anticipate that the formation of multiple byproducts during the reaction is the reason behind the low yield and inability to isolate any of the byproducts made it impossible to characterize them. The initial ^{1}H NMR analysis showed a significant difference in peak distribution compared to the benzannulated product with the same mass (HRMS-APCI, calculated for $C_{58}H_{49}N_4^+$: $[M + H]^+$ = 801.3952, found = 801.3956). These results demonstrate the formation of a new cyclic system which can be described as a regio-isomer of **6**. The X-ray crystallographic results unambiguously proved the presence of a 2-fold formal 7-*endo-dig* cyclization at the C3 and C6 positions, resulting in a nonalternant aromatic heterocycle (Figure 2). This distinct arrangement of two adjacent pentagons positioned between two heptagons is recognized as an inverse Stone−Thrower−Wales defect in graphene.

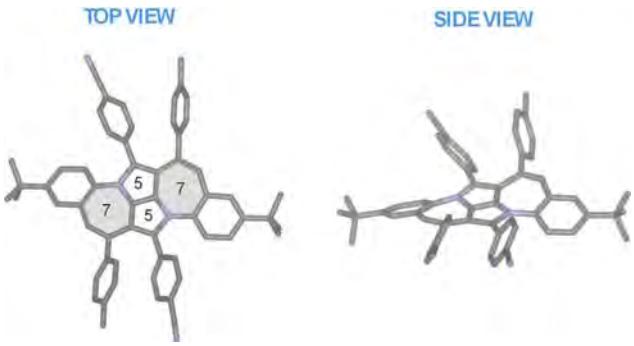

Figure 2. Crystal structure (CCDC 2379282) of heptagon-embedded nonalternant aromatic heterocycle **5aa**. Solvent molecules and hydrogen atoms were omitted for clarity.

This transformation was quite intriguing as it could only be catalyzed using $HNTf_2$. Subsequently, we tested a range of catalysts which are commonly utilized for alkyne annulation reactions, including cationic gold catalysts with different ancillary ligands and counteranions compared to the ones we used in our prior work[38] (see Table S1 in the Supporting Information for details). However, none of them gave a similar outcome. Alcarazo and co-workers did a comparative study on the hydroarylation of alkynes using Brønsted acid and cationic gold catalysts.[25] They showed that the 7-*endo-dig*-type annulation is induced by acid only when the vinyl carbocation intermediate is stabilized by electron-donating groups on benzene rings attached to it and Au-catalysis toward this product is governed by steric factors around the reaction center. Extensive literature studies focusing on the exo vs endo selectivity of this carbocyclization are limited to gold catalysts.[42−44] Intriguingly, Langer and co-workers found that depending on the choice of Brønsted acid and solvent, alkyne annulation in the case of imidazo[1,2-*a*]pyridines can be steered toward the formation of either a six-membered ring or seven-membered ring.[45]

Computational Studies—Mechanism. For a better understanding of the dichotomy in reactivity under Brønsted acid and gold catalysts, the annulation of model TAPP **Ia** (bearing phenyl group at the alkyne terminus) triggered by $HNTf_2$ was investigated computationally (Scheme 1). The pathway preferred for gold catalysis,[38] encompassing *6-endo-dig* annulation followed by a 1,2-aryl shift, is also plausible but only when cyclization is triggered by the protonation of the alkyne moiety (**TS1a**, $\Delta G^{\ddagger}$ = 168.8 kJ/mol) to give rise to intermediate **IIIa** that easily undergoes 1,2-aryl shift (**TS3a**, $\Delta G^{\ddagger}$ = 64.2 kJ/mol). In contrast, despite extensive research on the potential energy surface, we did not locate a transition state associated directly with *7-endo-dig* cyclization. However, attack of the protonated alkyne at position **3a** of the 1,4-dihydropyrrolo[3,2-*b*]pyrrole (DHPP) system producing **IIa** is not only possible (**TS2a**, $\Delta G^{\ddagger}$ = 154.8 kJ/mol) but also kinetically preferred over another *6-endo-dig* cyclization proceeding through **TS1a**. Intermediate **IIa** is capable of rearranging with ring expansion through a 1,2-vinyl shift (**TS4a**, $\Delta G^{\ddagger}$ = 81.2 kJ/mol) toward **IVa**, which after deprotonation delivers a thermodynamically less preferred product bearing a 7-membered ring. Similar profiles were found for both cyclization manifolds of annulation of analogues TAPP **Ib**, bearing *p*-methoxyphenyl groups at the alkyne. The rate-limiting steps, however, proceeding through **TS1b** and **TS2b** were associated with considerably lower activation barriers ($\Delta G^{\ddagger}$ = 143.9 and 120.6 kJ/mol, respectively) compared to phenyl-substituted alkynes proceeding through **TS1a** and **TS2a** ($\Delta G^{\ddagger}$ = 168.8 and 154.8 kJ/mol, respectively).

Scope and Limitations. To showcase the functional group tolerance and synthetic utility of this reaction, we began the synthesis of precursor TAPPs **4** which possessed electronically different substituents at the para-position of the benzene ring

https://doi.org/10.1021/acs.joc.4c02538
J. Org. Chem. 2025, 90, 614−622

Scheme 3. Synthesis of a Non-planar, π-Extended Pyrrolo[3,2-*b*]pyrroles via $HNTf_2$-Mediated Two-fold Alkyne Annulation of Alkyne Bearing TAPPs 4. (I) Substrates; (II) Successful Examples; (III) Pd-Catalyzed Intramolecular Arylation of 5ac; (IV) Unsuccessful Examples[a,b]

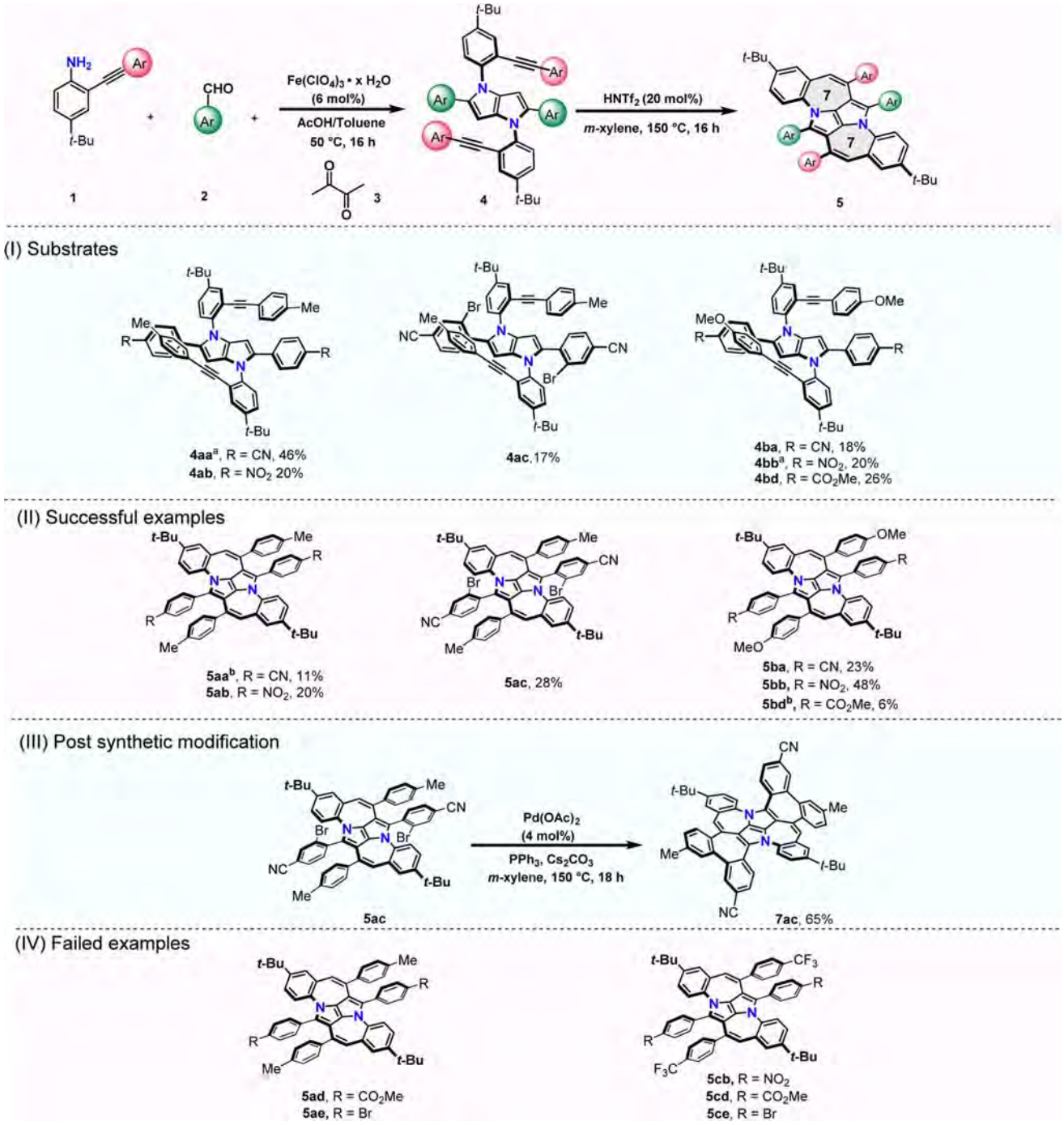

[a]Compound has been reported previously.[38] [b]Reaction kept at 160 °C for 6 h.

attached to the triple bond. These rationally chosen precursors were synthesized by following the method described in our previous work.[38] The $HNTf_2$-catalyzed annulation turned out to be highly selective as it worked only on specific substrates (Scheme 3). It is quite evident that the formal *7-endo-dig* cyclization is favored only when the triple bond is activated by electron-donating groups (MeO or Me) present on the benzene ring connected to it. Failed examples of **5cb**−**ce** confirm this hypothesis [Scheme 3(IV)]. Nevertheless, the presence of these groups is not the only requirement. Arene rings on positions 2 and 5 must be electron-deficient (with substituents CN, CO_2Me, or NO_2) to a degree that ensures the stability of the final product. When we changed the electron-withdrawing ability of the substituents from low (Br as in the case of **5ae** [Scheme 3(IV)] to high (NO_2 in **5ab**), the reaction outcome changed from a complex mixture of byproducts to

https://doi.org/10.1021/acs.joc.4c02538
J. Org. Chem. 2025, 90, 614−622

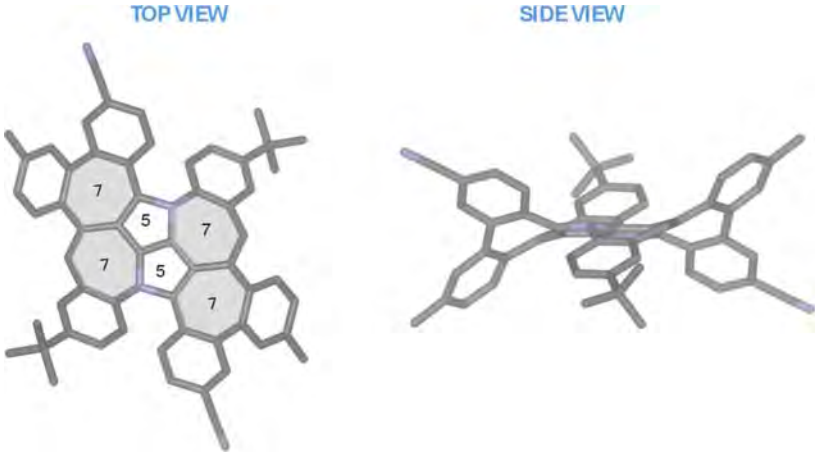

Figure 3. Crystal structure (CCDC 2381915) of multiple heptagon-embedded double helical nanographene **7ac**. Solvent molecules and hydrogen atoms were omitted for clarity.

Table 1. Photophysical Properties of the π-Extended Pyrrolopyrroles 5 and 7ac

	solvent	λ_{abs}^{max}/nm	λ_{em}^{max}/nm	stokes shift/cm^{-1}	ϕ_{fl}[a]	ε/M^{-1} cm^{-1}
5aa	toluene	450	575; 618	4800	0.04	18,000
	THF	449	572; 614	4700	0.05	21,000
5ab	toluene	515	676	4600	0.02	12,000
	THF	515	747	6000	<0.001	12,000
5ac	toluene	462	585; 630	4500	0.01	9000
	THF	465	590; 630	4500	0.01	9000
5ba	toluene	453	573; 613	4600	0.01	18,000
	THF	451	570; 613	4600	0.05	14,000
5bb	toluene	515	641	3800	0.01	11,000
	THF	514	644	3900	<0.001	10,000
5bd	toluene	449	613	5900	0.05	14,000
	THF	449	613	5900	0.04	14,000
7ac	toluene	502	670	5000[b]	0.01	9000
	THF	503	645	4300[b]	0.01	12,000

[a]Standard: 9,10dDiphenyl anthracene in cyclohexane (ϕ_{fl} = 0.7). [b]Stokes shift calculated from absorption corresponding to lowest energy (λ = 502 and 503 nm).

predominantly yielding the bis-annulated product. We also tested the possibility of performing the reaction on substrates with halogen handles so as to demonstrate the postsynthetic utility of this reaction [Scheme 3(III)]. Alkyne annulation occurred smoothly to obtain **5ac**, which then underwent intramolecular direct arylation to form the completely fused nonplanar double helical nanographene **7ac** (Figure 3).

Photophysical Properties. The fused dyes **5** exhibit distinct photophysical properties compared to previously reported π-expanded TAPPs (Table 1 and Section S5.1, Supporting Information).[34,35] In particular, they show a very weak ϕ_{fl} (typically around 0.01), which indicates low-radiative emission. This is confirmed by theoretical calculations (see below). Their absorption showed a significant vibronic structure with a low energy absorption band ranging from 449 to 515 nm. The substituents at positions 2 and 5 significantly influence the locations of the absorption and emission maxima. Specifically, substituting CN to NO_2 (**5aa** and **5ab**) causes a red shift of ≈65 and 100 nm, respectively. Similar effects are seen in **5ba** and **5bb**. Compared to their structural isomer S-shaped, π-expanded pyrrolopyrroles,[38] these dyes exhibit a bathochromic shift of emission at ≈80 nm. As expected, further extension of the π system (**7ac**) induces red shifts of absorption and emission, relative to the precursor.

Computational Studies—Photophysics. To understand the peculiar photophysical properties of these systems, clearly differing from the ones of usual TAPPs, we have performed theoretical calculations (see the Supporting Information for details). Let us first discuss **5bb** which is a relevant example; the main conclusions and trends to all systems except **7ac**. Given the symmetric chemical substitution in **5bb**, we performed ground-state optimizations in both the C_2 and C_i point groups and found that both were stable minima but that the former is significantly favored (by ca. 7 kcal·mol^{-1} on the Gibbs energy scale). The electron density difference (EDD) plots obtained for the five lowest transitions of this stable C_2 structure are displayed in Figure 4. As can be seen, the lowest transition of *A* symmetry is very weakly dipole-allowed. For this transition, the EDD reveals a delocalization on the TAPP core as well as the side seven-membered rings, whereas the contribution of the nitrophenyls is limited. Such topology is very original since for the vast majority of TAPPs developed to date, the lowest transition corresponds to a bright quadrupolar charge-transfer (CT) from the dye core to the side groups located at positions 2 and 5.[38,46−48] This is in fact the topology found for the third transition here, i.e., that of *B* symmetry (see

https://doi.org/10.1021/acs.joc.4c02538
J. Org. Chem. 2025, 90, 614−622

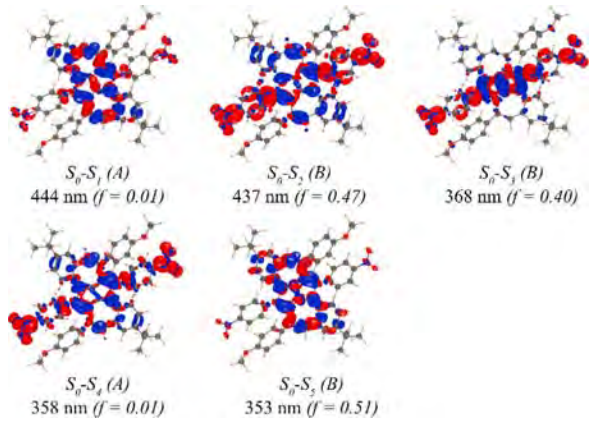

Figure 4. EDD plots for the 5 lowest excited states of **5bb**. The red and blue lobes are regions of decrease (red) and increase (blue) in density upon absorption. For each state, we provide the symmetry, vertical excitation wavelength, and oscillator strengths computed at a TD-DFT level with the (LR,neq)-PCM(toluene) solvent model. Contour threshold: 0.001 au. See Figures S4 and S5 in the Supporting Information for other compounds.

Figure 4) which is significantly upshifted. The second transition is located at almost the same energy as the first but is bright. It represents intermediate features between the first and third states with a marked CT character, yet with significant contributions to the seven-membered rings. As can be seen from Table S5 in the Supporting Information, the same conclusions (state ordering and dipole strengths) are obtained at both the TD-DFT and CC2 levels of theory, giving confidence in the result.

To give a qualitative comparison with the experiment, one should note that the two first transitions are very close in energy, causing them to form two peaks, which is consistent with the measurements; e.g., the nearly dark lowest transition is likely buried under absorption to the second excited state that should be responsible for the measured λ_{abs}^{max}. The presence of such a nearly dark transition is of course detrimental for emission since it is indicative of a very low radiative rate (the oscillator strength obtained on the S_1 minimum is also very small). In other words, dark-state quenching happens in these compounds. Very similar trends are obtained in the full series of compounds **5** and are not further detailed. More quantitative theory/experiment comparisons have also been obtained; see the Supporting Information for details (Table S6). Eventually, **7ac** shows some specificities. First, the most stable structure we could obtain belongs to the C_i point group. While this dye still presents two nearly degenerated excited states — the lowest (A_g) being dark and the second (A_u) being bright — it is noteworthy that the CT character of the second transition is much less marked than in **5aa** (see EDDs in the SI).

Cyclic Voltammetry. Voltammetric experiments were performed to investigate the electrochemical properties of all of the synthesized compounds (**5**, **7ac**, and their precursors **4**) (Table 2). The parent TAPP **4** underwent one reversible oxidation process. While **4ac** and **4ba** showed one quasireversible reduction event, **4ab** exhibited three reduction events, out of which the first two are quasireversible and the third irreversible. Fused compounds **5** displayed two or three

Table 2. Redox Potentials of the π-Extended Pyrrolopyrroles 5, 7ac, and Precursors 4

compound[a]	event	E_{OX}^{PA} [V]	E_{OX}^{PC} [V]	$E_{OX}^{1/2}$ [V]	E_{OX}^{ONSET} [V]	IP[c] [eV]	E_{RED}^{PA} [V]	E_{RED}^{PC} [V]	$E_{RED}^{1/2}$ [V]	E_{RED}^{ONSET} [V]	EA[d] [eV]
4ab	1	1.03	0.94	0.98	0.91	5.2	−0.72	−0.79		−0.68	−3.60
	2						−0.93	−1.17			
	3							−1.71			
4ac	1	1.10	1.00	1.05	0.99	5.1	−0.66	−0.90		−0.70	−4.22
4ba[b]	1	0.99	0.90	0.94	0.87	5.1	−0.70	−0.90		−0.74	−3.53
4bd	1	0.85	0.75	0.80	0.74	5.0					
5aa	1	0.73	0.66	0.69	0.63	4.9	−0.62	−0.89		−0.67	−3.61
	2	1.14									
5ab	1	0.76	0.69	0.72	0.65	4.9	−0.67	−0.86		−0.68	−3.60
	2	1.12	1.06				−0.99	−1.09			
	3							−1.49			
5ac	1	0.76	0.65	0.70	0.65	4.9					
	2	1.22	1.12								
5ba	1	0.71	0.64	0.67	0.60	4.9	−0.65	−0.92		−0.67	−3.61
	2	0.94						−1.35			
	3	1.13									
5bb	1	0.73	0.65	0.64	0.62	4.9	−0.68	−0.83		−0.67	−3.61
	2	1.11	1.02	1.06			−0.95	−1.14			
	3						−1.29	−1.48			
5bd	1	0.63	0.57		0.53	4.8	−0.65	−0.92		−0.69	−3.59
	2	0.91	0.77					−1.37			
	3	1.04	0.97								
7ac	1	0.88			0.60	4.9	−0.68	−0.92		−0.68	−3.60
	2	1.22						−1.29			

[a]Measurement conditions: electrolyte (NBu_4PF_6, c = 0.1 M), dry CH_2Cl_2, potential sweep rate: 100 mV s^{-1}, working electrode: glassy carbon (GC), auxiliary electrode: Pt wire, reference electrode: Ag/AgCl/$NaCl_{sat}$; all measurements were conducted at room temperature. [b]Potential sweep rate: 50 mV s^{-1}. [c]Ionization potential. [d]Electron affinity. Calculated according to the equations: IP(eV) = $[E_{OX}^{ONSET} - E_{1/2}(Fc/Fc^+) + 4.8]$; EA(eV) = $-[E_{RED}^{ONSET} - E_{1/2}(Fc/Fc^+) + 4.8]$. $E_{1/2}(Fc/Fc^+)$ = 0.52 V under the above-mentioned conditions.

https://doi.org/10.1021/acs.joc.4c02538
J. Org. Chem. 2025, 90, 614−622

oxidation events with a reversible first oxidation. The only exception is **5bd**, where all three oxidation events are quasireversible. Considering reduction, these compounds showed one, two, or three quasireversible or nonreversible reduction events. However, molecule **5ac** did not show any reduction event. Cyclic voltammetry measurements demonstrated that the fused DHPPs have a lower first oxidation potential than the nonfused parent systems, following the general pattern that as the degree of conjugation increases, the first oxidation potential decreases. A similar trend is visible for the ionization potential as well. However, completely fused molecule **7ac** showed higher first oxidation potential than that of the precursor.

■ CONCLUSIONS

In conclusion, the direction of double intramolecular alkyne annulation for dihydropyrrolopyroles can be controlled through the choice of acids. The use of exceptionally strong Brønsted acids induces the formation of a two-seven-membered-ring-containing dye, which possesses an inverse Stone−Thrower−Wales topology. Based on computational studies, we reasoned that the reaction course can be rationalized by the kinetic forces. The presence of conjugated ring systems 7−5−5−7 and 7−7−5−5−7−7 shifts both absorption and emission bathochromically.

■ ASSOCIATED CONTENT

Data Availability Statement

The data underlying this study are available in the published article and its Supporting Information.

Supporting Information

The Supporting Information is available free of charge at https://pubs.acs.org/doi/10.1021/acs.joc.4c02538.

Experimental procedures, X-ray crystallography data, mechanistic computational studies, photophysical properties, computational studies, and copies of the NMR spectra of all products (PDF)

Accession Codes

Deposition Numbers 2379282 and 2381915 contain the supplementary crystallographic data for this paper. These data can be obtained free of charge via the joint Cambridge Crystallographic Data Centre (CCDC) and Fachinformationszentrum Karlsruhe Access Structures service.

■ AUTHOR INFORMATION

Corresponding Authors

Michał K. Cyrański − *Faculty of Chemistry, University of Warsaw, 02-093 Warsaw, Poland*; Email: mkc@chem.uw.edu.pl

Denis Jacquemin − *Nantes Université, CNRS, CEISAM UMR 6230, F-44000 Nantes, France; Institut Universitaire de France, F-75005 Paris, France*; orcid.org/0000-0002-4217-0708; Email: denis.jacquemin@univ-nantes.fr

Wojciech Chaładaj − *Institute of Organic Chemistry, Polish Academy of Sciences, 01-224 Warsaw, Poland*; orcid.org/0000-0001-8143-3788; Email: wojciech.chaladaj@icho.edu.pl

Daniel T. Gryko − *Institute of Organic Chemistry, Polish Academy of Sciences, 01-224 Warsaw, Poland*; orcid.org/0000-0002-2146-1282; Email: dtgryko@icho.edu.pl

Authors

Gana Sanil − *Institute of Organic Chemistry, Polish Academy of Sciences, 01-224 Warsaw, Poland*; orcid.org/0000-0001-7570-0544

Łukasz Dobrzycki − *Faculty of Chemistry, University of Warsaw, 02-093 Warsaw, Poland*; orcid.org/0000-0002-4426-963X

Complete contact information is available at: https://pubs.acs.org/10.1021/acs.joc.4c02538

Author Contributions

The manuscript was written through contributions of all authors. All authors have given approval to the final version of the manuscript.

Notes

The authors declare no competing financial interest.

■ ACKNOWLEDGMENTS

This project has received funding from the European Union's Horizon 2020 research and innovation programme under the Marie Skłodowka-Curie grant agreement No. 860762. This work was supported by the Polish National Science Center, Poland (grants OPUS 2020/37/B/ST4/00017). DFT calculations were carried out using resources provided by the Wroclaw Centre for Networking and Supercomputing (https://wcss.pl), grant no. 518. The X-ray structure was determined in the Advanced Crystal Engineering Laboratory (aceLAB) at the Chemistry Department of the University of Warsaw. MKC acknowledges Dr. Arkadiusz Ciesielski and Prof. Ilona Turowska-Tyrk for their support. This research used resources from the GLiCID Computing Facility (Ligerien Group for Intensive Distributed Computing, 10.60487/glicid, Pays de la Loire, France). The collaboration between the Gryko and Jacquemin groups is supported by the Maria Skłodowska-Curie and Pierre Curie Polish-French Science Award.

■ REFERENCES

(1) Rana, S. S.; Choudhury, J. Orchestrated Octuple C−H Activation: A Bottom-Up Topology Engineering Approach toward Stimuli-Responsive Double-Heptagon-Embedded Wavy Polycyclic Heteroaromatics. *Angew. Chem., Int. Ed.* **2024**, *63* (31), No. e202406514.

(2) Luo, H.; Wan, Q.; Choi, W.; Tsutsui, Y.; Dmitrieva, E.; Du, L.; Phillips, D. L.; Seki, S.; Liu, J. Two-Step Synthesis of B2N2-Doped Polycyclic Aromatic Hydrocarbon Containing Pentagonal and Heptagonal Rings with Long-Lived Delayed Fluorescence. *Small* **2023**, *19* (34), 2301769.

(3) Wagner, J.; Kumar, D.; Kochman, M. A.; Gryber, T.; Grzelak, M.; Kubas, A.; Data, P.; Lindner, M. Facile Functionalization of Ambipolar, Nitrogen-Doped PAHs toward Highly Efficient TADF OLED Emitters. *ACS Appl. Mater. Interfaces* **2023**, *15* (31), 37728−37740.

(4) Liu, B.; Chen, M.; Liu, X.; Fu, R.; Zhao, Y.; Duan, Y.; Zhang, L. Bespoke Tailoring of Graphenoid Sheets: A Rippled Molecular Carbon Comprising Cyclically Fused Nonbenzenoid Rings. *J. Am. Chem. Soc.* **2023**, *145* (51), 28137−28145.

(5) Stępień, M.; Gońka, E.; Żyła, M.; Sprutta, N. Heterocyclic Nanographenes and Other Polycyclic Heteroaromatic Compounds: Synthetic Routes, Properties, and Applications. *Chem. Rev.* **2017**, *117* (4), 3479−3716.

(6) Wang, C.; Deng, Z.; Phillips, D. L.; Liu, J. Extension of Non-Alternant Nanographenes Containing Nitrogen-Doped Stone-Thrower-Wales Defects. *Angew. Chem., Int. Ed.* **2023**, *62* (35), No. e202306890.

(7) Luo, H.; Liu, J. Facile Synthesis of Nitrogen-Doped Nanographenes with Joined Nonhexagons via a Ring Expansion Strategy. *Angew. Chem., Int. Ed.* **2023**, *62* (21), No. e202302761.
(8) Tanaka, T.; Kise, K. Non-Planar Polycyclic Aromatic Molecules Including Heterole Units. *Heterocycles* **2022**, *104* (8), 1373.
(9) Qiu, Z. L.; Chen, X. W.; Huang, Y. D.; Wei, R. J.; Chu, K. S.; Zhao, X. J.; Tan, Y. Z. Nanographene with Multiple Embedded Heptagons: Cascade Radical Photocyclization. *Angew. Chem., Int. Ed.* **2022**, *61* (18), No. e202116955.
(10) Messersmith, R. E.; Siegler, M. A.; Tovar, J. D. Aromaticity Competition in Differentially Fused Borepin-Containing Polycyclic Aromatics. *J. Org. Chem.* **2016**, *81* (13), 5595−5605.
(11) Caruso, A.; Tovar, J. D. Functionalized Dibenzoborepins as Components of Small Molecule and Polymeric π-Conjugated Electronic Materials. *J. Org. Chem.* **2011**, *76* (7), 2227−2239.
(12) Mokrai, R.; Mocanu, A.; Duffy, M. P.; Vives, T.; Caytan, E.; Dorcet, V.; Roisnel, T.; Nyulászi, L.; Benkő, Z.; Bouit, P. A.; Hissler, M. Stereospecific Synthesis of Chiral P-Containing Polyaromatics Based on 7-Membered P-Rings. *Chem. Commun.* **2021**, *57* (59), 7256−7259.
(13) Scott, L. T.; Hashemi, M. M.; Meyer, D. T.; Warren, H. B. C. Corannulene. A convenient new synthesis. *J. Am. Chem. Soc.* **1991**, *113* (18), 7082−7084.
(14) Goldfinger, M. B.; Swager, T. M. Fused Polycyclic Aromatics via Electrophile-Induced Cyclization Reactions: Application to the Synthesis of Graphite Ribbons. *J. Am. Chem. Soc.* **1994**, *116* (17), 7895−7896.
(15) Senese, A. D.; Chalifoux, W. A. Nanographene and Graphene Nanoribbon Synthesis via Alkyne Benzannulations. *Molecules* **2019**, *24* (1), 118.
(16) Magiera, K. M.; Aryal, V.; Chalifoux, W. A. Alkyne Benzannulations in the Preparation of Contorted Nanographenes. *Org. Biomol. Chem.* **2020**, *18* (13), 2372−2386.
(17) Pankova, A. S.; Shestakov, A. N.; Kuznetsov, M. A. Cyclization of Ortho-Ethynylbiaryls as an Emerging Versatile Tool for the Construction of Polycyclic Arenes. *Russ. Chem. Rev.* **2019**, *88* (6), 594−643.
(18) Liu, J.; Li, B. W.; Tan, Y. Z.; Giannakopoulos, A.; Sanchez-Sanchez, C.; Beljonne, D.; Ruffieux, P.; Fasel, R.; Feng, X.; Müllen, K. Toward Cove-Edged Low Band Gap Graphene Nanoribbons. *J. Am. Chem. Soc.* **2015**, *137* (18), 6097−6103.
(19) Yang, W.; Lucotti, A.; Tommasini, M.; Chalifoux, W. A. Bottom-Up Synthesis of Soluble and Narrow Graphene Nanoribbons Using Alkyne Benzannulations. *J. Am. Chem. Soc.* **2016**, *138* (29), 9137−9144.
(20) Yang, W.; Longhi, G.; Abbate, S.; Lucotti, A.; Tommasini, M.; Villani, C.; Catalano, V. J.; Lykhin, A. O.; Varganov, S. A.; Chalifoux, W. A. Chiral Peropyrene: Synthesis, Structure, and Properties. *J. Am. Chem. Soc.* **2017**, *139* (37), 13102−13109.
(21) Storch, J.; Sýkora, J.; Čermak, J.; Karban, J.; Císařová, I.; Růžička, A. Synthesis of Hexahelicene and 1-Methoxyhexahelicene via Cycloisomerization of Biphenylyl-Naphthalene Derivatives. *J. Org. Chem.* **2009**, *74* (8), 3090−3093.
(22) Storch, J.; Čermák, J.; Karban, J.; Císařová, I.; Sýkora, J. Synthesis of 2-Aza[6]Helicene and Attempts to Synthesize 2,14-Diaza[6]Helicene Utilizing Metal-Catalyzed Cycloisomerization. *J. Org. Chem.* **2010**, *75* (9), 3137−3140.
(23) Weimar, M.; Correa Da Costa, R.; Lee, F. H.; Fuchter, M. J. A Scalable and Expedient Route to 1-Aza[6]Helicene Derivatives and Its Subsequent Application to a Chiral-Relay Asymmetric Strategy. *Org. Lett.* **2013**, *15* (7), 1706−1709.
(24) Li, Y.; Concellón, A.; Lin, C. J.; Romero, N. A.; Lin, S.; Swager, T. M. Thiophene-Fused Polyaromatics: Synthesis, Columnar Liquid Crystal, Fluorescence and Electrochemical Properties. *Chem. Sci.* **2020**, *11* (18), 4695−4701.
(25) Sprenger, K.; Golz, C.; Alcarazo, M. Synthesis of Cycloheptatrienes, Oxepines, Thiepines, and Silepines: A Comparison between Brønsted Acid and Au-Catalysis. *Eur. J. Org Chem.* **2020**, *2020* (39), 6245−6254.
(26) Shao, J.; Zhao, X.; Wang, L.; Tang, Q.; Li, W.; Yu, H.; Tian, H.; Zhang, X.; Geng, Y.; Wang, F. Synthesis and Characterization of π-Extended Thienoacenes with up to 13 Fused Aromatic Rings. *Tetrahedron Lett.* **2014**, *55* (41), 5663−5666.
(27) Labella, J.; Durán-Sampedro, G.; Krishna, S.; Martínez-Díaz, M. V.; Guldi, D. M.; Torres, T. Anthracene-Fused Oligo-BODIPYs: A New Class of π-Extended NIR-Absorbing Materials. *Angew. Chem., Int. Ed.* **2023**, *62* (5), No. e202214543.
(28) Kurpanik, A.; Matussek, M.; Szafraniec-Gorol, G.; Filapek, M.; Lodowski, P.; Marcol-Szumilas, B.; Ignasiak, W.; Małecki, J. G.; Machura, B.; Małecka, M.; Danikiewicz, W.; Pawlus, S.; Krompiec, S. APEX Strategy Represented by Diels−Alder Cycloadditions—New Opportunities for the Syntheses of Functionalised PAHs. *Chem. - Eur. J.* **2020**, *26* (53), 12150−12157.
(29) Márquez, I. R.; Castro-Fernández, S.; Millán, A.; Campaña, A. G. Synthesis of Distorted Nanographenes Containing Seven- and Eight-Membered Carbocycles. *Chem. Commun.* **2018**, *54* (50), 6705−6718.
(30) Qiu, Z.; Asako, S.; Hu, Y.; Ju, C. W.; Liu, T.; Rondin, L.; Schollmeyer, D.; Lauret, J. S.; Müllen, K.; Narita, A. Negatively Curved Nanographene with Heptagonal and [5]Helicene Units. *J. Am. Chem. Soc.* **2020**, *142* (35), 14814−14819.
(31) Chaolumen; Stepek, I. A.; Yamada, K. E.; Ito, H.; Itami, K. Construction of Heptagon-Containing Molecular Nanocarbons. *Angew. Chem., Int. Ed.* **2021**, *60* (44), 23508−23532.
(32) Kawai, K.; Kato, K.; Peng, L.; Segawa, Y.; Scott, L. T.; Itami, K. Synthesis and Structure of a Propeller-Shaped Polycyclic Aromatic Hydrocarbon Containing Seven-Membered Rings. *Org. Lett.* **2018**, *20* (7), 1932−1935.
(33) Yamada, K. E.; Stepek, I. A.; Matsuoka, W.; Ito, H.; Itami, K. Synthesis of Heptagon-Containing Polyarenes by Catalytic C−H Activation. *Angew. Chem., Int. Ed.* **2023**, *62* (51), No. e202311770.
(34) Sanil, G.; Koszarna, B.; Poronik, Y. M.; Vakuliuk, O.; Szymański, B.; Kusy, D.; Gryko, D. T. The Chemistry of 1,4-Dihydropyrrolo[3,2-b]Pyrroles. *Adv. Heterocycl. Chem.* **2022**, *138*, 335−409.
(35) Stecko, S.; Gryko, D. T. Multifunctional Heteropentalenes: From Synthesis to Optoelectronic Applications. *JACS Au* **2022**, *2* (6), 1290−1305.
(36) Mishra, S.; Krzeszewski, M.; Pignedoli, C. A.; Ruffieux, P.; Fasel, R.; Gryko, D. T. On-Surface Synthesis of a Nitrogen-Embedded Buckybowl with Inverse Stone-Thrower-Wales Topology. *Nat. Commun.* **2018**, *9* (1), 1714.
(37) Krzeszewski, M.; Dobrzycki, Ł.; Sobolewski, A. L.; Cyrański, M. K.; Gryko, D. T. Saddle-Shaped Aza-Nanographene with Multiple Odd-Membered Rings. *Chem. Sci.* **2023**, *14* (9), 2353−2360.
(38) Sanil, G.; Krzeszewski, M.; Chaładaj, W.; Danikiewicz, W.; Knysh, I.; Dobrzycki, Ł.; Staszewska-Krajewska, O.; Cyrański, M. K.; Jacquemin, D.; Gryko, D. T. Gold-Catalyzed 1,2-Aryl Shift and Double Alkyne Benzannulation. *Angew. Chem., Int. Ed.* **2023**, *62* (49), No. e202311123.
(39) Zhao, W.; Sun, J. Triflimide (HNTf2) in Organic Synthesis. *Chem. Rev.* **2018**, *118* (20), 10349−10392.
(40) Gicquiaud, J.; Hacıhasanoğlu, A.; Hermange, P.; Sotiropoulos, J. M.; Toullec, P. Y. Brønsted Acid-Catalyzed Carbocyclization of 2-Alkynyl Biaryls. *Adv. Synth. Catal.* **2019**, *361* (9), 2025−2030.
(41) Hermange, P.; Gicquiaud, J.; Barbier, M.; Karnat, A.; Toullec, P. Y. Bronsted Acid Catalyzed Carbocyclizations Involving Electrophilic Activation of Alkynes. *Synth.* **2022**, *54* (24), 5360−5384.
(42) Praveen, C.; Szafert, S. Homogeneous Gold Catalysis for Regioselective Carbocyclization of Alkynyl Precursors. *ChemPlusChem* **2023**, *88* (7), No. e202300202.
(43) Shibata, T.; Ito, M.; Inoue, D.; Kawasaki, R.; Stephen Kanyiva, K. Cationic Au(I)-Catalyzed Cycloisomerization of N-(2-Alkynylphenyl)Indolines for the Construction of Indolobenzazepine Skeleton. *Heterocycles* **2017**, *94* (12), 2229.
(44) Mandal, M.; Pradhan, R.; Lourderaj, U.; Balamurugan, R. Dodging the Conventional Reactivity of O-Alkynylanilines under

https://doi.org/10.1021/acs.joc.4c02538
J. Org. Chem. 2025, 90, 614−622

Gold Catalysis for Distal 7-Endo-Dig Cyclization. *J. Org. Chem.* **2023**, *88* (4), 2260−2287.
(45) Khomutetckaia, A.; Ehlers, P.; Villinger, A.; Langer, P. Synthesis and Properties of Benzo[h]Imidazo[1,2-a]Quinolines and 1,2a-Diazadibenzo[Cd,f]Azulenes. *J. Org. Chem.* **2023**, *88* (13), 7929−7939.
(46) Clark, J. A.; Kusy, D.; Vakuliuk, O.; Krzeszewski, M.; Kochanowski, K. J.; Koszarna, B.; O'Mari, O.; Jacquemin, D.; Gryko, D. T.; Vullev, V. I. The Magic of Biaryl Linkers: The Electronic Coupling through Them Defines the Propensity for Excited-State Symmetry Breaking in Quadrupolar Acceptor-Donor-Acceptor Fluorophores. *Chem. Sci.* **2023**, *14* (46), 13537−13550.
(47) Łukasiewicz, Ł. G.; Rammo, M.; Stark, C.; Krzeszewski, M.; Jacquemin, D.; Rebane, A.; Gryko, D. T. Ground- and Excited-State Symmetry Breaking and Solvatofluorochromism in Centrosymmetric Pyrrolo[3,2-b]Pyrroles Possessing Two Nitro Groups. *ChemPhotoChem.* **2020**, *4* (7), 508−519.
(48) Tasior, M.; Kowalczyk, P.; Przybył, M.; Czichy, M.; Janasik, P.; Bousquet, M. H. E.; Łapkowski, M.; Rammo, M.; Rebane, A.; Jacquemin, D.; Gryko, D. T. Going beyond the Borders: Pyrrolo[3,2-b]Pyrroles with Deep Red Emission. *Chem. Sci.* **2021**, *12* (48), 15935−15946.

https://doi.org/10.1021/acs.joc.4c02538
J. Org. Chem. 2025, 90, 614−622

7. Declaration of the Authors of Publications

Institute of Organic Chemistry
Polish Academy of Sciences

M.Sc. Gana Sanil

+48 22 343 20 26
gana.sanil@icho.edu.pl

Institute of Organic Chemistry, PAS
ul. Marcina Kasprzaka 44/52
Warsaw 01-224

Warszawa Date.

I declare that my contribution to the following publication consisted of:

- Gana Sanil, B. Koszarna, Y. M. Poronik, O. Vakuliuk, B. Szymański, D. Kusy, D. T. Gryko, *Adv. Heterocycl. Chem.* 2022, *138*, 335–409. DOI 10.1016/bs.aihch.2022.04.002 ." *The chemistry of 1,4-dihydropyrrolo[3,2-b]pyrroles"*

  Collection of research papers and writing the sections "previous synthetic methods towards pyrrolo[3,2-*b*]pyrroles" and "Synthesis of π-expanded 1,4-dihydropyrrolo[3,2-*b*]pyrroles". Incorporation of the description from all co-authors to prepare the final draft and editing the chapter.

- Gana Sanil, M. Krzeszewski, W. Chaładaj, W. Danikiewicz, I. Knysh, Ł. Dobrzycki, O. Staszewska-Krajewska, M. K. Cyrański, D. Jacquemin, D. T. Gryko, *Angew. Chem. Int. Ed.* 2023, 62, e202311123. DOI 10.1002/anie.202311123. *"Gold-Catalyzed 1,2-Aryl Shift and Double Alkyne Benzannulation"*

  Co-development of research concept and interpretation of results. I carried out the synthesis of starting material anilines **1a-e**, used them for the synthesis of precursors **4ea-ec**. I developed and carried out the final alkyne annulation to synthesize products **5aa-ec**. Performed the complete chemical analysis of all new compounds, carried out their photophysical measurements and tabulated the results. Carried out all the additional experiments mentioned in the ESI. Prepared the supporting information and participated in the manuscript writing.

- Gana Sanil, Ł. Dobrzycki, M. K. Cyrański, D. Jacquemin, W. Chaładaj, D. T. Gryko, *J. Org. Chem.* 2024. DOI:10.1021/acs.joc.4c02538. "1,4-Dihydropyrrolo[3,2-*b*]Pyrroles with Two Embedded Heptagons via Alkyne Annulation"

  Co-development of research concept and interpretation of results. I carried out the synthesis of synthesis of precursors **4aa-cc**. I developed and carried out the final alkyne annulation to synthesize products **5aa-bc** and synthesized the completely cyclized product **7ac**. Performed the complete chemical analysis of all new compounds, carried out their photophysical and cyclic voltametric measurements, tabulated and interpreted the results. Carried out the additional experiments mentioned in the ESI. Prepared the supporting information and wrote the first draft of the manuscript.

Institute of Organic Chemistry
Polish Academy of Sciences

Professor Daniel Gryko
Director

+48 22 343 23 21
daniel.gryko@icho.edu.pl

Warsaw 8th January 2025

I declare that my contribution to the following publications consisted of:

› Gana Sanil, B. Koszarna, Y. M. Poronik, O. Vakuliuk, B. Szymański, D. Kusy, D. T. Gryko, *Adv. Heterocycl. Chem.* **2022**, *138*, 335–409. DOI 10.1016/bs.aihch.2022.04.002 ." *The chemistry of 1,4-dihydropyrrolo[3,2-b]pyrroles"*

Development of the review concept, writing the introduction and summary/outlook as well as editing of the final version of the manuscript.

› Gana Sanil, M. Krzeszewski, W. Chaładaj, W. Danikiewicz, I. Knysh, Ł. Dobrzycki, O. Staszewska-Krajewska, M. K. Cyrański, D. Jacquemin, D. T. Gryko, *Angew. Chem. Int. Ed.* **2023**, 62, e202311123. DOI 10.1002/anie.202311123. *"Gold-Catalyzed 1,2-Aryl Shift and Double Alkyne Benzannulation"*.

Co-development of research concepts, interpretation of results and preparation of the final version of the manuscript.

› Gana Sanil, Ł. Dobrzycki, M. K. Cyrański, D. Jacquemin, W. Chaładaj, D. T. Gryko, *J. Org. Chem.* **2024**. DOI:10.1021/acs.joc.4c02538. "1,4-Dihydropyrrolo[3,2-*b*]Pyrroles with Two Embedded Heptagons via Alkyne Annulation".

Co-development of research concepts, interpretation of results and preparation of the final version of the manuscript.

Yours sincerely

Institute of Organic Chemistry
Polish Academy of Sciences

dr Beata Koszarna

+48 22 343 20 37
beata.koszarna@icho.edu.pl

Warsaw 20th September 2024

Hereby I would like to declare that my contribution to the publication:

Gana Sanil, B. Koszarna, Y. M. Poronik, O. Vakuliuk, B. Szymański, D. Kusy, D. T. Gryko, *Adv. Heterocycl. Chem.* **2022**, *138*, 335–409. DOI 10.1016/bs.aihch.2022.04.002. " *The chemistry of 1,4-dihydropyrrolo[3,2-b]pyrroles"*

I contributed to writing the section of the publication that discusses the reactivity of 1,4-dihydropyrrolo[3,2-b]pyrrole derivatives.

Beata Koszarna

Yours sincerely

Institute of Organic Chemistry
Polish Academy of Sciences

dr Yevgen Poronik

+48 22 343 20 26
yevgen.poronik@icho.edu.pl

Institute of Organic Chemistry, PAS
ul. Marcina Kasprzaka 44/52
Warsaw 01-224

Warsaw 2nd of December 2024

I declare that my contribution to the following publication:

- Gana Sanil, B. Koszarna, Y. M. Poronik, O. Vakuliuk, B. Szymański, D. Kusy, D. T. Gryko, *Adv. Heterocycl. Chem.* **2022**, *138*, 335–409. DOI 10.1016/bs.aihch.2022.04.002 ." *The chemistry of 1,4-dihydropyrrolo[3,2-b]pyrroles*"

was writing the section 'Photophysical Properties' along with the final correction.

Yevgen Poronik

Yours sincerely,

Instytut Chemii Organicznej
Polskiej Akademii Nauk

Dr Olena Vakuliuk

+48 22 343 20 20
olena.vakuliuk@icho.edu.pl

Institute of Organic Chemistry
Polish Academy of Sciences
Kasprzaka 44/52, 01-224 Warsaw
Poland

Warsaw, 5th of November 2024 r.

Hereby I would like to declare that my contribution to the publication:

Gana Sanil, B. Koszarna, Y. M. Poronik, O. Vakuliuk, B. Szymański, D. Kusy, D. T. Gryko, *Adv. Heterocycl. Chem.* **2022**, 138, 335–409. DOI 10.1016/bs.aihch.2022.04.002 ." The chemistry of 1,4-dihydropyrrolo[3,2-b]pyrroles"

consisted in writing the section discussing the synthesis of 1,4-dihydropyrrolo[3,2-*b*]pyrrole derivatives.

Yours sincerely

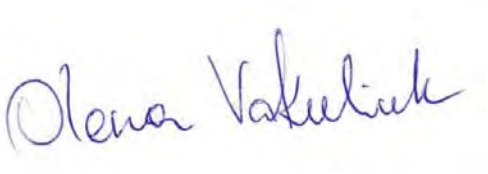

Warsaw, 17.09.2024r.

Statement

Hereby I would like to declare that my contribution to the publications:

Gana Sanil, B. Koszarna, Y. M. Poronik, O. Vakuliuk, B. Szymański, D. Kusy, D. T. Gryko, *Adv. Heterocycl. Chem.* **2022**, *138*, 335–409. DOI 10.1016/bs.aihch.2022.04.002 . *"The chemistry of 1,4-dihydropyrrolo[3,2-b]pyrroles"*

I collected the data about modern approaches in pyrrolo[3,2-b]pyrrole synthesis and wrote the part of the chapter regarding these synthetic methods.

Bartosz Szymański

Bartosz Szymański
PhD Student at Doctoral School in
Mathematics and Natural Sciences,
University of Warsaw

Institute of Organic Chemistry
Polish Academy of Sciences

Dr Damian Kusy

+48 22 343 20 08
damian.kusy@icho.edu.pl

Institute of Organic Chemistry, PAS
ul. Marcina Kasprzaka 44/52
Warsaw 01-224

Warszawa 07.11.2024

I declare that my contribution to the following publication consisted of:

- **Gana Sanil**, B. Koszarna, Y. M. Poronik, O. Vakuliuk, B. Szymański, D. Kusy, D. T. Gryko, *Adv. Heterocycl. Chem.* **2022**, *138*, 335–409. DOI 10.1016/bs.aihch.2022.04.002 ." *The chemistry of 1,4-dihydropyrrolo[3,2-b]pyrroles"*

  I contributed to writing the section of the publication related to the part Applications: "Optoelectronic applications, Metal-organic frameworks and related applications, Other applications".

Yours sincerely,

Damian Kusy

Institute of Organic Chemistry
Polish Academy of Sciences

Dr Maciej Krzeszewski

+48 22 343 20 26
maciej.krzeszewski@icho.edu.pl

Warszawa 13th September 2024

I declare that my contribution to the following publication consisted of:

Gana Sanil, M. Krzeszewski, W. Chaładaj, W. Danikiewicz, I. Knysh, Ł. Dobrzycki, O. Staszewska-Krajewska, M. K. Cyrański, D. Jacquemin, D. T. Gryko, *Angew. Chem. Int. Ed.* 2023, *62*, e202311123. DOI 10.1002/anie.202311123. *"Gold-Catalyzed 1,2-Aryl Shift and Double Alkyne Be*nzannulation"

I carried out the synthesis of substrates 4aa to 4da and 4mix, contributed to the preparation of the final version of the manuscript and supervised the experimental part. Furthermore, I was involved in editing the Supporting Information.

Yours sincerely,

Dr. Iryna Knysh
Iryna.Knysh@univ-nantes.fr

Nantes, le 12/09/2024

I hereby declare that my contribution to the listed publication below is as follows:

1. G. Sanil, M. Krzeszewski, W. Chaładaj, W. Danikiewicz, I. Knysh, Ł. Dobrzycki, O. Staszewska-Krajewska, M. K. Cyrański, D. Jacquemin, D. T. Gryko, *Angew. Chem. Int. Ed.* **2023**, 62, e202311123. "Gold-Catalyzed 1,2-Aryl Shift and Double Alkyne Benzannulation"

I have theoretically modelled vibrionic absorption and emission spectra for selected compounds.

Iryna Knysh

CEISAM
www.ceisam.univ-nantes.fr
Faculté des Sciences et Techniques
Nantes Université
2 Rue de la Houssinière,
BP 92208
44322 NANTES CEDEX 3
T : +33 (0)276 64 51 49
UMR CNRS 6230

Institute of Organic Chemistry
Polish Academy of Sciences

Dr. Olga Staszewska-Krajewska
Laboratory for Analysis of Bioactive Compounds

+48 22 343 25 52
olga.staszewska@icho.edu.pl

Warszawa Date 16.09.2024

I declare that my contribution to the following publication consisted of:

Gana Sanil, M. Krzeszewski, W. Chaładaj, W. Danikiewicz, I. Knysh, Ł. Dobrzycki, O. Staszewska-Krajewska, M. K. Cyrański, D. Jacquemin, D. T. Gryko, *Angew. Chem. Int. Ed.* **2023**, *62*, e202311123. DOI 10.1002/anie.202311123. "*Gold-Catalyzed 1,2-Aryl Shift and Double Alkyne Benzannulation*"

I was responsible for planning and performing NMR measurements of the studied compounds. I was involved in the results interpretation and editing process of the supplementary.

Yours sincerely,

Olga Krajewska

Institute of Organic Chemistry
Polish Academy of Sciences

Witold Danikiewicz
Head of the Mass Spectrometry Group

+48 22 343 22 15
witold.danikiewicz@icho.edu.pl

Warszawa September 24th, 2024

I declare that my contribution to the following publication consisted of:

Gana Sanil, M. Krzeszewski, W. Chaładaj, W. Danikiewicz, I. Knysh, Ł. Dobrzycki, O. Staszewska-Krajewska, M. K. Cyrański, D. Jacquemin, D. T. Gryko, Angew. Chem. Int. Ed. 2023, 62, e202311123. DOI 10.1002/anie.202311123. “Gold-Catalyzed 1,2-Aryl Shift and Double Alkyne Benzannulation”

Performing part of the quantum chemical calculations and writing the respective paragraph in the manuscript.

Yours sincerely,

Witold Aleksander Danikiewicz

Elektronicznie podpisany przez Witold Aleksander Danikiewicz
Data: 2024.09.24 12:22:30 +02'00'

Prof. Denis Jacquemin
Denis.Jacquemin@univ-nantes.fr

Ref. **Contribution Letter**

Nantes, 07/01/2025

To whom it may concern,

I hereby declare that my contribution to the publications below:

1. **Gana Sanil**, M. Krzeszewski, W. Chaładaj, W. Danikiewicz, I. Knysh, Ł. Dobrzycki, O. Staszewska-Krajewska, M. K. Cyrański, D. Jacquemin, D. T. Gryko, *Angew. Chem. Int. Ed.* **2023**, *62*, e202311123. DOI 10.1002/anie.202311123. "*Gold-Catalyzed 1,2-Aryl Shift and Double Alkyne Be*nzannulation"

2. **Gana Sanil**, Ł. Dobrzycki, M. K. Cyrański, D. Jacquemin, W. Chaładaj, D. T. Gryko, *J. Org. Chem.* **2024**. DOI:10.1021/acs.joc.4c02538. "1,4-Dihydropyrrolo[3,2-*b*]Pyrroles with Two Embedded Heptagons via Alkyne Annulation"

I supervised the theoretical parts of this work and wrote the theoretical section of all manuscripts. For publications 2, I also performed all the DFT and TD-DFT calculations. In both contributions, I was involved in the proof checking of the full manuscript.

With best regards

Prof. Denis Jacquemin

CEISAM
www.ceisam.sciences.univ-nantes.fr
UMR CNRS 6230
Faculté des Sciences et Techniques
Université de Nantes
2 Rue de la Houssinière,
Nantes, France

Institute of Organic Chemistry
Polish Academy of Sciences

Wojciech Chaładaj
associate professor

+48 22 343 30 65
wojciech.chaladaj@icho.edu.pl

Institute of Organic Chemistry, PAS
ul. Marcina Kasprzaka 44/52
Warsaw 01-224

Warsaw, 09.01.2025

I declare that my contribution to the following publication consisted of:

- Gana Sanil, M. Krzeszewski, W. Chaładaj, W. Danikiewicz, I. Knysh, Ł. Dobrzycki, O. Staszewska-Krajewska, M. K. Cyrański, D. Jacquemin, D. T. Gryko, *Angew. Chem. Int. Ed.* **2023**, 62, e202311123. DOI 10.1002/anie.202311123. "*Gold-Catalyzed 1,2-Aryl Shift and Double Alkyne Benzannulation*"

  Carrying out DFT calculations of the reaction mechanism, analysis and interpretation of the obtained data and preparation of the manuscript section concerning DFT investigation of the reaction mechanism.

- Gana Sanil, Ł. Dobrzycki, M. K. Cyrański, D. Jacquemin, W. Chaładaj, D. T. Gryko, *J. Org. Chem.* **2024**. DOI:10.1021/acs.joc.4c02538. "1,4-Dihydropyrrolo[3,2-*b*]Pyrroles with Two Embedded Heptagons via Alkyne Annulation"

  Carrying out DFT calculations of the reaction mechanism, analysis and interpretation of the obtained data and preparation of the manuscript section concerning DFT investigation of the reaction mechanism.

Yours sincerely,

Wojciech Jan Chaładaj

Digitally signed by Wojciech Jan Chaładaj
Date: 2025.01.09 13:28:02 +01'00'

UNIWERSYTET WARSZAWSKI

Wydział Chemii Uniwersytet Warszawski

Warsaw, January 14th 2025

I declare that my contribution to the following publications

Gana Sanil, M. Krzeszewski, W. Chaładaj, W. Danikiewicz, I. Knysh, Ł. Dobrzycki, O. Staszewska-Krajewska, M. K. Cyrański, D. Jacquemin, D. T. Gryko, *Angew. Chem. Int. Ed.* **2023**, *62*, e202311123. DOI 10.1002/anie.202311123. "*Gold-Catalyzed 1,2-Aryl Shift and Double Alkyne Be*nzannulation"

Gana Sanil, Ł. Dobrzycki, M. K. Cyrański, D. Jacquemin, W. Chaładaj, D. T. Gryko, *J. Org. Chem.* **2024**. DOI:10.1021/acs.joc.4c02538. "1,4-Dihydropyrrolo[3,2-*b*]Pyrroles with Two Embedded Heptagons via Alkyne Annulation"

concerned X-ray experimental part and discussion of the resulting (structural) results.

Sincerely Yours,

Michał K. Cyrański

Prof. dr hab. Michał K. Cyrański
Pasteura 1
02-093 Warszawa
e-mail: mkc@chem.uw.edu.pl
Tel: 22 55 26 360

Gainesville FL, 12 JAN 2025

STATEMENT

I hereby declare that my contribution to the following publications consisted on:

1. **Gana Sanil**, M. Krzeszewski, W. Chaładaj, W. Danikiewicz, I. Knysh, Ł. Dobrzycki, O. Staszewska-Krajewska, M. K. Cyrański, D. Jacquemin, D. T. Gryko, *Angew. Chem. Int. Ed*. **2023**, 62, e202311123. DOI 10.1002/anie.202311123. "*Gold-Catalyzed 1,2-Aryl Shift and Double Alkyne Benzannulation*"

   - performing X-ray crystallographic measurement, analysis of the data to obtain final crystal structure and writing the supporting information section related to X-ray crystallography.

2. **Gana Sanil**, Ł. Dobrzycki, M. K. Cyrański, D. Jacquemin, W. Chaładaj, D. T. Gryko, *J. Org. Chem.* **2024**. DOI:10.1021/acs.joc.4c02538. *"1,4-Dihydropyrrolo*[3,2-*b*]*Pyrroles with Two Embedded Heptagons via Alkyne Annulation"*

   - performing X-ray crystallographic measurement, analysis of the data to obtain final crystal structure and writing the supporting information section related to X-ray crystallography.

Łukasz Dobrzycki